City Research Online

City, University of London Institutional Repository

Citation: Margrain, T. (1997). Recovery of Spatial Vision Following Intense Light Adaptation. (Unpublished Doctoral thesis, City, University of London)

This is the accepted version of the paper.

This version of the publication may differ from the final published version.

Permanent repository link: https://openaccess.city.ac.uk/id/eprint/31118/

Link to published version:

Copyright: City Research Online aims to make research outputs of City, University of London available to a wider audience. Copyright and Moral Rights remain with the author(s) and/or copyright holders. URLs from City Research Online may be freely distributed and linked to.

Reuse: Copies of full items can be used for personal research or study, educational, or not-for-profit purposes without prior permission or charge. Provided that the authors, title and full bibliographic details are credited, a hyperlink and/or URL is given for the original metadata page and the content is not changed in any way.

City Research Online: http://openaccess.city.ac.uk/ publications@city.ac.uk

RECOVERY OF SPATIAL VISION FOLLOWING INTENSE LIGHT ADAPTATION

by

THOMAS HENGIST MARGRAIN

A thesis submitted
for the degree of

DOCTOR OF PHILOSOPHY

Department of Optometry and Visual Science,
City University, London.

December, 1997.

CONTENTS

LIST OF TABLES

LIST OF FIGURES

ACKNOWLEDGEMENTS

Firstly, I would like to express my sincere thanks to my supervisor Dr W.D. Thomson for his guidance, advice and continual support during this work.

I am also grateful to Prof. G.B. Arden for his helpful comments on experimental methods and rod-cone interactions; Dr R. Summers and Dr R. Hovorka for their advice on modelling and Dr R. Douglas for proof reading sections of this manuscript.

My thanks also go to the students, in particular my colleague Chris Owen, who helped to make my time at City such a happy one.

Most importantly, I would like to thank Kath for putting up with me for more years than I care to remember.

DECLARATION

I grant powers of discretion to the university librarian to allow this thesis to be copied in whole or in part without reference to me. This covers only single copies made for study purposes, subject to normal conditions of acknowledgement.

ABSTRACT

This thesis presents a series of investigations that describe the recovery of spatial vision following a period of intense light adaptation.

The first investigation in this thesis (Chapter 2) shows, for the first time, how threshold to sinusoidal gratings (0.6-14 c.p.d.), presented in the parafovea, varies during the course of dark adaptation (30 min). For all subjects (n=7) threshold to low spatial frequency gratings declined throughout the experiment, showing discrete cone and rod limbs. For subjects with normal colour vision, threshold to high spatial frequency gratings (14 c.p.d.) increased during the 'rod' phase of dark adaptation, a phenomenon known as suppressive rod-cone interaction (SRCI). This increase in threshold, was not observed in the 2 protanopes studied which suggests a distil site for this interaction.

From a functional perspective, the most important quantity for the visual system to extract form the environment is contrast. Therefore, a technique has been developed for measuring contrast sensitivity (CS) during recovery from a period of intense light adaptation. Results were obtained for 2 subjects, for 5 spatial frequencies (0.6-19.9 c.p.d.) at 5 luminances (50-0.005 cdm^{-2})(Chapter 3). These results provide a practical description of visual performance under such conditions.

The effect of 'bleach' intensity and duration on CS recovery was investigated in Chapter 4. Equal energy 'bleaches' that differed in intensity (I) and duration (t) (i.e. $I \times t = k$) produced different CS recovery functions. This suggests that CS recovery is only partly explained by the concentration of a photoproduct (the photochemical hypothesis).

Although, there have been no previous investigations of CS recovery following a period of intense light adaptation, the time taken for acuity to return following a 'bleach' has been measured (e.g. the 'photostress' test). Clinically, long 'photostress' recovery times (PSRTs) are associated with retinal dysfunction. However, interpretation of PSRT results is difficult because a variety of bleaching techniques and 'normal' PSRTs have been described in the literature. The effect of bleaching technique, age and ametropia on PSRT was investigated in Chapter 5. Results from 50 normal subjects (aged 21-76 yrs) showed that the most appropriate 'bleaching' technique involved exposing the eye to the light form a direct ophthalmoscope for 30 seconds.

To obtain a fuller understanding of how visual performance changes during photostress testing, 50 subjects were tested using a modified version of the CS recovery technique. Contrast sensitivity recovery functions were modelled using a single exponential function. Analysis of the model variables showed that the time constant of CS recovery increases with age.

The investigations presented in this thesis extend the current understanding of the recovery of spatial vision following a period of intense light adaptation.

1. INTRODUCTION

1.1 Foreword

The world we perceive is a clever reconstruction of the 'real' world based upon variations in the quantity and quality of light falling on different parts of the retina. We are able to see an object only when the amount and / or spectral distribution of light it reflects is different from that of its surround.

The task for the visual system, to extract information about the difference in reflectance, is a difficult one because the amount of light illuminating a scene varies enormously depending on the illuminating source. Although the range of contrasts produced by the natural world is relatively small, spanning a factor of about 20 (Walraven *et al.,* 1990) the range of light intensities spans approximately 10 log units (Lamb, 1990).

The ability of the visual system to compensate for changes in ambient illumination is referred to as adaptation. Its purpose is to make the response of the visual system dependent upon contrast rather than intensity (Shapley and Enroth-Cugell, 1984). Adaptation is mediated by a number of mechanisms and each taking a finite length of time to readjust following a change in ambient illumination. Providing the change in illumination is small the adjustment takes place rapidly. However, the adjustment period can take seconds of even minutes following a large, abrupt drop in ambient illumination.

Sensitivity regulation is thought to take place mainly within the retina. It is important for adaptation to occur at this level because the retinal ganglion cells have a limited operating range. These cells, which carry information from the eye to the lateral geniculate nucleus, like many others in the nervous system, can only signal levels of activity accurately over a range of approximately 100 to 1 (Werblin, 1974). This is a much smaller range than the range of light intensities encountered in the natural environment. Additional evidence that the retina is the main site of sensitivity regulation has been provided by a number of psychophysical investigations which have shown that the state of light adaptation in one eye has little effect in determining sensitivity in the other eye, (Battersby and Wagman, 1962; Whittle and Challands, 1969).

This thesis describes a series of experiments designed to investigate the nature of spatial vision during the adaptation process, in particular during recovery from exposure to high intensities.

1.2 Anatomy and electrophysiology of the visual system

1.2.1 Overview of the visual system

The main anatomical structures of the visual system are the eye, the optic nerve, the chiasma, the optic tract, the lateral geniculate nucleus (LGN), the optic radiations and the visual areas of the brain.

Light entering the eye is refracted by the cornea and crystalline lens and forms an inverted image in the plane of the retina. The retina converts light into electrical activity and begins to process information contained within the retinal image. Visual information leaves the eye via the optic nerve and after being segregated into right and left fields at the chiasma, passes to the LGN. From there, information is relayed via the optic radiations to the visual cortex. A schematic diagram of the visual system is shown in Figure 1.1.

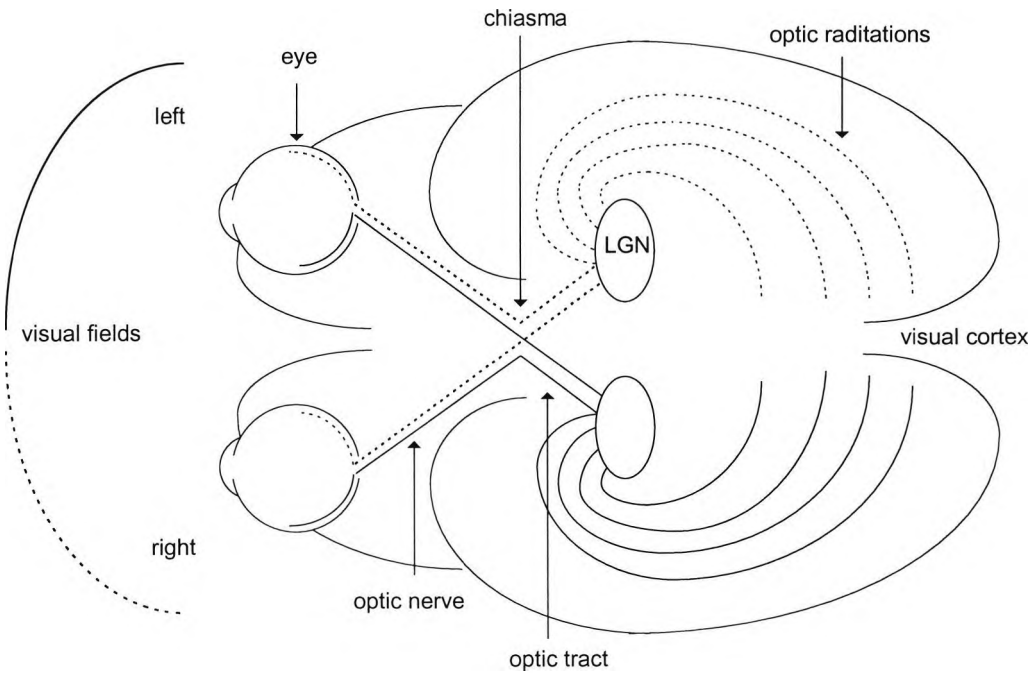

Figure 1.1 Schematic diagram of the visual system in humans viewed from the underside of the brain. Redrawn from Dowling (1987).

1.2.2 The retina

The retina is sandwiched between the vitreous body and the choroid. It possesses two distinct parts; the retinal pigment epithelium (RPE) and the sensory retina. The RPE is firmly attached to the choroid but only weakly attached to the sensory retina despite its intimate relationship. The sensory retina is securely attached to the globe at the ora seratta and the optic nerve head.

The retina is supplied with blood by the uveal blood vessels and the central retinal artery. These originate from the ophthalmic artery, the first branch of the internal carotid. Venous drainage of the choriocapillaris is mainly through the vortex vein system which in turn passes into the superior and inferior ophthalmic veins (Guyer *et al.*, 1989).

The thickness of the retina varies with retinal eccentricity, from 0.1 mm at the ora seratta and the foveola, increasing to 0.23 mm at the parafovea and is at its thickest adjacent to the optic nerve head (0.56 mm) (Ruskell, 1988; McDonnell, 1989).

Figure 1.2 shows a schematic diagram of the retinal surface including; the optic nerve head, retinal blood vessels and the relative location / size of different parts of the retina.

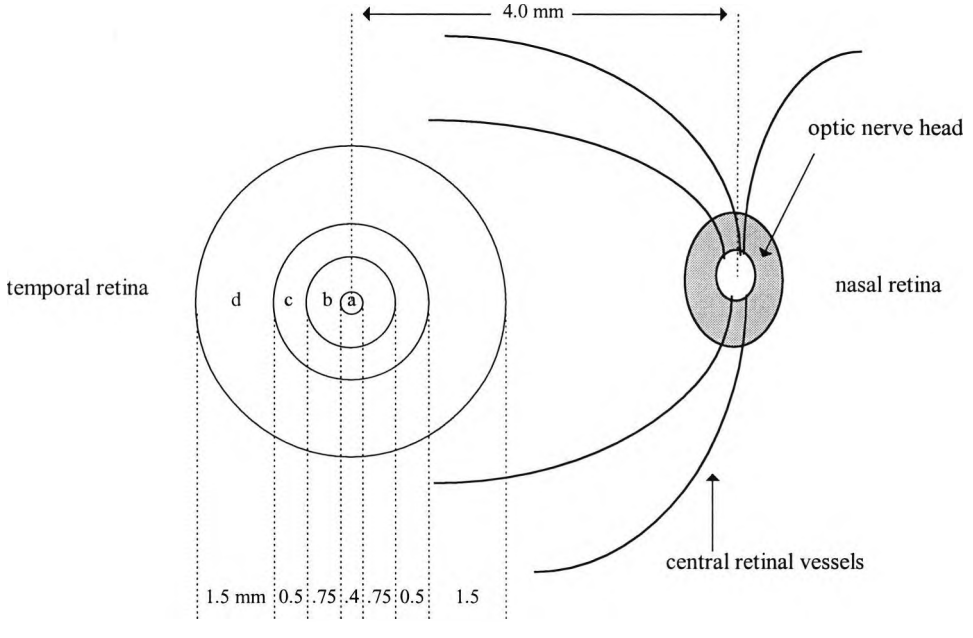

Figure 1.2 Schematic view of optic nerve head and central retinal blood vessels. Circles show, approximate location and diameter of the foveola (a), fovea (b), parafoveal area (c) and perifoveal regions (d). Together these areas constitute the macular.

The central part of the retina, which provides us with the highest acuity in photopic conditions, is known as the foveola. It is about 0.4 mm in diameter and located about 4 mm temporally and 0.8 mm inferiorly to the centre of the optic nerve head. The foveola is avascular, composed entirely of cones and found at the centre of the fovea (which has a diameter of about 1.5 mm). This portion of the retina is concave due to displacement of the inner retinal layers. The parafovea surrounds the fovea and contains approximately equal numbers of rods and cones. This in turn is surrounded by the perifoveal retina which extends out to about 2.95 mm from the foveola and marks the boundary of the central retina i.e. the macular. The peripheral retina extends from the macular region out to the ora seratta.

One of the retina's most striking features in cross section, is the well ordered structure and sharply defined layers (see Figure 1.3). The neurones of the retina are divided into three main layers: the most external is the photoreceptor layer, more centrally is the inner nuclear layer which contains horizontal, bipolar cells, amacrine and interplexiform cells, and the inner most layer is known as the ganglion cell layer. Synaptic connections between cells are limited to two plexiform layers. Conventionally the layers of the retina are numbered from the outer most layer as follows:

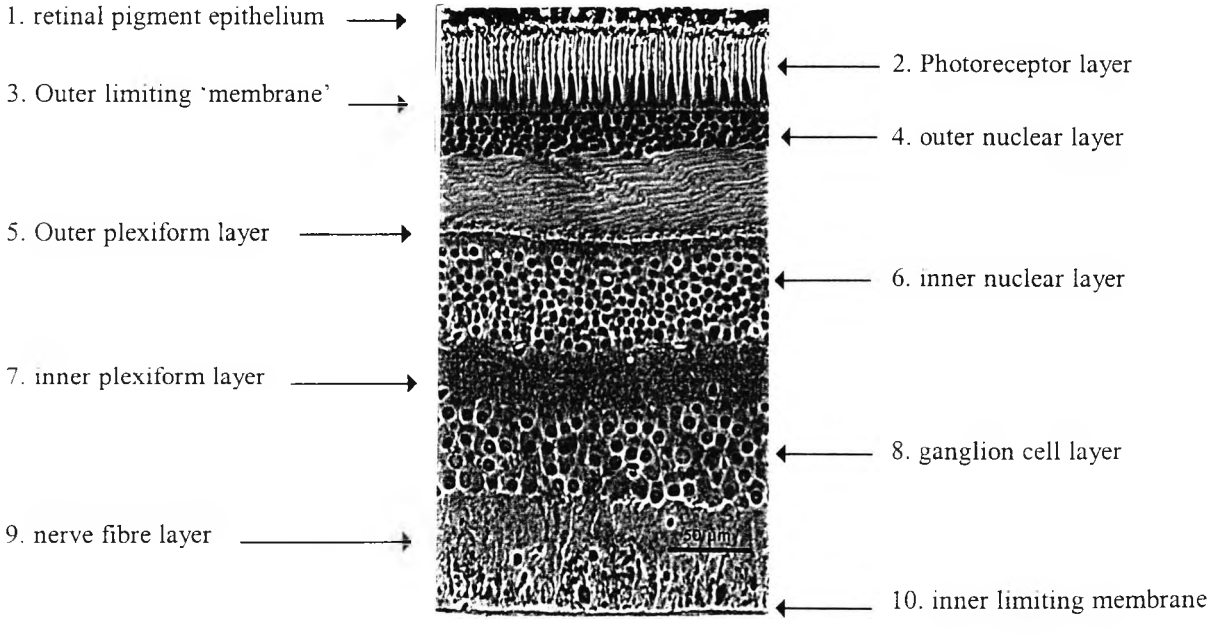

Figure 1.3 Vertical section through the human retina. After Dowling (1987).

1.2.3 Photoreceptors

The initial transduction of light into a neural signal takes place in the photoreceptors which form a mosaic of cells in the outermost layer of the sensory retina. Humans have a duplex retina i.e. one that consists of both rods and cones. Rods are extremely sensitive to light and mediate vision when illumination is low. Cones are less sensitive and hence only respond when illumination is relatively high. They mediate our perception of fine detail and colour.

There are about 110-125 million rods and 6-8 million cones in the human retina (Ruskell, 1988). Each receptor type is distributed unevenly across the retina. Cone density is maximal at the fovea (peak cone density at the foveola is approximately 161,900 cones per mm^2, Curcio *et al.,* 1987). Rods are absent from the central 0.3 mm of the retina, but their numbers increase rapidly further out in the retina. Their density reaches a peak at about 18° from the foveola (Ogden, 1989). Figure 1.4 shows how receptor density varies along the horizontal meridian in the human retina.

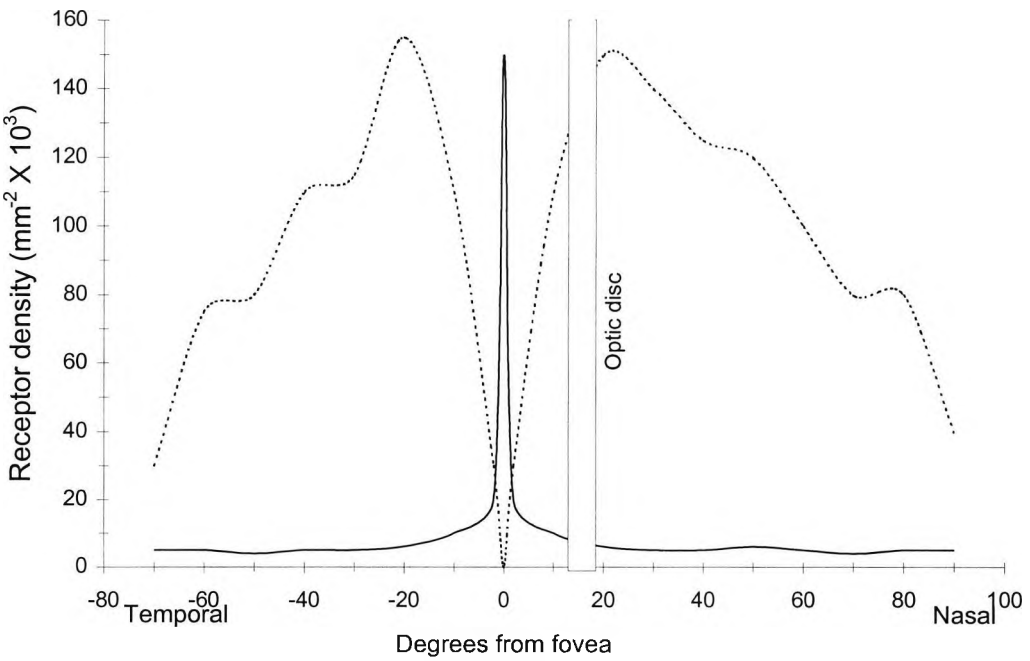

Figure 1.4 Rod and cone density along the horizontal meridian of the human retina. Cone density is greatest at the fovea (solid line) and rod density (dotted line) is greatest approximately 18° from the fovea, (After Ruskell, 1988).

1.2.3.1 Morphology

Photoreceptors have a highly differentiated and well-organised structure. At one end of the cell is the outer segment (so called because it lies closest to the outer most layers of the eye) which generates an electrical signal in response to light. The receptor inner segment contains the metabolic organelles (ellipsoid and myoid), a perikaryal region contains the nucleus and a terminal relays the light signal to other neurones. Although each receptor type is constructed from these basic elements the morphology of rods and cones is different.

The inner and outer segments of rods are cylindrical along their length and are approximately 1.4μm wide (Ruskell, 1988). Cone shape is dependant on retinal location. Peripheral cone outer segments are approximately conical, the apex being in close proximity to the RPE. However, at the fovea, cones resemble rods, having long slender cylindrical outer and inner segments and a maximum diameter of about 2.5μm in humans.

The outer segments of photoreceptors are composed of a stack of disk shaped double membranes that bind the light sensitive pigment (there are approximately 10^9 molecules of photopigment present in receptor outer segments, Dowling, 1987). Each cone contains one of three different light sensitive pigments that absorb strongly in the short (~ 420 nm), middle (~ 520 nm) or long (~ 565 nm) wavelength region of the spectrum. Rods only contain one type of photopigment that absorbs maximally at about 500 nm.

In cones the disk membranes are continuous with the cell membrane and hence are connected to one another. Rod disk membranes are distinct from the cell membrane and hence an internal messenger (cyclic GMP) is needed to convey information from the disks to the rest of the cell. In all receptors the disks are stacked on top of each other, perpendicular to incident light, to maximise the efficiency of photon capture.

Photoreceptors communicate with second order neurones by modulating the release of a neurotransmitter, glutamate (Yau, 1994). Transmitter release is maximal in the dark and least when the receptor is stimulated by light. Each class of photoreceptor has distinct synaptic terminals. Cones have large wide terminal endings called pedicles and rods have smaller endings called spherules. Fine processes or telodendria may also be

observed at cone terminals, extending laterally and usually contacting other receptors (Dowling, 1987). Processes from within the outer plexiform layer may invaginate cone terminals or end at flat basal junctions. These different types of junction determine whether the bipolar depolarises (invaginating type ending) or hyperpolarises (flat basal junction) in response to light.

Interconnections also exist between neighbouring receptors and it has been suggested that rod-cone gap junctions in primates may mediate rod-cone interaction (Nelson, 1977). These rod-cone gap junctions may permit transmission of rod signals in cone bipolars, (Stockman *et al.,* 1995). Recent evidence indicates that rods in the macaque monkey retina are functionally isolated from each other, but that they provide an excitatory input into cones, (Schneeweis and Schnapf, 1995).

1.2.3.2 Response to light

By placing a microelectrode inside the relatively large receptors of certain fishes, amphibians and reptiles, a transmembrane potential of approximately -40 mV is measurable in the dark. After light stimulation this potential increases to about -70 mV (Schnapf and Baylor, 1987). Figure 1.5 shows how receptor potential changes in response to light.

By drawing a receptor's outer segment into a microelectrode and measuring photocurrent rather than photo voltage, the response of a rod receptor to a single quantum may be recorded. Voltage recordings cannot measure the effects of a single photon hit in cold blooded animals because electrical gap junctions between receptors allows the voltage to be 'pooled'. In a rod the photocurrent produced by a single quantal hit is about one picoampere. The cone response is much smaller and has been estimated at about 10 femtoamperes (10×10^{-15}) (Schnapf and Baylor, 1987). This difference in response amplitude may partly explain why human cone vision is much less sensitive than rod mediated vision (Schnapf and Baylor, 1987).

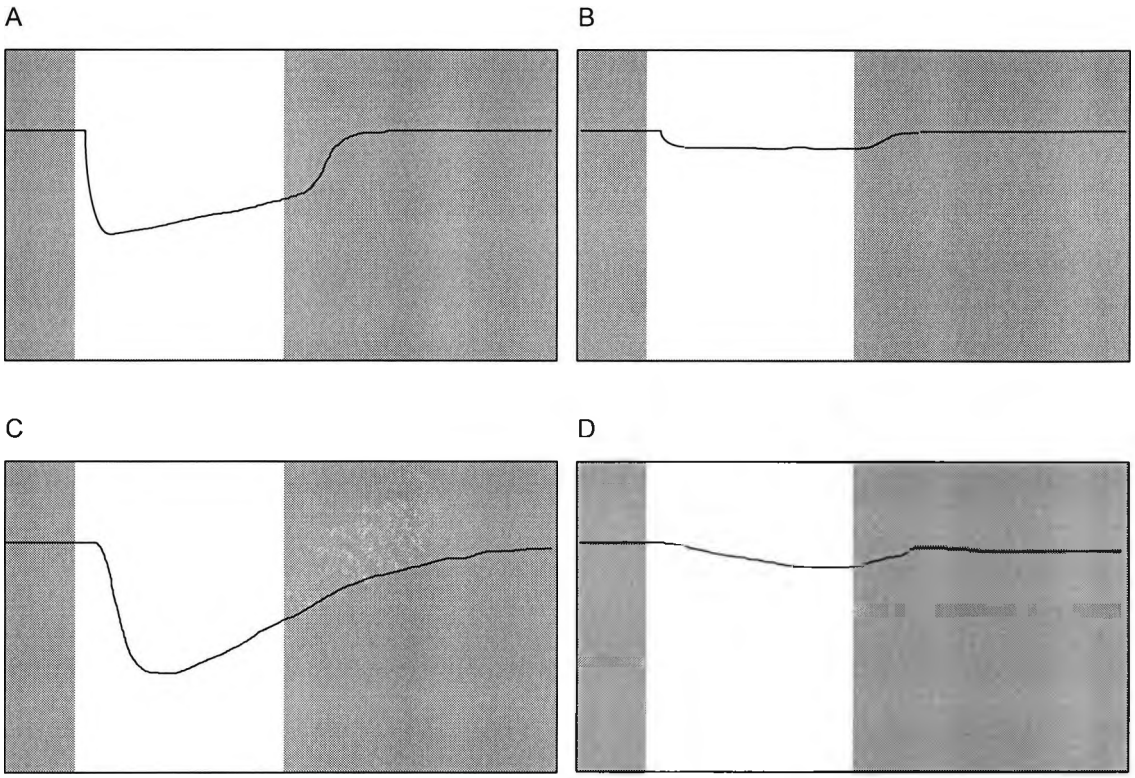

Figure 1.5 Electrical responses of a mudpuppy cone (top row) and a rod (lower row) to spot of light (100 µm in diameter) (A and C) and a centre spot with surround (B and D) (the unshaded portion of each record represents the period of light stimulation (1 second). Unlike most neurones, receptors hyperpolarize in response to illumination, and produce graded potentials rather than spike discharges. Redrawn from Werblin, (1974).

1.2.3.3 Visual pigment and the light response

Visual pigment molecules are bound to photoreceptor disk membranes. Rhodopsin accounts for more than 90% of the total protein found in disk membranes, (Palczewski, 1994). These proteins are orientated in a specific way, the amino terminal end of the molecule is always on the inside of the disk and the carboxyl terminal end is always on the outside, (Dowling, 1987).

Light sensitivity of the protein is due to the chromopore, a vitamin A aldehyde (retinal), which is bound to the visual pigment protein (opsin).

When visual pigments absorb light the first reaction is for the chromopore to isomerise from 11 *cis* retinal to all *trans* retinal (see Figure 1.6). This shape change causes conformational changes in the opsin part of the visual pigment which ultimately leads to a reduction in cGMP, a closing of sodium channels, hyperpolarization and a reduction in transmitter release rate.

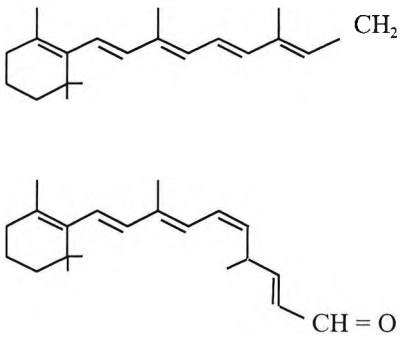

Retinal (all-*trans*)

Retinal (11-*cis*)

Figure 1.6. The structure of all-*trans* and 11-*cis* retinal. Light causes 11-*cis* retinal to isomerise to the all-*trans* form. After Dowling, (1987).

Immediately after reacting to light, rhodopsin changes through at least 6 intermediate states before separation of the chromapore from the opsin, (Dowling, 1987). The conversion of rhodopsin to metarhodopsin I takes several microseconds. Then, within a fraction of a millisecond, metarhodopsin I breaks down into metarhodopsin II. Metarhodopsin II, the catyliticaly active form of rhodopsin, mediates channel closure and is much longer lived, having a half life of several minutes at room temperature, (Dowling, 1987). Eventually, Metarhodopsin II breaks down into opsin and the all *trans* isomer of retinal. This scheme of events is summarised below:

Rhodopsin → metarhodopsin I → **metarhodopsin II** → all-*trans* retinal + opsin

All-*trans* retinal may be isomerised back to the 11-*cis* form directly, in which case it may rejoin with the opsin to form rhodopsin once more, or it may be converted into vitamin A and stored in the RPE (this takes place in the light) until it is needed again (in the dark to regenerate rhodopsin), (Dowling, 1987).

1.2.3.4 Activation of the light response

To understand how receptors respond to light it is first necessary to understand what receptors do in the dark.

When a photoreceptor is in the dark the concentration of ions on either side of the cell's membrane is very different. There is an excess of potassium ions inside the cell and an excess of sodium ions outside. This unequal distribution of ions is caused by the active extrusion of sodium ions from the cell by the 'sodium pump'. Because the concentration of potassium ions is higher inside the cell than outside, they diffuse across the cell

membrane down the concentration gradient. This movement of potassium ions results in charge being moved from the inner to the outer surface of the membrane. The transfer of charge causes the inside of the cell to become relatively negative with respect to the outside. In the dark the cell membrane is also permeable to sodium and again these ions flow down the concentration gradient, this time from outside of the cell to the inside. Charge moves into the cell as sodium ions diffuse across the membrane. This movement of charge into the cell by sodium and out of the cell by potassium results in the 'dark current' which is responsible for partial cell depolarisation, (Schnapf and Baylor, 1987). This relative depolarisation maintains a high steady release of neurotransmitter in the dark.

A small proportion of the dark current is due to the movement of calcium ions. Like sodium, calcium ions are actively pumped out of the photoreceptor and flow into the cell through 'light sensitive' channels found in the receptor outer segment, down the resulting concentration gradient (Pugh and Lamb, 1990).

When light strikes a photoreceptor the channels that allow sodium ions to diffuse into the cell close. This closure prevents sodium ions from entering the cell but does not prevent potassium ions from leaving. Cell hyperpolarization results because the outward movement of charge, carried by potassium ions, is no longer balanced by the inward movement of charge by sodium ions.

Sodium channel closure and opening is controlled by the concentration of intra-cellular cyclic guanosine monophosphate (cGMP). In the dark the concentration of cGMP is high. Molecules of cGMP bind to the sodium ion channels and cause them to open. In the light the concentration of cGMP drops and the nucleotide leaves its binding site which results in channel closure and the consequent blocking of sodium influx results in cell hyperpolarization and a decrease in transmitter release.

Metarhodopsin II, the active form of rhodopsin, binds another membrane bound protein known as Gt and causes GDP, which makes up part of the Gt protein, to be replaced with guanosine triphosphate (GTP). The resulting Gt-GTP complex falls apart and the α-sub unit which bears GTP activates cGMP phosphodiesterase (PDE). PDE activity produces a drop in cytoplasmic cGMP which leads to closure of cGMP gated channels, (Pugh and Lamb, 1990). This sequence of events is summarised in Figure 1.7.

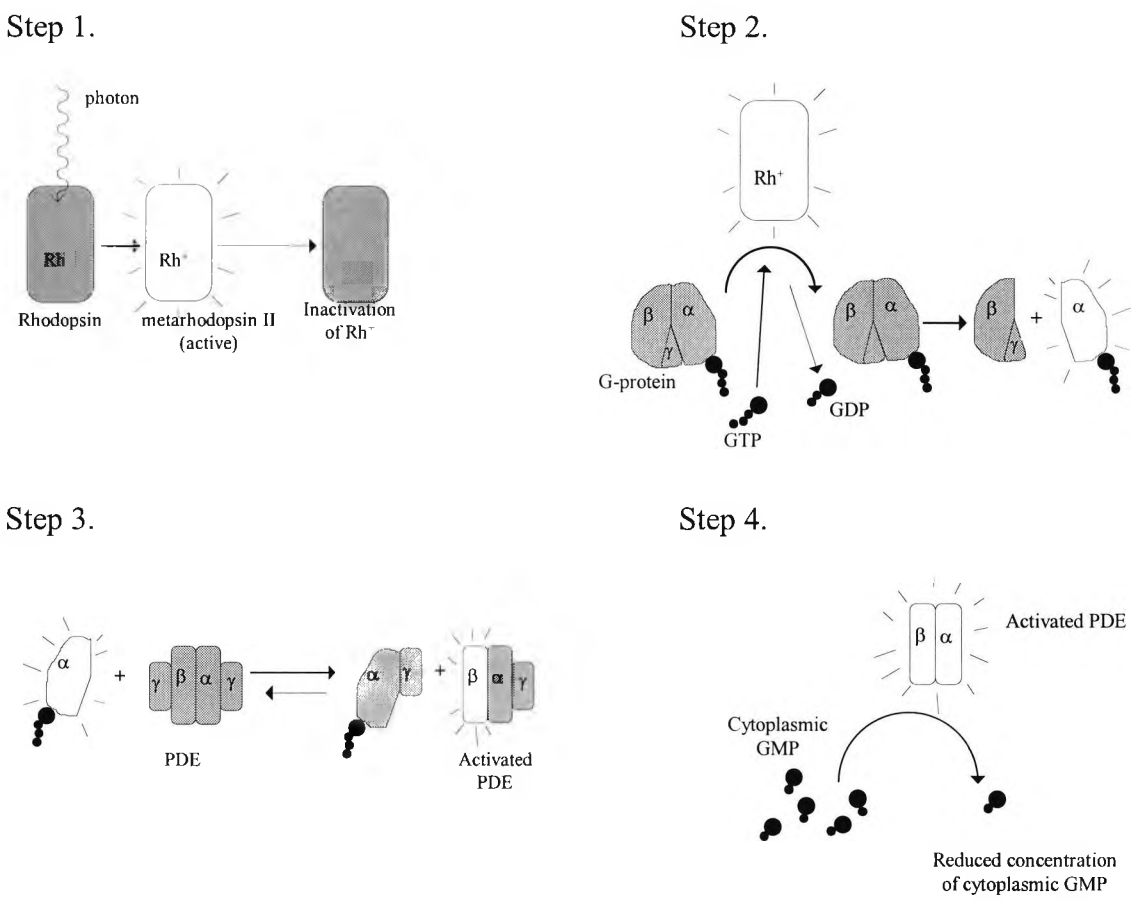

Figure 1.7 Schematic diagram showing the sequence of events that leads to closure of sodium channels and cell hyperpolarization. Step 1: light isomerises retinal and causes rhodopsin to form metarhodopsin II. Step 2: metarhodopsin II catalyses the exchange of GTP for GDP on the G-protein which produces activated Gα GTP. Step 3: activated Gα GTP binds to phosphodiesterase (PDE) and removes the inhibitory γ-sub unit. Step 4: activated PDE lowers the concentration of cytoplasmic GMP which results in channel closure.

Although there is little doubt about the events that lead to channel closure and receptor hyperpolarization, the events that lead to restoration of the unstimulated state are less well understood (Pugh and Lamb, 1990). Inactivation of the cascade may take place at several sites.

1.2.3.5 Inactivation of the light response

Metarhodopsin II, the catylitically active form of rhodopsin, decays for several minutes and binds to the G protein throughout this decay. However, quenching of the visual cascade happens much more rapidly than this. Therefore another mechanism other than metarhodopsin II decay must be involved (Palczewski, 1994).

Rhodopsin kinase and arrestin prevent activation of the G protein by metarhodopsin II. Rhodopsin kinase phosphorylates photolyzed rhodopsin and arrestin binds to phosphorylated metarhosopsin II and therefore prevents further activation of the G protein. This phosphorylation of metarhodopsin II by rhodopsin kinase followed by arrestin binding is the first step that leads to restoration of the dark state (Palczewski, 1994). Inactivation of metarhodopsin II by phosphorylation *in vivo* occurs with a time constant of 1-5 seconds at room temperature, (Pugh and Lamb, 1990).

Inactivation of the G protein is brought about by the hydrolysis of the GTP group, (Pugh and Lamb, 1990).

PDE is activated by the removal of the inhibitory γ subunit by the activated G-protein (transducin). Inactivation of PDE may result from reassociation of the γ subunit. However, the mechanism responsible for this reassociation is unknown (Pugh and Lamb, 1990).

1.2.3.6 A role for calcium feedback in adaptation

Inactivation of the light response is due to restoration of cGMP levels. Cyclic GMP is synthesised by the enzyme, guanylate cyclase. Guanylate cyclase activity is modulated by the calcium binding protein guanylyl cyclase activating protein (GCAP). Therefore cGMP levels are dependant on the concentration of intra cellular calcium ions. A reduction in calcium ions, brought about by channel closure and continuing calcium ion pump activity, increases the availability of GCAP which increases guanylyl cyclase activity leading to increased concentration of cGMP and a re-opening of the channels (Pugh and Lamb, 1990). Therefore, calcium exerts inhibitory feedback on the receptors light induced response. Such feedback may provide a site for light adaptation.

Calcium may exert inhibitory feedback at another stage of the phototransduction cascade. Photo-activated rhodopsin (metarhodopsin II) may have its activity prolonged by the calcium binding protein recoverin which prevents hydrolysis (Palczewski, 1994; Yau, 1994). In the light, intra cellular calcium concentration falls and this drop in concentration allows metarhodopsin II to be hydrolysed rapidly thereby speeding up the light response.

Therefore, calcium-mediated feedback has two effects. 1) it ensures that recovery from a brief flash of light is rapid and 2) it reduces the response of receptors to steady light. Therefore calcium is a potential candidate for receptoral adaptation (Yau, 1994).

1.2.4 Horizontal cells

Horizontal cells are located in the outer plexiform layer of the sensory retina. They form an important local circuit in the retina because their dendrites terminate in receptor ribbon terminals of cones where they surround the processes of invaginating bipolar cells (Kolb, 1994). Synaptic feedback from horizontal cells onto cones can modulate receptor sensitivity over a three fold range in the turtle retina, (Burkhardt, 1995). This local circuit also provides the bipolars with a spatially antagonistic receptive field. Horizontal cells make inhibitory synapses with receptors and electrical gap junctions with other horizontal cells (Kolb, 1994). The primary effect of these low resistance gap junctions is to increase the receptive field size of horizontal cells, (Dowling, 1987). Intriguingly, it has been suggested that this electrical coupling (and hence receptive field size) may be modulated by synaptic input from interplexiform cells and by the neuro-modulator dopamine (Dowling, 1987). Dopamine is produced by some amacrine and interplexiform cells. In isolated retinas it has been shown to decouple horizontal cell contacts over a period of 7-8 minutes (Dowling, 1987).

1.2.4.1 Morphology

Until recently it was thought that vertebrates possessed only two types of horizontal cells, a cell with a short axon that typically runs approximately 400 μm and an axonless cell (Dowling, 1987). This view has been challenged by Kolb *et al.* (1992) who identified three types of horizontal cells in humans (the HI, HII and HIII).

The HI cell is common in the human retina. It has a long axon and a dendritic tree whose size varies with retinal location. At the fovea the dendritic spread is 18 -20μm. At about 2.5 mm from the fovea the dendritic tree has enlarged to 25-30μm and approximately 7 cone pedicles are contacted. Further out in the periphery the dendrites may contact 15-20 cones and spread 75 -80μm. HI cells make dendritic contacts with all the cones within their dendritic tree. HI cells have a thick axon (2μm) that ends in a

group of distinctive 'lollipop' shaped terminals that innervate rod spherules (Kolb *et al.*, 1992).

The HII cell has a woolly appearance due to its many interwoven fine dendrites. It has a short curled axon that is thinner than HI cells (0.5μm). These axons arise from the ends of dendrites and innervate cone pedicles. HII cells tend to be specific to blue cones (Kolb *et al.*, 1992).

The HIII cell was first described by Kolb *et al.* (1992). This type of cell had previously been included in the HI category but Kolb *et al.* (1992) provided statistical evidence showing that 3 mm from the fovea, HIIIs have larger dendritic trees than HI type horizontal cells. HIII horizontal cells are usually highly asymmetric and have 1 or 2 dendrites that are distinctly longer than others. Unlike HI type cells, HIII cells appear to miss out some cones in their dendritic field area. Kolb *et al.* (1992) suggest that HIII horizontal cells selectively contact red and green cone pedicles and miss out blue ones. An additional feature of HIII horizontals is that they send thick processes from their cell bodies into the IPL where they branch in sublamina a (Kolb *et al.*, 1992).

1.2.4.2 Response to light

Like receptors, horizontal cells have a negative membrane potential (about -30 mV in the dark) and many hyperpolarise in response to light achieving a potential of about -60 mV. Figure 1.8 shows the electrical response of such a horizontal cell to centre and centre plus surround stimulation.

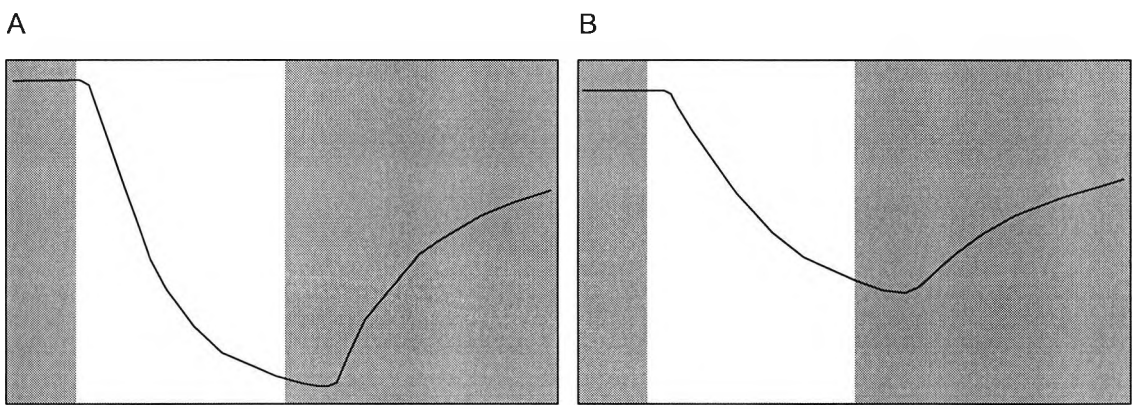

Figure 1.8 Electrical responses of a mudpuppy horizontal cell to a spot of light (100 μm in diameter) (A) and a centre spot with surround (B) (the un-shaded portion of each record represents the period of light stimulation (1 second). Like receptors horizontal cells depolarise in response to light and produce graded potentials. Redrawn from Werblin, (1974).

These hyperpolarising cells are called luminosity or L-type horizontal cells. Some animals that possess good colour vision have some horizontal cells that hyperpolarise to one wavelength of light and depolarise to others. These cells are known as chromaticity or C type horizontal cells (Dowling, 1987).

1.2.5 Bipolar cells

Bipolar cell bodies are found in the inner nuclear layer of the retina. They have concentrically organised antagonistic receptive fields and conduct information from the outer to the inner plexiform layers. There are several different types of bipolar cell. Midget bipolar cells may posses dendrites that invaginate cone pedicles (invaginating midget bipolars) or they may have dendrites that end in basal junctions on the surface of cone pedicles (flat midget bipolars) (Kolb, 1994). These different endings determine whether the cell is an ON or OFF centre bipolar. A remarkable anatomical specialisation exists in the inner plexiform layer to ensure that bipolars make appropriate connections with amacrine and ganglion cells. Bipolar cells that make invaginating contacts with cone pedicles (ON centre cells) terminate in sublamina b, the inner most layer, of the inner plexiform layer and flat midget bipolars (OFF centre cells) terminate in sublamina a (Miller, 1989).

1.2.5.1 Morphology

Cone bipolars are readily distinguished from rod bipolars by the shape of their dendrites. Cone bipolar dendrites end in clusters of terminals in the plane of the cone pedicles in the outer plexiform layer. Rod bipolars have multiple spiky dendrites that extend beyond the layer of cone pedicles to reach rod spherules, (Kolb *et al.,* 1992). Table 1.1 describes the types of bipolar cells that are found in the human retina.

Class	Sub class	Name	Dendritic contacts	Location of axon
Cone	Midget bipolar	fmB (flat midget)	small bouquet of fine terminals contact a single cone	sublamina a at the border of strata 1 & 2
		imB (invaginating)	invaginating	deep in sublamina b
	Small field diffuse	DBa	superficial basal contacts, that contact all cones within dendritic tree	sublamina a, stratum 2
		DBb	invaginating, contact all cones within dendritic tree	sublamina b, stratum 4
	Blue cone bipolars	BBa (putative)	innervate a sub-population of cones	stratum 1, sublamina a
		BBb	innervate a sub-population of cones	stratum 5
	Giant cone bipolars	GBa	innervate most overlying cones	stratum 1 and 4
		GBb		stratum 3
Rod		RBb	spiky dendrites reaching up to rod spherules	stratum 4 and 5

Table 1.1 Table showing the types of bipolar cell found in the human retina, (Kolb *et al.,* 1992).

1.2.5.2 Response to light

Bipolars, like receptors and horizontal cells, respond to light with a sustained graded potential. They have concentrically organised receptive fields which may either hyperpolarise or depolarise in response to stimulation at the centre of the receptive field. Depolarising and hyperpolarizing bipolars are also known as ON and OFF bipolars respectively (Dowling, 1987). Bipolar cells respond more rapidly to illumination falling at the centre of their receptive fields than light falling on the surround, therefore they tend to respond in a saw tooth fashion to uniform illumination, (Dowling, 1987).

The centre surround organisation of bipolar cells permits them to respond to local changes in contrast and may also contribute to sensitivity regulation. That is, the response of cells to contrast is maintained at different levels of illumination because stimulation of the surround tries to drive the cells potential back to its unstimulated level (Dowling, 1987).

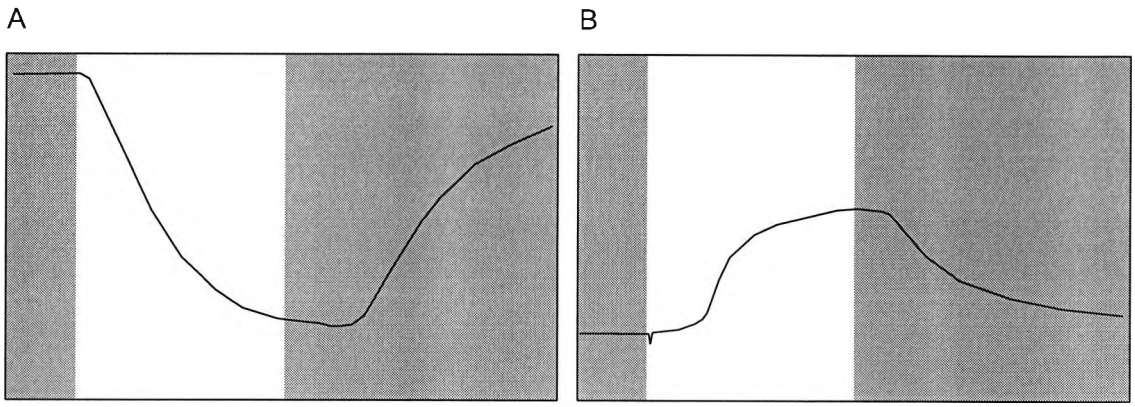

Figure 1.9 Electrical responses of a hyperpolarising mudpuppy bipolar cell to a spot of light (100 µm in diameter) (A) and with the central stimulation maintained, annular illumination (B) (the unshaded portion of each record represents the period of light stimulation (1 second). The hyperpolarising bipolar responds by hyperpolarising when the centre of its receptive field is illuminated, and a response of opposite polarity is observed when the antagonistic surround is illuminated. Redrawn from Werblin, (1974).

1.2.6 Amacrine cells

Amacrine cell bodies are found in the inner nuclear layer of the retina. They make connections with bipolar cells and ganglion cells and facilitate a lateral transfer of information. They play a particularly important role in the scotopic pathway. Rod bipolars, unlike cone bipolars, do not make direct contact with ganglion cells. Instead they contact several different types of amacrine cells, the most important of which are the AII and A17 type cells (Kolb, 1994). These amacrine cells spread out rod information before converging on ganglion cells. The dopaminergic amacrine cells and GABAergic interplexiform cells are also believed to be influential upon the rod pathway. Kolb (1994) suggests they may feed back and forth rod signals to reset the scotopic system's state of adaptation.

1.2.6.1 Morphology

Amacrine cells are a particularly diverse group of cells, with at least 26 different morphological types having been identified (Kolb *et al.,* 1992). They use a variety of neuro-transmitters such as GABA (gamma-aminobutyric acid), numerous peptides, glycine, acetylcholine, dopamine, seratonin and others (Miller, 1989). Table 1.2 shows the diversity of amacrine cells found in the human retina.

Basic category	Type	Stratification in IPL	Dendritic field
Small field amacrine	A1	S 1 and 2	60μm (9 mm)
	A2	S 2	
	A3	S 2 and 3	50-60μm (4 mm)
	A4	S 2, 3 and 4	96μm (11 mm)
	A5	S 4 and 5	75μm (10 mm)
	AII	sublamina a and b	70-80μm (periphery)
	A8	sublamina a and b	50μm (periphery?)
Medium field amacrine	A12	S5	185μm (7 mm)
	A14	S2 and S 4/5	140μm (location ?)
	tristratified	S 1/2, 2/3, 4/5 borders	170μm
	woolly	all strata	145 μm (8 mm)
	A13	all strata	290μm (mid periphery)
	spiny	S 3	400μm (mid periphery)
	spiny varicose	S3	400μm (mid periphery)
	Ach	S2 and S4	250μm (3 mm)
Large field amacrine	thorny type 1	S1	
	Thorny type 2	S3	800μm (periphery)
	Wavy	S1	500μm
	A18	S1	500μm
	Semilunar type 1	S1	700μm
	Semilunar type 2	2	600-700
	Semilunar type 3	4/5	800 8-9 mm
	Stellate wavy	3 and 4	600μm
	Stellate varicose	2 and 3	800μm
	A17 diffuse	5	1 mm (10 mm)
	Wiry	3	600μm

Table 1.2 Table showing the variety of amacrine cell types found in the human retina, after Kolb *et al.* (1992).

1.2.6.2 Response to light

Amacrine cells may respond with transient or sustained responses although most retinas contain a preponderance of transient types. Unlike receptors, horizontal cells and bipolar cells, transient amacrines always depolarise in response to light. Spikes are often observed superimposed on the transient depolarization's. They are particularly responsive to moving stimuli (Dowling, 1987) and most produce ON and OFF responses to illumination presented anywhere in their receptive fields. Generally they do not show an antagonistic centre-surround organisation. Figure 1.10 shows the electrical response of a transient amacrine cell.

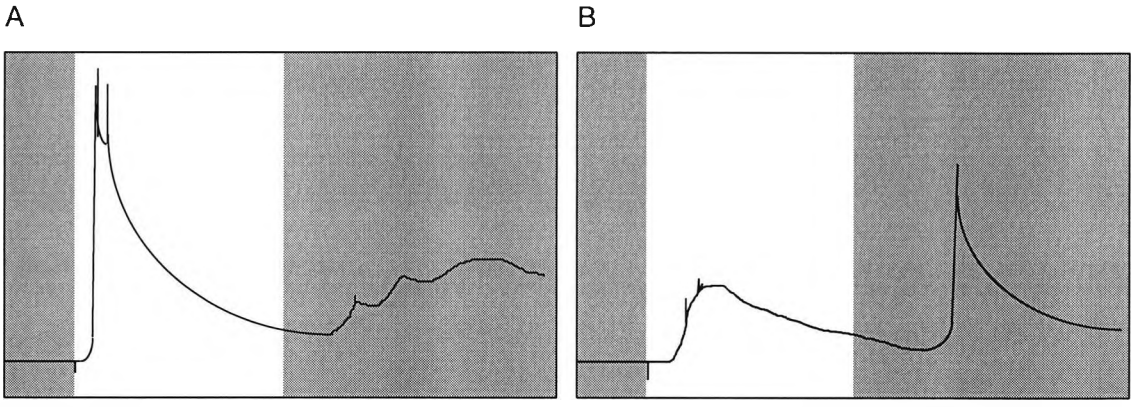

Figure 1.10 Electrical response of a transient amacrine cell to a spot of light (100 μm in diameter) (A) and a centre spot with surround (B), the unshaded portion of each record represents the period of light stimulation. Amacrine cells depolarise in response to light and generate spike discharges, (after Werblin, 1974).

1.2.7 Interplexiform cells

The cell body of the retinal interplexiform cell (IPC) lies amongst those of the amacrine cells. Unlike amacrine cells however, it sends processes to the OPL as well as the IPL. The existence of this class of cell was only established about 15 years ago. One of the reasons for its relatively late discovery is that the cell does not stain well using conventional Golgi techniques. In macaque monkeys there are two types of interplexiform cells; one which appears to be GABAergic and another that is dopaminergic, (Ryan and Hendrickson, 1987). There appear to be at least two types of interplexiform cells in the human retina (Linberg and Fisher, 1986).

In the inner plexiform layer, interplexiform cells make pre and post-synaptic connections with amacrine cells and are less frequently pre-synaptic to bipolar cells (Linberg and Fisher, 1986).

In the outer plexiform layer they are predominantly pre-synaptic to invaginating cone bipolars but they also make contact with rod and flat type bipolars and occasionally with cone pedicles (Linberg and Fisher, 1986). Interplexiform cells have also been observed contacting horizontal cells in the macaque monkey retina (Ryan and Hendrickson, 1987).

Interplexiform cells occupy an important position in the retina because their anatomical relationship with other retinal cell types may permit them to feed back information from the inner to the outer plexiform layer. Hence they may play a role in sensitivity regulation (Dowling, 1987).

1.2.8 Ganglion cells

Retinal ganglion cells are a diverse group of retinal neurones that send information from the retina to the LGN via the optic nerve. Ganglion cell dendrites ramify in the IPL and contact the processes of bipolar cells and amacrines. Their cell bodies are located in the ganglion cell layer of the retina and their axons leave the eye via the optic nerve.

In humans there are approximately 1.2 million ganglion cells (Ruskell, 1988). These cells are distributed unevenly across the retina. Ganglion cell bodies are absent at the fovea, where their presence would disrupt the image falling on the receptors, but are found in preponderance in the parafoveal region where they may lie up to 8 cells deep. Further from the macular their numbers decrease dramatically.

A plethora of terms have been used to classify ganglion cells according to their morphology and / or response to light. Ganglion cell terminology is further complicated because different terms are used to identify ganglion cells of different species.

1.2.8.1 Morphological classification of ganglion cells

Ganglion cells may be divided into two types on the basis of dendrite morphology: those which have dendrites confined to specific levels of the IPL and those whose dendrites are diffusely spread throughout the IPL, (Dowling, 1987; Blanks, 1989). These basic types may be further subdivided according to the size of their dendritic trees into small and large field types (Dowling, 1987). Polyak using the Golgi staining technique identified six morphological types of primate ganglion cell. He described five types of diffuse cell (the term diffuse, was used to indicate that the cell contacted more than one bipolar), namely; parasol, shrub, small diffuse, garland and giant cells. The midget cell has the smallest dendritic tree of all ganglion cells and contacts only one midget bipolar cell. Midget ganglion cells are only found in primate retinas.

More recent anatomical studies of primate ganglion cells classify them according to where their axons terminate in the LGN. Using this system of classification there are 2 main types of cells: P cells that project to the parvocellular layers of the LGN and M cells that project to the magnocellular layers. An additional heterogeneous group of primate ganglion cells terminate in the superior colliculus (Miller, 1989). They account

for approximately 10 % of all ganglion cells and are similar to the W cells of the cat. Kolb *et al.* (1992) identified 18 different types of ganglion cells in the human retina using golgi staining techniques. Some of these cell types are specific to primates and others are similar to those observed in cat retinas. Table 1.3 below summarises their findings of 'primate type' ganglion cells observed in the human retina.

	Cell Type		
	P1 type ganglion cell	**P2 type ganglion cell**	**M type ganglion cell**
Projection	Parvo	Parvo	Magno
Dendritic field size at fovea	5-7μm	9μm	25-30μm
Dendritic field size at 8 mm	20μm	60μm	160μm
Location of dendrites	sublamina a, stratum 1 and 2 or sublamina b, stratum 5	sublamina a, stratum 2 or sublamina b, stratum 3 and 4	sublamina a, stratum 2 or sublamina b stratum 3
Proportion of ganglion cells	P1 and P2 cells account for 80% of ganglion cells		10%
Other names (Polyak)	midget	small parasol	large parasol and giant cells
Number of contacts	1, v. occasionally 2 bipolars	one or more	many

Table 1.3 Main types of ganglion cell observed in the Human retina, based on classification by Kolb *et al.*, (1992).

1.2.8.2 Ganglion cell physiology

Hartline (1938) was the first to record the electrical response of single ganglion cells to light. He found that responses could be described as being ON (an increase in the sustained discharge rate), OFF (a decrease in the sustained discharge rate) or ON-OFF responses. Both ON and OFF type responses tended to be sustained when light fell in the cell's receptive field, whereas the ON-OFF cell responded transiently to the onset or offset of a light.

Kuffler (1953) discovered that ganglion cells not only respond to stimulation of their receptive field centres but that this response was antagonised by stimulation of the surrounding retina. Consequently he described ganglion cells as being ON-centre cells

or OFF-centre cells. If both centre and surround are stimulated simultaneously, the two regions antagonise one another and a weak response characteristic of the centre is observed. Consequently, the response of a ganglion cell to light is dependant on the spatial distribution of light falling on the retina (Dowling, 1987).

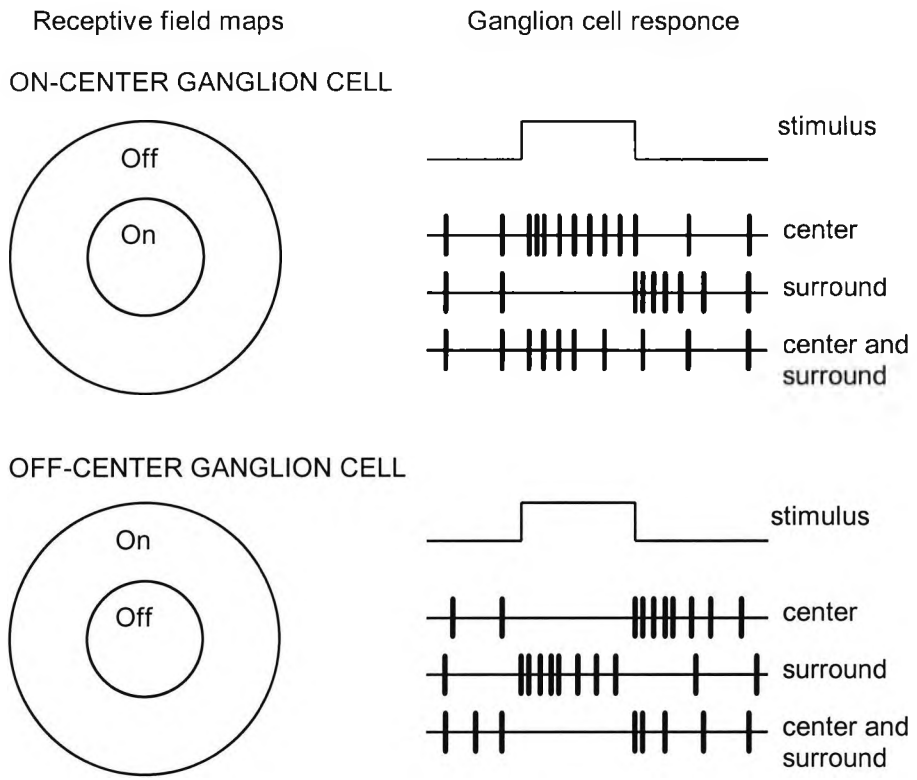

Figure 1.11 Receptive field maps (left) and idealised responses (right) for an ON-centre and OFF-centre retinal ganglion cell. After Dowling (1987).

The sensitivity profile of ganglion cell receptive fields was characterised by Rodieck (1965). He proposed that the sensitivity (gain) of the individual centre and surround mechanisms could be approximated by a Gaussian surface. The difference in gain between the large shallow Gaussian of the surround and the small peaked one of the centre mechanism characterises the response of the cell to light. This model of receptive field gain has been used by neurophysiologists to map out the properties of the centre and surround mechanisms of primate ganglion cells (Derrington and Lennie, 1984; Croner and Kaplan, 1995).

The response of the receptive field centre may be distinguished from that of its surround by exploiting the fact that field surrounds are very much larger than their centres. By stimulating the field with high spatial frequency gratings the cell's response is

determined by the centre of the receptive field only. This is because relatively high spatial frequency gratings are above the resolution limit of the surround.

Primate ganglion cell activity can be monitored by recording the extracellular excitatory potential using glass microelectrodes placed in the LGN of anaesthetised monkeys. Typically the response characteristics of the cell are probed using drifting sinusoidal gratings. A response by the cell to such stimuli is signalled by a modulation in the cell's sustained discharge rate (Kaplan and Shapley, 1986; Derrington and Lennie, 1984; Croner and Kaplan, 1995; Purpura *et al.,* 1988).

Enroth-Cugell and Robson (1966) identified another difference between ON and OFF centre cells in the cat retina. Some produced a sustained response while others responded transiently. Cells providing a sustained response were called X cells and cells that responded transiently were termed Y cells, (Miller, 1989). Subsequently, Stone and Hoffman (1972) identified an additional class of ganglion cells. These cells known as W-cells are a diverse group that account for almost 50% of all cat ganglion cells.

Another popular classification of cat ganglion cells was first proposed by Boycott and Wassle (1974). They identified two types of cells on morphological grounds, the alpha and beta cells, that appeared to match the physiological X and Y classification. Support for this method of classification was provided by recording electrophysiological responses from these cells before staining them and examining their morphology. The morphological substrate of W-cells are the gamma cells.

1.2.8.3 Response to light

A ganglion cell's response is determined predominantly by the input it receives from more distal retinal elements. Dowling (1987) proposed that the response of ganglion cells is determined by two basic types of retinal processing, one conducted in the OPL and the other in the IPL. Ganglion cells that produce a sustained response (ON and OFF centre units) receive most of their input from bipolar cells and consequently reflect processing that takes place predominantly in the OPL. Ganglion cells that respond transiently (ON-OFF units) receive most of their input from amacrines and hence, reflect processing in the IPL. Figure 1.12 shows the electrical responses of a sustained and a transient type ganglion cell.

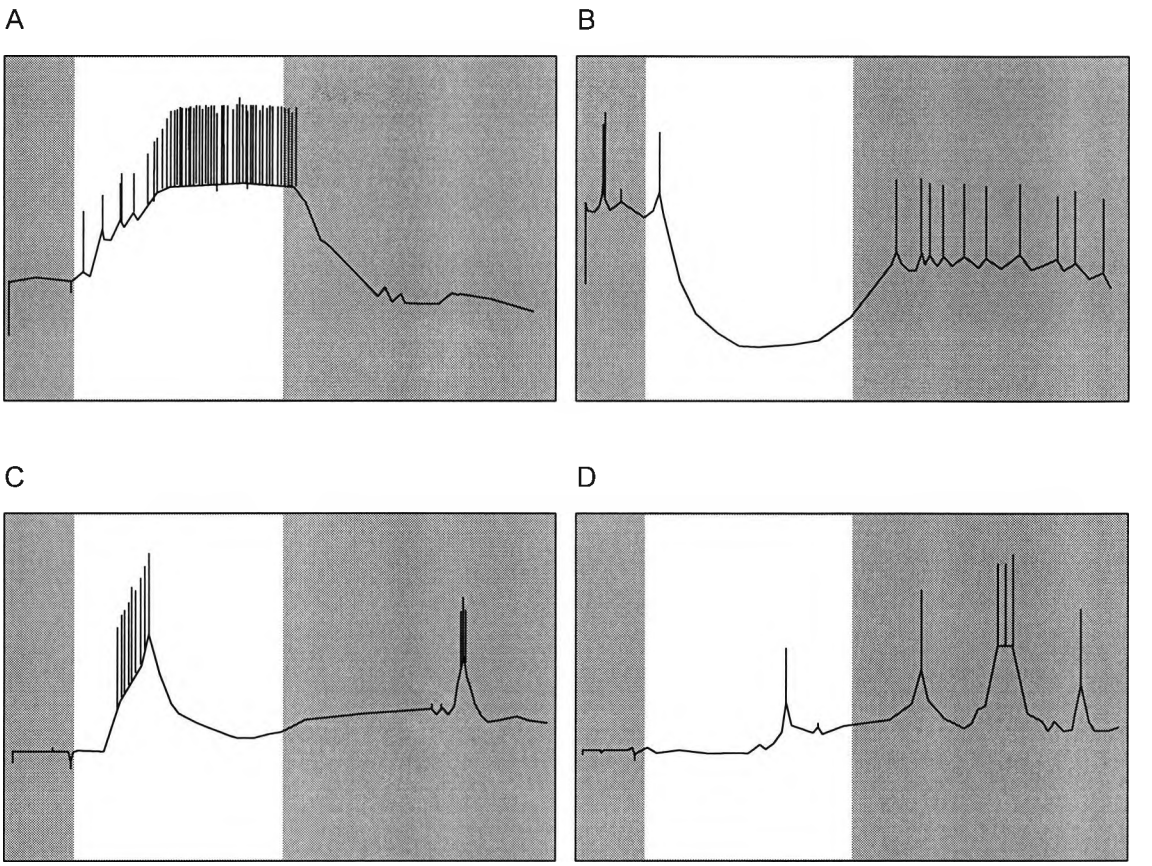

Figure 1.12 Electrical responses of mudpuppy ganglion cells. The top row shows the response of a sustained type ganglion cell to a spot (A) and spot and annulus of light (B). The lower row shows the response of a transient type ganglion cell to the same stimulation (C and D). The sustained type cell may reflect processing in the OPL and the transient type cell processing in the IPL. Redrawn from Werblin (1974).

1.2.9 Retinal pathways

Anatomical investigations show that neurones in the human retina have a similar morphology and architecture to those in the cat and monkey retina. On this basis it is reasonable to assume that the human retina contains a number of functional circuits (Kolb, 1994).

In conditions of low luminance, information flows from rod receptors to rod bipolars and on to several amacrines (the AII and A17 in particular). Synaptic input from AII amacrine cells drives OFF centre ganglion cells. ON centre ganglion cells, that mediate dim light information, receive input from AII amacrines indirectly, via cone bipolar cells. Recently, an additional rod pathway has been proposed, whereby rod signals are transmitted to cones via gap junctions, before passing through the cone bipolar cells which drive ganglion cells, (Stockman *et al.*, 1995).

In bright conditions, diffuse cone pathways are relatively direct. Information flows from cones via invaginating cone bipolars (depolarising type) to ON centre ganglion cells or via flat cone bipolar cells (hyperpolarizing type) to OFF centre ganglion cells. The ON or OFF centre characteristics of ganglion cells are predominantly determined by the type of cone to bipolar connection. Figure 1.13 summarises the main direct pathways that exist in the human retina. Although these pathways might be the main communication routes in the retina, many others are being discovered at a rapid rate (Kolb, 1994).

These retinal circuits play an important role in determining the response characteristics of ganglion cells. Two basic types of ganglion cell conduct information from the primate retina to the LGN: P cells (or colour opponent cells) that project to the parvocellular layers of the LGN and M cells (or broad-band cells) that project to the magnocellular layers (Kaplan and Shapley, 1986).

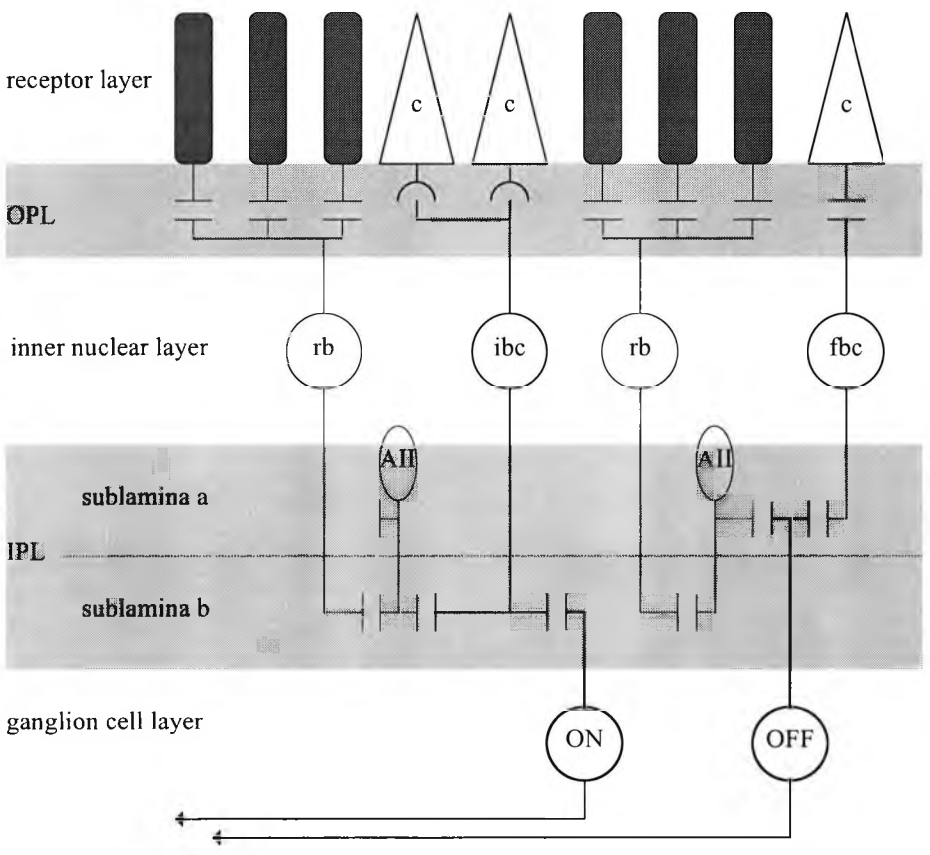

Figure 1.13 Summary of main direct pathways in the human retina. In dim conditions ON centre ganglion cells are driven by rods via rod bipolars (rb), AII amacrine cells and invaginating cone bipolar cells (ibc). In similar conditions OFF centre ganglion cells are driven by rods via rod bipolar cells and AII amacrine cells. In bright conditions cone / bipolar connections determine the response characteristics of the ganglion cell. Invaginating cone bipolars make direct contact with ON centre ganglion cells in sublamina b of the OPL the and flat bipolar cells contact OFF centre ganglion cells in sublamina a of the OPL.

1.2.9.1 Characteristics of the parvocellular pathway

About 80% of all retinal ganglion cells are of the P variety. All foveal receptors project to P type cells and they predominate in the central retina. Receptive field centres in the central 5° are small (median 0.03°, interquartile range 0.01°), (Croner and Kaplan, 1995) and at the fovea they measure 2μm, approximately the same size as a single cone (Derrington and Lennie, 1984). Centre radius increases to about 0.15° at 30° from the fovea and at all retinal locations the antagonistic surround is on average 6.7 times wider than the centre (Croner and Kaplan, 1995).

At 200 cdm^{-2}, P cells respond optimally to gratings drifted at 5 to 10 Hz (Derrington and Lennie, 1984). Over a wide range, P cell response is very nearly linear as a function of contrast and their responses rarely saturate at high contrast (Derrington and Lennie, 1984).

Schiller *et al.* (1990) trained 7 rhesus monkeys to perform a variety of visual tasks. Data about contrast sensitivity, flicker detection, stereopsis, texture and brightness perception were collected before and after small lesions were made to the parvocellular or magnocellular layers of the LGN. Their results show that P cells play an essential role in the perception of colour, texture, fine pattern and fine stereopsis. In particular contrast sensitivity at approximately 40 cdm^{-2} is primarily mediated by P type ganglion cells and not M cells despite the fact that the latter have a higher contrast gain. However, Purpura *et al.* (1988) were unable to measure a response from P cells for any stimulus when its illuminance was less than 0.43 td. Therefore it seems likely that the parvocellular pathway only mediates contrast sensitivity in relatively bright conditions.

1.2.9.2 Characteristics of the magnocellular pathway

Croner and Kaplan (1995) have shown that M cells are out numbered by P cells at all eccentricities and are not found at all within the central 3°. At any retinal eccentricity M cell receptive fields are approximately 1.6 times larger than those of P cells (Derrington and Lennie, 1984). Five degrees from the fovea their centres have a radius of 0.1° and at 20-30° this increases to 0.23°. M cell surrounds are approximately 4.8 times wider than their centres (Croner and Kaplan, 1995).

The magnocellular pathway responds optimally to relatively high temporal frequencies (20 Hz) and their response to lower temporal frequencies declines more rapidly than for the parvocellular pathway (Derrington and Lennie 1984). When stimulated optimally M cells are 5 to 10 times more sensitive to contrast than P cells. Their contrast gain (slope of the response vs. contrast graph) is greater than that of P cells but the response is only linear over a limited range of low contrasts (Kaplan and Shapley, 1986). M cell responses tend to saturate at high contrasts (Derrington and Lennie, 1984).

Behavioural studies have shown that the magnocellular pathway mediates the perception of flicker and motion. Merigan and Maunsell (1990) showed that contrast sensitivity to a Gaussian blob flickering a 10 Hz was greatly reduced by destruction of the magnocellular pathway but that sensitivity to a stationary 2 c.p.d. grating and to a 1 c.p.d. grating modulated at 10 Hz (counterphase) was unaffected. However, M cell lesions have virtually no effect on the contrast sensitivity function (Schiller *et al.*, 1990).

From a functional point of view, the primary role of the M cell pathway is to draw attention to objects moving in the peripheral retina. The high temporal frequency response and high contrast gain of the system are particularly important in enabling it to respond to movement. Objects moving in the periphery of the visual field are likely to be small relative to the size of peripheral receptive fields. Their relatively small spatial extent means that they are a relatively weak stimulus to the cell. However, the high contrast gain of M cells partly overcomes this problem because it permits them to respond to relatively small changes in flux, such as that caused by a small object moving into their receptive field.

1.2.10 Lateral geniculate nucleus

Most ganglion cells terminate in the lateral geniculate nucleus (LGN). The LGN is a relatively simple structure made up of 6 distinct layers. Fibres that cross over at the chiasma terminate in layers 1, 4 and 6, and uncrossed fibres terminate in layers 2, 3 and 5. Layers 1 and 2 contain magno cells and layers 3-6 are made up of parvo cells. The fibres of the LGN project to the primary visual cortex via the optic radiations.

1.2.11 Primary visual cortex

Fibres from the LGN terminate in the occipital lobes of the brain. This area is known as area 17, the striate cortex, the primary visual cortex or more simply V1. V1 is composed of 6 layers which are numbered from the cortical surface inward.

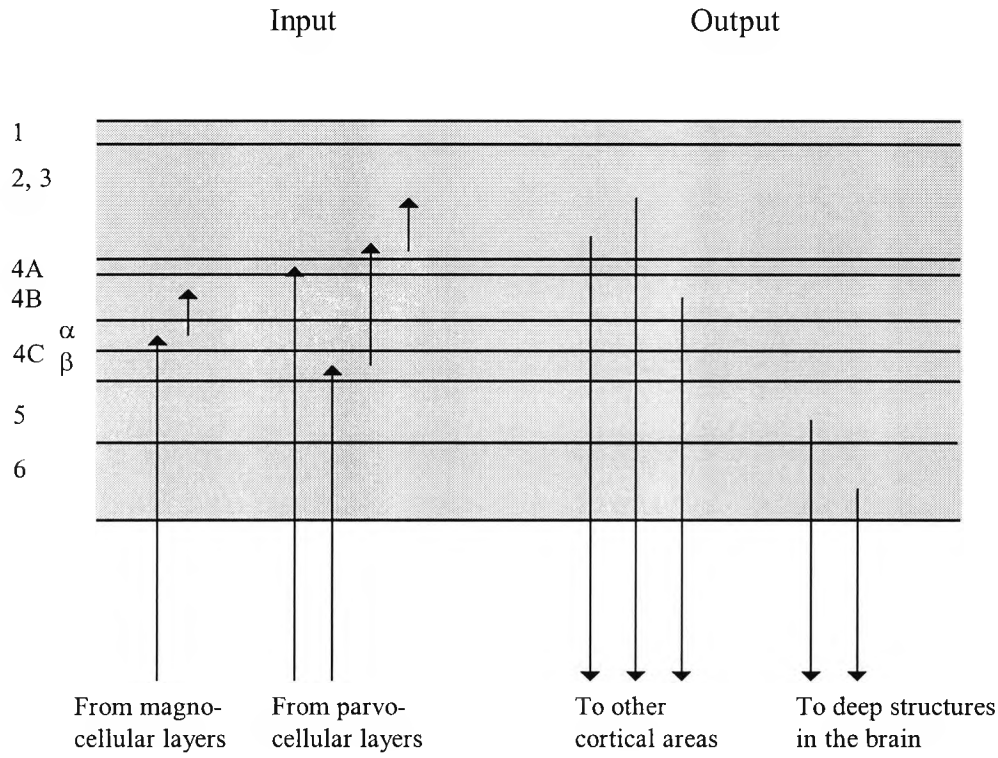

Figure 1.14 Cross section through V1 going from the outer surface layer 1 to deeper layers. The arrows on the left hand side show the main connections made by cells from the magno and parvocellular cells of the LGN and the arrows on the right hand side show the projections from V1 to other regions of the brain. Redrawn from Hubel (1988).

Cells from the magno and parvocellular layers of the LGN terminate in specific subdivisions of layer 4. V1, like other areas of the cortex, has a highly organized structure, information about various visual attributes is 'pigeon holed' in specific areas. The visual field is mapped onto the cortical surface i.e. the topographical relationship between different areas of the visual field is maintained on the cortical surface. Information from each eye initially remains distinct in a series of ocular dominance columns, this is particularly so in layer 4. Cells that respond to lines at a specific orientation are located in columns (orientation columns) perpendicular to the cortical surface. V1 also contains columns of cells in the middle of ocular dominance columns known as 'blobs'. Cells in 'blobs' have been shown to be wavelength sensitive.

Orientation sensitive cells that are insensitive to wavelength are found between 'blobs' in areas known as 'interblobs'. The organization of area V1 is shown in Figure 1.15.

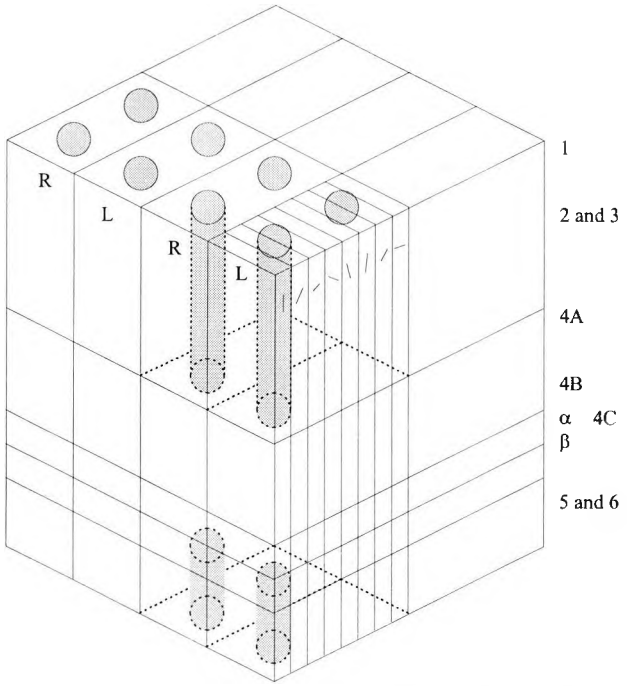

Figure 1.15 A model of the organization of area V1 showing: ocular dominance columns, orientation columns and 'blobs' (in grey). After Livingstone and Hubel, 1984, redrawn from Zeki 1993.

V1 contains a number of specific cell types:

Concentric cells, predominate in layer 4 of V1. They are driven monocularly and have concentrically organised receptive fields with distinct 'on' and 'off' regions, similar to ganglion cells.

Simple cells, have antagonsitically organised receptive fields but the antagonistic regions are arranged as parallel bands. Consequently, they respond maximally to lines of a specific orientation. These cells are also driven monocularly.

Complex cells, do not have an antagonistically organised receptive field, instead they respond to bars presented anywhere in their receptive field. They are particularly responsive to moving stimuli and some are directionally selective.

End stopped cells, respond best to lines of a specific length. Therefore they are particularly sensitive to breaks in lines and corners.

Colour coded cells, may have a similar organisation to the simple, complex or end stopped cells but they respond according to wavelength.

1.2.12 Extra striate cortex

Information contained in the visual scene is not only mapped onto V1 but onto other extra-striate areas of the cortex, for example V2, V3, V4, V5 and V6. Each area has a characteristic architecture, specific set of inputs and outputs and is thought to be functionally distinct.

V2 is similar to V1 in that all aspects of vision are represented e.g. motion, orientation, wavelength and depth. Like V1, V2 sends processes to other areas.

V3 contains cells that are sensitive to lines of a specific orientation but insensitive to colour. This area may be responsible for processing information about form.

The cells in V4 are predominantly wavelength sensitive but it also contains some that are sensitive to stimulus orientation.

V5, sometimes known as MT (when referring to owl monkeys), contains cells particularly sensitive to motion but like area V3 the cells are insensitive to wavelength.

V6 has a particularly unconventional retinal map. The cells in V6 respond to stimuli presented at a particular point in space, independent of fixation. Therefore, it may process information about the representation of space, (Zeki, 1993).

Taken together there are at least 4 main pathways in the visual cortex: a motion pathway (M-cells, layers 1 & 2 of the LGN, layer 4B of V1 and V5); a dynamic form pathway (M-cells, layers 1 and 2 of the LGN, layer 4B of V1 and V3); a colour pathway (P-cells, LGN layers 3-6, layers 2 and 3 of V1, 'blobs', V4 and a form pathway (P-cells, LGN layers 3-6, layers 2 and 3 of V1, 'interblobs', V4). In each case information may flow directly from V1 to the extra striate regions or it may be relayed to these centres via V2. As adaptation is mainly a function of the retina, further information about extra-striate visual areas is not included here. For a review of the anatomy and function of the visual cortex see Zeki (1993).

1.3 Mechanisms of sensitivity regulation

Sensitivity may be modified at any site in the visual system but investigations such as those conducted by Whittle and Challands (1969) have shown that sensitivity is primarily regulated within the eye itself. They showed that the adaptive state of one eye has little effect on the sensitivity of the other eye.

Identifying the site of sensitivity control within the human retina is not straightforward. The main problem is that there is little electrophysiological information on how stimulus response functions for primate interneurones vary with background illumination. There are considerable species differences in how the burden of the task of adaptation is distributed amongst the retinal neurones, which limits the value of information gained from lower animals (Green, 1986; Dowling, 1987). The gaps in our understanding have been highlighted by relatively recent anatomical and pharmacological discoveries. A whole class of retinal interneurones, the retinal interplexiform cell, have only recently been identified in humans (Linberg and Fisher, 1986). Although these cells are ideally located in the retina to regulate sensitivity, we can only speculate about their role in modifying sensitivity, (Walraven *et al.,* 1990). Even more recently, dopamine has been implicated in regulating sensitivity. Dopamine is released in the light-adapted retina of the rabbit, which inhibits the response of the AII amacrine cell and therefore inhibits the transfer of rod signals to ganglion cells. Therefore it may play an important role in the switch from scotopic to photopic vision. Although it acts relatively slowly and diffusely in the retina, evidence suggests that it may produce 'flip flop' like switch effects within the retina, possibly turning on and off whole classes of interneurones (Witkovsky and Dearry, 1992). Our general state of knowledge about sensitivity regulation is perhaps best described by Shapley *et al.* (1993) as being 'confusing and contradictory'.

Although there are gaps in our understanding of adaptation, it seems likely that a multiple hierarchical system of sensitivity regulation exists. This section describes several mechanisms that may contribute to sensitivity regulation.

1.3.1 Pupil

The most obvious mechanism for altering the visual system's sensitivity is the iris. However, in man the pupil can only alter its area approximately 10 fold and therefore can only account for adaptation over a 1 log unit range. Despite the limited effect of the pupil it may be a useful adaptational mechanism in some circumstances. In particular it can respond relatively rapidly, peak constriction occurring within about 600 msec, (Sharp and Nordby, 1990). Barlow (1972) suggested that the relatively rapid pupil response may circumvent some of the problems caused by the slow regeneration of photopigment.

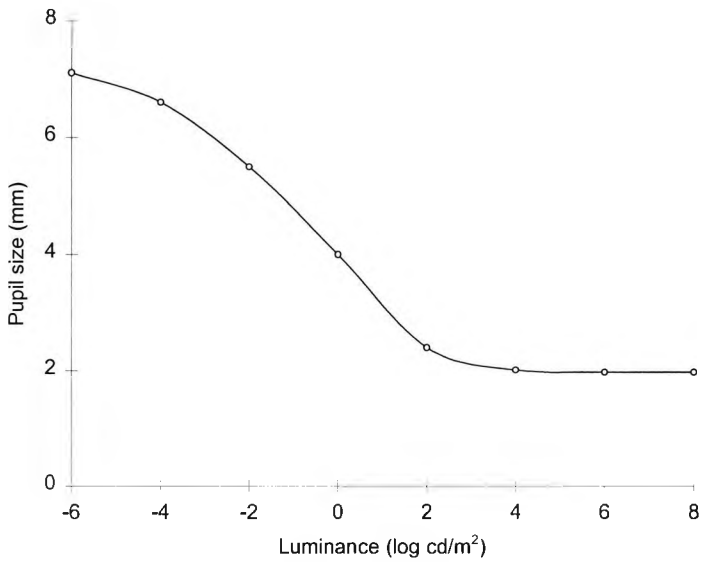

Figure 1.16 Pupil size as a function of luminance. After Walraven *et al.* (1990).

1.3.2 Noise

Although noise is not an adaptation mechanism, it does play a role in determining the sensitivity of the visual system because any psychophysical threshold is dependant upon a signal to noise ratio. The visual system is subject to two very different sources of noise, the quantal fluctuations of light itself and noise inherent to cells throughout the visual system.

1.3.2.1 Quantal noise

The number of quanta in a background field is not constant, but follows a Poisson distribution with a mean of n and a standard deviation of $n^{0.5}$, (Makous, 1990). Therefore at low light levels the visual system must extract information from a 'noisy' stimulus. The visual system will only be able to detect the presence of an object when the signal generated by that object exceeds that generated by the fluctuations in the number of quanta making up the background. The ability of the retina to integrate over space and time is likely to minimise the effect of quantal fluctuations in the background. Consequently, quantal fluctuations are most likely to impose a limit on sensitivity when small brief test stimuli are used. Psychophysical evidence supporting the idea that threshold is partly dependant upon noise is provided by increment threshold functions that obey the de Vries-Rose law. Increment threshold functions having a slope of 0.5 are observed for small, short flashes, detected by the rod system (Barlow, 1957). As background intensity increases, photon noise becomes relatively less important except for very small stimuli (Walraven *et al.,* 1990).

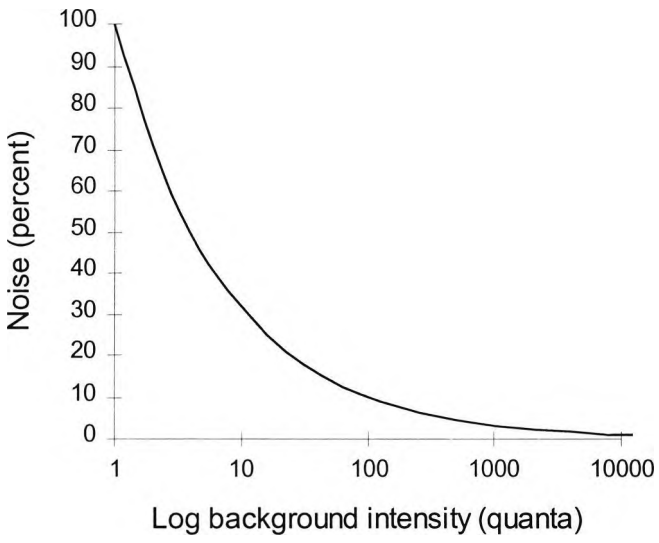

Figure 1.17 Quantal noise expressed as a percentage of background intensity. At low background intensities quantal noise is relatively great but at higher background intensities quantal noise, as a percentage of total background intensity, reduces.

1.3.2.2 Internal noise

Noise may also originate within the visual system itself. Schnapf and Baylor (1987) reported that spontaneous quantal-like events occur in monkey rods approximately once

every 150 seconds even when the retina is in absolute darkness. These events and other sources of neural noise contribute to the quantity known as 'dark light'. Measurement of 'dark light' in the rods of the toad as a function of temperature suggest that much of this noise is due to the thermal decomposition of visual pigment (Baylor *et al.,* 1980). Cone 'dark light' has received relatively little attention but has been estimated to be of the order of 10 to 100 isomerizations per cone per second, (Walraven *et al.,* 1990).

Noise may also originate proximal to the receptors. When dark adaptation functions are obtained after light adaptation of both eyes, the resulting function is lower than that obtained by light adapting the test eye only (Makous, 1990). It has been proposed that this lowering of the dark adaptation function is due to a reduction in the noise input of the non-test eye to the visual system, (Makous, 1990).

1.3.3 Duplicity

Another way in which the visual system copes with a large operating range is by having two types of receptors, the rods and cones. In humans, rods operate over the lowest 3 log units of retinal illuminance, from approximately -3 log scotopic trolands to 0.1 log td at which point the cones take over (Shapley and Enroth-Cugell, 1984). The precise rod-cone break point is dependant on retinal location and test / background parameters. Although having two receptor types reduces the range over which each type must operate, each must still adapt over a considerable range. In the photopic (cone) system, most adaptation is thought to occur within the receptors themselves. This is in contrast to the scotopic (rod) system, for although rods do alter their gain depending on background illumination, much of the scotopic system's adaptational machinery is post-receptoral, (Lamb, 1990).

1.3.4 Pigment density

Early workers postulated that pigment depletion accounted for the eye's loss of sensitivity in the light (Hecht, 1924). Threshold was thought to be directly related to the concentration of bleached photopigment, e.g. bleaching half the pigment would result in a 2 fold increase in threshold. Only when it became possible to measure pigment density in the living human eye was it proven that no such relationship existed (Campbell and Rushton, 1955). The relative unimportance of pigment density to scotopic threshold is

most easily shown in a rod monochromat. Although rhodopsin concentration does decline monotonically with increasing ambient illumination, it only does so above 3 log scot td when the rod threshold vs. intensitiy (t.v.i.) function is already 'saturating' (Sharpe, 1990).

In the photopic system, photopigment bleaching plays a more significant role in determining sensitivity than does rhodopsin concentration in the scotopic system. This can be seen from Figure 1.18 below. As the high end of the normal photopic range is approached, a significant amount of pigment is bleached. For example, at 4.5 log td about 50% of the pigment is bleached and therefore a two fold reduction in sensitivity may be expected. On the same basis, a 2 log unit reduction in sensitivity may be expected at 6.5 log td.

Boynton and Whitten (1970) showed that a simple model of response compression and photopigment depletion could describe adaptation in macaque cones.

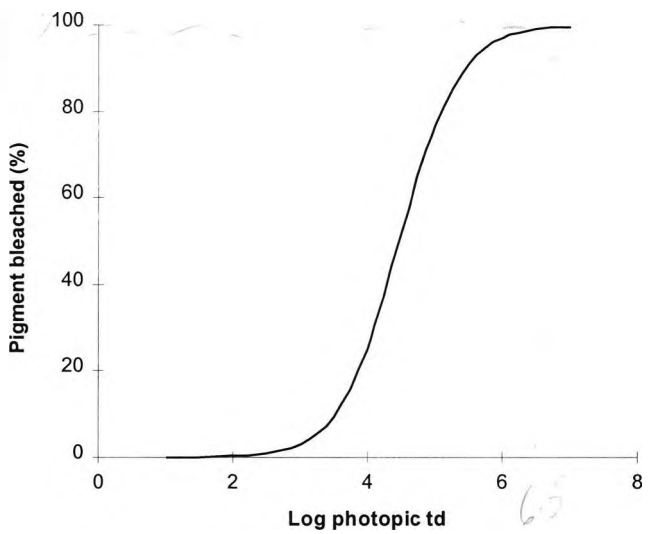

Figure 1.18 Graph showing how the percentage of bleached pigment varies with intensity in cones. After Hollins and Alpern (1973).

1.3.5 Receptoral adaptation

All receptors have a finite number of channels in their outer segments which can close in response to light. This limitation on channel numbers means that all receptors are liable to suffer the ill effects of response compression i.e. saturation. Some types of receptors are able to avoid or stave off saturation by implementing an active adaptational mechanism.

1.3.5.1 Rods

Several species have rods that are capable of avoiding saturation by speeding up their response to light e.g. the rods of the turtle (Baylor and Hodgkin, 1974), the toad (Fain 1976), and those of the cat (Tamura *et al.,* 1989). Other species such as the mudpuppy (Werblin, 1974) and macaque (Baylor *et al.,* 1984) appear to have rods that do not adapt. Sharpe (1990) compared electrical data from macaque rods (Baylor *et al.,* 1984) with the threshold vs. intensity (t.v.i.) function obtained from a rod monochromat. He showed that although primate rods begin to desensitise at 1 log td (based on a calculation converting macaque 2 log photo-isomerisations sec^{-1} rod^{-1} to human equivalent retinal illumination), the human rod t.v.i. function begins to rise at about -2.5 log td. It appears that primate rods (and presumably human ones as well) suffer response compression and saturate without adapting. Consequently, the site of adaptation in the scotopic system must be proximal to the photoreceptors. The dashed line in Figure 1.19 describes the results of physiological experiments with single macaque rods. The vertical axis gives the amount of light (ΔL) in the test flash needed to elicit a criterion response, relative to the amount needed in the absence of the background (ΔL_o). The solid line shows a psychophysically measured increment threshold function obtained from a rod monochromat.

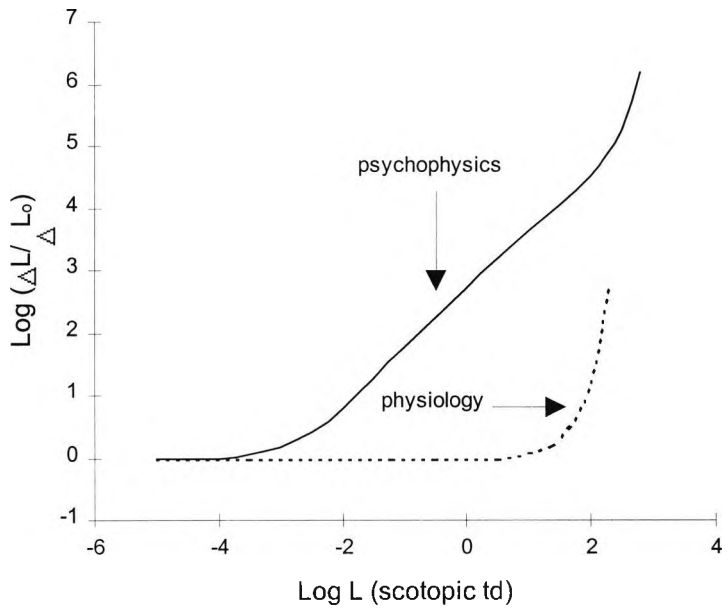

Figure 1.19 Psychophysically measured increment threshold function obtained from a rod monochromat compared to physiological data obtained from a single rod. The physiological response is described by a function based on response compression. Redrawn from Walraven *et al.* (1990) based on the data of Baylor *et al.* (1984).

1.3.5.2 Cones

Electrical recordings from the cones of the mudpuppy (Werblin, 1974; Norman and Werblin, 1974) the ground squirrel (Dawis and Purple, 1982) and the turtle (Baylor and Hodgkin, 1974) indicate that they adapt.

Evidence for primate cone adaptation is equivocal. Boynton and Whitten (1970) obtained electrical recordings from macaque cones and showed that the data could be explained by response compression and photopigment depletion only, i.e. there was no evidence for an active adaptational process. However, similar investigations have shown that an additional adaptational process is required to explain primate cone response to light (Valeton and van Norren, 1983). Recently Shapley *et al.* (1993) used data obtained by others (Sneyd and Tranchina, 1989; Purpura *et al.,* 1990) to compare the effect of mean illumination on cone and ganglion cell dynamics. The temporal frequency response functions for P type ganglion cells and M type cells (at high levels of illumination) are qualitatively similar to those obtained from cone photoreceptors. This observation indicates that photoreceptor adaptation is the predominant determinant of ganglion cell sensitivity in photopic conditions (see Figure 1.20).

Cone photoreceptors may have access to several types of gain control mechanism. It has been proposed that one type of photoreceptor adaptation depends upon a calcium based feed-back mechanism (Shapley *et al.,* 1993; Fain and Cornwall, 1993; for a review of how this mechanism works see Yau, 1994).

Another mechanism capable of regulating sensitivity is synaptic gain, from cones to horizontal and bipolar cells. One characteristic of cone synapses is that they continuously release glutamate at a relatively high rate in the dark. This high rate of release is facilitated by ribbon synapses and is calcium dependant. Synaptic gain from cones to bipolar cells is high at potentials close to the cone's dark membrane potential and lower at more hyperpolarized potentials. Therefore, direct light stimulation that hyperpolarises the cone, reduces the synaptic gain (for a review of synaptic gain see Verweij, 1996). When illumination is diffuse (a good stimulus to horizontal cells) synaptic gain is further modified by horizontal cell feedback, (Verweij, 1996).

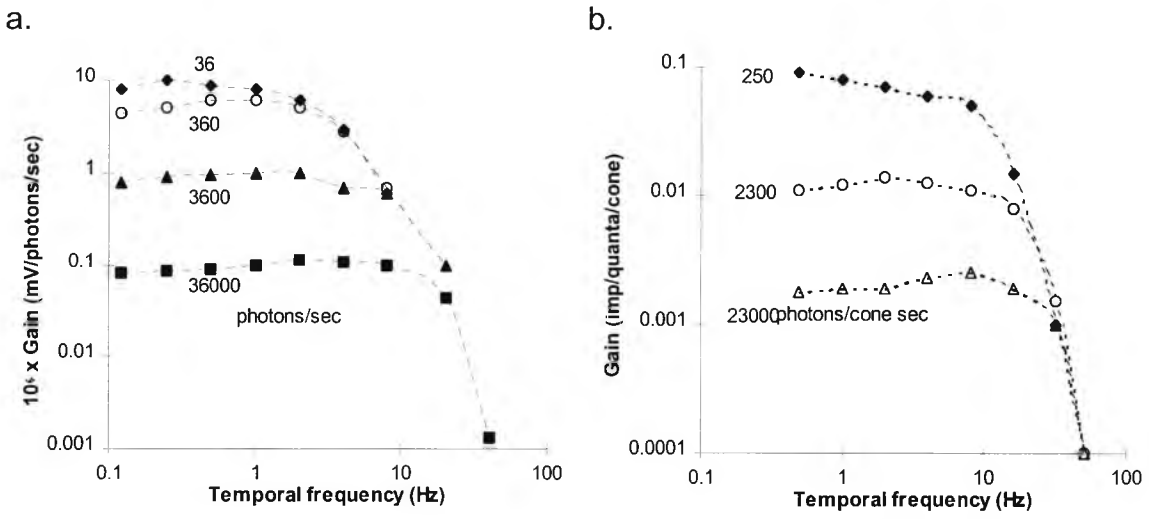

Figure 1.20 Temporal frequency responses of a turtle cone (a) and a P type retinal ganglion cell (b) at different mean illuminations The similarity of the plots indicates that receptor adaptation plays a large role in determining ganglion cell sensitivity. Redrawn from Shapley *et al.* (1993) based on data from Sneyd and Tranchina (1989) and Purpura *et al.* (1990).

Although cone receptors may be capable of adapting, measurements of membrane current in macaque cones indicates that desensitisation of the photopic system occurs at backgrounds 200 times dimmer than required to reduce the photon response of cones themselves (Baylor, Nunn and Schanpf unpublished cited in Walraven *et al.,* 1990). Therefore it seems likely that both receptoral and additional post receptoral mechanisms are required to explain sensitivity regulation in the photopic system (Walraven *et al.,* 1990).

1.3.6 Post-receptoral adaptation

Post receptoral mechanisms are particularly important to the scotopic system since rods themselves seem unable to adapt. However, as we have seen, they may also play a role in determining photopic sensitivity. The existence of a post-receptoral adaptation mechanism in the scotopic system has been clearly demonstrated by Rushton (1965). He proposed that adaptation in the human scotopic system must take place at a site beyond the receptors in an 'adaptation pool'. Two pieces of evidence supported this assertion. Firstly, a background so dim that only approximately 1 in 10 rods received a photon hit in a second, was sufficient to raise threshold 0.5 log units above absolute threshold. Secondly, threshold to a square wave grating presented in phase or out of phase with a

background grating was found to be the same[1]. The physiological basis for Rushton's 'adaptation pool' is likely to be the ganglion cell receptive field.

The site of post-receptoral adaptation has been studied electrophysiologically by Green *et al.* (1975). They measured the isolated receptor potential, the s-potential (from horizontal cells), b-wave (generated by Müller cells) and ganglion cell thresholds in the all rod retina of the skate. They adapted the retina to different intensity backgrounds and used a test flash to probe sensitivity. Their data show that low levels of illumination have no effect on receptor or horizontal cell response, but a significant effect on the b-wave and ganglion cell thresholds. Sensitivity to dim backgrounds is apparently modulated by a post receptoral 'network' mechanism. At higher levels of illumination Green *et al.* (1975) showed that the sensitivity of all the retinal neurones studied was altered by background intensity.

Green *et al.* (1975) also showed that the early phase of dark adaptation is dependant on a post-receptoral 'neural' mechanism. Following exposure to a dim light that bleached an insignificant amount of photopigment, the isolated receptor potential recovered rapidly but threshold for the b-wave and ganglion cell discharge rate recovered relatively slowly (see Figure 1.21). It is unfortunate that there is no information concerning the site of the 'neural' component of dark adaptation in any species other than the skate, (Dowling, 1987).

Recently Frishman and Seiving (1995) compared the effects of background illumination on the STR (cornea negative scotopic threshold response, an inner retinal signal) and PII (cornea positive, b-wave) components of the monkey ERG. They showed that the STR was reduced by backgrounds 100 times weaker than those necessary to reduce the PII component. This result indicates the existence of at least 2 post-receptoral adaptation sites because the STR is generated more proximally in the retina than the PII component. More recently, Frishman *et al.* (1996) examined the effect of background illumination on the STR and PII components of the human ERG and psychophysical

[1] Rushtons findings were disputed by Barlow and Andrews (1967). They conducted a similar grating investigation but found that threshold was always higher when the test grating was in phase with the background.

threshold. Psychophysical threshold was raised by backgrounds 5 times less intense than those necessary to reduce the STR component and 50 times less intense than those necessary to reduce the PII component. This finding suggests that dim backgrounds that first reduce retinal sensitivity have their effect at a site more proximal than the bipolar cells possibly involving amacrine and ganglion cells. It also suggests that very weak backgrounds have a desensitizing effect that originates at a site more proximal than the STR, Frishman *et al.* (1996).

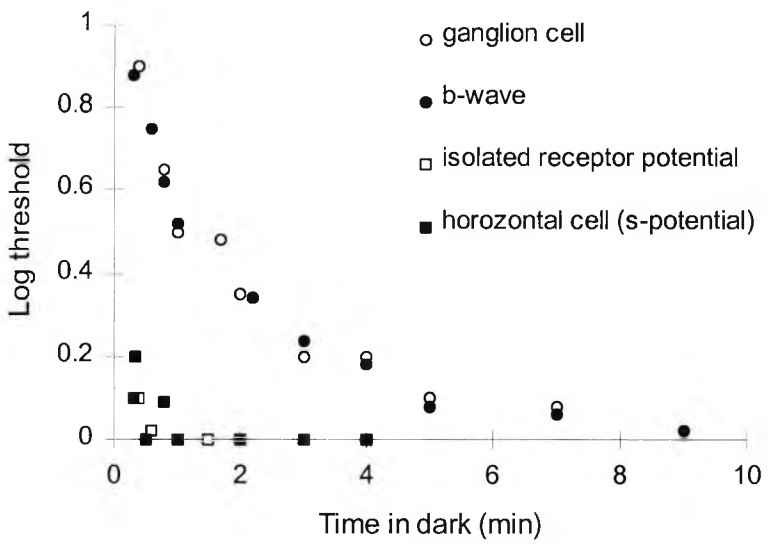

Figure 1.21 Dark adaptation of receptor potential, b-wave, ganglion cell and the horizontal cell (s-potential).Threshold data are plotted relative to the dark adapted threshold for each type of response. The receptor potential and s-potential follow the same time course and full sensitivity has returned after 1 minute. Recovery of sensitivity for the ganglion cell and b-wave is slower and takes about 8 minutes to fully dark adapt. Redrawn from Green *et al.* (1975).

1.3.7 Retinal gain control

Retinal gain control mechanisms not only regulate sensitivity to light, they also mediate the perception of contrast. Consider a visual pathway whose receptive field is 'looking' at a background. Over a large range of intensities, the gain (amplification) of that pathway is approximately proportional to the reciprocal of the luminance of the background (Barlow and Levick, 1969). That is, the gain of the pathway alters according to:

$$\text{gain} = K / Lb$$

Where Lb is the luminance of the background and K is a proportionality constant. When an eye movement allows the receptive field to 'see' an object (Lo) there is an

instantaneous change in the amount of light striking the receptive field. This change in intensity is the stimulus (Lo - Lb) that generates a neural signal. Therefore the presence of a border (contrast) is signalled by:

$$\text{signal} = K \times (Lo - Lb) / Lb$$

Consequently, the visual system's responsiveness to contrast is primarily a result of the gain control that produces light adaptation (Shapley and Enroth-Cugell, 1984; Shapley, 1991; Shapley *et al.*; 1993). It is of interest to note that the gain in a pathway alters according to light flux, i.e. illumination per unit area, (Croner and Kaplan, 1995). Therefore, pathways that posses large receptive fields 'collect' more quanta than smaller ones at any particular background luminance. Hence, the gain of a pathway with a relatively large receptive field is lower than one with a smaller field i.e. pathways that have large receptive fields are more light-adapted than smaller ones.

Previous paragraphs have indicated that sensitivity is likely to be controlled at numerous sites in the retina and that this sensitivity control forms the basis of contrast perception. One way of determining the combined effects of all retinal adaptational mechanisms is to examine the electrophysiological properties of ganglion cells, the output cells of the eye.

Ganglion cell discharge rate is primarily determined by changes in contrast, but over a considerable range, it is also influenced by steady ambient illumination. The response of primate M and P-type ganglion cells to different contrasts at various background intensities was determined by Purpura *et al.* (1988). Some of their results are shown in Figure 1.22.

The results of Purpura *et al.* (1988) have several important features. Ganglion cell discharge rate is largely dependant upon contrast e.g. when there was no contrast the discharge rate of both P and M cells (impulses per second) was at a minimum. Up to a point, the responsiveness of P and M cells to contrast improves as illumination increases i.e. contrast gain (the slope of the response vs. contrast graph) increases with increasing illumination. However, when retinal illuminance exceeds 2.5 log td for M cells and 3 log td for P cells, discharge rate becomes relatively independent of illumination (Purpura *et al.,* 1988). This can be seen more clearly in Figure 1.23 which shows how contrast gain varies with retinal illumination.

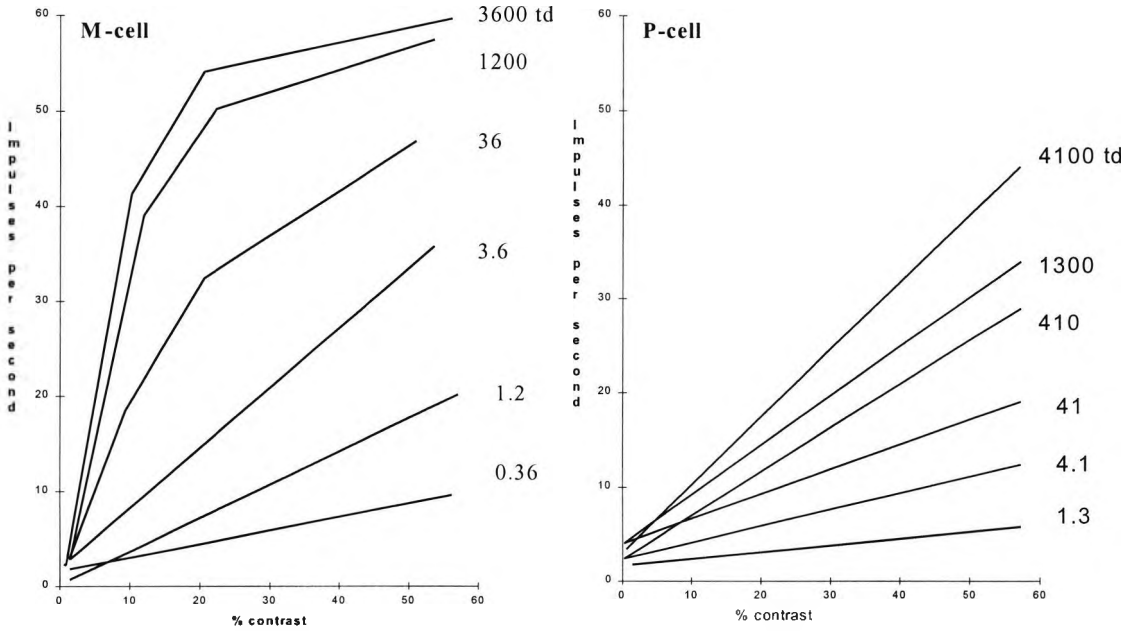

Figure 1.22 Graph showing how P and M cell responses vary with contrast and illumination. Note: in the absence of contrast, ganglion cell response is at a minimum and cell response increases in proportion to stimulus contrast. The response is relatively independent of illumination except at low light levels (after Purpura *et al.,* 1988).

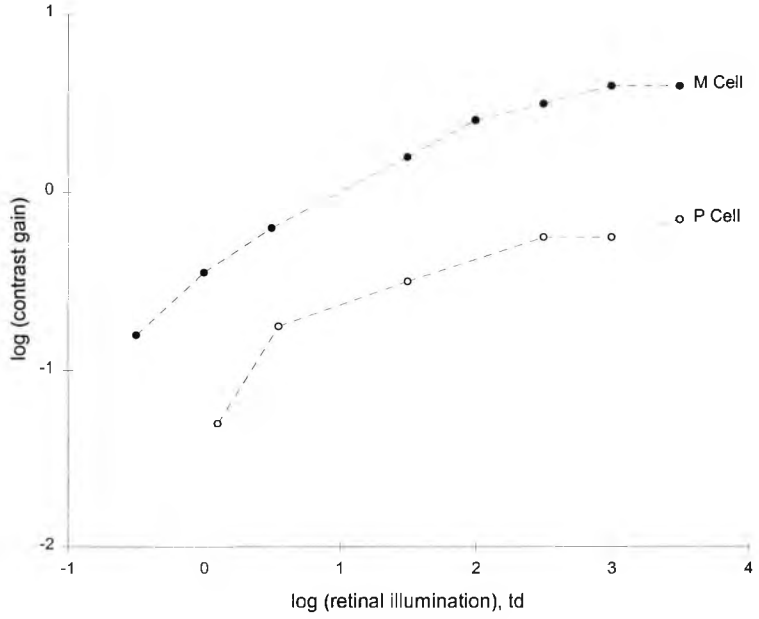

Figure 1.23 Graph showing how contrast gain (slope of response vs. contrast) varies with increasing illumination. Contrast gain has units of impulses per second per % contrast. M cell and P cell contrast gain becomes independent of illumination above approximately 2.5 log td and 3 log td respectively (after Purpura *et al.,* 1988).

1.4 Visual performance at different light levels

It is helpful at the outset to distinguish between two psychophysical methods of studying adaptation; steady state investigations and temporal investigations. Steady state (often referred to as light adaptation) investigations probe the sensitivity of the visual system when the eye is adapted to a given light level and is in equilibrium. Temporal adaptation investigations determine how sensitivity changes over time following a change in retinal illuminance. Dark adaptation investigations are a special subset of temporal adaptation investigations and typically refer to studies that monitor the recovery of visual performance in the dark following exposure to a light that bleaches a substantial fraction of photopigment.

It has been said that the purpose of adaptation is to make the retinal response to contrast independent of changes in illumination (Shapley and Enroth-Cugell, 1984). Contrast, a physical property of the visual stimulus, is typically defined in one of two ways. When aperiodic stimuli such as spots of light are used, contrast is usually defined as:

$$\text{Contrast} = (L_o - L_b) / L_b$$

where L_o is the luminance of the object and L_b that of the background. This definition of contrast (Weber contrast) is more usually written as:

$$\text{Contrast} = \Delta L / L_b$$

where ΔL is the incremental luminance of the spot. More recently stimuli that vary sinusoidally over space and time have been used to probe the performance of the visual system. Periodic stimuli have been used increasingly in psychophysical investigations because the visual system has been shown to contain filters that respond optimally to stimuli that posses specific spatial and temporal frequency envelopes (Campbell and Robson, 1968; Enroth-Cugell and Robson, 1966). When periodic stimuli, such as a sinusoidal contrast grating are used, contrast is defined as:

$$\text{Contrast} = (L_{max} - L_{min}) / (L_{max} + L_{min})$$

where L_{max} is the peak luminance of the grating and L_{min} the minimum luminance. This definition of contrast is known as Rayleigh or Michelson contrast. The minimum contrast required to perceive a stimulus is known as the contrast threshold. Contrast sensitivity is the reciprocal of contrast threshold.

1.4.1 Studies of steady-state visual performance using aperiodic stimuli

The performance of the visual system in steady-state conditions is typically determined by studying increment thresholds. Increment threshold studies require subjects to adjust the intensity of a test field presented on a relatively large adapting background, to the point at which it is just discernible i.e. threshold. This measurement is repeated over a range of background intensities and typically the data is presented graphically as log increment threshold as a function of log background intensity. Such graphs are known as increment threshold or threshold vs. intensity (t.v.i.) functions.

1.4.1.1 Scotopic increment threshold

Perhaps the best known study of this type was that conducted by Aguilar and Stiles (1954). They chose an experimental method designed to isolate the scotopic system. The test was blue green in colour (520 nm), large (9°), 200 msec in duration and located 9° form fixation. To further isolate rod responses the test was projected through the periphery of the pupil (to reduce the directional effectiveness of cones) and the adapting background field was red (620 nm), to desensitise the cones. Figure 1.24 shows their averaged results.

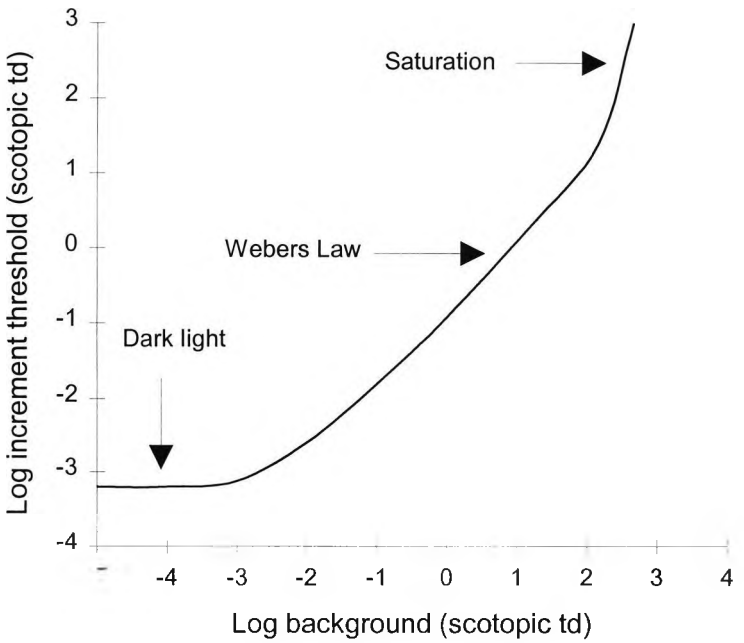

Figure 1.24 Increment threshold function for a 520 nm, 9° spot displayed for 0.2 seconds, centred 9° from fixation in a 20°, 620 nm background. From the averaged results of Aguilar and Stiles (1954).

Their data, plotted as log increment threshold vs. log background intensity, has several features. At very low background luminance levels (up to 2 x 10^{-3} scotopic td), the increment threshold is approximately constant and independent of the retinal illuminance of the background luminance. At slightly higher background intensities, Aguilar and Stiles (1954) showed that increment threshold increased in proportion to background intensity. Specifically, threshold was equal to the background intensity times a constant (Webers law: $\Delta I = k \times I$). The value of the Weber constant (k) found in this study was averaged as 0.21 (Barlow, 1972). At higher background levels increment threshold rose steeply, a phenomenon often referred to as 'rod saturation'.

The lower asymptote of this function is usually attributed to 'noise' (Walraven *et al.,* 1990). Barlow (1972) referred to this noise as 'dark light', a source of excitation which acts like real light and adds to it. A physiological substrate for 'dark light' has been found by Schnapf and Baylor (1987) who showed that spontaneous quantal-like events occurred in monkey rods approximately once every 150 seconds.

The gradient of the linear Weber portion of the graph was approximately 0.9 which indicated that the contrast sensitivity of the rods for large, long-duration presentations was approximately constant over a considerable range of background intensities. This suggests that some form of active adaptational process must be in operation. However, recent evidence has shown that the red background used by Aguilar and Stiles (1954) stimulated the cones which contributed to the slope (Sharpe *et al.,* 1993). In a complete achromat who has normal rods but no cones, the slope of the Weber portion under similar test conditions was only 0.77 (Sharpe *et al.,* 1993). The steep rise in increment threshold above 2 log scot td, often referred to as 'saturation', indicates a failure of sensitivity control (the Weber fraction (ΔI /I) increases dramatically) and has been attributed to rods reaching the ceiling of their response range (Walraven *et al.,* 1990). Saturation of the rod system may be advantageous because it prevents the rods interfering with visual processing under photopic conditions.

The form of the increment threshold function is highly dependant upon experimental conditions. Barlow (1965) conducted a rod isolation investigation but used a smaller test (0.75°) presented for 8 msec, 10° from fixation on a 10° orange background. This investigation showed that, after the lower asymptote (the 'dark light' region), threshold

on log log co-ordinates rose with a slope of approximately 0.5 over a 2 log unit range. This was the range over which Rose (1948) proposed that sensitivity would be limited by quantal fluctuations of the background. In particular, the number of quanta making up the background field is not constant but follows a Poisson distribution with a mean of n and a standard deviation of $n^{0.5}$. Consequently the quanta making up the test (the signal) are liable to be confused with the fluctuating quanta that make up the background (the noise). Therefore, the brighter the background the greater the noise and the higher threshold will be. In fact, threshold would have to increase in proportion to the standard deviation of the noise i.e. $n^{0.5}$. This square root portion of the increment threshold function is generally known as the de Vries-Rose law. Shapley and Enroth-Cugell (1984) point out that this decrease in sensitivity is not strictly light adaptation but an inevitable loss of sensitivity due to the nature of the stimulus. For a full discussion of the effects of quantal noise see Makous (1990).

Although an increment threshold slope approaching one is usually taken as being indicative of an active adaptational process, this need not be the case. Aperiodic stimuli, like most visual objects, are broad band in nature, i.e. they contain a variety of spatial and temporal frequencies. We now know that the visual system contains an array of spatio-temporal filters and the most sensitive filter for a particular set of conditions, will determine threshold. Therefore, it is quite possible that a spot may be detected by one filter at a low background luminance and others at higher background luminances. Consequently, the increment threshold function for aperiodic stimuli is likely to be an envelope of individual filter responses. Therefore to some extent, adaptation to every day objects may be a filter based operation (Hess, 1990).

Under normal conditions, (i.e. when the rod system is not isolated), the cones 'take over' at approximately 10^{-1} td (Wyszecki and Stiles, 1982). The intrusion of the cones is first evident by a second plateau in the increment threshold function (cone 'dark light', Barlow, 1958b). The intrusion of the cones prevents the rods from attaining stable contrast sensitivity i.e. a slope of unity, and over most of their normal operating range rod increment thresholds approximate to the square root law (Shapley and Enroth-Cugell, 1984).

Working on experimental data produced by Blackwell (1946), Shapley and Enroth-Cugell (1984) calculated that maximum contrast sensitivity (CS) for large test stimuli in the rod system was about 12 and for small tests (18 min) only 1.5.

1.4.1.2 Photopic increment thresholds

The t.v.i. curves obtained for the photopic system are similar to those obtained for the scotopic system. There is an initial lower asymptote due to cone 'dark light'. The slope then rises showing square root and Weber law behaviour (depending on field size) but unlike the rod system there is no evidence of saturation (Wyszeki and Stiles, 1982). The avoidance of saturation has been attributed to photopigment bleaching which takes place above 10^4 td (Walraven *et al.*, 1990).

Contrast sensitivity improves dramatically at photopic background luminances when the cones are operating (CS of 125 or more), (Shapley and Enroth-Cudgell, 1984).

1.4.2 Periodic stimuli

More recently, periodic stimuli have been used to investigate sensitivity at different background luminances. Such stimuli, unlike abruptly presented spots (aperiodic stimuli), contain well defined spatial and temporal frequency components. Perhaps the best known studies of how contrast sensitivity varies with mean luminance for periodic stimuli are those conducted by van Nes and Bouman (1967), Daitch and Green (1969) and Kelly (1972).

Daitch and Green (1969) described the performance of the visual system at different light levels with a series of contrast sensitivity functions. Before presenting their results the contrast sensitivity function (CSF) is described.

1.4.2.1 The human contrast sensitivity function

Clinically, spatial vision is usually measured using letter charts. Snellen acuity for normal young adults may range from 6/6 to 6/4 which corresponds approximately to a grating of 30 to 45 c.p.d. Unfortunately, this method of assessing spatial vision only indicates how well an individual is able to resolve fine detail at high contrast. A more

complete description of visual function is provided by the contrast sensitivity function (CSF). To measure the CSF the contrast of a sinusoidal grating is adjusted until the pattern is just visible. The sensitivity (the reciprocal of threshold contrast) is then plotted as a function of spatial frequency. The precise shape of the CSF is dependant upon the temporal characteristics of the presentation, the retinal location, display area, the method of measurement and the mean luminance of the grating.

When gratings are presented foveally at low temporal frequencies, the resulting CSF is a band pass function with peak sensitivity occurring at 2-5 c.p.d., declining on either side.

Compared with foveal measurement, the CSF (for a fixed grating size) in the peripheral retina is depressed particularly for higher spatial frequencies. There is a reduction in the highest resolvable spatial frequency and the spatial frequency which corresponds to peak sensitivity (Rovamo *et al.,* 1978).

1.4.2.2 Determinants of CSF shape

A number of factors determine the shape of the CSF including the optics of the eye, the anatomy of the retina and the properties of underlying spatial frequency tuned channels.

The optics of the eye may determine the high frequency cut off point (acuity). On the basis of the line spread function (about 1.2 min arc at half height) determined by Campbell and Gurbish (1966), Wilson *et al.* (1990) argue that gratings above 60 c.p.d. are unresolvable because the contrast of such a grating is degraded by a factor of about 100 by the optics of the human eye. However, acuity decreases with increasing eccentricity to a greater extent than predicted by optical factors alone. Therefore, the optics of the human eye may impose a limit on grating acuity at the fovea but not at more peripheral locations (Wilson *et al.,* 1990).

Another factor limiting acuity may be photoreceptor packing density. For a sinusoidal grating to be resolved it must be sampled at least twice per cycle. The period of the highest spatial frequency that can be resolved is half the angular subtense of the row to row spacing of cones packed in a perfect triangular lattice (Nyquist frequency) (Curcio and Sloan, 1992). Typically grating acuity at different retinal eccentricities is parallel to but slightly less than that suggested by the cone Nyquist limit indicating that acuity is largely determined by cone spacing (0 to 10°) (Rovamo and Virsu, 1979). One problem

with this idea is that although the mean packing density of the cones declines with increasing eccentricity the minimum spacing at any eccentricity is approximately constant (6-8μm). Therefore at least some high frequencies at the correct orientation may be accurately sampled in the peripheral retina (Curico and Sloan, 1992).

Further sampling limits are imposed by the number of ganglion, LGN and cortical neurones. At the fovea the ratio of cones to ganglion cells is 1:1 and therefore the Nyquist sampling limit of the cones may indeed be the limiting factor for acuity. However, peripheral ganglion cells under-sample the cone mosaic resulting in a decline in acuity. Wilson *et al.* (1990) suggest that there are 100 times more striate cells per cone at the fovea than in the far periphery. Rovamo and Virsu (1979) proposed that cortical magnification could account for the variation of CSF high frequency cut off with eccentricity.

In summary, it appears that optical factors may limit acuity at the fovea but that the sampling limits imposed by the cone mosaic and ganglion cell density limit acuity in the periphery.

At lower spatial frequencies, the CSF is thought to represent an envelope of the thresholds of a number of spatial frequency tuned channels. Contrast sensitivity at a particular spatial frequency is determined by the channel most sensitive to that frequency. Therefore factors that limit the sensitivity of individual channels will also have an effect on the overall system and determine the shape of the CSF. The main factors limiting a pathway's sensitivity are receptive field size and contrast gain (Shapely and Enroth-Cugell, 1984).

1.4.2.3 Scotopic (peripheral) CSF

Daitch and Green (1969) used a cathode ray tube (CRT) display to present sinusoidal contrast gratings to the peripheral retina. The colour of the monitor was adjusted using filters to maximally stimulate rods and light from the grating was made to enter the periphery of the pupil. Contrast threshold to a variety of gratings (0.5 to 8 c.p.d. approximately) was measured over a range of luminances (-2.5 to 1.5 log td). They presented their data graphically as a series of contrast sensitivity functions (see Figure 1.25).

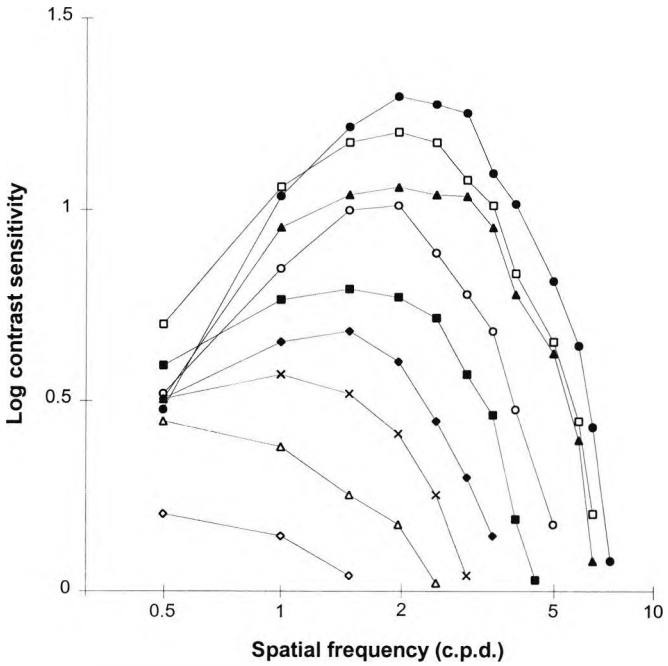

Figure 1.25 Contrast sensitivity of the peripheral retina at various luminances and spatial frequencies. The grating measured 8° x 3° and was centred 12° from fixation in the temporal retina. A straight line connects measurements taken at each luminance. The open diamond symbol represents measurements taken at -2.5 log td; open triangle, -2.0 log td; cross, -1.5 log td; solid diamond, -1.0 log td; solid square, -0.5 log td; open circle, 0.0 log td; solid triangle, 0.5 log td; open square, 1.0 log td, solid circle, 1.5 log td. Re-drawn from Daitch and Green (1969).

The contrast sensitivity functions have a number of interesting features: at the highest mean illuminance (1.5 log td), the CSF is a band pass function having a peak contrast sensitivity of approximately 20 for a 2 c.p.d. grating. Peak contrast sensitivity shifts towards lower spatial frequencies as mean retinal illumination reduces e.g. at -1.5 log td peak contrast sensitivity of approximately 4 is observed for a 1 c.p.d. grating. The shape of the CSF changes from band pass to low pass below -1.5 log td. Acuity (the highest resolvable spatial frequency) declines from approx. 8 c.p.d. at 2.5 log td to only 1.75 c.p.d. at -2.5 log td. Weber's law (constant contrast sensitivity) is only observed for the coarsest grating (0.5 c.p.d.) between -1.5 and 0.5 log td. Contrast sensitivity for higher spatial frequencies increases as mean illuminance increases indicating that the corresponding increment threshold functions would have a slope less than 1.

The preponderance of square root behaviour indicates that rods do not light adapt and that their sensitivity is limited by the quantal fluctuations of the stimulus. Shapley and Enroth-Cugell (1984) calculated how many quanta are available to detect threshold contrast in scotopic conditions (1 scot td and below) and concluded that quantum

fluctuations must limit sensitivity in the scotopic range. Although this is largely true, some sort of sensitivity regulation must occur for pathways that are sensitive to low spatial frequencies (because sensitivity drops more steeply than the square root law). Two possible mechanisms of sensitivity regulation have attracted psychophysical investigation; photopigment depletion (a minor factor in the scotopic system) and the 'adaptation pool'.

Daitch and Green's (1969) data shows that the peak of the CSF moves slightly toward higher spatial frequencies as mean illuminance increases. Such a finding may be explained on the basis that the centre and surround mechanisms of concentrically organised ganglion cells adjust their gain independently. At very low light levels the gain (amplification) of the centre and surround mechanisms are at a maximum. As background luminance is increased, the gain of the centre mechanism is reduced before that of the surround. Therefore the surround becomes relatively more dominant and the filter becomes more sensitive to a slightly higher frequency (Enroth-Cugell and Lennie, 1975).

This effect is only likely to account for a shift in spatial frequency tuning at low light levels because above 1 td the gains of the centre and surround are reduced equally (Enroth-Cugell and Lennie, 1975).

1.4.2.4 Photopic (foveal) CSF

A similar investigation for foveal vision has been conducted by van Nes and Bouman (1967). They used a Maxwellian view optical system to image photographically produced contrast gratings onto the retina. The gratings subtended 8.25° by 4.5°, had a dominant wavelength of 525 nm and were presented continuously i.e. 0 Hz. Their results (shown in Figure 1.26) were not presented as a series of CSFs but as threshold contrast (% modulation) as a function of spatial frequency (0.5 to 48 c.p.d.) for different mean retinal illuminances (-3.0 to 2.95 log td).

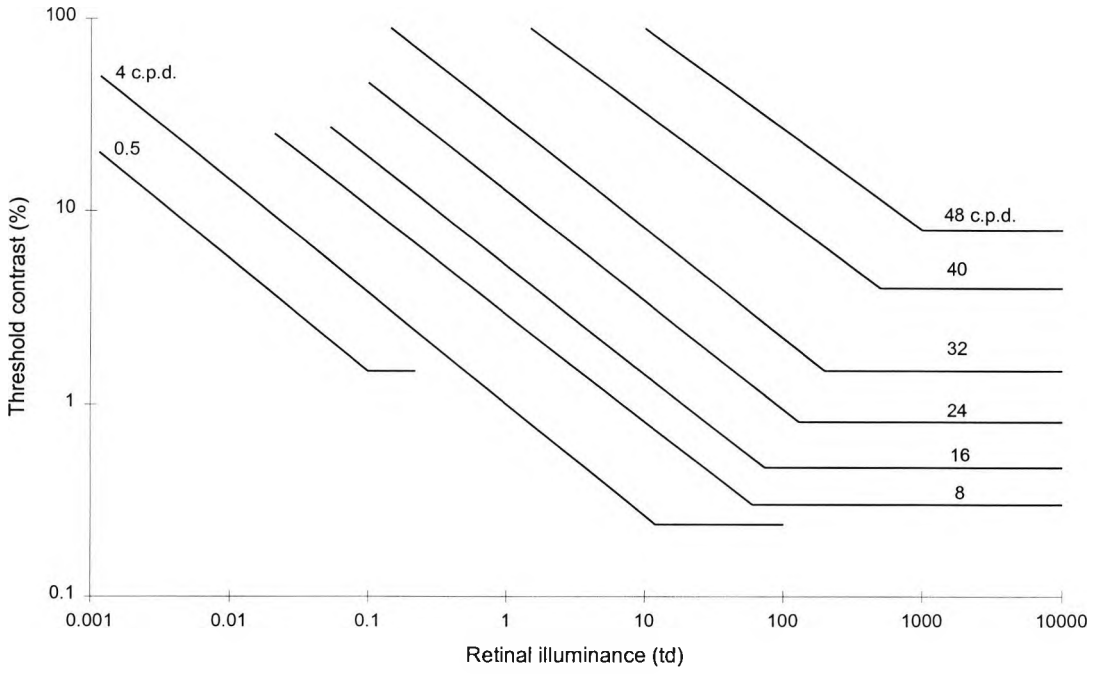

Figure 1.26 Graph showing the dependence of threshold modulation on retinal illumination for a variety of spatial frequencies. The flat portions of the graph indicate where contrast sensitivity is constant and the sloping portions of the graph are consistent with the square root law. Re-drawn from van Nes and Bouman (1967).

The data has a number of interesting features:

a) Above approximately 3 log td, contrast sensitivity to all spatial frequencies was constant i.e. Weber's law was observed.

b) As background illumination was reduced, below 3 log td, contrast sensitivity for the higher spatial frequencies began to fall i.e. grating threshold began to rise. The point at which contrast sensitivity first began to fall was directly proportional to spatial frequency. For all spatial frequencies, the reduction in contrast sensitivity associated with reducing background illumination obeyed the square root law, indicating that quantal fluctuations play a role in determining sensitivity at the fovea.

Peak contrast sensitivity was obtained for a 4 c.p.d. grating. Shapley and Enroth-Cugell (1984) calculated that the peak contrast sensitivity for this frequency was in excess of 200.

One explanation for the finding that contrast sensitivity is greater at the fovea than in the peripheral retina is that there are fewer ganglion cells in the periphery than at the fovea. Information about stimuli presented to the fovea, over a fixed area, is conveyed to the

cortex by a vast number of ganglion cells but relatively few convey the information from the periphery. When the area of the grating is varied so that the number of ganglion cells stimulated is kept constant, contrast sensitivity in the periphery and at the fovea are similar (Rovamo *et al.,* 1978).

1.4.2.5 Effect of temporal frequency

Kelly (1972) extended the findings of van Nes and Bouman (1967) by showing that the transition of square root to Weber's law was dependant upon temporal frequency. He used a CRT display (subtending 7°) centred on the fovea to display gratings of various spatial and temporal frequencies. The mean retinal illuminance provided by the screen was adjusted using ND filters (approx. 1.5 log td to 3 log td). His results, presented as amplitude threshold as a function of spatial or temporal frequency, show that Weber's law is observed for all spatial frequencies (0.5 to 12 c.p.d.) over this illumination range provided the grating is modulated at low temporal frequencies (<1 Hz). At higher temporal frequencies (8 Hz) a square root law is obeyed over this illumination range and at very high temporal frequencies (>= 32 Hz), sensitivity to all gratings is independent of retinal illumination (Kelly, 1972).

1.4.3 Psychophysical identification of adaptational mechanisms

The various mechanisms that contribute to the steady state sensitivity of the visual system may be teased apart by psychophysical investigation because the visual system's various adaptational mechanisms take a finite length of time to operate. Increment threshold functions obtained when a test is presented simultaneously with a background rise steeply because the operating range of the system is used up by responding to the background therefore less is available to signal the presence of a test. Such curves reflect what Boynton and Whitten (1970) referred to as 'response compression'. This effect was first observed by Crawford (1947) who measured foveal increment thresholds against flashed backgrounds. He found that there was a large transient threshold rise during the first 100 msec of a flashed background. This technique, often referred to as 'Crawford masking' has been used in a modified form by other psychophysicists to study different adaptational processes.

1.4.4 Adaptational processes

Apart from response compression (which is not really adaptation, but a feature of a system with a definite operating range) there are two types of adaptational process; multiplicative and subtractive.

1.4.4.1 Multiplicative adaptation

Multiplicative adaptation attenuates the response to backgrounds and tests equally, rather like looking through a neutral density filter. This type of adaptation is sometimes referred to as 'dark glasses' adaptation. Such adaptation may be provided by pupil constriction, photopigment depletion, receptor adaptation etc.

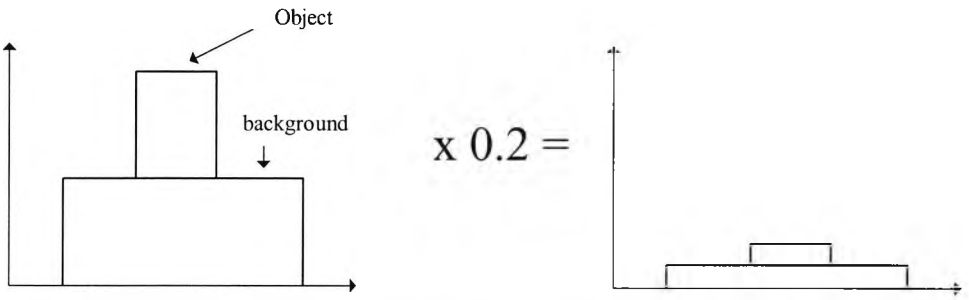

Figure 1.27 Plot showing how the luminance profile of a background and object are transformed by a multiplicative adaptational mechanism. Object and background are attenuated by the same amount.

1.4.4.2 Subtractive adaptation

Subtractive adaptation reduces the response to backgrounds but leaves transients unaffected, rather like a zero offset device on an amplifier. This type of adaptation may be provided by temporal or spatial filtering (Geisler, 1983; Hayhoe *et al.,* 1992; Hayhoe and Smith, 1989).

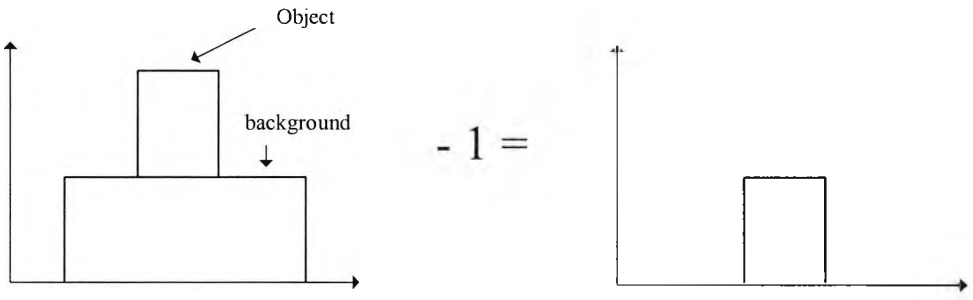

Figure 1.28 Plot showing how the luminance profile of an object and background are transformed by a subtractive adaptational mechanism.

1.4.5 Psychophysical isolation of adaptation mechanisms

Most neurones in the visual system can only respond over a limited range compared to the range of light intensities found in the environment. This limited range is revealed by the ability of brief flashes of light to drastically increase threshold, (Crawford, 1947). When an increment threshold function is obtained for a test presented simultaneously with the onset of an adapting background, the resulting function rises dramatically at relatively low adapting background intensities i.e. the curve 'saturates' (see Figure 1.29, Panel A). When threshold is measured on a background that has been presented for some time, adaptational mechanisms have sufficient time to adjust and threshold is very much lower. These mechanisms may permit Weber's law i.e. constant contrast sensitivity, to be obtained up to high light intensities.

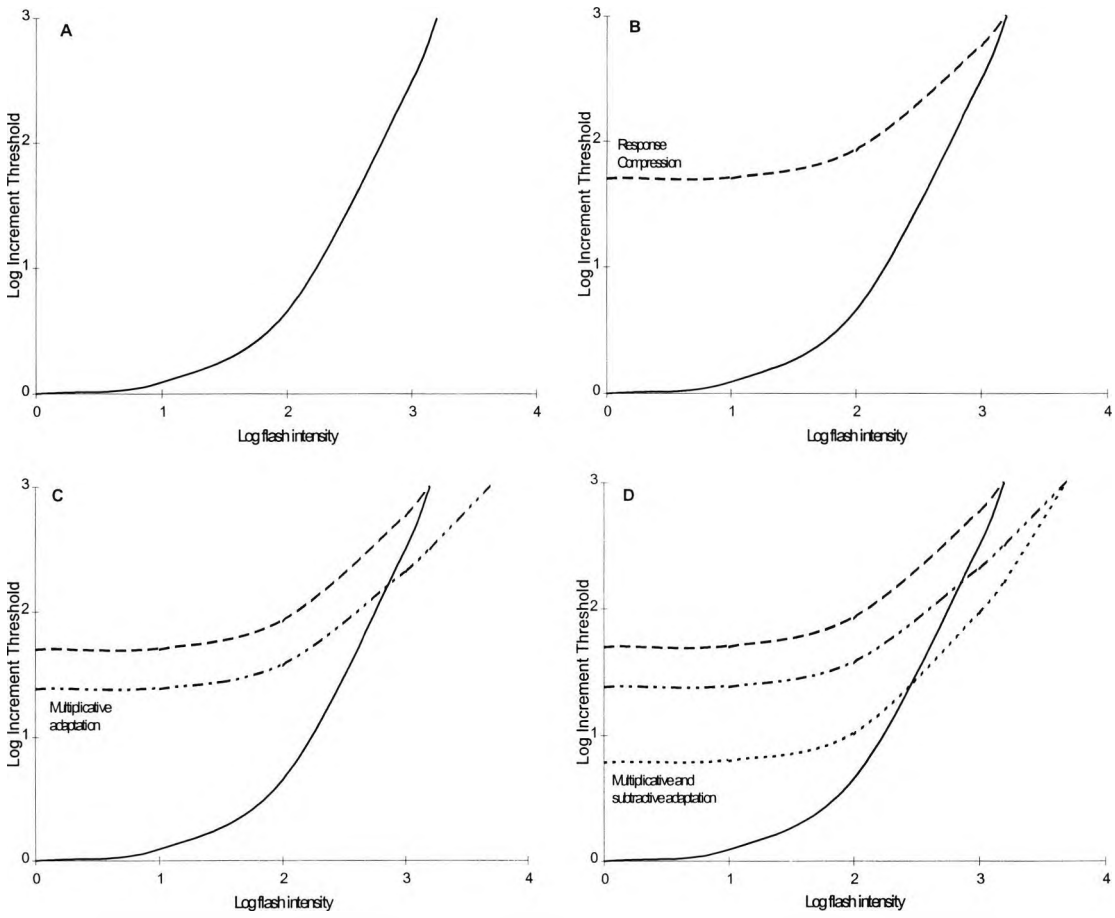

Figure 1.29 Effect of adaptation on the increment threshold function. Panel (A) shows the increment threshold function when the test flash and background are presented simultaneously (probe-flash curve). In Panel (B) the dashed curve shows how the probe-flash curve would be affected by the presence of an additional background and no adaptation i.e. effect of response compression. In Panel (C) the dot-dash curve shows the effects of multiplicative adaptation, the curve shifts down and to the right. In Panel (D) all the previous curves are repeated and a new curve (dots) shows the effects of both multiplicative and subtractive adaptation. Redrawn from Hayhoe *et al.* (1987).

The properties of the adaptational mechanisms may be revealed by studying the transition from a saturating increment threshold function (i.e. one where only response compression is operating) to a non-saturating function obtained on steady backgrounds.

Each type of adaptational process is evident by comparing the increment threshold functions obtained when a test flash is presented simultaneously with a flashed background (probe flash functions) in darkness and in the presence of an additional fixed background. If the visual system responded to the steady background in the same way that it did to the flashed background, the two would have an additive effect. The added background field would be particularly effective at raising threshold at low flash intensities when it is intense relative to the flashed background. As the flash intensity increases it becomes relatively more intense compared to the steady background and the increment threshold function, at these higher flash intensities, would approximate that obtained without the steady background. Therefore, with response compression but without active adaptation, the floor of the flash probe increment threshold function obtained in the presence of an additional fixed background would be raised (see Figure 1.29, panel B).

Multiplicative adaptation is evident in flash probe increment threshold functions obtained in the presence of a steady background by a shift in the curve down and to the right i.e. the effect of the steady background is reduced which lowers the floor of the function and it takes a brighter background flash to saturate the response, hence the shift to the right (see Figure 1.29, panel C).

Subtractive mechanisms differ from multiplicative ones in that only the response to the steady adapting field is attenuated. Transients, such as the flashed background, are unaffected. Subtractive adaptation manifests itself in the flash probe increment threshold function by a downward shift in the floor of the function only (see Figure 1.29, panel D). A more detailed description of the rationale behind this type of investigation is provided by Hayhoe *et al.* (1987).

1.4.6 Time course of adaptation in the scotopic system

Adelson (1982) used the flash probe technique to study the time course of adaptational processes in the scotopic system. He obtained several increment threshold functions for test flashes that were presented at various times after the onset of a background. The test was a 4.5°, blue (480 nm) square presented for 30 msec in the centre of a large 11° red adapting background, centred 12° from fixation. One increment threshold function was obtained when the onset of the test flash coincided with the onset of the background, others were obtained when the test flash was presented 200, 500, or 1000 msec after background onset and another was obtained in steady state conditions when the adaptational processes were at equilibrium. Adelson's (1982) data show that rod saturation (i.e. total failure of adaptation) occurs on relatively dim backgrounds when the test is presented simultaneously with (or shortly after) the onset of the background.

In steady state conditions he found that the rod system saturated at approximately 2 log scotopic td, but when the test presentation coincided with that of the background, saturation occurred at approximately 0 log scotopic td i.e. 2 log units earlier. His data show that 200 msec after presentation of the background the saturation point has moved up 1 log unit of background intensity indicating the presence of a rapid adaptational process. Between 200 and 1000 msec there was a slow increase in the background intensity at which saturation occurred but it took '2 or 3 min' for the saturating background intensity to asymptote. In the time between the onset of a background and the time at which steady state conditions are obtained there are adaptational changes in the rod system that improve the operating range of the rods by approximately 2 log units.

To determine whether multiplicative or subtractive mechanisms were altering the sensitivity of the scotopic system, Adelson (1982) used the probe flash plus background technique described in the previous section. By changing the time between the onset of the adapting background and the probe flash measurement he was also able to determine the time course of each mechanism. He showed that multiplicative mechanisms dominate in the first 200 msec following onset of a background but that subtractive mechanisms are most important after that time.

Adelson (1982) suggests that the transient saturation that occurs when a test is presented simultaneously with a dim background (0.5 log scot td) takes place proximally to the rods, possibly at the bipolars or ganglion cells, because the background used in his investigation did not contain enough light to saturate the responses of the rods. This hypothesis is supported by evidence that bipolars and ganglion cells saturate at lower flash intensities than receptors (Werblin, 1974). When the background is presented 1 second before the test, saturation occurs at higher background intensities but is likely to originate in the rods themselves.

1.4.7 Time course of adaptational processes in the photopic system

Hayhoe *et al.* (1992) used the flash probe technique to investigate adaptational mechanisms in the photopic system. By modelling their data they not only distinguished between multiplicative and subtractive processes but were able to determine the time course of such processes after the onset of a background. Their results indicate that multiplicative changes take place very rapidly (<100 msec). They also showed that a slow subtractive process was present that took 10 to 15 seconds to asymptote.

To determine if centre-surround antagonism could account for subtraction in both the photopic and scotopic systems, Hayhoe and Smith (1989) obtained a series of increment threshold functions for tests presented on different sized backgrounds. The increment threshold function obtained when using a small (55′) background in photopic conditions, rose very much more steeply than that obtained when using a larger (45°) background. This result indicates that input from the surround protects the system from saturation. When the scotopic system was isolated, altering background field size had little effect on the slope of the increment threshold function. They concluded that spatial filtering is an important adaptational mechanism in the photopic system but that it is less important in the scotopic system. Centre-surround effects are likely to take effect very rapidly, therefore it is very unlikely that the mechanism observed by Hayhoe and Smith (1989) is the same as the slow subtractive mechanism observed by Hayhoe *et al.* (1992) or by Hayhoe *et al.* (1987).

Slow subtractive mechanisms are more likely to be due to temporal rather than spatial filtering.

Although the study by Hayhoe *et al.* (1992) investigated adaptational processes at background onset, the same mechanisms presumably take time to switch off at background offset, i.e. during early dark adaptation.

Geisler (1983) used the flash probe technique to examine adaptational mechanisms operating in the cone system during early dark adaptation. After the offset of a 4 log td background, Geisler showed that sensitivity to the flash probe fell in 2 stages. The initial change, which took place rapidly (within 100 msec), was attributed to a subtractive mechanism and a slower process that was still operating for approximately 10 seconds was identified as being multiplicative. Geisler (1983) suggests that there are at least 3 (approximately multiplicative) mechanisms that operate after the first 100 msec of dark adaptation, 'a short-term neural or network mechanism, a long-term receptor or bleaching mechanism and photopigment depletion'.

1.5 Dark adaptation

Dark adaptation investigations typically involve exposing the eye to a bright light that 'bleaches' a substantial fraction of photopigment and then measuring of the recovery of sensitivity in complete darkness.

Perhaps the best known dark adaptation investigation was that conducted by Hecht *et al.* (1937). They exposed the eye to bright 'bleaching' lights of different intensities. Following a period of light-adaptation the subject, who was otherwise in darkness, was required to adjust the intensity of a violet test light (presented for 200 msec) so that a black cross could just be seen. The results of this investigation were presented graphically as a series of dark adaptation functions (a plot of log threshold as a function of time) and are shown in Figure 1.30. Following exposure to a weak light, threshold initially fell relatively rapidly at first then more slowly. Following exposure to strong adapting lights, recovery took place in two phases. The first phase consisted of an initial rapid drop in threshold that lasted approximately 5 minutes, threshold then remained relatively constant for a further 7 minutes (during this time the colour of the violet test was apparent). After approximately 12 minutes threshold fell again before gradually asymptoting after 30-40 minutes. During the latter part of the study, the colour of the test was not apparent. Hecht *et al.* (1937) attributed the first phase of dark adaptation to cones and the later part to rods.

During dark adaptation, sensitivity is thought to be largely dependant upon processes that originate in the retina. This belief originates from the work of Craik and Vernon (1941) who showed that a dark adaptation function obtained in an eye that was pressure blinded during the initial period of light adaptation and the same eye when not pressure blinded, were very similar. Pressure blinding is believed to prevent retinal signals reaching the cortex, and therefore the similarity in the dark adaptation functions indicates that dark adaptation takes place within the eye itself.

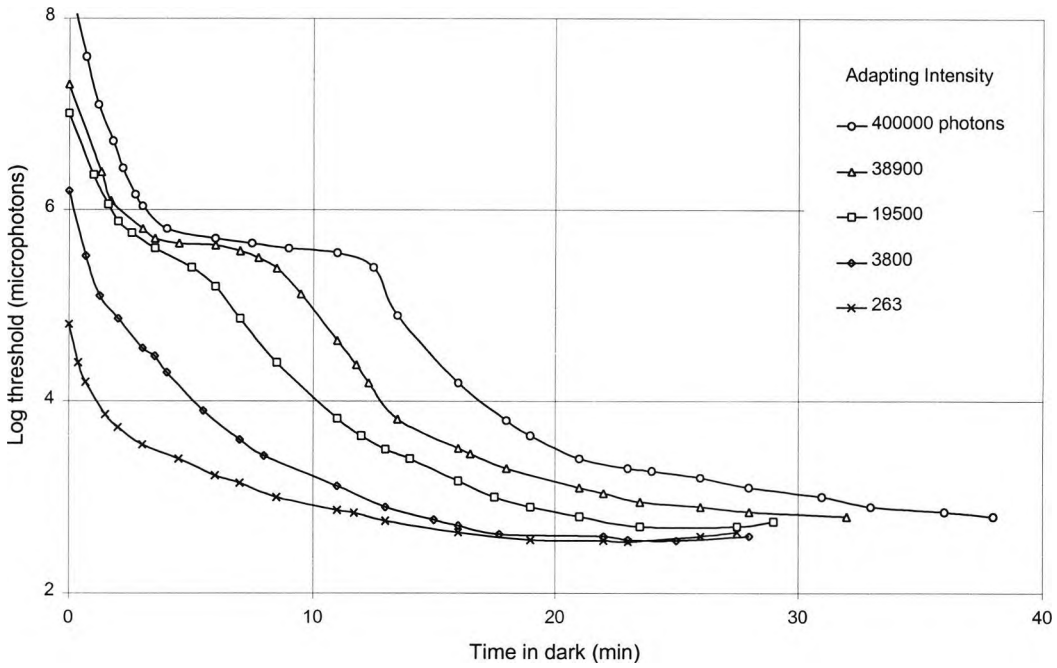

Figure 1.30 Dark adaptation functions for a normal observer. After Hecht *et al.* (1937).

However, in some conditions post-retinal sites may also influence the shape of the dark adaptation function. Lansford and Baker (1969) obtained monocular dark adaptation functions following light adaptation of the test eye and following light adaptation of both eyes. They found that the rod-cone transition occurred approximately 3 min earlier when both eyes had previously been light-adapted, indicating that sites beyond the retina may also influence the shape of the dark adaptation function.

There are two useful and enduring hypothesis about dark adaptation. One is that sensitivity at any time in the dark may be described in terms of an 'equivalent background' (Stiles and Crawford, 1932), a sort of invisible afterglow that determines threshold just as a real background would. Another, originally proposed by Hecht (1937), is that sensitivity at any time in the dark is governed by the concentration of a photo-product, the 'photochemical hypothesis'.

Before examining these hypothesis and the mechanisms that determine sensitivity in the dark several classic dark adaptation studies are reviewed.

1.5.1 Dark adaptation measured with aperiodic stimuli

1.5.1.1 The early stages of dark adaptation

There are several components to the recovery of sensitivity in the dark, not all of which are apparent in typical dark adaptation investigations such as that conducted by Hecht *et al.* (1937).

Over the first second of dark adaptation there is a large and rapid decline in threshold that is only apparent by using special techniques. Baker and Donovan (1982) examined the change in threshold over the first second of dark adaptation, an example of their data and its relation to a normal dark adaptation function is shown in Figure 1.31.

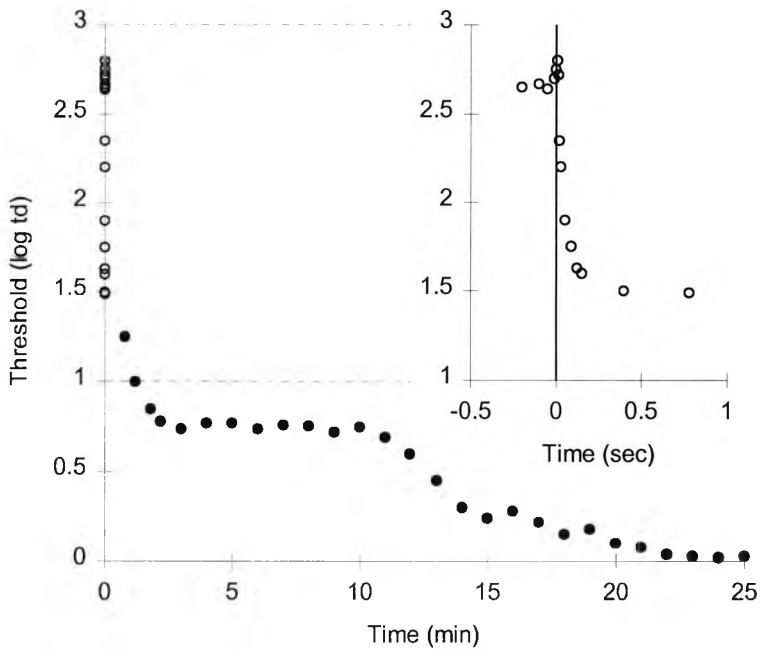

Figure 1.31 Normal dark adaptation (●) and early dark adaptation(O); 5° from fixation using a white test spot 1° in diameter presented for 20 msec. Early dark adaptation measurements are repeated in the inset graph on an expanded time scale. After Baker and Donovan (1982).

Over the first second of dark adaptation a brief and relatively small increase in threshold is followed by a relatively large and sudden drop in threshold. Baker and Donovan (1982) suggest that this early phase of dark adaptation is largely attributable to the decay of the receptor potential that was generated by the adapting light. The form of this early change in threshold is also likely to be influenced by lateral inhibitory effects. Kitterle and Leguire (1975) have shown that the shape of the early dark adaptation curve is

dependant upon the spatial configuration of the adapting field, i.e. whether it was a disk or an annulus of the same diameter.

1.5.1.2 Dark adaptation of the scotopic system

One of the most complete descriptions of dark adaptation in the scotopic system was provided by Pugh (1975). He obtained a series of dark adaptation functions for a 1.9°, 450 nm test presented for 55 msec 13.4° from fixation following exposure to bleaching lights of different energies. (4.7, 5.0, 5.3, 5.6, 5.9, 6.1, 6.4, 6.7, 7.0 and 7.3 log scot. td sec).

Following exposure to the least intense light, that bleached 2% of rod photopigment (according to Lamb, 1990), threshold was initially elevated by approximately 2.5 log units. It then fell rapidly over the first minute and then more gradually for a further 10 minutes by which time recovery was approximately complete.

After a more intense period of light adaptation that bleached 98% (according to Lamb, 1990), the initial rise in threshold was relatively large, (approximately 5.5 log units). Subsequently there was a rapid drop in threshold of several log units that lasted approximately 1 minute, then a plateau region was reached. This phase of dark adaptation was due to recovery of the cones. After 10 minutes, threshold began to fall again but this time more slowly. The decline in threshold (approx. 3.5 log units) continued for the next 30 minutes.

Pugh showed that identical dark adaptation functions were obtained with a 30 second period of light adaptation or a quantum equivalent 600 msec flash. The significance of this finding is discussed later.

The recovery of the rod system can be followed above the level corresponding to cone threshold in subjects who lack functioning cones. Blakemore and Rushton (1965a) examined such a subject and showed that after a 50% rhodopsin bleach, threshold was initially raised by approximately 7 log units; sensitivity then returned but recovery was not complete until almost 40 minutes had elapsed.

1.5.1.3 Dark adaptation of the photopic system

Hollins and Alpern (1973) studied dark adaptation in the photopic system. They bleached cone pigment with a variable intensity 7° field centred on the fovea and subsequently monitored sensitivity to a centrally-presented, 1° red (675 nm) test spot, that was presented for 83 msec twice per second. Following a weak 'equilibrium bleach' (10 sec intense plus 1 min weaker) that bleached 10% of cone photopigment, threshold was raised initially by 1 log unit before declining rapidly, asymptoting after approximately 1.5 min. After an intense (100%) bleach, threshold was raised by at least 3 log units (threshold was higher than this for the first 20 seconds but not measured). It then declined in an approximately exponential fashion over the next 5 minutes.

Coile and Baker (1992) obtained similar results for foveal dark adaptation on a large sample of subjects (n=58). They exposed subjects to a 5.8 log td, 5° bleaching field for 1 min and then measured threshold to a 1.4°, foveally-presented test. Following the bleach, threshold was initially raised by approximately 4 log units. Over the following 5-10 minutes threshold fell back to pre-exposure levels. Coile and Baker (1992) showed that recovery was somewhat slower for older subjects.

Even very weak bleaches are capable of elevating threshold for a considerable time. Brown (1983) showed that exposure to an adapting field that bleached only 0.2% of cone photopigment raised threshold to a small (20 min) red (650 nm) brief (10 msec) test flash by 0.5 log units and that recovery was not complete after 1 minute.

1.5.2 Dark adaptation hypotheses

Two hypothesis about dark adaptation have attracted much research, namely; the photochemical and equivalent background hypotheses.

1.5.2.1 The photochemical hypothesis

One of the most enduring hypothesis about dark adaptation is that sensitivity is determined by the concentration of a substance in the receptors the 'photochemical hypothesis'. This idea was first proposed by Hecht *et al.* (1937). They proposed a linear relationship between threshold and the amount of pigment in the bleached state. If half

the pigment was bleached, threshold would double. Unfortunately this assertion could not be tested at that time because there was no means of determining the concentration of photopigment in the intact retina.

Almost two decades later, the rate at which photopigment regenerates in the intact human eye was measured by Campbell and Rushton (1955) using a technique known as retinal densitometry. They showed that photopigment regenerates in a exponential manner and that the time constant is similar to one obtained by fitting an exponential curve to a dark adaptation function. A similar result was obtained for cones by Rushton (1957).

In 1960, Dowling compared the amount of light necessary to evoke a threshold b wave in the rat electroretinogram and the rhodopsin concentrations in the eyes of rats killed and frozen at the same time after a bleach. His results indicated that log threshold is proportional to the amount of bleached rhodopsin. Rushton (1961) showed that a similar relationship existed in man. He obtained dark adaptation functions from a rod monochromat and measured rhodopsin concentration by densitometry. The relationship between bleached photopigment and log threshold is known as the Dowling-Rushton relationship:

$$\log (I_t/I_o) = kB$$

where I_t is test flash threshold, I_o is the threshold of the completely dark-adapted eye, B is the percentage of bleached photopigment and k is a constant (3 in cones and 20 in rods according to Frumkes, 1990). Although this equation was accepted as an adequate description of dark adaptation for many years, it is only valid under specific conditions, namely in the late stages of dark adaptation following exposure to light that bleaches a significant amount of photopigment, (Lamb, 1990).

Hollins and Alpern (1973) examined the validity of the Dowling-Rushton relationship for human cones. They obtained dark adaptation functions for a 1°, brief (85 msec), red (675 nm) test spot presented at the fovea and photopigment regeneration curves in the same subject for a variety of bleach conditions (10-100% bleaches). After long bleaches, both threshold recovery and pigment regeneration could be described by a single exponential curve with a time constant of 105 sec for one subject, (for the other subject the time constant for threshold recovery was 116 sec but no pigment regeneration data

were obtained). For shorter bleaches (about 10 seconds) the time constant of recovery for threshold and pigment regeneration was less, (about 65 seconds). Except for the first 30 seconds following a weak bleach (when threshold is higher than predicted) their data supported the Dowling-Rushton relationship for human cones.

When the bleach is relatively weak, rod threshold is initially substantially above that predicted by the Dowling-Rushton relationship. For example, the equation predicts that after a 1.5 per cent bleach, threshold should be raised by 0.285 log units (assuming k=20). However by examining the data of Rushton and Powell (1972) who used such a bleach, the initial rise in threshold is almost 2.5 log units. The equation also fails to adequately describe initial threshold elevation after large bleaches. In such situations the predicted threshold elevation is much higher than that observed. Lamb (1990) calculated that following a 90% bleach, the Dowling-Rushton relationships prediction could be as much as 8 log units higher than that observed. Another problem with the equation was highlighted by Pugh (1975). He adjusted the intensity of a 1.9° circular test patch presented for 55 msec, 13.4° from fixation, to threshold following various bleaches (2 to 98%). He fitted exponential curves to the resulting dark adaptation functions and found that the 'constant' in the equation was not constant at all but varied from approximately 3.5 min for weak bleaches to more than 11 min for intense ones. An additional problem with the Dowling-Rushton relationship is that identical dark adaptation functions can be obtained following a very intense flash or a long duration quantum equivalent bleach (30 sec) despite the fact that the long exposure, bleaches much more pigment than the photoflash, a phenomena Pugh (1975) described as 'Rushton's paradox'.

From what we now know about the complexity of the visual system, it is not surprising that the Dowling-Rushton relationship has been shown to be an oversimplification. Alpern *et al.* (1970) describes the relationship as a 'compact parcel of trouble' and Lamb (1990) criticises it because it is without theoretical foundation.

Rushton (1972) proposed two reasons why the Dowling-Rushton relationship is a poor description of threshold during the initial stage of dark adaptation following a weak bleach. Firstly the rise may be due to a 'change in nerve organisation' following the offset of the background light and secondly, the rise may be due to an unidentified photoproduct (Rushton, 1972). Support for the idea that some photoproduct is

responsible for the initial rise in threshold is provided by Rushton and Powell (1972). They used a 15° circular bleaching field centred 8° from fixation that was split horizontally into two half fields. The bleach in each half field differed in that the exposure in one field was relatively weak and long and in the other intense and brief, but the product of the intensity and time was constant (I.t=k). The 7.5° circular test was also split horizontally so that each half fell on the two different bleach areas. If the initial threshold rise is due to a photoproduct one would expect the amount of this product to be the same as long as I.t was constant (Bunsen-Roscoe Law) and hence the initial threshold rise should be similar. Rushton and Powell (1972) found that the Bunsen-Roscoe Law held for a range of bleaching intensities and durations (t=0.5 sec to 30 sec) and consequently argued that some photoproduct must be responsible for the rise in threshold. Rushton and Powell (1972) called this photoproduct 'X-opsin' and Rushton (1972) suggested that the photoproduct was metarhodopsin II. Similar results were obtained by Pugh (1975) who also showed that as long as I.t = constant, rod thresholds followed a similar time course. In his investigation initial light adaptation was produced either by exposure to a xenon photo flash (that bleached 47% of rod photopigment) or an energy equivalent exposure to a xenon arc for 30 seconds (that bleached all the photopigment). He showed that the course of dark adaptation was similar despite the fact that the two bleaching methods bleached a different amount of rhodopsin. This led Pugh (1975) to the conclusion that the threshold raising photo-product must be from a 'side reaction in the normal chain of events in scotopic excitation' that originates before the Metarhodopsin I to Metarhodopsin II transition.

Lamb (1981) re-evaluated Pugh's (1975) data and noted that the recovery of log threshold could be described accurately by several straight lines rather than the usual exponential. Hence threshold elevation (as opposed to log threshold elevation) appears to decline exponentially with time. Lamb (1981) identified 3 components with time constants of 5, 100 and 400 seconds and related these to the presence of 3 photoproducts produced by the rod transduction mechanism.

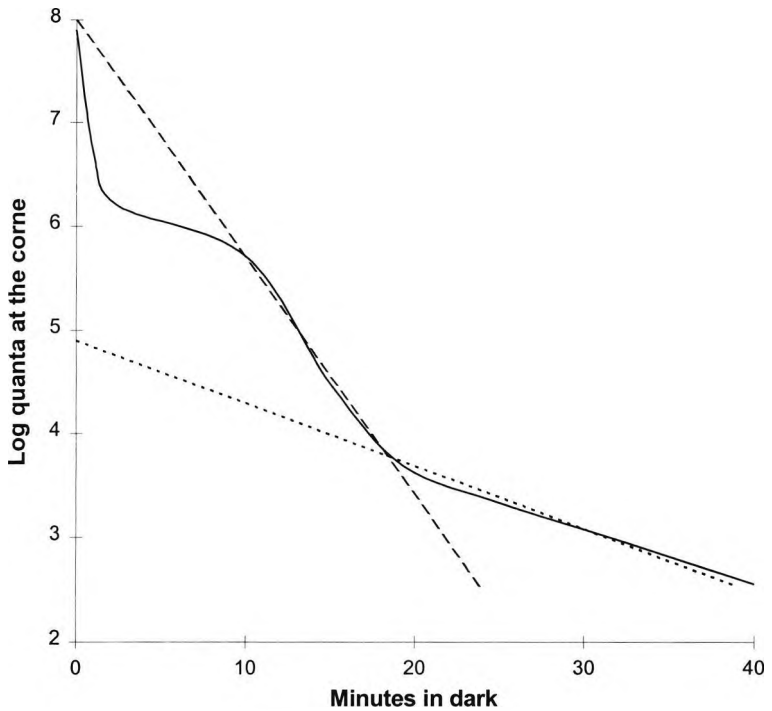

Figure 1.32 Dark adaptation curve for a normal observer following a period of light adaptation that bleached 98% of rod photopigment (after Pugh, 1975). The two broken lines show that log threshold elevation can be accurately described by several straight line sections rather than the more usual exponential curve (after Lamb, 1981). The dashed line indicates that threshold recovers exponentially with a time constant of 100 seconds and the dotted line shows another component with a time constant of 400 seconds.

1.5.2.2 Equivalent background hypothesis

During dark adaptation the elevation of threshold may be described in terms of an 'equivalent background', (Stiles and Crawford, 1932; Crawford, 1937). This equivalent background is a sort of invisible afterglow, produced by exposing the eye to light, which acts just like a real background light. As dark adaptation proceeds the equivalent background gradually fades and threshold declines. This theory suggests that dark adaptation is simply a special case of light adaptation, in which the adapting background is stabilised on the retina.

According to the equivalent background hypothesis, threshold elevation, spatial resolution, temporal resolution and pupil size measured at any point in time during dark adaptation, should be exactly equivalent to those found in the presence of a real stabilised background light.

The strength of this hypothesis is evident in the results of Blakemore and Rushton (1965a). They obtained dark adaptation functions and increment threshold functions, for a variety of tests, from a rod monochromat.

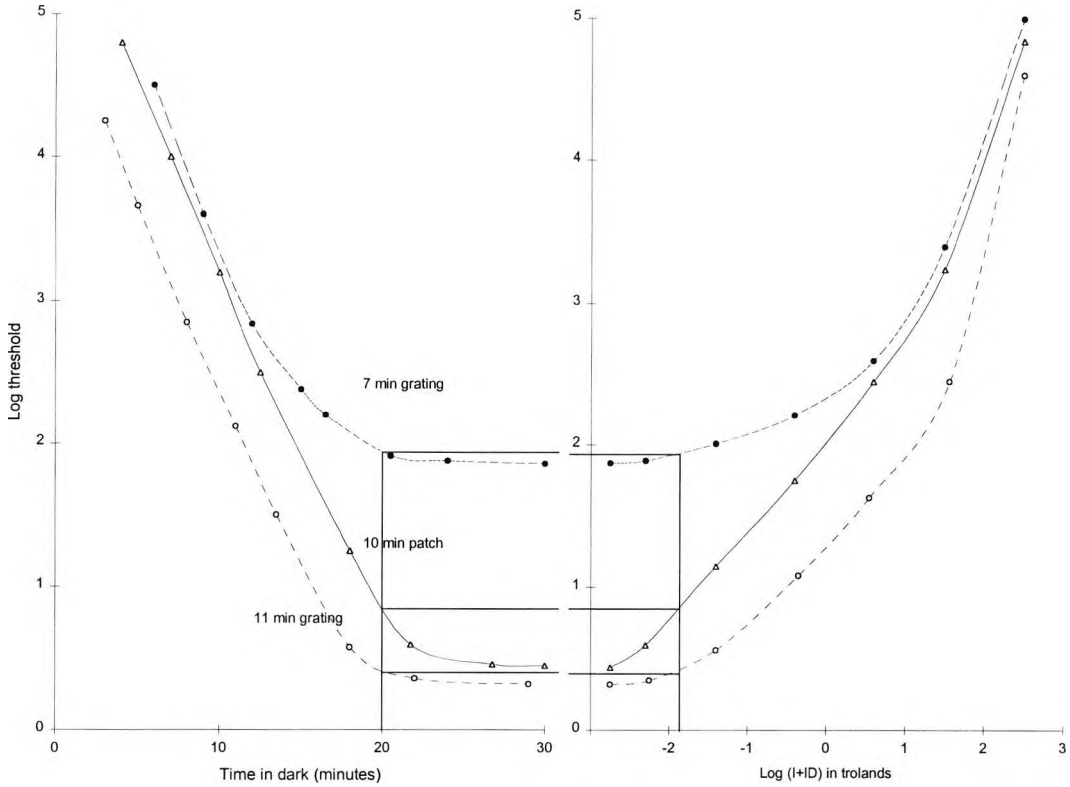

Figure 1.33 Dark adaptation function (left) and increment threshold function (right). Although the shape of the dark adaptation and increment threshold functions are very different for each test stimulus, threshold at any time in the dark for any test may be described in terms of an equivalent background. For example after 20 minutes of dark adaptation threshold for all tests is the same as if threshold had been measured on a real background of approximately -2 Log trolands.

Figure 1.33 shows dark adaptation and increment threshold functions obtained with a 7′ grating, 11′ grating and an 11′ uniform patch of light. Blakemore and Rushton's (1965a) results showed that threshold at any time in the dark, for any test, was the same as that measured on a steady background. This is exemplified in Figure 1.33 where threshold (for each of the test stimuli) after 20 minutes of dark adaptation is the same as threshold measured on a background of approximately -2 log trolands.

Hollins and Alpern (1973) and Rushton and Powell (1972) have shown that it is useful to distinguish between the initial phase of dark adaptation which is controlled by a mechanism that recovers rapidly and a slower mechanism controlled by bleached photopigment (or related photoproduct). The equivalent background hypothesis may

hold for either or both phases. The results of Blakemore and Rushton (1965a) show that the equivalent background hypothesis holds for the slower mechanism in the scotopic system.

Geisler (1979) showed that the equivalent background hypothesis also holds for the slower mechanism in photopic conditions (he corrected his data for photopigment depletion because pigment depletion accounts for a sizeable component of the photopic dark adaptation function (Geisler, 1980) but a much smaller component of increment threshold functions).

However the equivalent background hypothesis breaks down in other situations, e.g. when a test spot is presented simultaneously with a flashed background (Geisler 1981) or when temporal modulation sensitivity is measured following a long dim bleach (the hypothesis holds for the same test when the bleach is brief and intense) (Hayhoe and Chen, 1986).

1.5.3 Mechanisms of dark adaptation

Ideally, the eye would adjust its sensitivity to a sudden drop in ambient illumination instantaneously. However, as we have seen, this is not the case. Following a sudden drop in illumination, the visual system takes a finite length of time to adjust to the new light levels. The sensitivity of the eye at a given time during dark adaptation may by limited by any of the components that make up the visual system. Different components may limit sensitivity at different times following light offset.

1.5.3.1 Photopigment depletion

Although Hecht's (1937) original assertion that threshold was directly proportional to the fraction of bleached photopigment has been shown to be incorrect, photopigment depletion is an important factor in determining cone dark adaptation thresholds. If 99% of cone photopigment is bleached the retina's ability to catch quanta is reduced a 100 fold, therefore a 2 log unit rise in threshold would be attributable to photopigment depletion alone (Geisler, 1979). In the scotopic system, photopigment depletion accounts for a negligible increase in threshold because almost all rod photopigment has regenerated by the time rods determine sensitivity.

1.5.3.2 Photochemistry of receptoral dark adaptation

The validity of the Bunsen-Roscoe law confirms that dark adaptation is largely determined by the concentration of a photoproduct in the retina. Electrical recordings from receptors have shown that this photoproduct, produced by bleaching, mimics the effect of real light: sensitivity is decreased, circulating current is reduced and the decay time of the response to light flashes is accelerated. Such observations suggest that the photoproduct produces an 'equivalent background' excitation of the transduction process, Cornwall and Fain (1994).

Recently there has been interest in determining which photo-intermediary is responsible for activating the cascade. When Rhodopsin is activated by light, it passes through a number of stages before becoming Metarhodopsin II (the photoproduct that activates the transduction cascade). Metarhodopsin II then decays to Meta III and to Opsin. Cornwall and Fain (1994) suggest that during dark adaptation the transduction cascade may be activated by:

1. A small and decreasing amount of Meta II in the receptor due to reversible phosphorylation.
2. Meta II produced by reversible reactions from other photoproducts i.e. a fraction of Meta III or Opsin may recycle to Meta II.
3. One of the photoproducts (although much less efficacious) itself might activate the cascade i.e. opsin might directly activate the cascade.

If the equivalent background is produced by the regeneration of Metarhodopsin II then it would be expected that noise should be observed in the electrical recordings of dark adapting rods. This is because a single regeneration would be indistinguishable from a single quantal absorption. Unfortunately it is not clear if such noise exists. It has been observed for small bleaches (<1%) in toad and primate rods (Lamb, 1980; Schnapf and Baylor, 1987) but not following large bleaches (Cornwall and Fain, 1994) which are more typical in dark adaptation investigations. There is now evidence to suggest that Rushton's (1965) proposal that the equivalent background is produced by opsin itself is correct. It has been shown that inactivation of opsin (e.g. by analogues of 11 cis retinal

that bind to opsin and produce an inactive pigment) removes the desensitisation usually observed following a bleach (Corson *et al.* 1990, Jin *et al.* 1994).

Although opsin may produce an 'equivalent background' by activating both phosphodiesterase (PDE) and guanylyl cyclase (Cornwall and Fain, 1994) this background is not exactly the same as the one produced by light because it is relatively noise free (Fain and Cornwall, 1993).

Regeneration of the visual pigment and hence the return of sensitivity requires that opsin be combined with 11-*cis* retinal. In rod retinas it is believed that all-*trans* retinal is first converted to all-*trans* retinol in the photoreceptor outer segment before it moves to the RPE where it is esterified. This esterification permits all-*trans* retinol to isomerise to 11-*cis* retinol, which is then converted to 11-*cis* retinal in the RPE. The reformed 11-*cis* retinal then moves back into the retina so that visual pigment may regenerate, Saari 1990, Jin *et al.* 1994. Regeneration of visual pigment in cones is considerably faster than in rods (Rushton, 1972). Unlike rods, cone visual pigment may regenerate in the isolated retina i.e. when the RPE has been removed (Normann and Perlman, 1990). This finding indicates that 11-*cis* retinal may be resynthesised by the sensory retina itself. In cone-dominated retinas significant isomerisation has been observed to take place in the neural retina, most likely in the Müller cells (Das *et al.,* 1992). This source of 11-*cis* retinal is only available to cones because cones, unlike rods, permit 11-*cis* retinal to diffuse from the cell body to the outer segment.

Receptoral dark adaptation is rate limited by the local availability of 11-*cis* retinal. Rods only have access to one supply of 11-*cis* retinal from the RPE but cones may obtain theirs from a store in Müller cells and from the RPE.

If the local availability of 11-*cis* retinal is the primary limiting factor that determines the rate of dark adaptation, topographical differences in retinal anatomy such as Müller cell density and photoreceptor length may influence the rate at which dark adaptation proceeds for different spatial frequencies.

The technique of retinal densitometry has been used to determine how rapidly photopigment can regenerate. Early investigations showed that all cone photopigments regenerated in an exponential manner with a time constant of about 120 seconds for long bleaches, (Rushton and Henry, 1968). Following a shorter (1 second) period of

light adaptation that bleached the same amount of photopigment, the time constant of recovery was 60 seconds. Rushton and Henry (1968) proposed that dark adaptation may be rate limited by the local availability of 11-*cis* retinal. After a long bleach, any store of 11-*cis* retinal would be depleted therefore pigment regeneration would be slow. After a brief bleach there would not be sufficient time for photopigment regeneration to occur during the bleach itself. Therefore at the end of the bleach the plentiful supply of 11-*cis* retinal may allow rapid photopigment regeneration. This view, that the availability of 11-*cis* retinal is responsible for rapid recovery following short bleaches, is supported by Coolen and van Norren (1988).

If it is accepted that the regeneration of photopigment is limited by the availability of 11-*cis* retinal and that receptors have access to different sources of 11-*cis* retinal then it is remarkable that photopigment regeneration follows a single exponential time course. Indeed it now appears that the regeneration of photopigment does not strictly adhere to an exponential function. Smith *et al.* (1983) measured cone photopigment regeneration following exposure to a 6 log td bleach that lasted for either 10 seconds or 2 minutes. Their densitometric data indicate that an exponential function provides a good description for regeneration following a 10 second period of light adaptation but not for longer exposures.

Although considerable emphasis has been placed upon retinal densitometry it is important to realise that inactivation of metarhodopsin II involves multiple phosphorylation of the opsin followed by binding to s-antigen, reactions that are very likely to effect threshold but ones that do not alter the spectral absorbency of the retina (Lamb, 1990).

It is of interest to note that the regeneration of cone pigment in protanopes, deuteranopes and in colour normal subjects follows a similar time course, (Rushton, 1965; Baker and Rushton, 1965; Rushton and Henry, 1968). This finding has been confirmed more recently by Smith *et al.* (1983).

In summary, receptoral threshold is raised during dark adaptation because a photoproduct resulting from the period of light adaptation (most likely opsin) produces an 'equivalent background' excitation. This excitation acts very much like light itself and consequently invokes the adaptational mechanisms associated with light adaptation.

The rate at which receptoral threshold declines during dark adaptation is determined by the rate at which opsin can recombine with 11-*cis* retinal. Cones may obtain 11-*cis* retina from several sources and therefore the return of sensitivity is relatively rapid but rods may only obtain 11-*cis* retinal from the RPE and hence the return of scotopic sensitivity is relatively slow.

1.5.3.3 Post receptoral mechanisms in dark adaptation

Photopigment bleaching and activation of the transduction cascade by opsin are only two of the mechanisms involved in dark adaptation. Additional receptoral and post receptoral processes also contribute to the dark adaptation function obtained in psychophysical investigations. Some of the post-receptoral processes are discussed below:

Rushton (1965) introduced the idea of the 'adaptation pool' to explain the finding that non uniform bleaches produced by an array of spots produces almost identical dark adaptation curves to those obtained following a uniform bleach which on average bleached the same amount of pigment. This result indicated that the rate of dark adaptation is not limited by the rods themselves but at a post-receptoral pooling centre. The idea that signals from individual rods are pooled is supported by Rushton's assertion that the scotopic increment threshold begins to rise when on average, individual rods receive less than one quantum hit per second, indicating that the desensitisation produced by a weak light must be as a result of pooled signals (Rushton, 1965). Shapley and Enroth-Cugell (1984) suggest that the 'adaptation pool' has its origins in the receptive fields of ganglion cells. By bleaching the retina with gratings that differed in spatial frequency Cicerone and Hayhoe (1990) determined that the area desensitised by a bleaching light corresponds to the receptive field size of the bipolar cell. In the scotopic system at least, threshold during dark adaptation is not directly determined by receptors but rather by the gain of a post-receptoral site, which is set by signals originating from all the rods that make up its receptive field.

Recently, Cicerone *et al.* (1990) examined the spread of bleaching adaptation for human cone vision in the fovea and parafovea. They bleached retinal photopigment with a variety of square wave gratings (the bars of the gratings subtended 10, 7.5, 5 or 2.5 min

of arc) and an equal energy uniformly illuminated field. Following the period of light adaptation, threshold was measured using a circular test that subtended 0.5° (following exposure to the 2.5 and 5 min grating bleaches) or one that subtended 1° (following exposure to the 10 min grating). Cicerone *et al.* (1990) concluded that there is little spread of bleaching adaptation for cone vision. However there are several problems with the study. Firstly there is no mention of the test sizes used for the uniform bleach or the 7.5 min grating. This is unfortunate because test size has been shown to influence the course of dark adaptation. Threshold falls more rapidly for large tests than small ones (Arden and Weale, 1954). Therefore, the relatively rapid recovery in sensitivity following the 10 min grating bleach (and possibly the 7.5 min grating) may simply be due to the fact that the investigators used a 1° test for this condition rather than the 0.5° test used for finer gratings. Secondly, although the investigators collected data on 4 sessions, only data from 1 session is presented. Presumably this data was typical? Thirdly, the authors claim that the dark adaptation functions obtained in the parafovea and fovea are similar for the uniform and 5 min gratings bleaches but dissimilar for 7.5 and 10 min gratings. Examination of their data does not reveal a clear distinction (except for the 10 min grating but this may be due to test size).

Lateral interactions in the retina are also required to explain the large and sustained threshold rise observed following small brief bleaches. Hayhoe (1979) obtained dark adaptation functions for small, brief tests centred 5° from fixation following exposure to a brief (50 msec) bleach of 7.7 log td that was either 27 min or 115 min in diameter. In the investigation of cone function the test was red (630 nm cut off), 20 msec in duration and 3 min in diameter (see Figure 1.34).

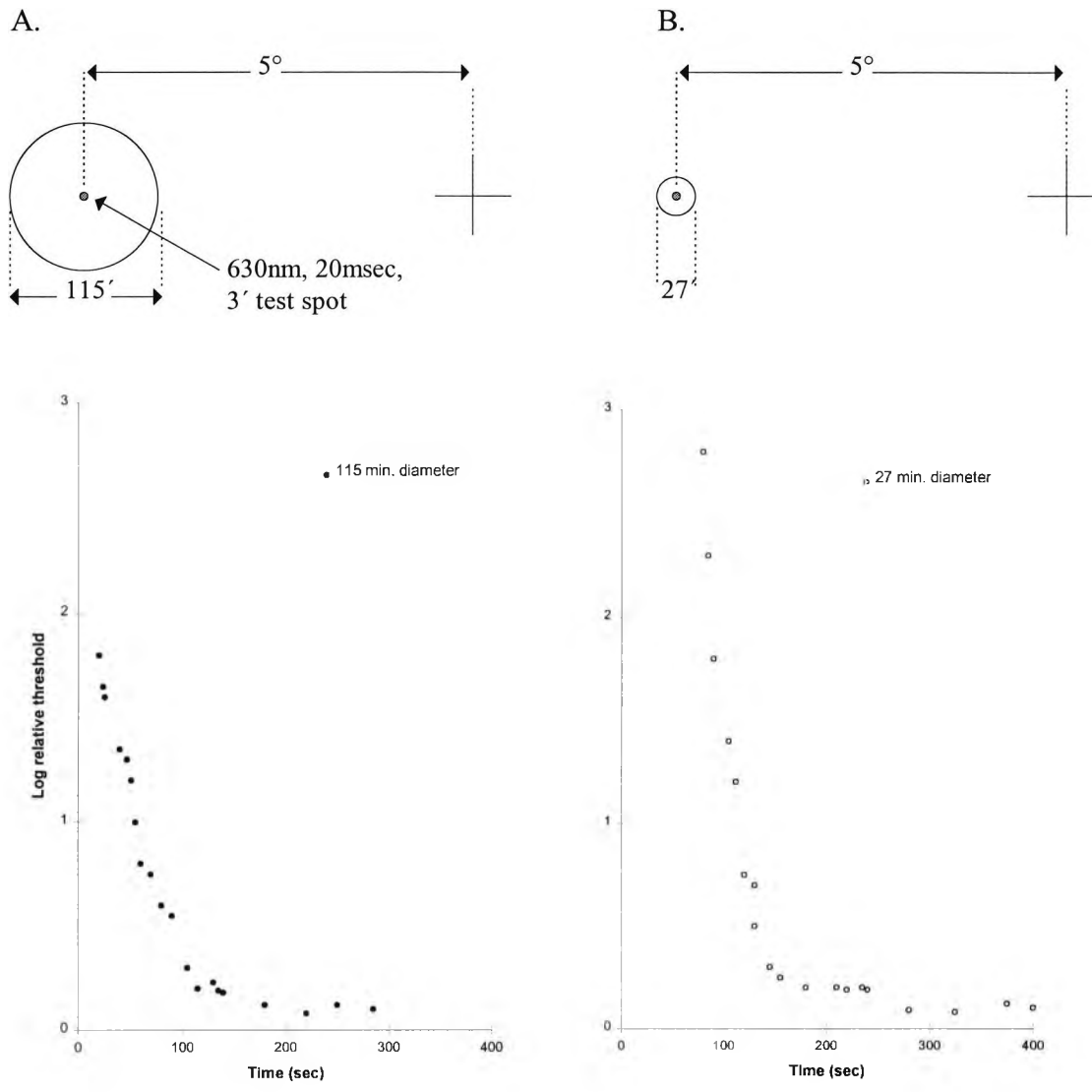

Figure 1.34 Schematic diagram of experimental parameters (top) and results of cone dark adaptation (after Hayhoe, 1979). After exposure to a relatively large bleach (A) threshold falls rapidly and asymptotes after approximately 150 seconds. When a small bleach is used (B) recovery is delayed and initial threshold elevation high. This is followed a precipitous drop in threshold.

Following exposure to the large bleaching field, threshold was initially elevated by 2 log units. Thereafter threshold fell rapidly and asymptoted after approximately 150 seconds. After exposure to the small field, recovery was much delayed and no measurements were possible for 70 seconds. After this, threshold fell precipitously over more than 3 log units and asymptoted again after approximately 150 seconds. In the investigation of rod function the test flash was 486 nm but conditions were otherwise identical. In this case the resulting dark adaptation functions were the same following large (115 min) or small (36 min) bleaches. These results indicate that lateral interactions operate during

dark adaptation. Horizontal cells have large receptive fields and are therefore poorly stimulated by small fields. Following the bleach, lateral antagonism provided by the horizontal cells in response to the 'equivalent background' excitation in the receptors, is minimal following the tiny bleach but much greater following the large one. The relatively large antagonistic input following a large bleach may be sufficient to bring bipolar cells back to their normal operating range allowing them to respond to the test.

Further evidence that post-receptoral elements are involved in dark adaptation was provided by Arden and Weale (1954) who used a Crooks adaptometer to investigate the effect of test size on the dark adaptation function. Following a 5 minute period of light adaptation, dark adaptation functions were obtained for tests of different sizes placed at different retinal locations. The test was either a 7° circular field which was presented 8° from fixation or a 2.7 min triangular test presented at the same retinal location or at the fovea, see Figure 1.35. Threshold for the smaller test was higher throughout dark adaptation but both showed rod and cone phases when the test was located 8° from fixation. When the small triangular test was centred on the fovea, threshold was lower than when presented in the parafovea but no rod branch was apparent. Their results showed that the rate of dark adaptation is dependant upon test size. Specifically, during the rod phase of dark adaptation, the rate of adaptation is found to increase with the size of the test field.

Test size then determines threshold magnitude and the rate at which dark adaptation proceeds, e.g. after 8 minutes in the dark, the rate of dark adaptation for a small 2.7 min test positioned 8° from fixation was 0.16-0.22 log units /min but for a large 7° field at the same retinal location it was 0.44 log unit/min. Arden and Weale (1954) attributed this difference in recovery rate to an increase in the integrating power of the retina as dark adaptation proceeds.

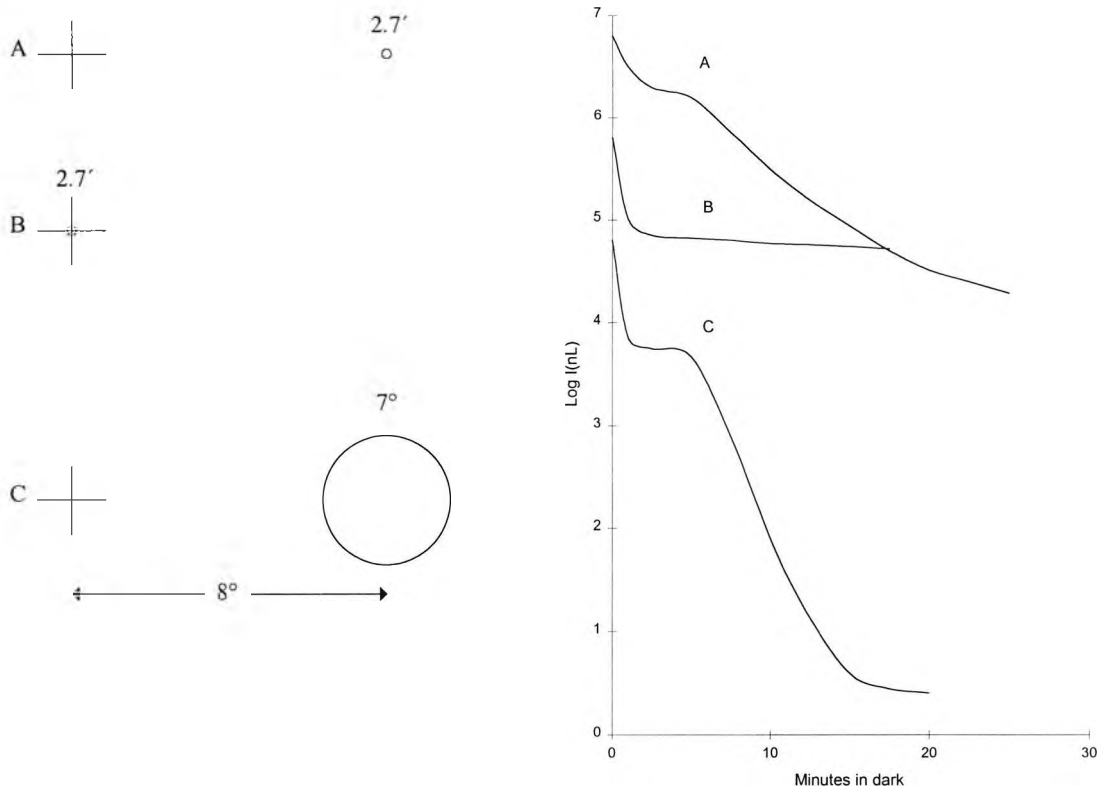

Figure 1.35 Dark adaptation curves measured 8° from fixation (A = 2.7′ test, C = 7° test) and at the fovea (B = 2.7′ test) (after Arden and Weale, 1954).

There are several possible reasons why spatial summation increases during dark adaptation. One possibility is that the receptive fields in the retina increase in size during dark adaptation. Using sinusoidal gratings and measuring CS in cat ganglion cells (X cells), Enroth-Cugell and Robson (1966) found that receptive field size almost doubled when mean illumination was varied from 3.3 log cdm^{-2} to 1.2 log cdm^{-2}. Such an increase in receptive field size may also explain the finding that any spatial frequency appears to be relatively higher to the dark adapted eye (Virsu, 1975). Virsu (1975) presented two sets of drifting gratings to one eye. The luminance of one grating was varied (0.05 to 5 td) and the subject adjusted the spatial frequency of a grating of fixed luminance (5 td) so that it appeared similar to the lower luminance grating. However, the effect observed by Virsu was relatively small (a 4 c.p.d. grating appeared to have a spatial frequency of approximately 4.8 c.p.d. (a 20% increase) when grating luminance was reduced by 2 log units. Shapley and Enroth-Cugell (1984) argue on the basis of the results of Enroth-Cugell *et al.* (1977b) that the receptive field centre size is relatively constant from mid-scotopic to mid-photopic levels and that centre size only increases

slightly in the low scotopic range. Therefore, it seems unlikely that increasing receptive field size accounts for the large observed increase in spatial summation during dark adaptation.

A more likely explanation for the increase in spatial summation during dark adaptation is that large receptive fields mediate detection in dark adapted conditions but cells with smaller receptive fields mediate detection at earlier stages following light adaptation. One explanation why large receptive fields mediate vision after a long time in the dark but not immediately after a period of intense light adaptation is that such fields are relatively more light adapted at any point in time following a bleach than other ganglion cells (Shapley and Enroth-Cugell, 1984). Therefore, following exposure to bright light ganglion cells with large receptive fields are relatively more desensitised than smaller ones and hence are not capable of mediating vision until relatively late in dark adaptation.

If the difference in recovery rates observed in Arden and Weale's (1954) data are due to threshold being determined by different spatial filters at different times during dark adaptation, then dark adaptation functions using stimuli localised in space and time should produce dark adaptation functions that recover at the same rate.

1.5.4 Periodic studies

Stimuli that vary sinusoidally over space and time are particularly useful in examining the properties of the visual system because the response of the system at threshold is determined by a single pathway. Although periodic stimuli have been used extensively to study steady-state adaptation (e.g. van Nes and Bouman 1967, Daitch and Green 1969) they have only been used occasionally to study dark adaptation. There have been several investigations of sinusoidal flicker sensitivity during dark adaptation but only one of sinusoidally-modulated gratings.

In steady state investigations periodic stimuli are usually described by their contrast. In the dark this unit is meaningless because light of any intensity compared to darkness has a contrast of 1. Therefore, the few studies that have been conducted present the data as modulation amplitude or illuminance (of Imax) as a function of time.

Both flicker and grating studies are discussed below.

1.5.4.1 Flicker sensitivity during dark adaptation

Most studies of dark adaptation determine the visual system's sensitivity to the presence of light (detection threshold). However changes in detection threshold do not necessarily reflect changes in other visual attributes (Frumkes, 1990).

A dark adaptation function obtained by adjusting the luminance of a low frequency flickering test to threshold is qualitatively similar to a typical dark adaptation function. Threshold falls throughout such an investigation and cone and rod limbs are evident. When the frequency of the test is increased (above about 7 Hz) the dark adaptation function undergoes a profound change. Threshold falls during the initial stage of dark adaptation but then rises at approximately the same time that rods would be expected to determine threshold.

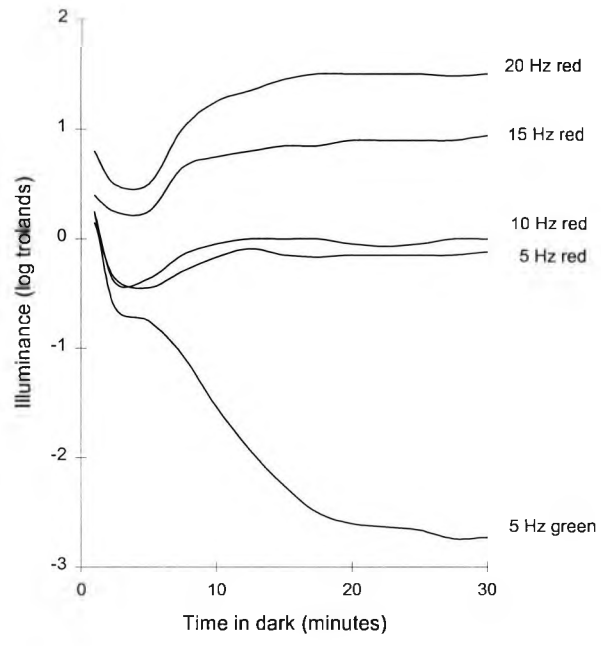

Figure 1.36 Dark adaptation functions for a variety of flickering test stimuli. Threshold was the point at which flicker could just be detected. After Goldberg *et al.* (1983).

Several studies have provided evidence that dark adapted rods tonically inhibit cone mediated flicker detection. This phenomenon is known as suppressive rod-cone interaction (SRCI) and was first observed by Goldberg *et al.* (1983). They presented a sinusoidally flickering test 2.33° in diameter, 7° from fixation following exposure to a

46000 td white field for 1 minute. The subject's task was to adjust the intensity of the test to the point where flicker was just apparent. Data from a 5 Hz green test resembled the usual 2 phase dark adaptation function. The upper limb was attributed to cones and the lower limb to rods. Sensitivity increased throughout dark adaptation providing the test flickered below 7 Hz. Sensitivity to red, green or yellow 20 Hz flicker also increased during the cone phase of dark adaptation but during the rod phase of dark adaptation, sensitivity declined. Only the cones are thought to be able to respond to such high frequencies and therefore the increase in threshold was attributed to loss of cone sensitivity, (temporal acuity of the rod system is 25 Hz at 13×10^{1} scot td but only 5 Hz at 13×10^{-3} scot td (Hess and Nordby, 1986)). Goldberg *et al.* (1983) also measured flicker sensitivity using a, scotopically equated, red / green test that flickered in counterphase. Sensitivity to this test also declined during the rod phase of dark adaptation even though it did not provide a stimulus to the scotopic system. It was concluded that the loss of high frequency flicker sensitivity is due to a tonic inhibitory effect exerted by dark-adapted rods on cones. Similar effects have been reported by Coletta and Adams (1984) and Alexander and Fishman (1984). Suppression of cone mediated flicker was attributed to rod activity because altering the wavelength of the bleach had no effect on the data corresponding to the rod phase of dark adaptation providing the scotopic illuminance of the bleach was fixed (Goldberg *et al.,* 1983). Additional evidence that suggests that the effect is due to rods is that the rise in cone-mediated flicker threshold coincides with the time that the rod-cone break is usually observed (however there are exceptions[2]).

Several studies have examined this flicker SRCI effect in individuals with retinal pathology and attributed the effect to processing in the distil retina (Alexander and Fishman, 1985; Arden and Hogg, 1985). More specifically flicker SRCI has been attributed to an inhibitory influence of horizontal cells on cone pathways which is determined by the rods (Arden and Hogg, 1985). Further evidence that the rod effect is

[2] Such coincidence is not evident in the data of Alexander and Fishman (1984) Sensitivity to a 25 Hz, 1.733° white test presented 20° from fixation fell after approximately 2 minutes of dark adaptation but when the subjects task was to detect the presence of the same test flashed for 500 msec the rod cone break occurred after 10 minutes.

mediated by horizontal cells has been provided by electrical recordings from the mudpuppy retina. Pharmacological agents that selectively block horizontal cell activity abolish the flicker SRCI effect (Eysteinson and Frumkes, 1989).

The finding that flicker SRCI is absent in protanopes (Coletta and Adams, 1985; Frumkes *et al.,* 1988; Goldberg and Frumkes, 1983) suggests that the interaction takes place between rods and a long wavelength sensitive cone mechanism.

Interestingly, the initial recovery of sensitivity to high frequency flicker (< 2 minutes) is dependant upon the duration of the bleach. Recovery of sensitivity to high frequency flicker is relatively rapid following a brief bleach but is delayed after a long one. This is remarkable because bleach duration has no effect on recovery of sensitivity to low frequency flicker, (Hayhoe and Chen, 1986).

1.5.4.2 Grating detection during dark adaptation

Several authors have studied grating acuity during dark adaptation (Brown *et al.,* 1953; Blakemore and Rushton, 1965a; Brown *et al.,* 1969; Coletta *et al.,* 1986; Naarendorp *et al.,* 1988 and Hahn and Geisler, 1995).

Despite these studies, knowledge about how spatial vision changes during dark adaptation is both limited and equivocal.

Our knowledge is limited because none of the studies have measured sensitivity using sinusoidal gratings throughout the course of dark adaptation. Most previous studies of spatial vision during dark adaptation have used square wave gratings and modulated grating intensity using neutral density filters. Although this arrangement keeps the contrast of the grating constant, the harmonics contained in a square wave grating may have influenced the results. The only study to have used sinusoidal gratings was that of Hahn and Geisler (1995) and in their experiment, thresholds were only recorded for the first 15 minutes of dark adaptation.

The results of previous studies are equivocal in as much that some studies show a rise in high spatial frequency grating threshold during the rod phase of dark adaptation, a grating SRCI effect, (Coletta *et al.,* 1986; Naarendorp *et al.,* 1988) and others do not,

(Brown *et al.,* 1953; Brown *et al.,* 1969). The following paragraphs describe these studies in detail.

Brown *et al.* (1953) measured the recovery of grating acuity during dark adaptation in 2 normal subjects. Initial light adaptation was achieved by exposing both eyes to a surface with a luminance of 1500 millilamberts for 5 minutes. For the following thirty minutes, gratings (which subtended 7.3°) were presented to the subject's fovea once every minute (to minimise the possibility that the test would produce light adaptation). Subjects were required to identify the orientation of the grating and 'threshold had to be estimated.....on the basis of data for several sessions'. For low spatial frequency gratings (1.25 and 2.5 c.p.d.) dark adaptation functions obtained in this way show the typical 2 stage recovery of sensitivity. For finer gratings (7.5, 18 and 31.2 c.p.d.) thresholds were elevated and the rod branch of the recovery was absent but there was no evidence of a rise in threshold during the rod phase of dark adaptation.

Blakemore and Rushton (1965a) obtained both dark adaptation and increment threshold functions using a variety of gratings as the test stimuli. Although their data provide strong support for the concept of an 'equivalent background' it tells us relatively little about how spatial vision changes during dark adaptation in normal subjects because their subject was a rod monochromat.

Evidence that rods may inhibit cone function during dark adaptation (Granit, 1947 cited in Brown *et al.,* 1969) led Brown *et al.* (1969) to re-examine the recovery of spatial vision during dark adaptation. After exposing one eye to 1500 millilamberts for 4 minutes to light adapt the retina, subjects (n=2) were required to report the orientation of a 7.5 c.p.d. ('0.25 acuity') grating. The gratings subtended 3° and were presented 3° from the fovea. The results show that threshold drops rapidly over the first 5 minutes to a plateau that continued to the end of the data collection period (30 minutes). The authors concluded that 'recovery of the rod process...is not accompanied by any suppression or any special effect on the photopic process'.

Following a pre-adaptation bleach (unspecified in the abstract), Coletta *et al.* (1986) obtained dark adaptation functions for various high spatial frequency gratings (unspecified). The gratings which subtended approximately 0.4° were viewed foveally. Maximum sensitivity to the gratings was observed after 1-2 minutes of dark adaptation

and after 4 minutes sensitivity declined by 0.1 to 0.4 log units. The authors concluded that 'rods may have a small influence on cone spatial resolution'.

A considerably larger effect was described by Naarendorp *et al.* (1988). The author and one other subject participated in the experiment, but only the dark adaptation data from one of the subjects was presented. After exposure to approximately 30000 td for 1 minute dark-adaptation functions were obtained for a variety of spatial frequencies (1.75, 7, 14 and 21 c.p.d.). The gratings, presented for 600 msec once every 5 seconds, were centred 3° from fixation and subtended 6°. Subjects continuously adjusted grating luminance to threshold until adaptation was complete. The data presented by Naarendorp *et al.* (1988) showed that threshold to high spatial frequency gratings (7, 14 and 21 c.p.d.) rose during the rod phase of dark adaptation. For the 7 c.p.d. grating the effect was small but for the 21 c.p.d. grating there was an approximately 0.8 log unit rise in threshold. The data in the original study (Naarendorp, 1987) for the other subject is less impressive. There is no evidence of a rise in threshold for the 7 c.p.d. grating and only a 0.5 log unit rise in threshold for the 14 c.p.d. grating. No data was obtained for the 21 c.p.d. grating.

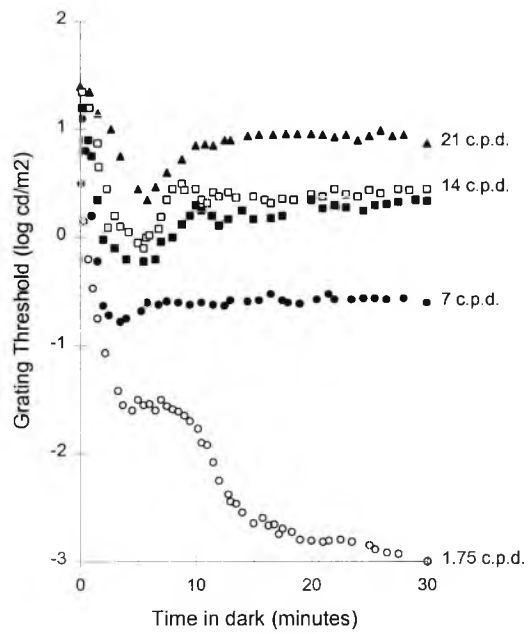

Figure 1.37 Threshold grating luminance as a function of time in the dark. Each shape represents a different spatial frequency square wave grating. The open symbols represent data obtained with a 'green' grating and the filled symbols represent data obtained with a 'red' grating. After Naarendorp *et al.* (1988).

Naarendorp *et al.* (1988) established that the effect was due to the rods by showing that the action spectrum of a dim field that removed the suppression of cone-mediated spatial vision matched that of the scotopic V'(λ) function.

More recently Hahn and Geisler (1995) used sinusoidal gratings to examine the recovery of spatial vision during dark adaptation. Two subjects participated in the experiment. Following exposure to a 5.77 log td field for 2 minutes, a Gaussian damped increment gabor (1,3,7,10 and 15 c.p.d.), positioned at the fovea, was presented for 250 msec once every second. Threshold was determined using the method of adjustment for 15 minutes in the dark. Sensitivity recovered monotonically throughout the investigation and the authors summarised their data with a simple exponential decay function of the following form:

$$\log A(t) = \alpha e^{-t/to} + \beta$$

where $A(t)$ is the amplitude threshold at time t, β is the dark adapted threshold, α is the initial rise in log threshold and *to* is the time constant of recovery. There was no evidence of a decline in sensitivity at any time during the investigation. However, the absence of a grating SRCI effect in this study is not in conflict with the findings of Coletta *et al.*, 1986 and Naarendorp *et al.*, 1988. Hahn and Geisler (1995) only measured dark adaptation for the first 15 minutes and it is quite possible that grating SRCI would have been delayed until beyond the end of their measurement period.

One further criticism of Hahn and Geislers' (1995) study is that they used a CRT to display sinusoidal 'increment gabors' and modulated the intensity of the light bars of the grating (I_{max}) directly. While this stimulus configuration has a number of advantages, the contrast of the grating will only remain constant if $I_{min} = 0$. Since I_{min} cannot be 0 on a CRT display it is likely that the contrast of the display varied to some degree with I_{max}.

The study reported in the following chapter re-examines the recovery of spatial vision during dark adaptation. It is the first to obtain dark adaptation functions throughout the full course of dark adaptation (30 min) using sinusoidal gratings as the test stimuli.

1.6 Summary

This chapter started by describing the basic anatomy and electrophysiology of the visual system with particular emphasis on the retina where most sensitivity regulation is thought to take place. The neural retina is composed of 6 basic types of cells. Information is transmitted longitudinally through the retina from the receptors to the ganglion cells via bipolar cells. Lateral interactions are possible at the outer plexiform layer which contains horizontal cells and at the inner plexiform layer that contains amacrine cells. Retinal interplexiform cells may subserve a feedback pathway from inner to outer plexiform layers. Information contained in the visual scene is transmitted to proximal visual centres by several parallel pathways. Different pathways subserve different aspects of vision and their sensitivity may be determined by any of the components that make up that pathway.

Although, sensitivity may be regulated by any of the components of the visual system it is thought that most sensitivity regulation takes place within the eye itself. Sensitivity may be determined by; pupil size, quantal noise, noise from within the visual system itself, the class of receptors mediating detection, photopigment density as well as receptoral and post-receptoral adaptational processes.

The steady state sensitivity of the visual system has been described in several ways. For aperiodic stimuli (such as abruptly presented test spots) sensitivity is typically described by the increment threshold function (a plot of increment threshold as a function of background intensity). Stable contrast sensitivity (the goal of sensitivity regulation) is denoted by an increment threshold function with a slope of 1 (Webers law). In the scotopic system slopes approaching 1 are only observed for large, long duration test stimuli. In the photopic system a slope of 1 may be achieved for any test providing the background luminance is sufficiently great. For periodic stimuli sensitivity is typically described in terms of contrast sensitivity. The steady state sensitivity of the visual system may then be described by a series of contrast sensitivity functions (plot of log contrast sensitivity as a function of spatial frequency) at different mean luminances.

Adaptational mechanisms take a finite length of time to adjust following an abrupt change in retinal illuminance. This feature has been exploited to show that adaptational mechanisms may work in a multiplicative or subtractive manner.

The recovery of sensitivity following a period of intense light adaptation is usually described by a dark adaptation function (plot of log threshold as a function of time). During a typical dark adaptation investigation threshold falls in 2 phases. The initial phase has been attribute to cone function and the second phase, which usually occurs after 5-10 minutes, has been attributed to rods. In total it can take up to about 45 minutes for the visual system to attain maximum sensitivity. This slow recovery is thought to be largely determined by the concentration of a photoproduct in the receptors (the photochemical hypothesis). At any time during dark adaptation the sensitivity of the visual system may be described in terms of an 'equivalent background' (the equivalent background hypothesis). This background may be produced by opsin, which is capable of activating the transduction cascade.

When the sensitivity of the visual system is probed using high frequency flicker (stimuli that are only be detected by cones) threshold does not decline throughout the course of dark adaptation. Rather, the initial fall in threshold is followed by a rise in threshold which occurs at about the same time that rods usually determine sensitivity. This loss of sensitivity has been attributed to rod suppression of cone-mediated vision and is known as flicker suppressive rod-cone interaction (SRCI).

Relatively little is known about how spatial vision changes during dark adaptation. There have been no studies of how sensitivity to sinusoidal gratings varies throughout the full course of dark adaptation and there is equivocal evidence as to the existence or otherwise of grating SRCI.

The following chapter shows how threshold to sinusoidal gratings varies throughout the course of dark adaptation in normal and dichromatic subjects.

2. Recovery of spatial vision during dark adaptation

2.1 Introduction

Since the pioneering experiments of Hecht *et al.* (1937), there have been numerous studies of dark adaptation. Most of these studies have measured changes in the absolute sensitivity of the eye to a circular test patch presented in darkness. Relatively little is known about the characteristics of spatial vision during the course of dark adaptation.

Most previous studies have used square wave gratings as the test stimulus, (Brown *et al.*, 1953; Blakemore and Rushton, 1965a; Brown *et al.*, 1969; Coletta *et al.*, 1986; Naarendorp *et al.*, 1988). Such stimuli contain harmonics that may have influenced the results. Furthermore, data obtained using square wave gratings is contradictory, with regard to the existence of grating suppressive rod-cone interaction (SRCI), and there is no information about how sensitivity to sinusoidal gratings varies during the full course of dark adaptation, (see section 1.5.4.2, in Chapter 1, for a description of each of the studies)

2.1.1 Grating suppressive rod-cone interaction

The rise in threshold observed for high spatial frequencies after 5-10 minutes of dark adaptation by Coletta *et al.* (1986) and Naarendorp *et al.* (1988) has been attributed to grating SRCI. This effect is qualitatively similar to that observed for high frequency flicker, (the flicker SRCI effect). This similarity led to the belief that both effects had a similar origin (Frumkes, 1990). However recent evidence suggests that the flicker and grating SRCI effects originate at different sites in the visual system. Lange and Frumkes (1992) examined the influence of a large rod stimulating background of $0.01 cdm^{-2}$ upon the visibility of a 1° display centred 5° from the fovea. This display was modulated in both spatial and temporal domains. The effect of the rod-stimulating background was maximal when low frequency gratings were flickered rapidly or when high frequency gratings were flickered slowly. This result suggested that there is at least some independence between these effects. Similar results were obtained by Lange and

Frumkes (1993) who concluded that "rod-adaptation exerts separate influences upon cone-mediated temporal and spatial resolution."

The distinction between grating and flicker SRCI has been further demonstrated by the observation that partial rod light adaptation of the non test eye abolishes grating SRCI but has no effect on flicker SRCI (Frumkes *et al.*, 1995). This result suggests a distil origin for flicker SRCI but a central one for grating SRCI. However, this recently proposed idea, seems to be contradicted by an earlier observation. In a brief report, Frumkes *et al.* (1988) described the results of an investigation which showed that grating SRCI was present in colour normal subjects but was absent in a protanopic subject. Protanopes then do not exhibit flicker or grating SRCI. The similarity of the flicker and grating results for protanopes would suggest that both effects have a similar distil retinal origin namely, some interaction between rods and long wavelength sensitive cones.

This apparent contradiction suggests that there are either multiple sites for the grating SRCI effect (one in the outer retina and another beyond the chiasma) or a single central site that is abnormal in protanopes.

An alternative explanation is that light adaptation of the non-test eye improves high frequency grating detection by a mechanism distinct from the one that causes grating SRCI, i.e. grating SRCI is present when the non-test eye is partly light adapted but its desensitizing effects are overcome by an improvement in the absolute sensitivity of the system. If the two effects balance out then the rise in threshold associated with grating SRCI would no longer be apparent. Makous (1990) has shown that partial light adaptation of one eye reduces absolute threshold in the other eye and attributed this effect to a reduction in noise emanating from the non-test eye. If this reduction in noise is particularly important to processing in area V3 and V4 of the cortex (which subserves form vison) and less important to V5 (which subserves our perception of motion and flicker) then light adaptation of the non-test eye could conceivably abolish grating SRCI but have no effect on flicker SRCI.

2.1.2 Flicker SRCI is absent in Protanopes?

Flicker SRCI has been attributed to a mechanism that involves long wavelength sensitive (LWS) cones. However, there is little published data supporting this assertion. Frumkes (1989) states that flicker SRCI "particularly relates to the activity of the long wavelength cone mechanism", and in a separate article he says that flicker SRCI is "totally lacking in the four protanopes carefully investigated" (Frumkes, 1990). However, only 2 published studies support these assertions.

Goldberg and Frumkes (1983) examined flicker SRCI in normals, anomalous trichromats, deuteranopes and protanopes. They showed that steady-state flicker SRCI is absent in protanopes but present in the other subjects. Coletta and Adams (1984) examined the magnitude of the effect for stimuli of different wavelengths. The greatest effect was observed when long-wavelength stimuli were used.

Contradictory results were obtained by Coletta and Adams (1985) who examined flicker sensitivity in dichromats and colour normal observers. They used a 10min, 25Hz, 640nm test and showed that both protanopes and deuteranopes exhibit a similar SRCI effect. A study by Alexander and Fishman (1983) was cited by Coletta and Adams (1984) as providing evidence that protanopes do not exhibit a rise in flicker threshold during dark adaptation. However, although this abstract does indicate that subjects with retinitis pigmentosa, cone-rod dystrophy, congenital stationary night blindness, juvenile x-linked retinoschisis, autosomal dominant optic atrophy and colour deficiency were studied it does not describe the results of the colour deficient observers. In a subsequent paper (Alexander and Fishman, 1985) the authors present the results of all subjects except for the colour deficient observers.

2.1.3 Purpose

The purpose of this study was to:

1. provide basic information about how threshold to sinusoidally modulated contrast gratings varies throughout the course of dark adaptation.
2. examine grating SRCI in colour normals and dichromats.

2.2 Methods

2.2.1 Subjects

Four colour normal, two protanopes and one deuteranope participated in the experiment. Colour perception was quantified using the Nagel anomloscope. Dichromats were distinguished by determining the amount of yellow necessary to match pure green and red. All subjects had a normal fundal appearance and corrected log MAR of 0.00 or better. All subjects were experienced observers and participated in a practice session prior to data collection. Subject details are provided in Table 2.1 below:

	Clinical details		
Subject	Refraction	Log MAR acuity	Colour vision
W.D.T.	-1.75 / -0.75 x 5	-0.08	Normal
T.M.	+0.25 / -0.50 x 45	-0.10	Protanope
D.T	-0.25 DS	-0.10	Protanope
C.G.O	+1.25 DS	-0.14	Normal
J.M	-3.00 DS	-0.08	Normal
N.P	-0.25 / -0.25 x 140	-0.18	Normal
B.A	-2.75/+1.25 x 15	-0.12	Deuteranope

Table 2.1 Subject details.

2.2.2 Apparatus

A schematic diagram of the apparatus and test field is shown in Figure 2.1. The "bleaching" field was produced by a Maxwellian view optical system. The system was arranged to give a uniform circular field subtending 16° and a retinal illuminance of 6 log photopic trolands. Subjects were protected from excessive exposure to infra-red radiation by a suitable filter placed in the optical system. A computer-controlled shutter positioned at a secondary focus of the optical system was used to expose the "bleaching" field for a precise duration (10 seconds). Under these conditions approximately 96% of cone photopigment was bleached by the adapting field (assuming a half bleach constant of $3x10^4$ and a time constant of recovery of 73 seconds, (Hollins and Alpern, 1973)).

Subjects viewed the test stimuli through a 4mm artificial pupil, a neutral density (ND) wedge (OD range 0.05-3.56) and an electronic shutter. The position of the ND wedge

was recorded by the computer via a gear-driven 10 turn potentiometer linked to an analog-to-digital converter. A supplementary ND filter (OD 3.0) was added when required giving a total luminance range of 6.56 log units. The electronic shutter was operated under computer control and used to regulate exposure of the test stimuli. A bite-bar was used to maintain subject alignment.

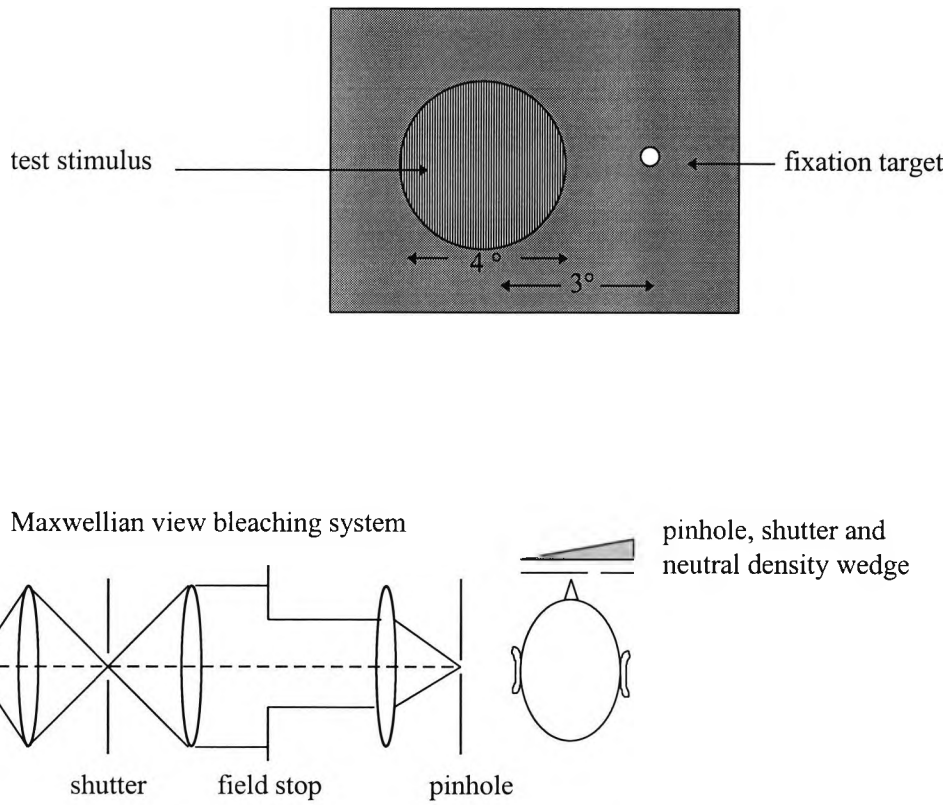

Figure 2.1 Schematic diagram of apparatus and test stimulus.

Gratings were generated by a Millipede Prisma VR1000 pattern generator interfaced to an IBM PC. All gratings had a contrast of 0.9 and were displayed on a "white" (P4) CRT display (maximum mean luminance 70 cdm^{-2}). Subjects fixated a small LED; the CRT display (masked to produce a 4° circular field) was centred 3° temporal to fixation.

The luminance / contrast of the CRT display was calibrated using an LMT photometer. Changes in screen luminance over time were minimised by displaying a blank screen at the mean luminance of the gratings used in the study (70 cdm^{-2}) for 1½ hours prior to each experimental session. The retinal illuminance produced by the Maxwellian view bleaching field was determined using a UDT photodiode and Oriel radiometer.

2.2.3 Determination of presentation sequence

For high spatial frequency gratings, the mean luminance required to resolve the grating may be as much as 4 log units higher than that required to detect the grating field. Clearly, presentation of the test field under these conditions may cause some light adaptation. In order to minimise the possibility of light adapting the retina it was important to minimise exposure to the test grating. A preliminary investigation was conducted in order to determine the optimum number of test presentations necessary to establish a stable threshold value while minimising light adaptation.

Two subjects participated in this pilot study. Two drops of 0.5% cyclopentolate were instilled 30 minutes before the experiment to paralyse accommodation and dilate the pupil. Subjects were then dark adapted for 30 minutes.

Before each threshold measurement the ND wedge was rotated to a random position. Gratings were then "flashed on" for 250 msec every 2 seconds and subjects were required to adjust the position of the ND wedge until the bars of the grating could just be perceived. After a predetermined number of presentations the shutter was closed and subjects sat in complete darkness for 20 seconds before the onset of the next presentation sequence. The position of the ND wedge was automatically recorded 1 second after the last grating presentation. The presentation cycle is summarised in Figure 2.2.

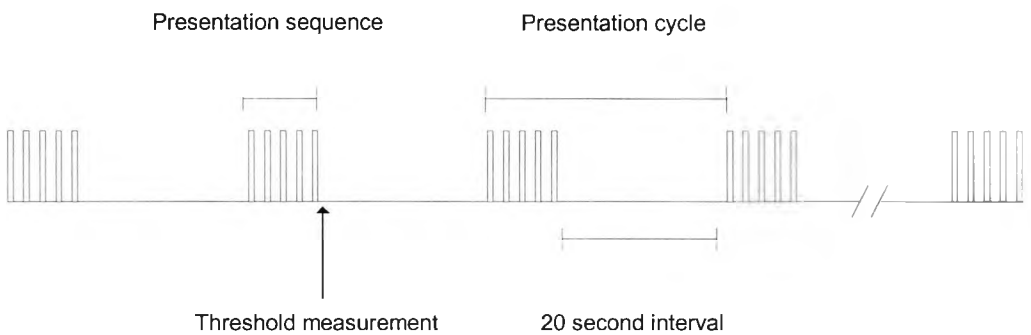

Figure 2.2 Presentation cycle, showing presentation sequence, point at which threshold was measured (1 sec after the last presentation) and 20 second rest period.

The number of exposures in each presentation sequence was varied (1, 3, 5, 7, and 10). Mean threshold for each spatial frequency and the standard error obtained for 10 repeated measurements for each subject is shown in Figure 2.3. On the basis of these

results, a presentation sequence that included 5 grating presentations was chosen, being the fewest presentations required to establish a reliable estimate of threshold.

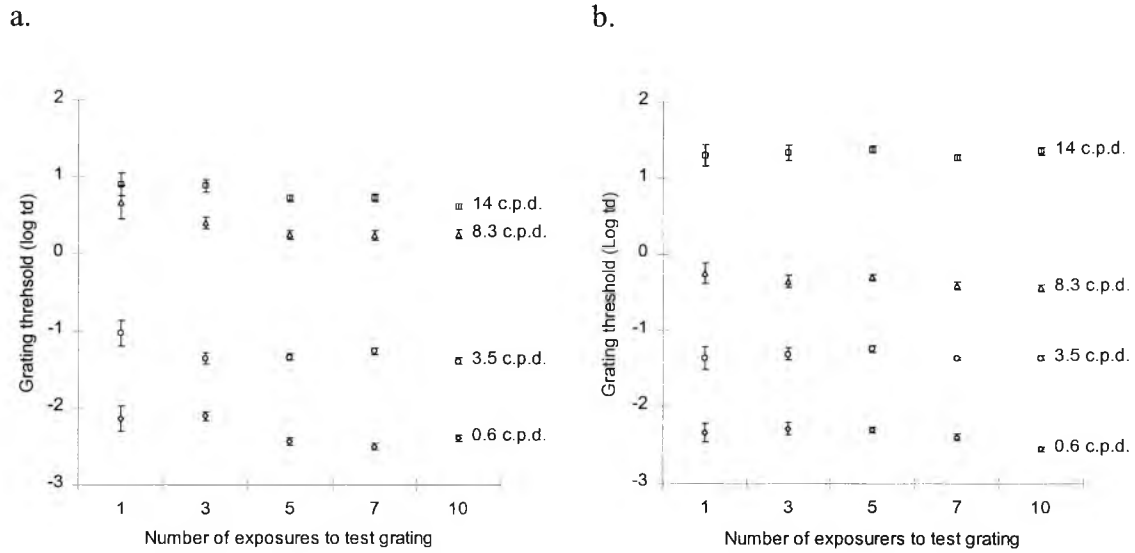

Figure 2.3. Effect of number of grating exposures on threshold for both subjects. Each point is the mean of 10 ND wedge settings. Error bars show ± 1 standard error. Panel a. shows the results obtained from subject T.M. and panel b. from subject C.G.O.

The final presentation sequence is summarised in Figure 2.4.

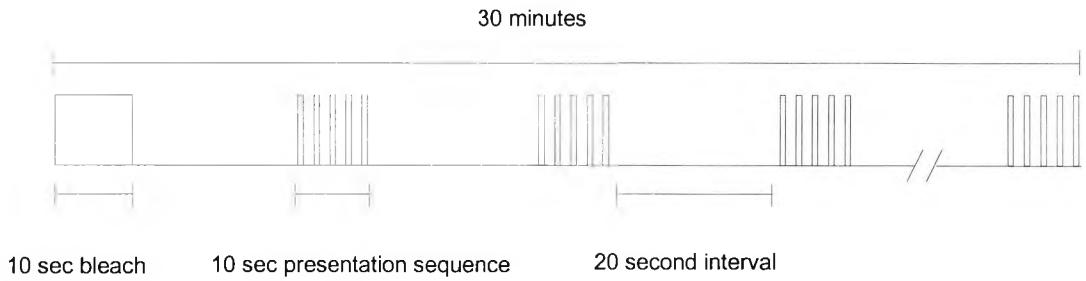

Figure 2.4 Stimulus presentation paradigm. Following a 10 second bleach the test grating was presented intermittently for 30 minutes in the dark.

2.2.4 Procedure

Two drops of 0.5% cyclopentolate were instilled 30 minutes before the experiment to paralyse accommodation and dilate the pupil. Results were particularly sensitive to

residual accommodation[1]. The refractive correction required to place the subjects' far point in the plane of the CRT display was then determined by refraction.

Following a 10 second exposure of one eye to the "bleaching" field, subjects turned to view the sinusoidal test grating through the artificial pupil, ND wedge and appropriate refractive correction. During each 10 second presentation sequence, subjects rotated the ND wedge until the bars of the grating were just perceived (subjects had no difficulty distinguishing, the task of resolving the bars of the grating from detection of the test field). The position of the ND wedge was automatically recorded 1 second after the last grating presentation, before a 20 second rest period in the dark. This test presentation cycle was repeated for 30 minutes in the dark.

2.3 Results

Results for each subject are plotted as log grating threshold as a function of time.

2.3.1 Colour normal subjects

Data for each of the colour-normal subjects is plotted in Figures 2.5 to 2.8 and presented elsewhere, (Margrain and Thomson, 1997).

Although only one data set for each subject is shown here, similar results were obtained from one normal and one protanope on a separate occasion. A slightly different paradigm was used on this occasion (the test was presented for 250 msec once every 2 seconds continuously throughout the course of dark adaptation).

---

[1] Results obtained from a preliminary investigation on 2 subjects using 1% Tropicamide as the cycloplegic produced variable results for high frequency gratings. This variability was attributed to residual accommodation, which in one case was as much as 2D. To minimise this source of error the amplitude of accommodation was measured using an RAF rule at the start of each experimental run. If it was found to be greater than 0.5D additional cyclopentolate was instilled.

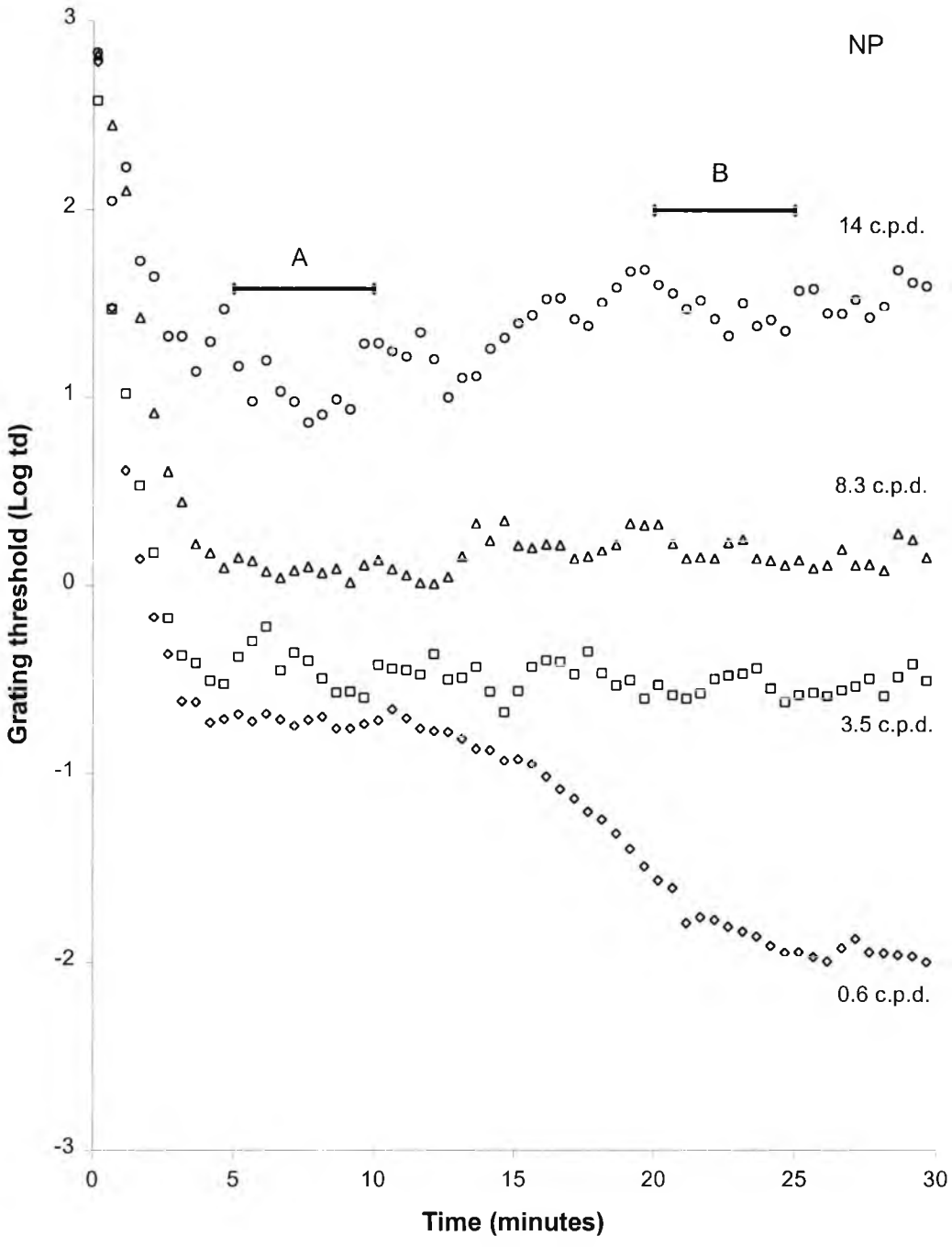

Figure 2.5 Log grating threshold as a function of time following following exposure to a 6 log td, white field for 10 seconds. All test gratings subtended 4° and were centred 3° from fixation. Each symbol represents a different spatial frequency and each point is a single data point. Subject NP had normal colour vision. Time interval A corresponds to the cone plateau period and interval B corresponds to a part of the dark adaptation function usually associated with rod function.

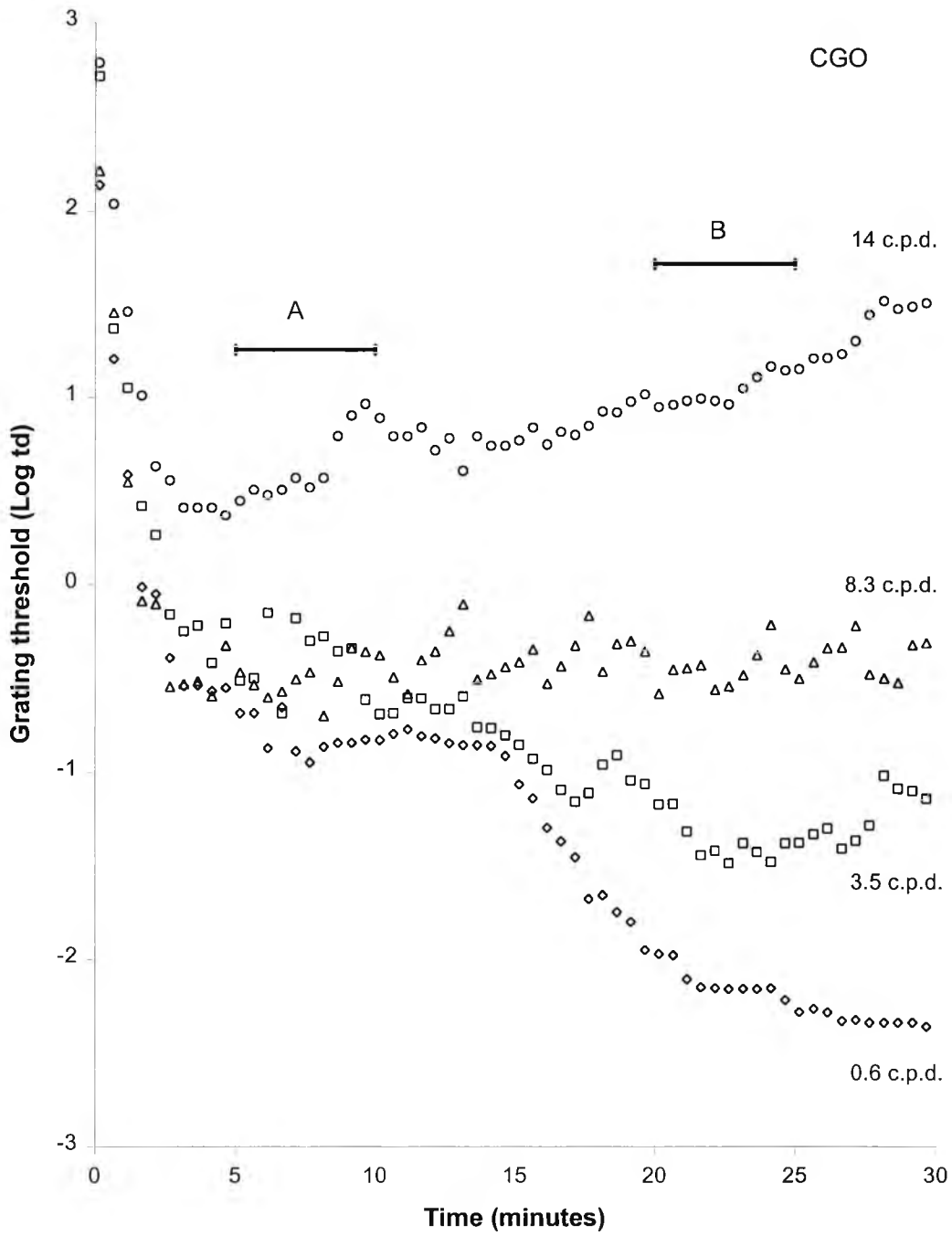

Figure 2.6 Log grating threshold as a function of time following following exposure to a 6 log td, white field for 10 seconds. All test gratings subtended 4° and were centred 3° from fixation. Each symbol represents a different spatial frequency and each point is a single data point. Subject CGO had normal colour vision. Time interval A corresponds to the cone plateau period and interval B corresponds to a part of the dark adaptation function usually associated with rod function.

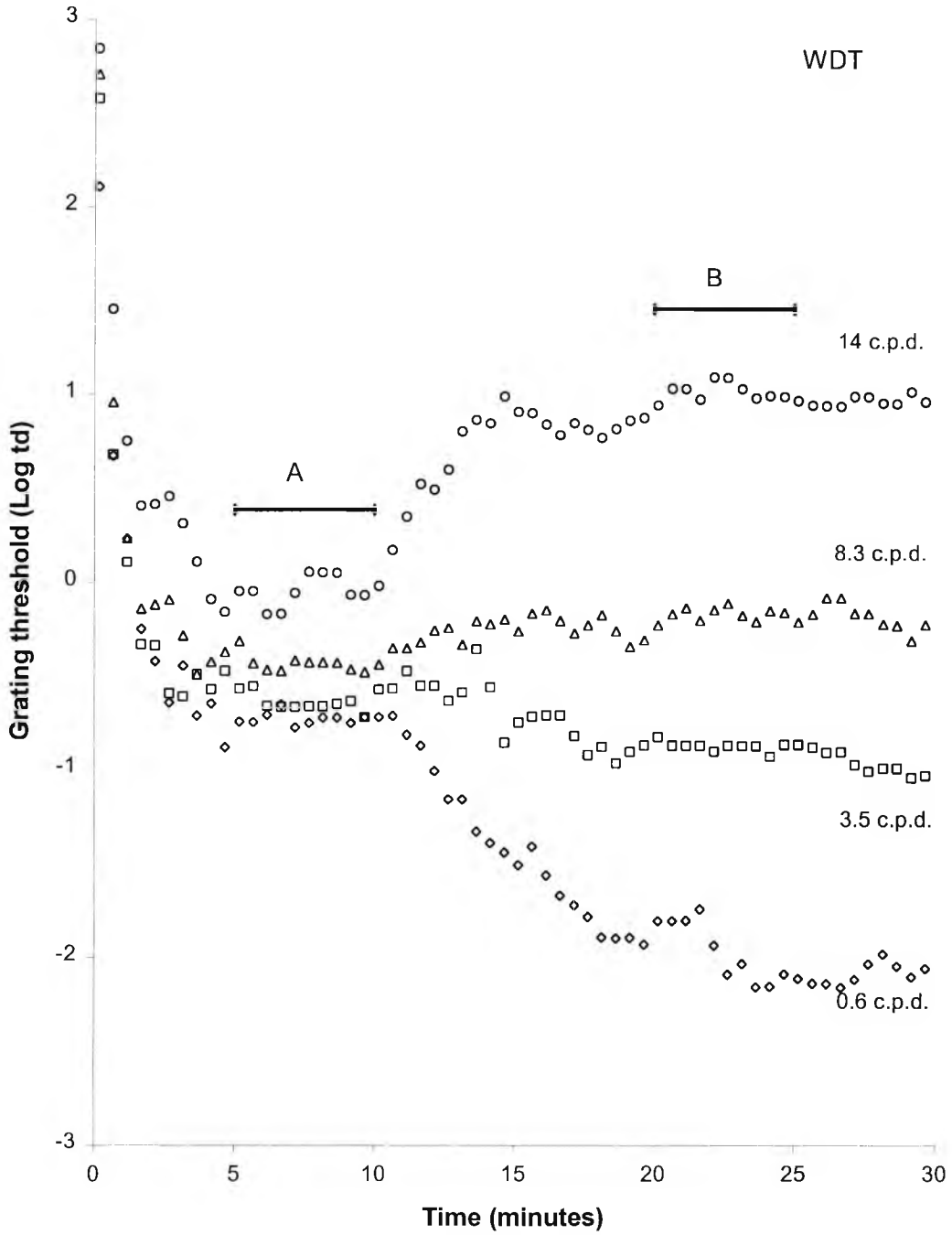

Figure 2.7 Log grating threshold as a function of time following following exposure to a 6 log td, white field for 10 seconds. All test gratings subtended 4° and were centred 3° from fixation. Each symbol represents a different spatial frequency and each point is a single data point. Subject WDT had normal colour vision. Time interval A corresponds to the cone plateau period and interval B corresponds to a part of the dark adaptation function usually associated with rod function.

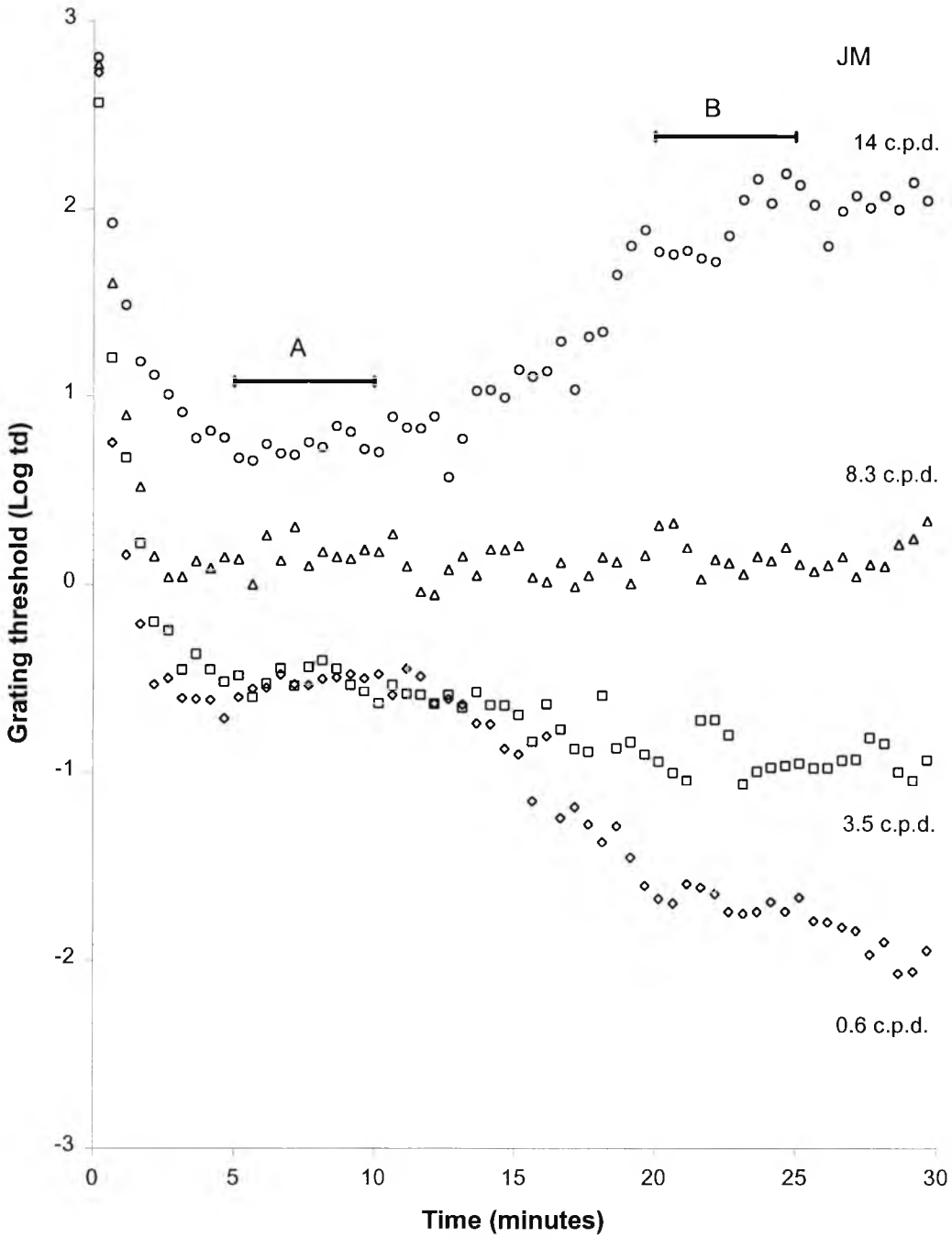

Figure 2.8 Log grating threshold as a function of time following following exposure to a 6 log td, white field for 10 seconds. All test gratings subtended 4° and were centred 3° from fixation. Each symbol represents a different spatial frequency and each point is a single data point. Subject JM had normal colour vision. Time interval A corresponds to the cone plateau period and interval B corresponds to a part of the dark adaptation function usually associated with rod function.

It can be seen from Figures 2.5 to 2.8 that threshold for the lowest spatial frequency was similar to a classical dark adaptation function, showing the typical cone and rod limbs. Although, threshold for the 3.5 c.p.d. grating showed a similar initial drop in threshold (attributable to recovery of cone sensitivity), the rod branch of the recovery is reduced / absent because this frequency is at the rod resolution limit, (Hess and Nordby, 1986).

The change in threshold for the 14 c.p.d. gratings is different from that of other frequencies in that after 5-10 minutes, threshold rises. Although this threshold rise is observed for all subjects there are subtle differences in the magnitude and form of the rise. To analyse this difference, mean threshold for the data collected after 5-10 minutes of dark adaptation, which approximately coincides with the cone plateau, (interval A in Figures 2.5 to 2.8) and mean threshold between 20-25 minutes (interval B in Figures 2.5 to 2.8) was compared. The difference in mean threshold over these two time periods for subjects NP, CGO, WDT and JM was 0.42, 0.40, 1.06 and 1.18 log units respectively. In all cases the increase in threshold was highly significant (t-test, $df = 9$, $p < 0.01$). Figures 2.5 to 2.8 also show differences in the form of the recovery. After 10 minutes of dark adaptation, WDT's threshold (Figure 2.7) for the 14 c.p.d. grating shows a relatively abrupt rise in threshold which then levels off after 15 minutes. The other subjects show a more gradual rise in threshold which continues until the end of the recording (30min).

Figure 2.9 shows the mean data for all subjects. The average standard error across all data points is shown by the error bars at the end of each dark adaptation function. Threshold for the 14 c.p.d. grating shows a mean threshold rise of 0.76 log units between 5-10 minutes (Figure 2.9 interval A), (which coincides with the cone plateau), and the mean threshold over the 20-25 minute interval (Figure 2.9 interval B). This increase was highly significant (t-test, $p< 0.01$). A similar but less marked effect (0.1 log units, $p< 0.01$) was found for the 8.3 c.p.d. grating.

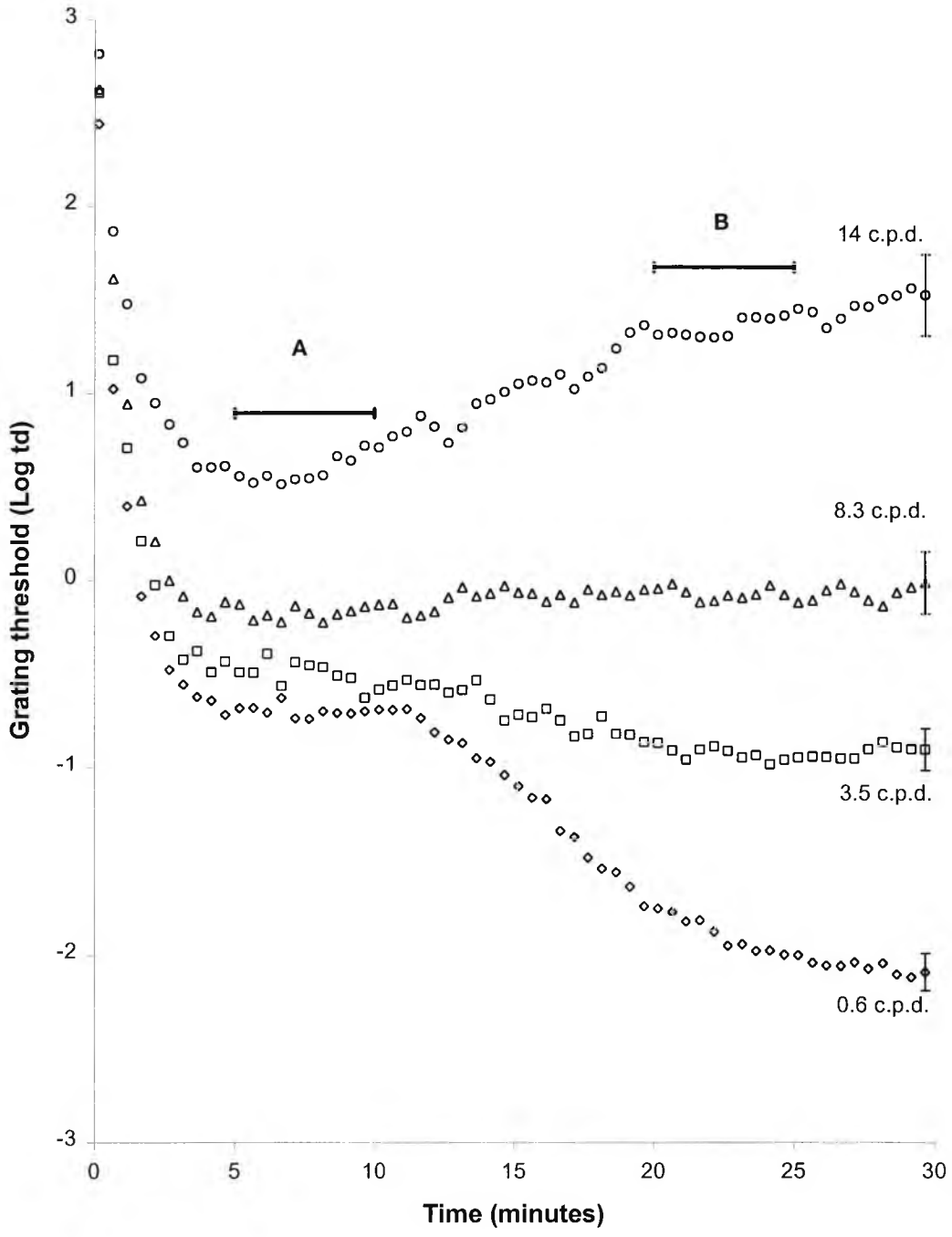

Figure 2.9 Dark adaptation curves for 4 spatial frequencies. Each point is the mean threshold value for all subjects with normal colour vision. The error bar at the end of each dark adaptation function indicates the size of the mean standard error. Time interval A (5-10 minutes) corresponds to the "cone plateau" and interval B (20-25 minutes) to the "rod phase" of dark adaptation. Note the relatively large rise in threshold for the 14 c.p.d. grating between intervals A and B (0.76 log units), and the much smaller rise for the 8.3 c.p.d. grating (0.1 log units).

2.3.2 Protanopes

Figure 2.10 and 2.11 show the results obtained from both protanopic subjects. The most striking feature of this data is that the rise in threshold observed with the highest spatial frequencies (8.3 c.p.d. and 14 c.p.d.) for normal subjects is absent. There is a small rise in threshold for the 14 c.p.d. grating for subject DT after 25 minutes in the dark. However, this rise coincided with the subject complaining of fatigue.

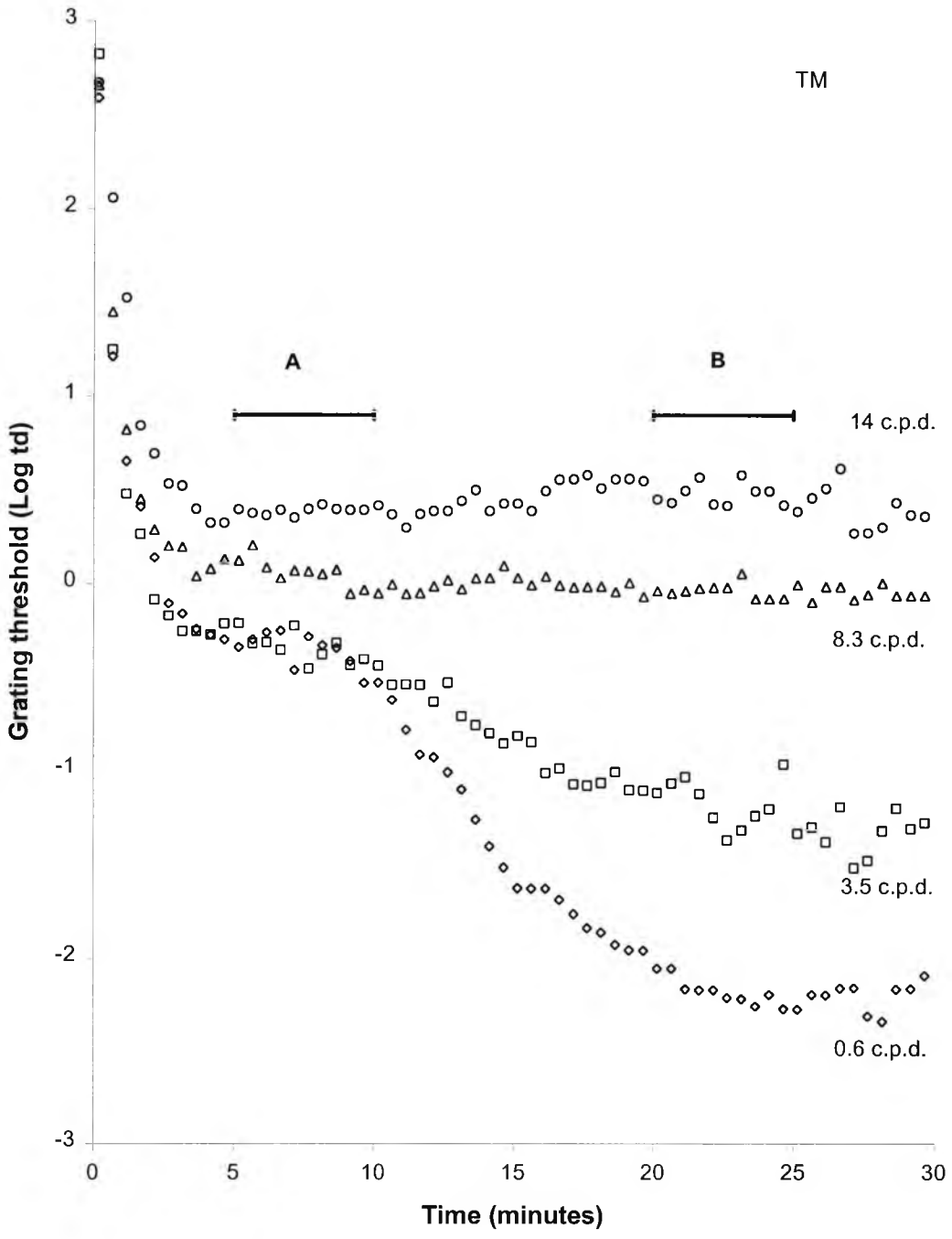

Figure 2.10 Dark adaptation function for subject TM who does not posses functioning LWS cones. Note that threshold for the 14 c.p.d. grating does not rise during the rod phase of dark adaptation.

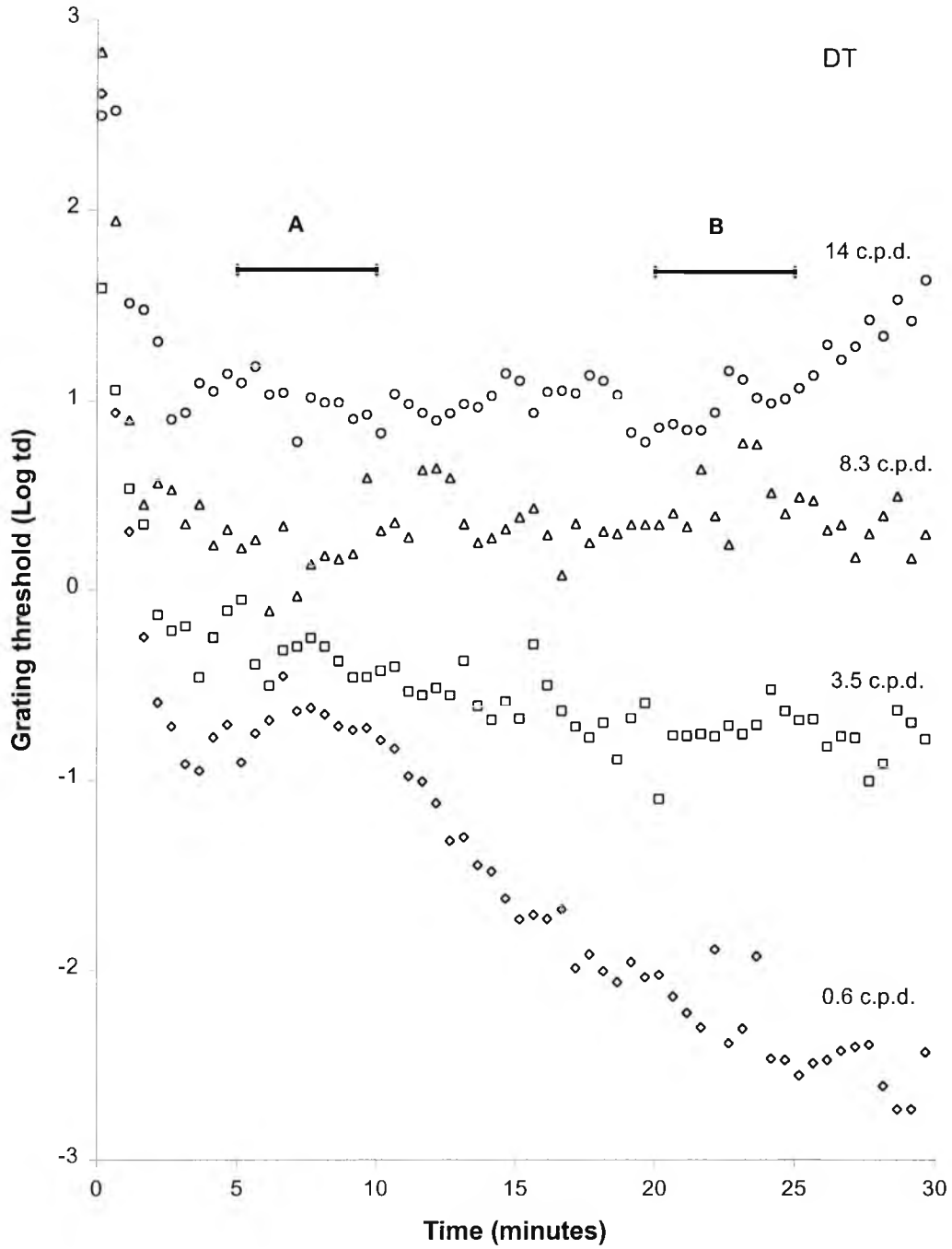

Figure 2.11 Dark adaptation function for subject DT who does not posses functioning LWS cones. Note that threshold for the 14 c.p.d. grating does not rise during the rod phase of dark adaptation.

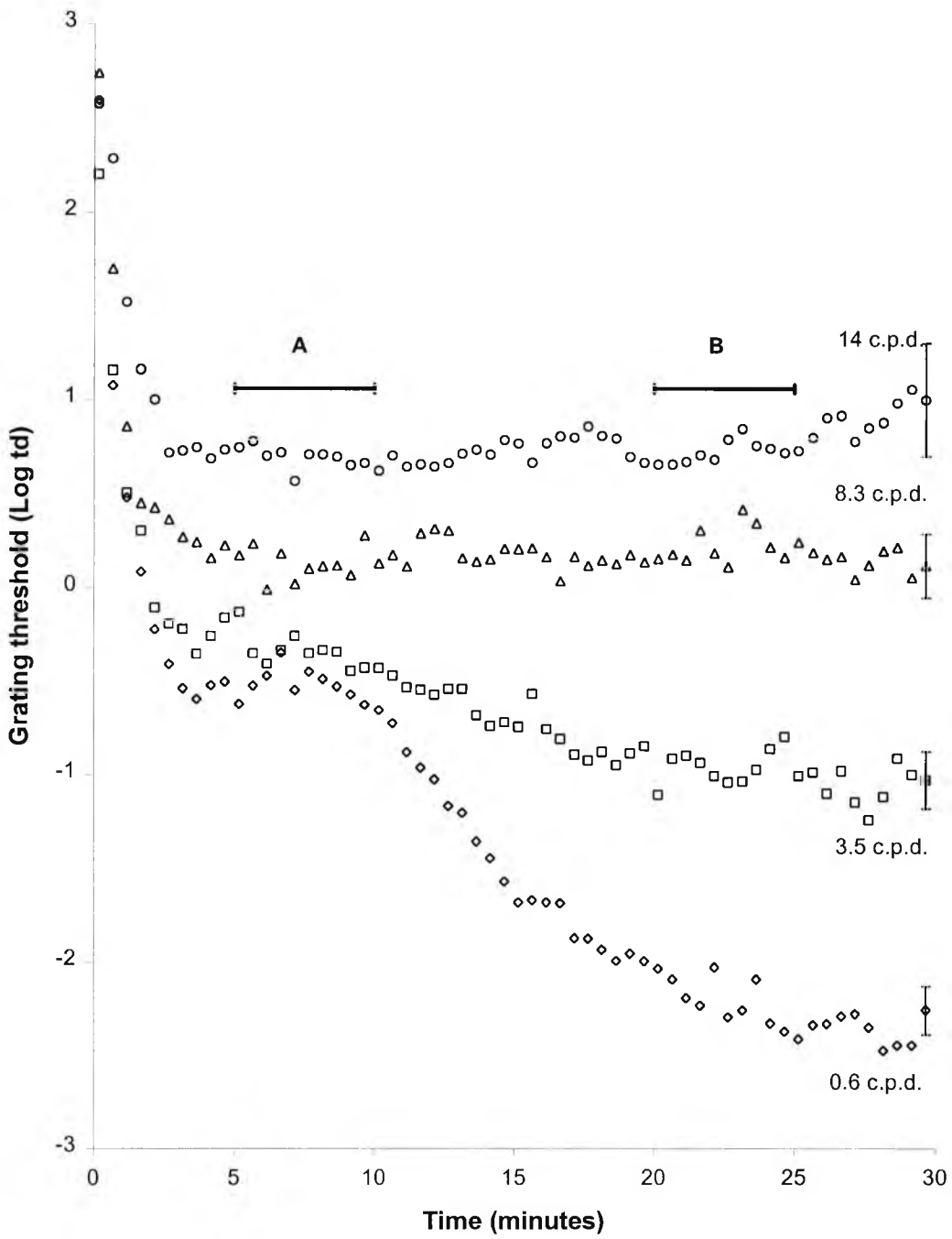

Figure 2.12 Dark adaptation curves for 4 spatial frequencies. Each point is the mean threshold value for the protanopic subjects. The error bar at the end of each dark adaptation function indicates the size of the mean standard error. Time interval A (5-10 minutes) corresponds to the "cone plateau" and interval B (20-25 minutes) to the "rod phase" of dark adaptation. Note there was no significant increase in threshold for the 14 c.p.d. between time interval A and B (rise in threshold = 0.03 log units, paired t-test p=0.34), nor was there a rise over the same period for the 8.3 c.p.d. grating (rise in threshold = 0.09 log units, paired t-test p=0.054).

2.3.3 Deuteranope

Figure 2.13 plots the data obtained from the only deuteranope to have taken part in the study. The data is similar to that obtained from normal subjects in as much that threshold to the 14 c.p.d. grating rises during the rod phase of dark adaptation.

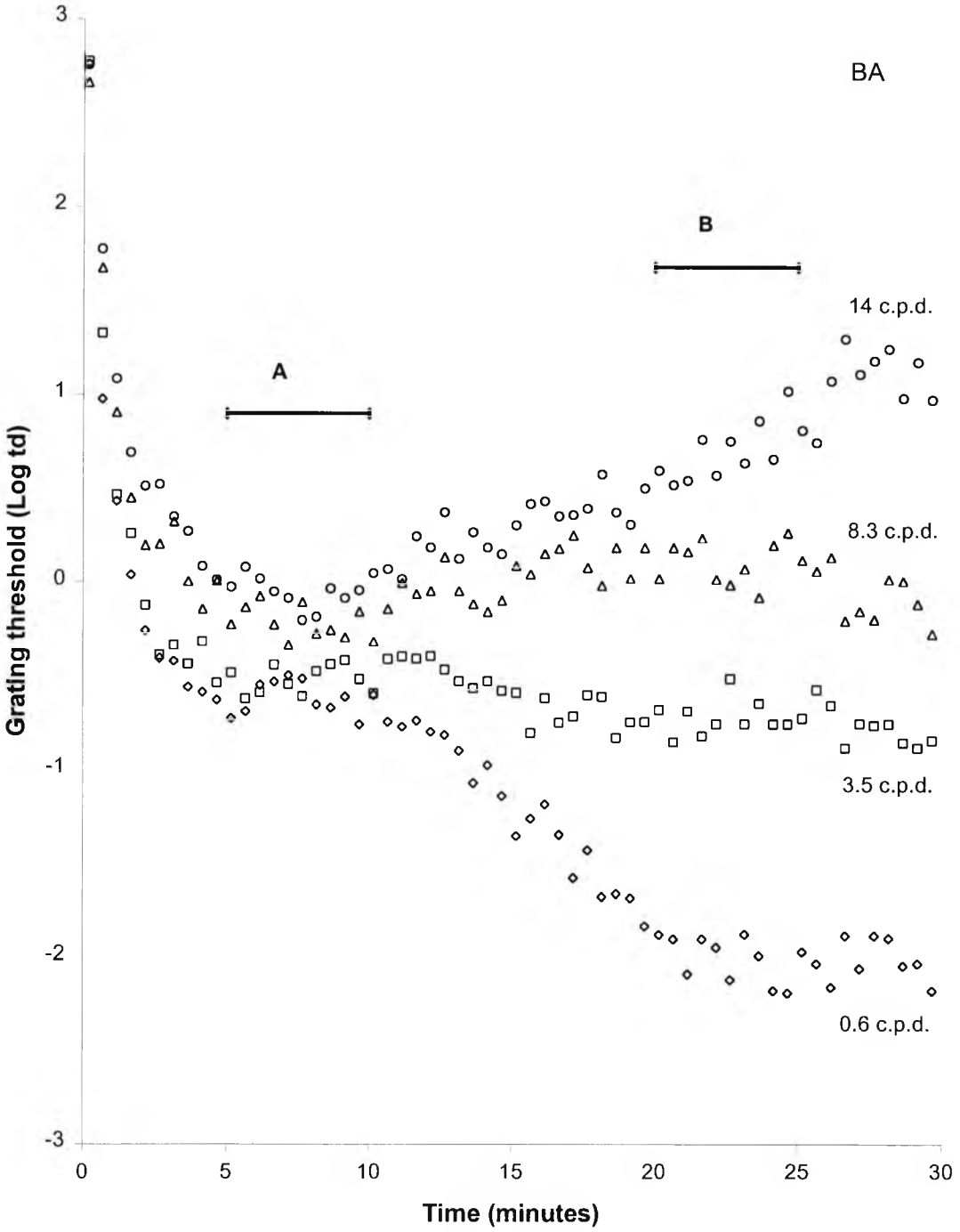

Figure 2.13 Dark adaptation function for subject BA who has no functioning MWS cones. Note that threshold for the 14 c.p.d. grating rises after approximately 10 minutes of dark adaptation in a similar fashion to subjects who have normal colour perception.

2.4 Discussion

This study has shown for the first time how threshold for sinusoidal gratings varies throughout the course of dark adaptation. The results obtained from colour-normal subjects and dichromats are discussed below.

2.4.1 Colour normal subjects

Results are in good agreement with those obtained by Coletta *et al.* (1986) and Naarendorp *et al.* (1988) but differ in a number of respects in relation to the data obtained by Brown *et al.* (1953), Brown *et al.* (1969) and Hahn and Geisler (1995).

It is likely that these differences are attributable to differences in the configuration of the stimulus and experimental methodology. For example the magnitude of the grating SRCI effect varies with retinal eccentricity (Lange and Frumkes, 1993), spatial frequency (Naarendorp *et al.,* 1988) and temporal frequency (Lange and Frumkes, 1993).

The increase in threshold noted for the highest spatial frequency during the rod phase of dark adaptation (0.4 - 1.1 log units) is somewhat larger that that obtained by *Coletta et al.* (1986) who used a comparable spatial frequency. This discrepancy is not remarkable because suppression of cone-mediated spatial vision by dark-adapted rods has been shown to decrease as stimuli are moved closer to the macula, (Lange and Frumkes, 1993).

Results have shown that the magnitude of suppressive rod-cone interaction is highly spatial frequency dependant. This observation may explain why Brown *et al.* (1969) did not observe an increase in threshold during the rod phase of dark adaptation despite the fact that that the test grating was centred 3° from fixation. The finest grating used in their study corresponded to a visual acuity of "0.25" (equating to 7.5 c.p.d.) which was almost certainly not fine enough to show an obvious grating SRCI effect.

The results of Brown *et al.* (1953) are less readily explained. In this study they used fine gratings (up to 31.2 c.p.d. for one subject) and yet their data failed to show any grating SRCI. Although their gratings (which subtended 7.3°) were centred on the fovea, data obtained by Coletta and Adams (1986) would suggest that some grating SRCI should have been observed.

The investigation by Hahn and Geisler (1995) also failed to show SRCI. There are several possible explanations. One possibility is that the relatively long (120 second) bleach may have delayed any rod-cone interaction effects until after the recording period. Another possible explanation is that the luminance of their CRT display was sufficient to prevent complete dark adaptation of the rods. Lange and Frumkes (1993) have shown that a 3° annulus with a luminance of only $0.03cdm^{-2}$ is sufficient to abolish grating SRCI for a small (1°) centrally fixated grating. Whatever the reason, our results indicate that modelling the recovery of spatial vision during the first 15 minutes of dark adaptation with a simple exponential decay function is an oversimplification.

Grating SRCI has been attributed to rod suppression of cone-mediated spatial vision. However, the data presented here suggests that this is an incomplete description because not all cone-mediated spatial vision is affected equally. The effect is strongly spatial frequency dependant and this seems just as note worthy as the fact that such high frequencies are detected by cones. So what might account for this spatial frequency dependency? One explanation is that small receptive fields are less light-adapted than larger ones, consequently their gain in response to any background (real or equivalent) is relatively greater. The relatively high degree of amplification associated with small receptive fields may make them much more sensitive to noise. In the dark, rods are fully depolarised and quantal-like events occur on a random basis producing "dark light". This source of noise will be present in all pathways but is likely to have a greater effect on psychophysical threshold (determined by signal to noise ratio) if it is fed into a high gain (i.e. small receptive field) pathway. If the high gain of small fields is responsible for the grating SRCI effect, this would indicate that the site of the rod input should be before the site of the gain i.e. distil to the retinal ganglion cells. Such a proposition is in conflict with the inter-ocular effect observed by Frumkes *et al.* (1995).

An additional question is whether the effect originates from dark-adapted rods or from rods in response to the test?

The flicker SRCI effect is due to a tonic sustained lateral inhibitory influence of unstimulated rods on cone signals i.e. dark adapted rods. This has been demonstrated by using red and green flickering stimuli presented 180° out of phase. When the scotopic illuminance of both lights is equated (but the photopic illuminance is different) flicker

SRCI is still evident even though the stimulus provides rods with a steady stimulus Goldberg *et al.* (1983).

It is less clear whether the grating SRCI effect is due to dark-adapted rods or due to the rods responding to the test. Naarendorp *et al.* (1988) showed, in steady state conditions, that a dim rod stimulating annulus (around but not on the test) abolished the grating SRCI effect, indicating that the effect is largely mediated by rods adjacent to the test area. In addition, Narrendorp *et al.* (1988) produced nearly identical dark adaptation functions with both a 512 nm and a red (wratten 29 filter) 14 c.p.d. test whose photopic illuminance was matched, even though each of these grating tests would have provided a very different scotopic stimulus.

Contradictory evidence is provided by Stabell and Stabell (1993). They showed that cone-mediated form perception is influenced by the light response of rods. A small rectangular test was presented 7° from fixation. The investigators claim that the test was perceived as being a rectangle by the cones and as a circle by the rods when the test's luminance was reduced. Threshold for the rectangular form percept increased during the rod phase of dark adaptation in a similar way to the grating SRCI effect. However this effect was abolished when the test was red (670nm) and no longer a stimulus to rods.

The retina provides numerous anatomical possibilities for interactions between rods and cones. Some of these are listed below:

1. Gap junctions between rods and cones. Nelson (1977) suggested that this is a likely site for rod-cone interaction.
2. Telodendria (fine processes that extend from cone receptor terminals) make contact with rods (Dowling, 1987).
3. Horizontal cells contact both rods and cones in the outer plexiform layer (Kolb and Famiglietti, 1976)
4. Some horizontal cells (HI) have dendritic trees that contact only cones but their axons innervate rod spherules (Kolb, Linberg and Fisher, 1992). However this is likely to allow information from cones to reach rods, not the otherway around.
5. In the inner plexiform layer some rod and cone signals are transmitted by the same cells, in particular the ON cone bipolar. These pathways are summarised below (Miller, 1989):

cone receptor → cone bipolar → ganglion cell (ON and OFF centre)

rod receptor → rod bipolar → amacrine (AII) → OFF ganglion cell

rod receptor → rod bipolar → amacrine (AII) → cone ON bipolar → ON ganglion cells

6. Interplexiform cells feed back information from the inner plexiform layer to the outer plexiform layer where they predominantly contact cone invaginating bipolars (Linberg and Fisher 1986)

Frumkes and Eysteinsson (1988) endeavoured to identify the site of flicker SRCI by blocking the activity of retinal cells using various pharmacological agents. Their results indicated that flicker SRCI in amphibians is at least partly due to rod modulation of horizontal cell feed back onto cones. However they speculate that other circuits in the inner plexiform and interplexiform circuits may also play a role in SRCI.

2.4.2 Dichromats

The absence of a grating SRCI effect for the protanopic subjects and the presence of it in the deuteranope is analogous to a similar finding for high frequency flicker and suggests that both effects originate at a similar locus.

However, recent evidence suggests that grating SCRI has a large inter-ocular component where as flicker SRCI does not. Apparently a dim field presented to the non-test eye abolishes steady-state grating SRCI but has no effect on flicker SRCI (Frumkes *et al.*, 1995).

These apparently conflicting results may be reconciled if it is accepted that the interocular effect is due to an increase in grating sensitivity brought about by reduction in noise from the non-test eye rather than the abolition of grating SCRI.

This study indicates that the grating SRCI effect involves LWS cones. This suggests a distil origin for the effect. However, at this point in time there does not appear to be an anatomical substrate for the effect. There is evidence that HII horizontal cells make specific contacts with MWS and LWS cones but avoid SWS cones but there is no evidence to suggest that LWS cones are singled out by any retinal neurone.

3. Recovery of contrast sensitivity

3.1 Introduction

The previous chapter has provided a description of how sensitivity to gratings of different spatial frequency changes in the dark following a period of intense light adaptation. Although such a description of spatial vision is of interest academically, individuals rarely have to see in absolute darkness. More typically, the slow recovery of vision associated with dark adaptation manifests itself when we move from bright sunshine to the relative gloom of an unlit building interior or when we are temporarily dazzled by a vehicles headlights at night. In such situations it is the return of contrast sensitivity that is of particular importance. Given the practical importance of contrast sensitivity, it is perhaps surprising that there have been no previous studies of how contrast sensitivity changes after a sudden drop in illumination. Indeed measurements of CS in such situations might enable an individual's "real world" visual performance to be predicted, (Owsley and Sloan, 1987).

One brief report entitled "Contrast sensitivity functions measured during dark adaptation..." would suggest that the CSF has been measured in such situations (Hahn and Geisler, 1991). However this investigation simply measured amplitude threshold (*Imax*) and not contrast sensitivity ((*Imax* - *Imin*) / (*Imax* + *Imin*)). The results of this study were published in greater detail by Hahn and Geisler (1995) and have been discussed in Chapter 2. Hahn and Geisler (1995) state that the reason for not describing their gratings in terms of contrast is that it is inappropriate to express the visibility of a grating in terms of its contrast in a dark adaptation investigation because all gratings have a contrast of 1 when viewed in darkness i.e. *Imax* - 0 / *Imax* + 0 = 1. This simple explanation masks the fact that dark adaptation investigations are fundamentally different from those measuring contrast sensitivity recovery. In a conventional dark adaptation experiment a grating is presented intermittently in absolute darkness and the subject adjusts the intensity of *Imax* to threshold. As dark adaptation proceeds both *Imax* and the space averaged mean luminance of the grating are reduced. In an assessment of CS recovery the subject adjusts the contrast of a grating to threshold.

Changes in the luminance of *Imax* are offset by changes in *Imin* so that the space averaged luminance of the grating remains constant. Inevitably, this background luminance will have an affect on the adaptational process operating during dark adaptation.

Although dark adaptation functions, such as those presented in the previous chapter, cannot be used to determine contrast sensitivity they do provide us with some information about contrast sensitivity. To clarify the relationship between a dark adaptation function and contrast sensitivity, Figure 3.1 shows a conventional dark adaptation function (circles) and a solid line indicating the mean luminance of a grating that may be used to determine contrast sensitivity during dark adaptation. If the grating has a mean luminance of 0.05 cdm^{-2} and a contrast of c=0.9, then the light bars of the grating (Imax) would have a peak luminance represented by the upper dashed line and the dark bars (Imin) a minimum luminance represented by the lower dashed line (assuming the grating is viewed through a 4 mm pupil).

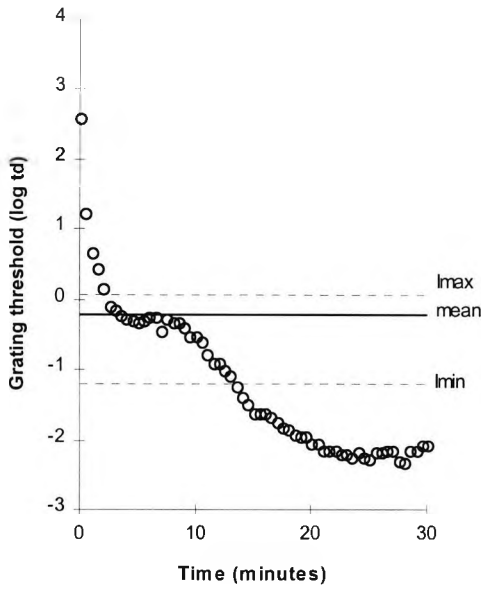

Figure 3.1 Dark adaptation function obtained using a 0.6 c.p.d. grating (circles). If a subjects task was to detect the presence of a high contrast grating (c=0.9) that had a mean luminance of 0.05 cdm^{-2} (mean) then it may be expected that approximately 2 minutes would elapse before the grating would become visible.

Assuming that at the start of the experiment the mean luminance of the grating is sufficiently dim that it does not significantly affect dark adaptation, the dark adaptation data (circles) would suggest that the grating (modulated in terms of its contrast) cannot

be seen until at least 2 minutes after the bleaching exposure, i.e. the visual system has become sufficiently sensitive at this point in time to detect the presence of the light bars of the grating. After this point the results for the conventional dark adaptation experiment show that sensitivity continues to improve until the end of the experiment (30 min). However, if contrast sensitivity is being measured, the mean luminance of the grating (0.05 cdm^{-2}) will arrest the process of dark adaptation, (Blakemore and Rushton, 1965b).

Although the conventional dark adaptation function may be used to predict approximately when CS will first return it cannot be used to determine how CS will increase after that point in time, in the same way that it cannot be used to provide an estimate of final (steady state) contrast sensitivity. Sensitivity to light and sensitivity to contrast are related but one cannot be used to predict the other.

If the mean luminance of a grating is known, information from a conventional dark adaptation function may be used to predict when the grating might first be seen but, how might CS improve subsequently? According to the equivalent background hypothesis the after-effects of a bleach are indistinguishable from the effects of real light. Therefore the visual system will respond to the grating as if it were superimposed on a steadily fading background. The grating will be perceived as having a lower contrast and higher mean luminance than it does in reality i.e.

$$Cp = \frac{(E + Imax) - (E + Imin)}{(E + Imax) + (E + Imin)} \tag{1}$$

$$MLp = E + \frac{\mathrm{Im}ax + \mathrm{Im}in}{2} \tag{2}$$

where Cp is the perceived contrast of the grating, MLp is the perceived mean luminance of the grating and E is the luminance of the equivalent background. Therefore contrast sensitivity will be low when the equivalent background is relatively intense and it will improve as the equivalent background fades. Contrast sensitivity to all spatial frequencies should return at the same rate because CS will be solely determined by the rate at which E reduces. However, this argument only holds when the perceived mean luminance of the grating is sufficient to permit the visual system to operate according to

Webers law. When the perceived mean luminance of the grating corresponds to the Weber / square root transition luminance the recovery rate will decline because the contrast sensitivity of the visual system reduces below this luminance. The transition luminance is directly proportional to spatial frequency (van Nes and Bouman, 1967). Therefore, the point in time at which the recovery rate declines should be spatial frequency dependant.

3.1.1 Purpose

This chapter describes a series of experiments in which contrast sensitivity was measured for gratings of different spatial frequency and mean luminance, following exposure to an intense adapting field. The purpose of this investigation was to provide basic, practical information about the recovery of contrast sensitivity following an abrupt drop in ambient illumination.

3.2 Methods

The methods used in this investigation were developed over many months in response to methodological shortcomings revealed by several preliminary investigations. All the methods were essentially similar in that after a period of light adaptation, contrast sensitivity to sine wave gratings of a variety of spatial frequencies was measured until recovery was judged to be complete.

The following paragraphs describe the development of this experiment by highlighting some of the difficulties encountered in preliminary investigations.

3.2.1 Preliminary investigation No.1

Initially the apparatus was similar to that shown in Figure 2.1. A single channel Maxwellian view optical system was used to light adapt the subject (10 second exposure to a 6 log td 16°, white field). The cyclopleged (2 drops, 1% tropicamide) subject then turned to fixate the centre of the monitor through a pinhole. The monitor surround was illuminated by fluorescent tubes in such a way that it had the same space-averaged luminance (70 cdm^{-2}) and colour appearance as the monitor. A dense afterimage was produced by the period of light adaptation and so four fixation markers surrounding the monitor were used to aid fixation. A schematic diagram of the bleaching field and test stimulus is shown in Figure 3.2.

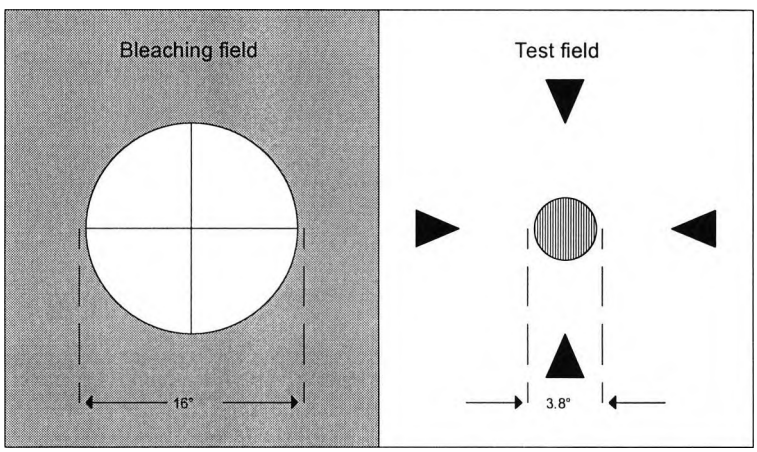

Figure 3.2 Bleaching and test field configuration.

As the afterimage faded the contrast of the screen was adjusted to threshold by the subject. Three sets of data were collected for each of the 6 spatial frequencies examined (0.5, 1, 2, 4, 8, 16 c.p.d.). An example of 1 data set for a 4 c.p.d. grating is shown in Figure 3.3.

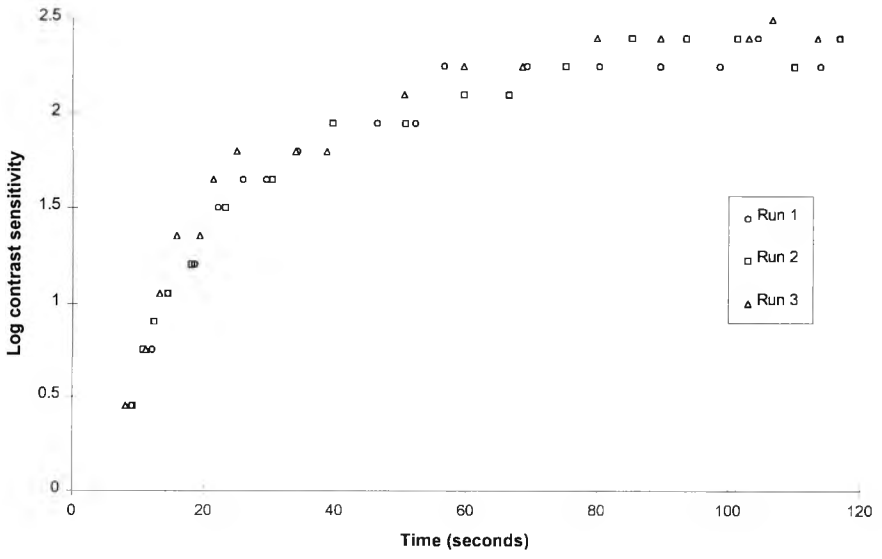

Figure 3.3 Recovery of contrast sensitivity to a 4 c.p.d. grating following a 10 second exposure to a 6 log td white field. Each symbol shape plots the data of a single experimental run. The subject adjusted the contrast of the grating and pushed a button to indicate that threshold had been reached.

This preliminary investigation revealed several shortcomings. Although the method of adjustment (used by others e.g. Hahn and Geisler, 1995) was simple and produced relatively consistent data, the subjects (n=2) were aware that threshold was being obtained in two different ways during the experiment. After an initial delay sensitivity rapidly returned. During this time subjects reduced the contrast of the grating and simply waited until the grating could first be seen again before pushing the button (there was no time to adjust the contrast to threshold). Later on in the experiment when sensitivity was not changing so rapidly, subjects had time to actively adjust the contrast of the grating before signalling that threshold had been obtained. This subtle difference in methods during each experimental run may have distorted the shape of the CS recovery function.

An additional difficulty was that high frequency gratings were being poorly reproduced on the monitor which was only capable of displaying 744 vertical lines (at a viewing distance of 1.5 meters each cycle of a 20 c.p.d. grating was represented by less than 4 lines).

3.2.2 Preliminary investigation No.2

A description of the methods used in the second investigation and its results may be found elsewhere (Margrain and Thomson, 1994). The investigation used the same apparatus and procedures used in investigation No.1 but the distance to the screen was increased to 2.8m. By doing this a single cycle of a 20 c.p.d. grating was represented by more than 7 lines (a sufficient number to represent a sinusoid, Barbur (1995)). In addition, the method of increasing limits was used as opposed to the method of adjustment.

Numerous psychometric methods have been used to determine contrast sensitivity e.g. method of adjustment, method of limits, method of constant stimuli (may employ forced choice), adaptive procedures (e.g. staircase methods), etc. (Woods and Thomson, 1995). Most of these techniques require several presentations to measure threshold and are not therefore, well suited to the measurement of a threshold that changes rapidly over time. Determination of threshold by the method of increasing limits is relatively rapid and has been shown to produce repeatable results (Ginsburg and Cannon, 1983; Woods and Thomson, 1995).

Initially, a high contrast sinusoidal grating (c=0.9) of a predetermined spatial frequency was displayed on the screen and subjects (n=5) were required to respond when it was first seen "through" the after image. Thereafter, the contrast of the grating was continuously ramped up from sub-threshold levels, under computer control, until the subject responded that it was just visible (ascending method of limits). Subjectively the detection criteria felt consistent throughout the recording period.

A considerable amount of data was collected using this method (approximately 15 hours per subject). Recovery of CS to a variety of gratings (0.6, 1.5, 3.5, 8.3 and 19.9 c.p.d.) was measured on several occasions (typically 3) over a range of mean luminances (50, 5, 0.5, 0.05, 0.005 cdm^{-2}).

Unfortunately this relatively simple apparatus required the subject to turn from the Maxwellian bleach to view the grating through the pinhole. Although this movement could be accomplished within 2-3 seconds and did not cause a problem with substantial bleaches (because the afterimage was so dense, vision was effectively obliterated after

turning to the screen) it became a problem when using relatively weak bleaches (during a pilot investigation into the effect of bleach duration and intensity on CS recovery, reported in Chapter 4) when threshold was found to change considerably in the first few seconds.

Therefore the apparatus was redesigned so that the subject did not have to move during the experiment. The methods eventually used in this investigation are described below.

3.2.3 Apparatus

The stimuli were all presented through an optical system. A schematic diagram of the apparatus is shown in Figure 3.4. Exposure to the bleaching field ('white', 16°, 5.67 log td) produced by Channel 1 was regulated by a computer controlled shutter (SH1) positioned at a secondary focus. Channel 2 produced an annular surround that had a luminance and colour matched to that of the monitor. The "hole" in the annulus was filled by the test grating from Channel 3 (which was not seen in Maxwellian view). The monitor was positioned 2.8m from the subject and was masked to produce a circular 4° display. A bite bar was used to maintain subject alignment. Fixation was aided by three LEDs positioned around the test grating and a line of letters on the surface of the monitor. In some experiments additional ND filters were placed in Channels 2 and 3 to alter the luminance of the monitor and its surround.

Gratings were generated by a Millipede Prisma VR1000 pattern generator interfaced to a PC. Hardware limitations and the rate at which thresholds changed dictated that gratings (of different contrast but the same spatial frequency) had to be generated before the start of each experimental run. This limited the number of possible contrasts to just 19 discrete steps. Resolution of the system was improved by interleaving the contrasts on subsequent runs. Following each response from the subject there was a random delay of 1 to 5 seconds (during which time the monitor was spatially-uniform) before grating contrast was ramped up from sub-threshold levels. Gratings alternated with a blank screen at a frequency of 1 Hz.

The retinal illuminance of channels 1 and 2 were calculated in the usual fashion (after Westheimer, 1966) on the basis of illuminance measurements obtained using a UDT photodiode (and Oriel radiometer) positioned 12 cm behind the pinhole. After removal

of the pinhole (PH) the luminance of the grating was determined with an LMT photometer.

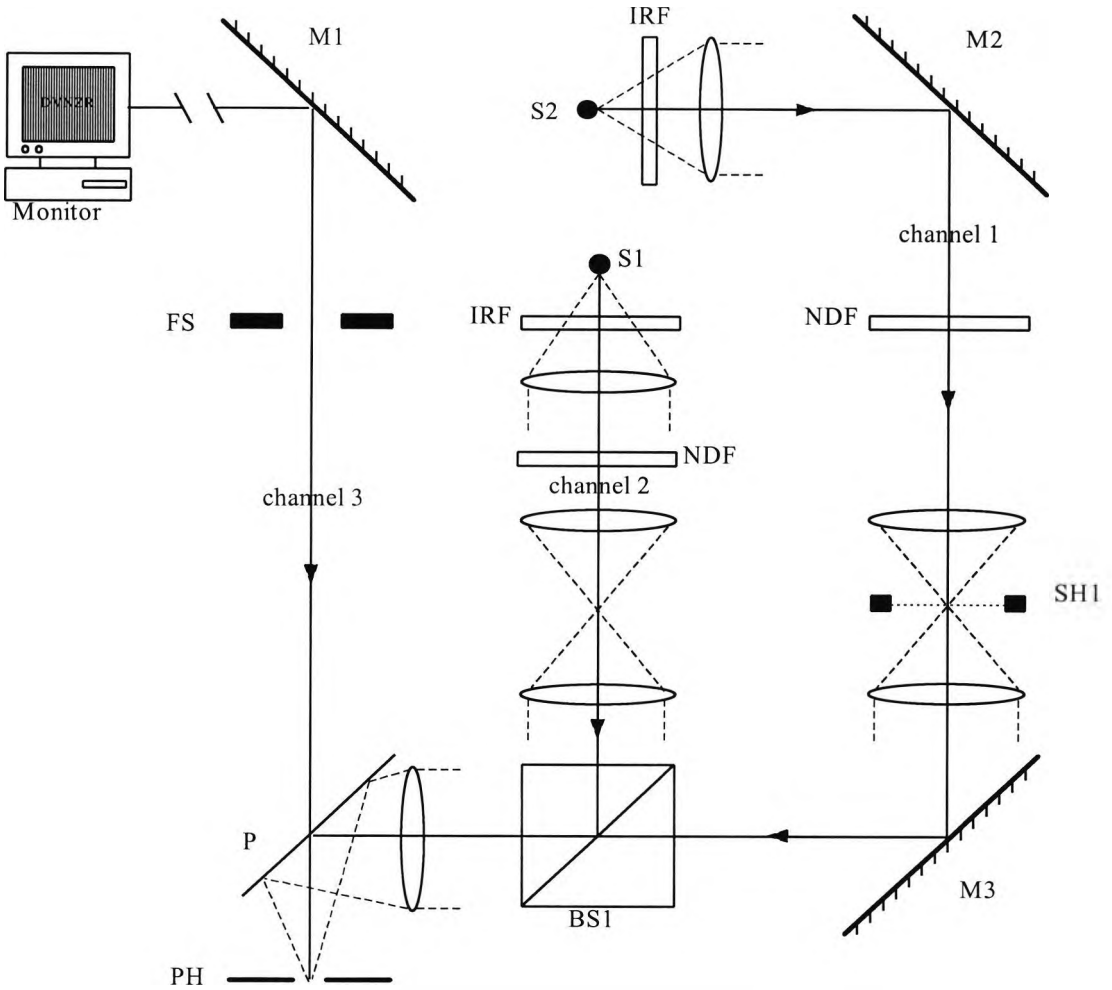

Figure 3.4 Schematic representation of the optical system. S1, S2 - quartz halogen lamp; BS1 - cube beam splitter; M1, M2, M3 - front surface mirrors; P - pellicle; NDF - neutral density filters; IRF - infra-red heat filter; SH1 - electro mechanical shutter; FS - field stop, PH - pin hole.

3.2.4 Procedure

Two drops of 0.5% cyclopentolate were instilled 30 minutes before the experiment to paralyse accommodation and dilate the pupil. The optical correction necessary to place the subjects' far point in the plane of the monitor was determined by refraction and placed immediately behind the pinhole (PH).

Prior to each experimental session, subject alignment was checked with a high contrast, high spatial frequency grating and the fixation letters on the monitor. Subjects signalled their readiness to begin each experiment by pressing a button. Following a 120 second exposure of one eye to the bleaching field, threshold was monitored continuously using

the method of increasing limits (MIL) until the end of the experiment. Five experiments were conducted. The duration of each recording and the mean luminance of the grating were different in each experiment (see Table 3.1).

	Luminance	Recording (min)	No. runs	Spatial frequencies	Total time (min)
Experiment No.1	50 cdm^{-2}	3	3	5	105
Experiment No.2	5 cdm^{-2}	5	3	5	135
Experiment No.3	0.5 cdm^{-2}	10	3	5	210
Experiment No.4	0.05 cdm^{-2}	30	2	4	240
Experiment No.5	0.005 cdm^{-2}	30	2	3	180

Table 3.1 Summary of experimental parameters. Luminance = mean grating luminance, Recording = duration of each experimental run, No. runs = number of sets of data collected per spatial frequency, Spatial frequencies = number of spatial frequencies examined, Total time = total length of each experiment.

In any experimental run, only one spatial frequency was examined. In experiments 1-3 three sets of data were collected for each spatial frequency. In experiments 4 and 5 only 2 sets of data were collected (all data sets were virtually identical to those collected during preliminary investigation No.2).

It can be seen from Table 3.1 that several of the experiments were very time consuming and therefore data for each experiment was often collected on different days. No experimental session lasted more than 90 minutes.

3.2.5 Data analysis / presentation

The experiments reported here yield a series of measurements taken at unspecified times. There are several approaches to analysing such serial measurements. Altman (1991) suggests two methods:

1. The commonest method is to perform independent analyses at each point in time. Data may by displayed graphically by a plot joining the mean values with error bars of ± 1 standard error. However, this approach may be criticised because no account is

taken of the fact that the values at each point in time are likely to be related to adjacent values.

2. A more useful approach is to reduce the data to a number of summary measures. One way of doing this is to fit a model to each data set. However, this approach relies on appropriate model choice.

Data analysis in a subsequent chapter uses the summary measures approach, but here the first approach was adopted. The main reason for doing this was to avoid making any assumptions about the data at this stage (i.e. by fitting a model).

One difficulty with this approach was that each measurement of threshold was made at a different time. To overcome this problem, data for each run was linearly interpolated between adjacent measurements. The mean threshold (for each second of the recovery) could then be determined. This approach is shown in Figure 3.5.

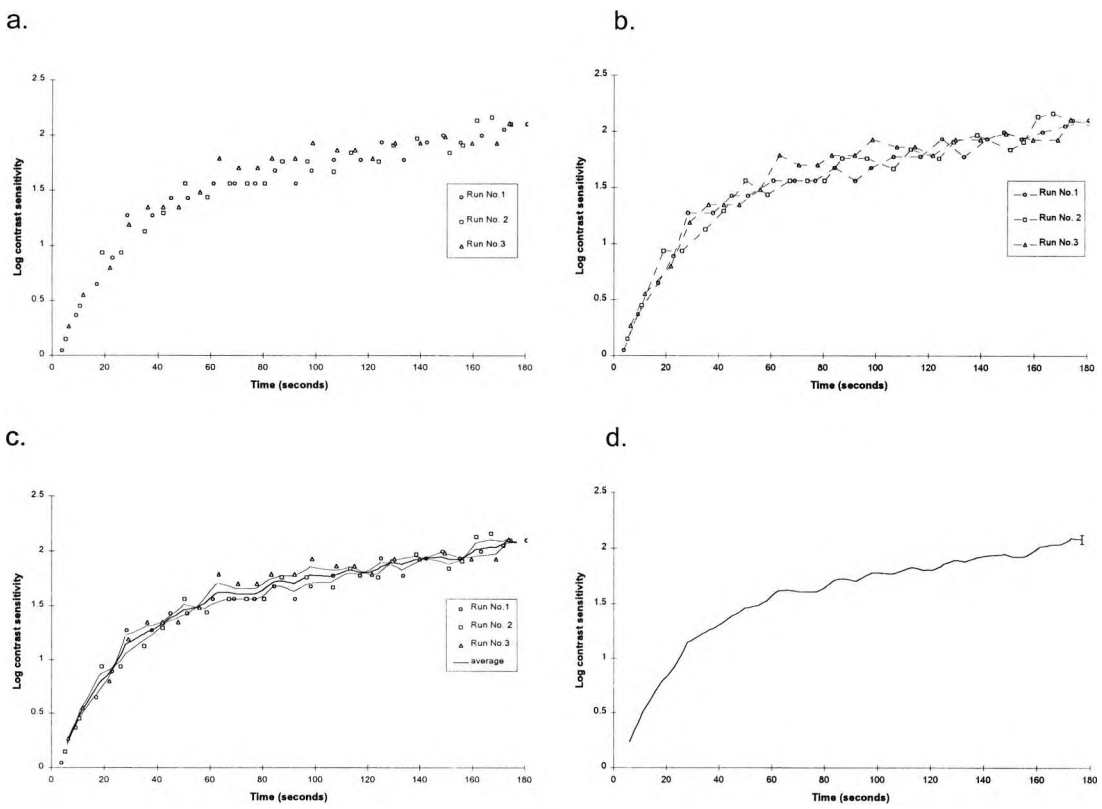

Figure 3.5 Four plots showing the process of data summary. Panel (a) shows the raw data. Note that each measurement is made at a different point in time. Panel (b) shows raw data and interpolated data. The heavy line in panel (c) shows the mean sensitivity and the thin dashed lines indicate the magnitude of the standard error throughout the investigation. Panel (d) shows how the original data was summarised by a line representing mean threshold and an error bar which is the mean standard error.

3.3 Results

The data obtained for each experiment is presented on the following pages. Figure 3.6 presents the data obtained for subject WDT and Figure 3.7 the data for subject TM. In each figure the left hand column shows log contrast sensitivity as a function of time (CS recovery function) for each of the spatial frequencies examined and the right hand column shows log contrast sensitivity as a function of spatial frequency at different times during the investigation. Going from top to bottom, each row shows data obtained when the grating had a mean luminance of 50, 5, 0.5, 0.05 and 0.005 cdm^{-2} respectively. The data is replotted in Figure 3.8 to show how CS recovered for a single spatial frequency for each of the luminances studied.

When the mean luminance of the grating was relatively high (50 cdm^{-2}, upper row of Figures 3.5 and 3.6) log contrast sensitivity recovers relatively rapidly. Contrast sensitivity recovery functions for the different spatial frequency gratings are similar in shape but translated along the vertical axis. This feature is more obvious in the right hand column where it may be seen that each contrast sensitivity function (CSF) has a similar shape. The CSF is band pass at all times following the bleach and peak CS was obtained for the 3.5 c.p.d. grating.

When the experiment was repeated with the grating at a lower luminance (5 cdm^{-2}, second row of Figures 3.5 and 3.6) CS returned more slowly than it had when the mean luminance of the display was 50 cdm^{-2}. Again, contrast sensitivity recovery functions for all spatial frequencies are approximately parallel and the CSFs obtained at different times after the bleach are band pass in shape. However there is a subtle change in the overall shape of the CSF function compared to that obtained at 50 cdm^{-2}. Although, contrast sensitivity to all spatial frequencies declines as the luminance of the display is reduced from 50 to 5 cdm^{-2}, the reduction in CS is greatest for the highest spatial frequency and least for the lowest spatial frequency. For example, for subject WDT final CS to the 19.9 c.p.d. grating was approximately 0.5 log units lower when the mean luminance of the display was 5 cdm^{-2} than it had been when the luminance was 50 cdm^{-2} but the reduction in CS observed for the 0.6 c.p.d grating was minimal.

When the luminance of the display was reduced to 0.5 cdm^{-2} (third row of Figures 3.5 and 3.6) the changes described in the previous paragraph were accentuated. CS returned

even more slowly and the loss of contrast sensitivity to the high spatial frequency gratings is more pronounced. Peak CS was obtained for the 1.5 c.p.d., rather than the 3.5 c.p.d. grating. Furthermore, the CSF appears to undergo a subtle change in shape as recovery proceeded. For subject WDT (see Figure 3.6, 3rd row) the CSF obtained after 101 sec is the same shape as that obtained after 151 sec. After this time (151 sec) CS to the high frequency gratings (19.9 and 8.3 c.p.d.) barely changes but CS to intermediate and low spatial frequencies continues to increase until about 340 sec have elapsed.

When the mean luminance of the grating was reduced to 0.05 cdm^{-2} (4th row of Figures 3.5 and 3.6) the shape of the CS recovery curves were different for each subject. Unlike the previous experiments the CS recovery functions are obviously not parallel and consequently the shape of the CSF changes during the course of CS measurement. For subject WDT the shape change is relatively subtle. For all spatial frequencies CS recovery begins after approximately 120 seconds. However, whilst contrast sensitivity to the highest spatial frequency grating (8.3 c.p.d.) asymptotes after about 4 minutes, CS for the lowest spatial frequency continues to improve for a further 4 minutes.

For subject TM the change in shape of the CSF is more profound. CS recovery is approximately similar for all spatial frequencies until a little after 10 minutes into the experiment when CS dramatically increases for the lower spatial frequencies.

When the mean luminance of the grating was reduced to only 0.005 cdm^{-2} CS recovery was greatly delayed in comparison with preceding experiments. With the exception of the 1.5 c.p.d. grating for subject WDT, none of the gratings were seen for the first 10 minutes following the bleach. After this, CS improved gradually until the end of the experiment. The lower rows of Figures 3.5 and 3.6 show that the CSF changes shape as recovery proceeds. Peak CS is initially observed for the 1.5 c.p.d. grating but after approximately 15 minutes peak CS shifts to the lowest spatial frequency and the CSF becomes a low pass function toward the end of the measurement period.

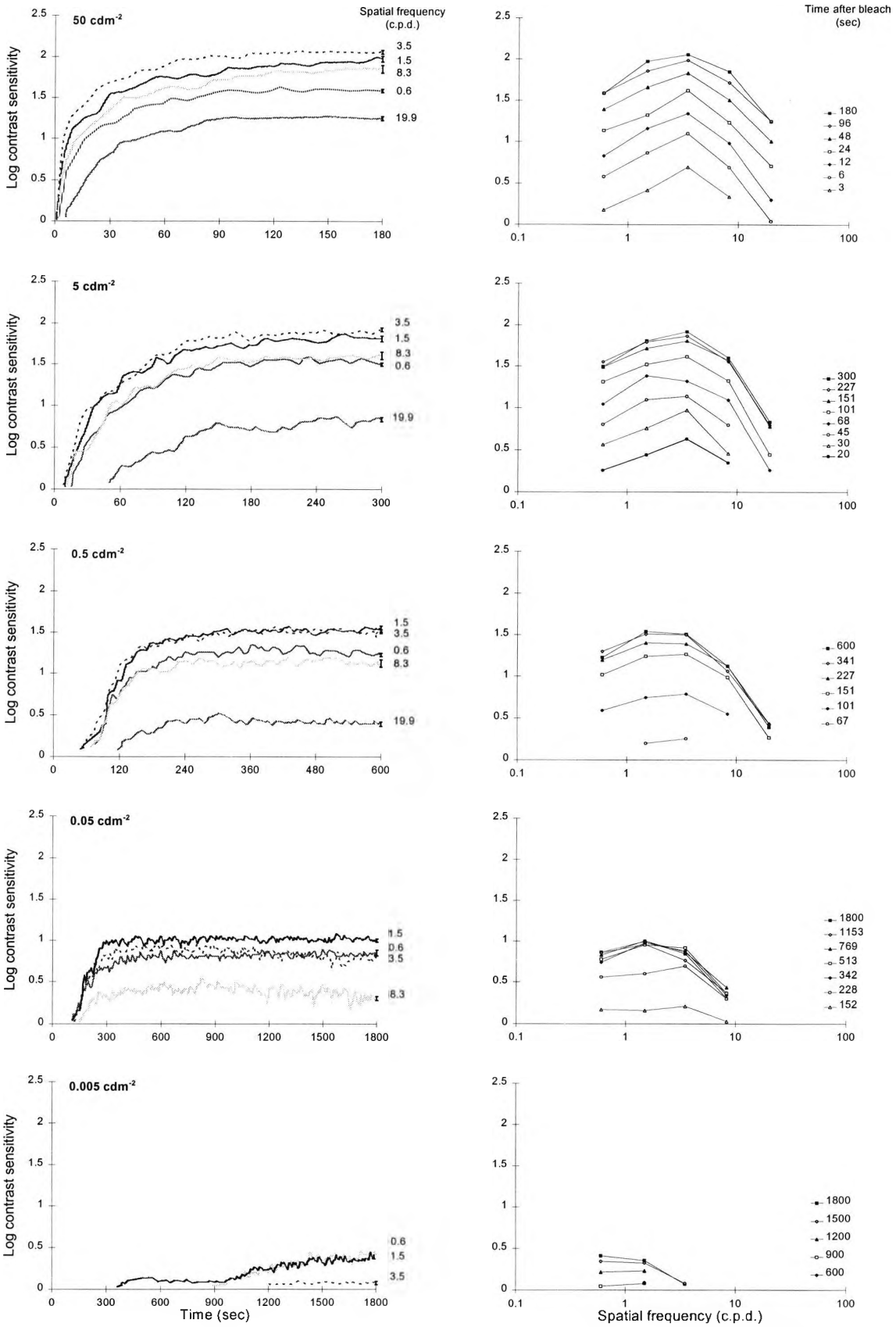

Figure 3.6 Recovery of CS following exposure to a 5.7 log td, white field for 120 seconds. The left hand column shows log CS as a function of time and the right hand column re-plots the data as a series of CSFs obtained at different times after the bleach. The mean luminance of the grating varies from 50 cdm^{-2} in the upper row to 0.005 cdm^{-2} in the lower row. Subject WDT.

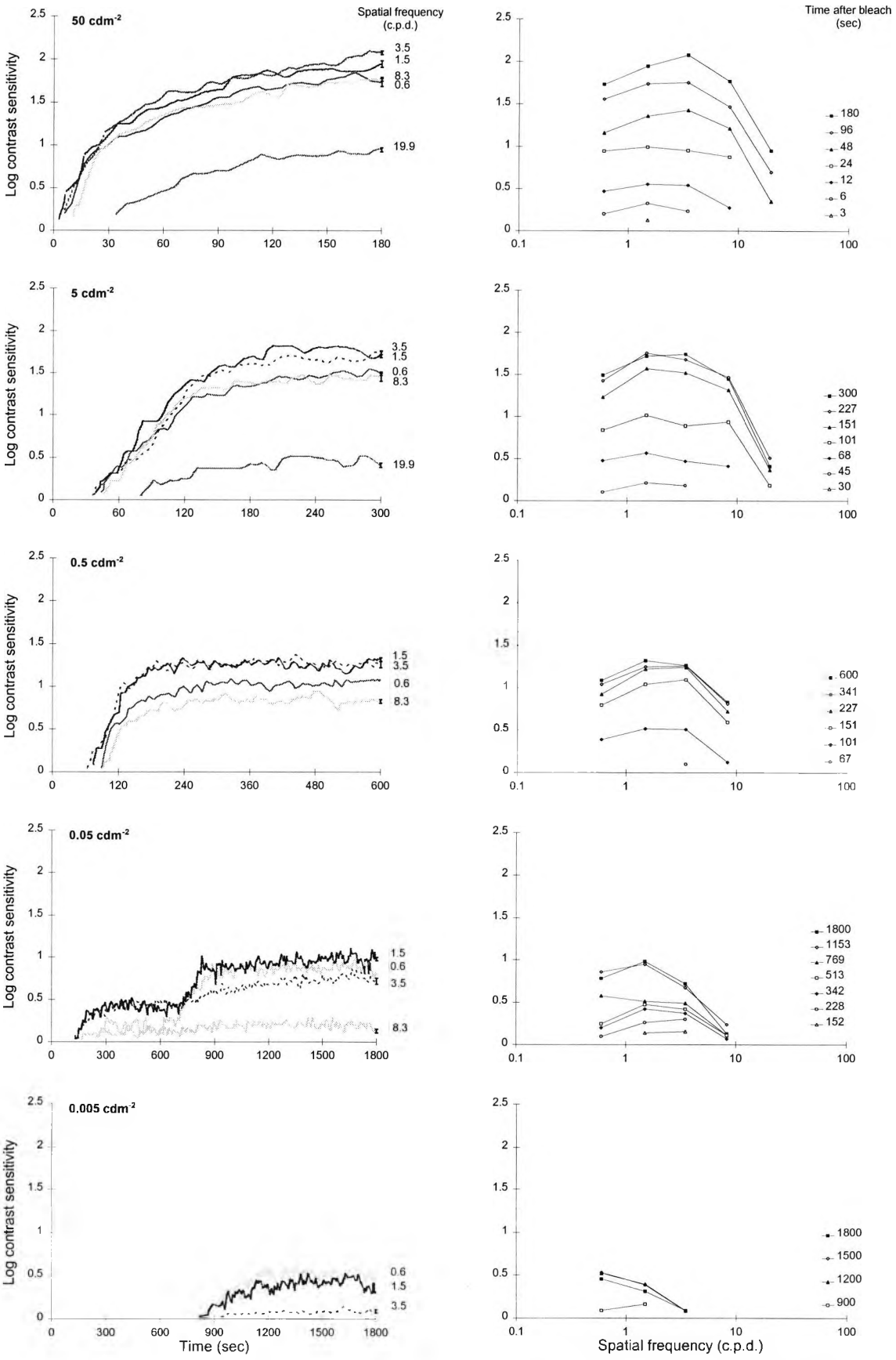

Figure 3.7 Recovery of CS following exposure to a 5.7 log td, white field for 120 seconds. The left hand column shows log CS as a function of time and the right hand column re-plots the data as a series of CSFs obtained at different times after the bleach. The mean luminance of the grating varies from 50 cdm^{-2} in the upper row to 0.005 cdm^{-2} in the lower row. Subject TM.

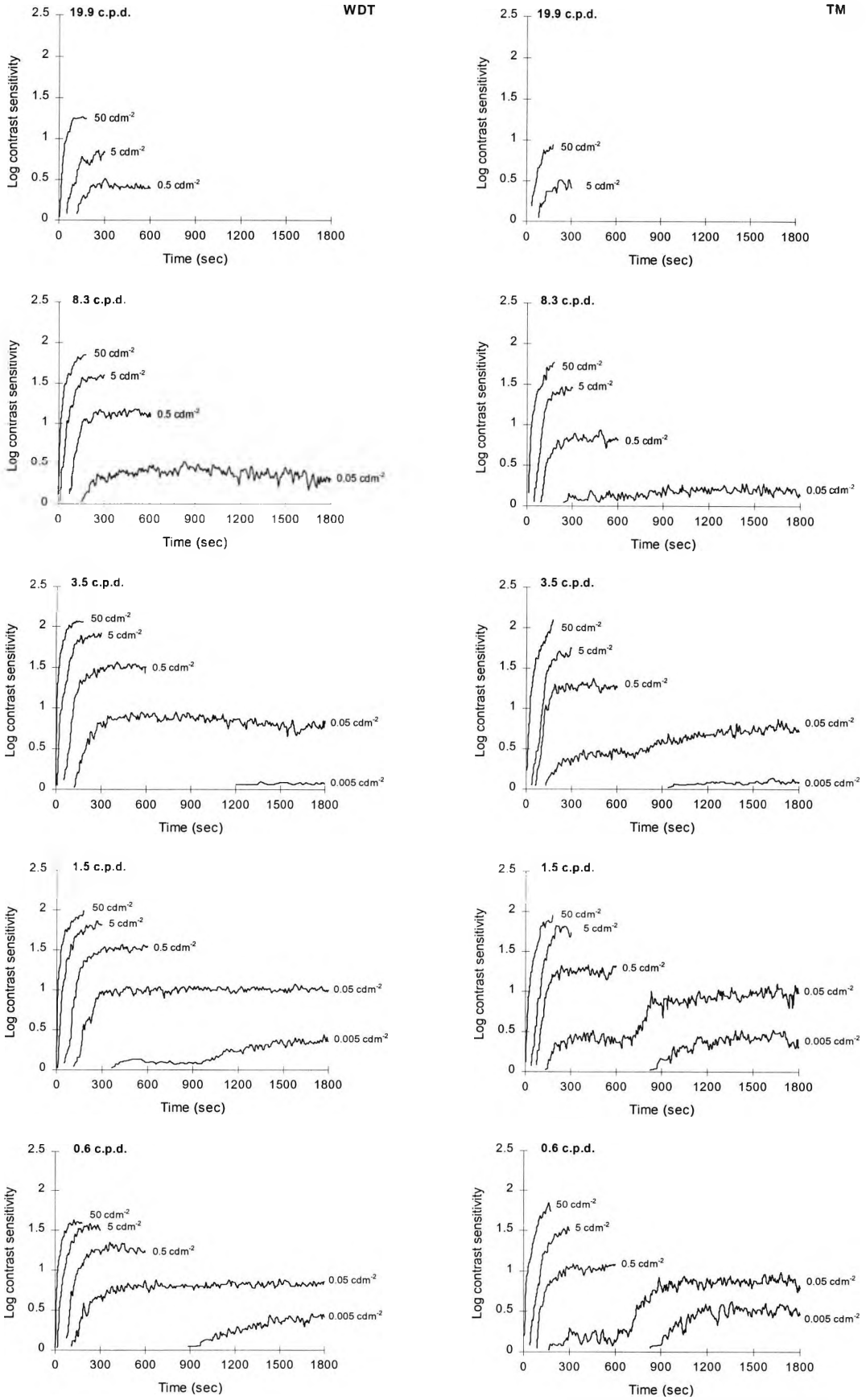

Figure 3.8 Contrast sensitivity plotted as a function of time. Each plot shows CS recovery functions obtained at different mean luminances for a single spatial frequency. The left hand column shows the data obtained from WDT and the right hand column data obtained from TM.

3.3.1 Contrast sensitivity at different mean luminances

At the end of each experiment CS recovery was complete therefore the last few measurements of CS provide a measure of steady state CS. Figure 3.9 describes steady state CS at each of the mean luminances studies. Each point is the mean of the last 10 measurements obtained at the end of each period of data collection.

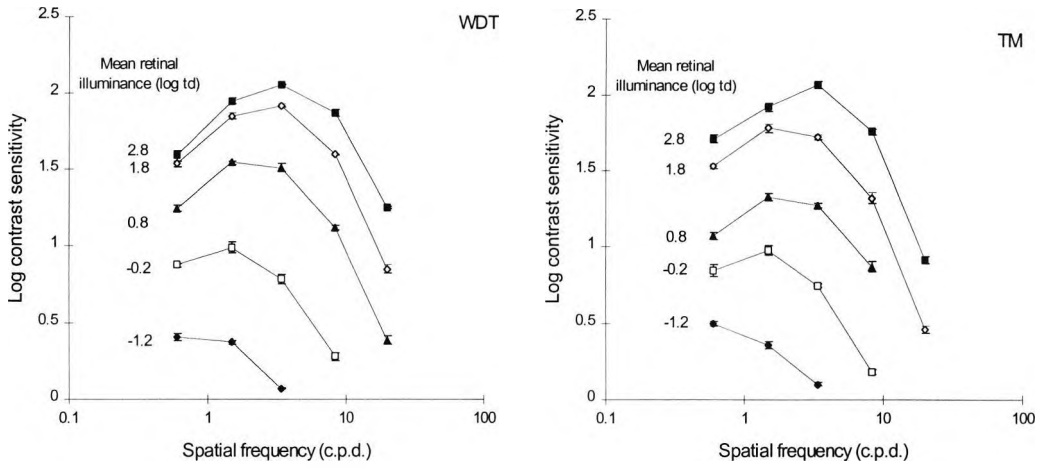

Figure 3.9 Contrast sensitivity functions obtained at different luminances. All gratings subtended 4° and were presented to the fovea. Each data point is the average of the last 10 measurements made during each of the preceding experiments and the error bars indicate the magnitude of the standard error.

The results are similar in a number of respects to those obtained by Daitch and Green (1969) and van Nes and Bouman (1967). As the mean retinal illuminance of the grating is reduced, steady state CS declines. This decline is more pronounced for the higher spatial frequencies and least for the lower ones. At the highest luminance studied, the CSF is a band pass function with peak CS being obtained for the 3.5 c.p.d. grating. As the luminance of the grating is reduced, peak CS shifts to lower frequency gratings, e.g. when the retinal illuminance of the grating is reduced to 0.8 log td, peak CS is obtained with a 1.5 c.p.d. grating. At the lowest illuminance the CSF becomes a low pass function.

3.4 Discussion

The purpose of this study was to measure, for the first time, the recovery of contrast sensitivity following intense light adaptation. Unlike dark adaptation investigations that measure sensitivity to light, this investigation measures sensitivity to contrast. Consequently the data provides a useful description of visual performance under such conditions.

When the mean luminance of the grating was high (>5cdm^{-2}) contrast sensitivity recovery began soon after the bleaching light was extinguished and once underway was relatively rapid, when the mean luminance was low CS recovery was delayed and relatively slow. This finding is in line with expectations because contrast sensitivity cannot begin to recover before the visual system regains sensitivity to the lightest bars of the grating. Despite these differences in recovery rate, Figure 3.9 shows that final CS for low spatial frequency gratings (0.6 c.p.d.) is similar whether the mean retinal illuminance of the grating was 2.8 or 1.8 log td. This indicates that the visual pathways responsible for mediating detection of low spatial frequency gratings are operating in accordance with Weber's law, (van Nes and Bouman, 1967). Contrast sensitivity to higher spatial frequencies declines as the mean luminance of the grating is reduced. This finding is similar to that obtained for the photopic system by van Nes and Bouman (1967) and for the scotopic system by Daitch and Green (1969).

In photopic conditions (2.8 and 1.8 log td), CS recovery curves were approximately parallel, i.e. CSFs obtained at different times after the bleach were simply translated along the vertical axis and were not associated with a change in shape. This finding is in accordance with a previous study (Hahn and Geisler, 1995) and indicates that there is no change in the size of the receptive field or the balance of antagonistic receptive field regions. It also suggests, that during CS recovery the visual pathways responsible for detecting the gratings are operating in accordance with Weber's law. The finding that different pathways regain CS at a similar rate suggests that the sensitivity of all pathways to contrast is determined by the same mechanisms. Cicerone *et al.* (1990) have shown that following a period of intense light adaptation, desensitisation of the retina is extremely localised. They interpreted their results as indicating that bleaching

adaptation takes place predominantly in cone photoreceptors themselves. Such a localised site for bleaching adaptation could also account for the simple translation of CSFs along the vertical axis. Hayhoe (1979) has shown that post-receptoral mechanisms may also contribute to the sensitivity of the photopic system when the bleach is spatially restricted. The desensitisation associated with small bleaches is likely to be due to saturation of a retinal neurone that has a spatially antagonistic receptive field. The relatively large bleaching field used in this set of experiments (16°) is unlikely to cause saturation at this site because it is sufficiently large to stimulate receptive field surrounds.

When the luminance of the grating was reduced to 0.5 cdm^{-2} (0.8 log td) the CSF underwent a subtle change in shape during the period of measurement (see Figure 3.6, row 3). Contrast sensitivity to low spatial frequency gratings continued to increase after CS recovery to high spatial frequency gratings was almost complete. This finding is consistent with the idea that pathways mediating detection of the low spatial frequency gratings operate in accordance with Weber's law while pathways mediating detection of the high frequency gratings do not. This observation is only apparent for data obtained from subject WDT.

At lower luminances (0.05 cdm^{-2} and below) the CS recovery functions obtained at different times after the bleach were not parallel (see Figure 3.6 and 3.7, row 4). Both sets of data show a sudden increase in CS for low spatial frequency gratings after about 10 minutes. There are two reasons for believing that this rise in threshold is due to activity of the rods: firstly, the rise takes place at approximately the same time that rods determine sensitivity during a conventional dark adaptation investigation, and secondly, CS to spatial frequencies above the rod resolution limit are unaffected. A more subtle change in CSF shape is observed during the rod phase of CS recovery for both subjects at the lowest luminance studies (0.005 cdm^{-2}, bottom row of Figures 3.5 and 3.6). At the start of the rod phase of recovery, CS to the 1.5 and 0.6 c.p.d. gratings was similar but toward the end of the period of data collection CS to the lower spatial frequency was greater. A similar observation was made by Blakemore and Rushton (1965a) who obtained a series of dark adaptation functions using gratings of different spatial frequency (see Figure 1.33). Threshold to gratings whose bars subtended 7′ and 11′ of

arc increased at approximately the same rate for about 15 minutes, then threshold to the 7′ grating asymptoted whereas threshold to the lower spatial frequency continued to decline for a further 5 minutes. The finding that CS returns at different rates for different spatial frequency gratings does not rule out a role for photopigment concentration in the regulation of sensitivity, (Geisler, 1980). However, if all receptors regain sensitivity at a similar rate then the difference in the shape of the CSF functions must be due to post receptoral differences in the way pathways respond to changing receptoral sensitivity. The most likely explanation is that large receptive fields are best able to make use of the increase in receptor sensitivity through spatial summation and the consequent improvement in the signal to noise ratio of the pathways.

4. The effect of 'bleach' parameters on CS recovery

4.1 Introduction

One of the most enduring hypothesis about dark adaptation is that sensitivity in the dark is controlled by the concentration of a substance in the receptors, i.e. the photochemical hypothesis. The most well known example of this hypothesis is the Dowling-Rushton relationship which suggests that log threshold in the dark is proportional to the fraction of bleached photopigment.

The Dowling-Rushton relation provides a relatively good description of the latter stages of rod dark adaptation following a relatively large, long duration, intense bleach. However, for small bleaches the equation consistently underestimates threshold, (Rushton and Powell, 1972). The equation also fails to provide an adequate description of the early stages of dark adaptation following an intense bleach, when threshold is much less than that predicted by the model, (Lamb, 1990).

The Dowling-Rushton relation also provides a relatively good description of cone dark adaptation, (Hollins and Alpern, 1973). However the relation also fails in certain circumstances, namely, during the first 30 seconds following a weak bleach and for the entire course of dark adaptation following very brief (<0.001 sec) bleaches. In both cases threshold is higher than predicted.

Failure of the Dowling-Rushton relationship to describe adequately rod and cone dark adaptation under certain conditions does not constitute failure of the more general photochemical hypothesis. Threshold may be determined by a substance other than bleached photopigment. The only convincing test of this more general hypothesis is to obtain dark adaptation functions following exposure to different bleaching lights that produce the same proportion of the substance (Geisler, 1980). Specifically, if the substance is produced as a result of a visual pigment molecule absorbing a photon, then observation of the Bunsen-Roscoe Law ($I \times t = k$) would provide strong proof of the photochemical hypothesis.

Rushton and Powell (1972) and Pugh (1975) tested this hypothesis and showed that bleaches that contained the same number of quanta but differed in intensity and duration, produced identical rod dark adaptation functions. Their results showed that even in situations where the Dowling-Rushton relationship failed, the more general photochemical hypothesis was upheld.

The limits of the more general photochemical hypothesis have not been investigated for the photopic system. However, Hayhoe and Chen (1986) did determine the effects of different bleach parameters on the temporal modulation sensitivity of the photopic system during dark adaptation. They bleached approximately 85% of cone photopigment using a relatively long, dim, bleach (150 sec, 5.2 log td) and a shorter, more intense one (0.2 sec, 7.5 log td). For the following 5 minutes, subjects adjusted a centrally-fixated, 3.8°, flickering test (2 or 25 Hz) to threshold (the time-averaged illuminance of the test was 140 td). Both bleach conditions reduced flicker sensitivity. Low frequency flicker sensitivity recovered equally rapidly following the brief and relatively long bleach, but high frequency flicker sensitivity recovered much more slowly after the long bleach.

The purpose of the experiments described in this chapter was to determine how systematic variations in the intensity and duration of the bleach affect photopic CS recovery. In the first experiment the validity of the Dowling-Rushton relationship was investigated by varying bleach parameters (intensity and duration) in such a manner that an identical proportion of cone photopigment would be bleached in each case[1]. In a second experiment, equal energy bleaches ($I \times t = k$) were used to test the validity of the more general photochemical hypothesis as it relates to the recovery of spatial vision in photopic conditions.

---

[1] Measurement of photopigment concentration (by densitometry) was beyond the resources of this investigation therefore the amount of pigment bleached was estimated from the equations described by Hollins and Alpern, (1973).

4.2 Methods (experiment No.1)

The general apparatus and procedure has been described in Chapter 3. The subject was positioned by means of a full mouth bite bar and accommodation was paralysed using 1% cyclopentolate. The same two subjects that took part in the previous investigation (Chapter 3) also participated in this study. Initially CS recovery for a single spatial frequency (3.5 c.p.d.) was measured. Photopigment was bleached by exposing subjects to an adapting field that could be varied in intensity and duration.

In the first experiment the intensity (I) and duration (t) of the adapting field were varied in such a way that different combinations of I and t bleached the same fraction of cone photopigment. Initially the intensity of the bleach was kept constant (5.71 log td) and the exposure duration was altered to bleach approximately 20, 50, 87 and 95% of cone photopigment. Subsequently, the duration of the exposure was kept constant (120 seconds) and the intensity was varied to bleach approximately 20, 50, 87 and 95% of cone photopigment. Tables 4.1 and 4.2 detail the bleach parameters used in each experiment and the resulting pigment bleach.

Run	1	2	3	4
t (sec)	1	3	10	120
Bleach (%)	20.5	49.5	86.2	94.5

Table 4.1 Experimental parameters used to determine the effect of bleach duration on CS recovery. In each case the retinal illuminance provided by the adaptation field was 5.7 log td. The final row indicates the percentage of photopigment bleached. Figures are based on the equations proposed by Hollins and Alpern (1973).

Run	1	2	3	4
I (log td)	3.92	4.48	5.34	5.71
Bleach (%)	19.5	48.3	88.0	94.5

Table 4.2 Experimental parameters used to determine the effect of bleach intensity on CS recovery. In each case the adapting field was presented for 120 seconds.

By bleaching similar amounts of cone photopigment using different I x t combinations, the validity of the Dowling-Rushton relationship could be tested. Specifically, if CS recovery is determined by the fraction of photopigment then different combinations of I and t that bleach the same quantity of photopigment should produce similar CS recovery functions.

4.3 Results (experiment No.1)

The results of the first experiment are presented in Figures 4.1 and 4.2 which show a series of CS recovery functions obtained from subject TM and WDT. In each figure the left hand panel shows the effect of varying bleach duration and the right hand panel shows the effect of varying bleach intensity. In each case the curves, going from top to bottom, were obtained by bleaching approximately 20, 50, 87 and 95% of cone photopigment.

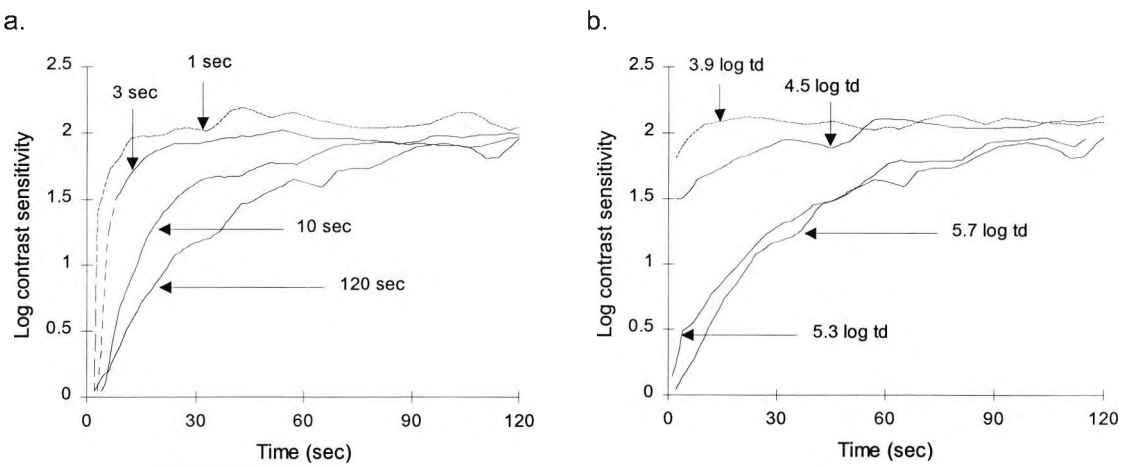

Figure 4.1 Contrast sensitivity recovery functions for subject TM following exposure to an adapting field that bleached approximately 20, 50, 87 and 95% of cone photopigment. In panel a. the adapting field produced a retinal illuminance of 5.71 log td and different bleaches were obtained by varying exposure duration. In panel b. the adapting field was displayed for 120 seconds and different bleaches were obtained by varying the retinal illuminance of the field.

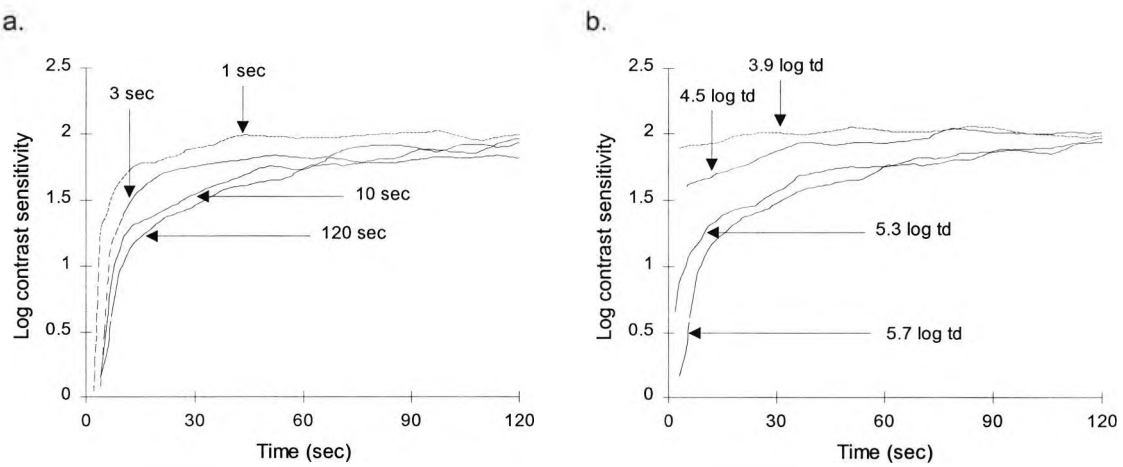

Figure 4.2 Contrast sensitivity recovery functions for subject WDT following exposure to an adapting field that bleached approximately 20, 50, 87 and 95% of cone photopigment. In panel a. the adapting field produced a retinal illuminance of 5.71 log td and different bleaches were obtained by varying exposure duration. In panel b. the adapting field was displayed for 120 seconds and different bleaches were obtained by varying the retinal illuminance of the field.

By comparing panels a. and b. in each figure, characteristic differences in CS recovery may be seen.

Following exposure to the intense adapting field (panel a. in Figures 4.1 and 4.2) CS was markedly depressed even when the exposure time was short (1 second). Immediately after each period of light adaptation, neither subject was able to see the high contrast grating (c=0.9). After a few seconds (2.5-6 seconds) the high contrast grating became visible and CS recovery began. Recovery of contrast sensitivity was most rapid following the shortest exposure and slowest following the longest exposure.

Following the long duration exposure (120 seconds) the pattern of CS recovery was markedly different (see panel b. in Figures 4.1 and 4.2). Only exposure to the most intense bleaching fields (5.34 and 5.7 log td) reduced CS < 1/0.9 i.e. subjects were unable to see the high contrast grating. Exposure to the 3.92 and 4.48 log td fields produced only a relatively small reduction in CS.

Comparison of panels a. and b. shows that short, intense, bleaches have a very different effect on CS recovery than longer, less intense ones, even when the amount of pigment bleached is the same. The greatest discrepancy is seen for the two conditions that bleached only 20% of cone photopigment (see upper curves in Figures 4.1 and 4.2). This finding demonstrates a clear failure of the Dowling-Rushton relation as it relates to CS recovery, i.e. CS recovery is not directly related to the fraction of bleached photopigment.

4.4 Methods (experiment No.2)

In the second experiment, the validity of the more general photochemical hypothesis was tested. The intensity and duration of the bleach were altered in such a way that the product of the two parameters remained constant i.e. (I x t = k, the Bunsen-Roscoe Law). Table 4.3 shows the combinations of I and t that were used together with the percentage bleach. The relatively brief exposure times used in this investigation (0.5 seconds) and the limited retinal illuminance (5.9 log td) that could be produced by the optical system dictated that the percentage of photopigment bleached would be relatively small.

Run	1	2	3
I (log td)	5.9	5.13	4.42
exposure time (sec)	0.5	2.7	13.8
bleach energy (I.t) td sec	5.6	5.6	5.6
Bleach (%)	15.2	15.0	13.9

Table 4.3 Experimental parameters used to determine the validity of the general photochemical hypothesis.

If a photoproduct is responsible for the initial reduction in CS and its subsequent recovery then equal energy bleaches (that presumably produce an equal concentration of a photoproduct) should produce identical CS recovery functions.

To determine if long and short bleaches had a different effect on different spatial frequencies, CS recovery was measured for three spatial frequencies (0.6, 3.5 and 19.9 c.p.d.).

The intensity of the bleach was varied by placing suitable ND filters in Channel 1 of the Maxwellian view optical system (see Chapter 3, Figure 3.4). Bleach duration was controlled by the electronic shutter (SH1, in Figure 3.4). The retinal illuminance produced by the optical system when using each ND filter was determined in the usual way. The accuracy of the shutter was determined by viewing the time profile, of the exposure, on a Nicolet 3091 storage oscilloscope which was connected to a United Detector Technologies (UDT) photodiode placed 12 cm from the pinhole.

4.5 Results (experiment No.2)

The results of the second investigation are presented in Figures 4.3 and 4.4. Although CS recovery was measured for 120 seconds, recovery was rapid and almost complete after 20 seconds. Therefore the following figures only present the first 20 seconds of CS recovery data.

The three upper panels in each figure show a series of CS recovery functions obtained following exposure to three equal energy bleaches that differed in intensity and duration. The lower three panels in each figure show contrast sensitivity functions obtained at different times after the bleach.

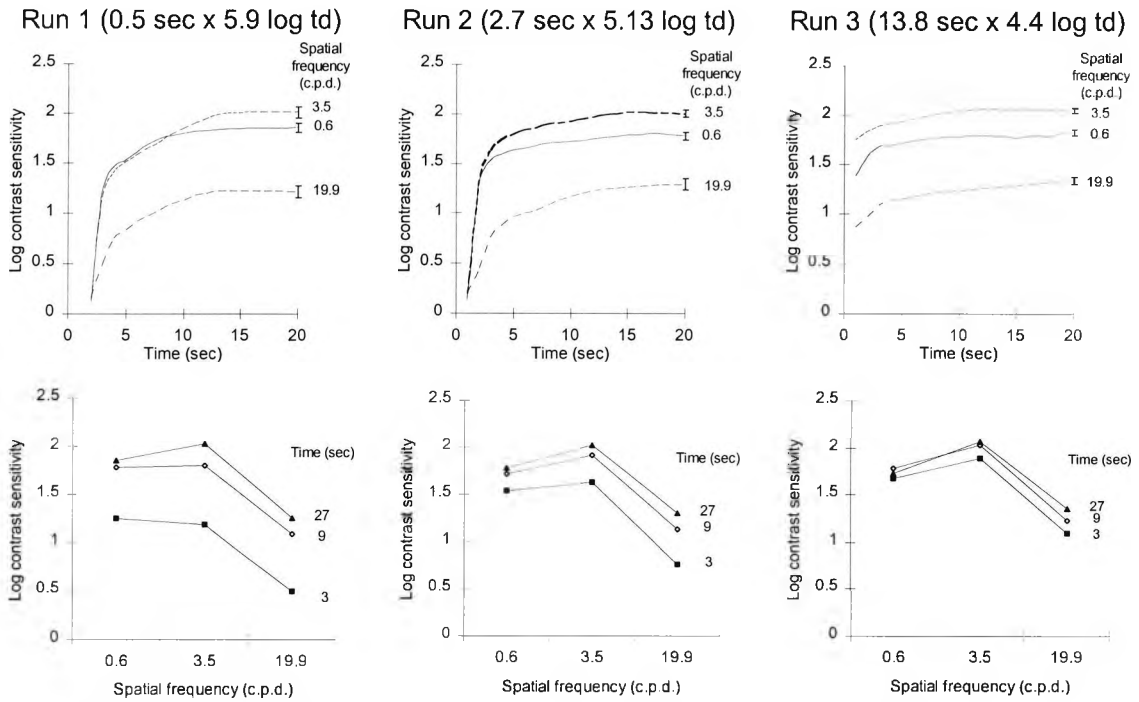

Figure 4.3 CS recovery following three equal energy bleaches that differed in intensity and duration for subject TM. The upper row shows CS recovery functions for the three spatial frequencies examined and the lower row shows a series of contrast sensitivity functions obtained at different times following the bleach. Time of measurement is indicated to the right of each contrast sensitivity function. The error bars at the end of each curve indicate the magnitude of the mean SE.

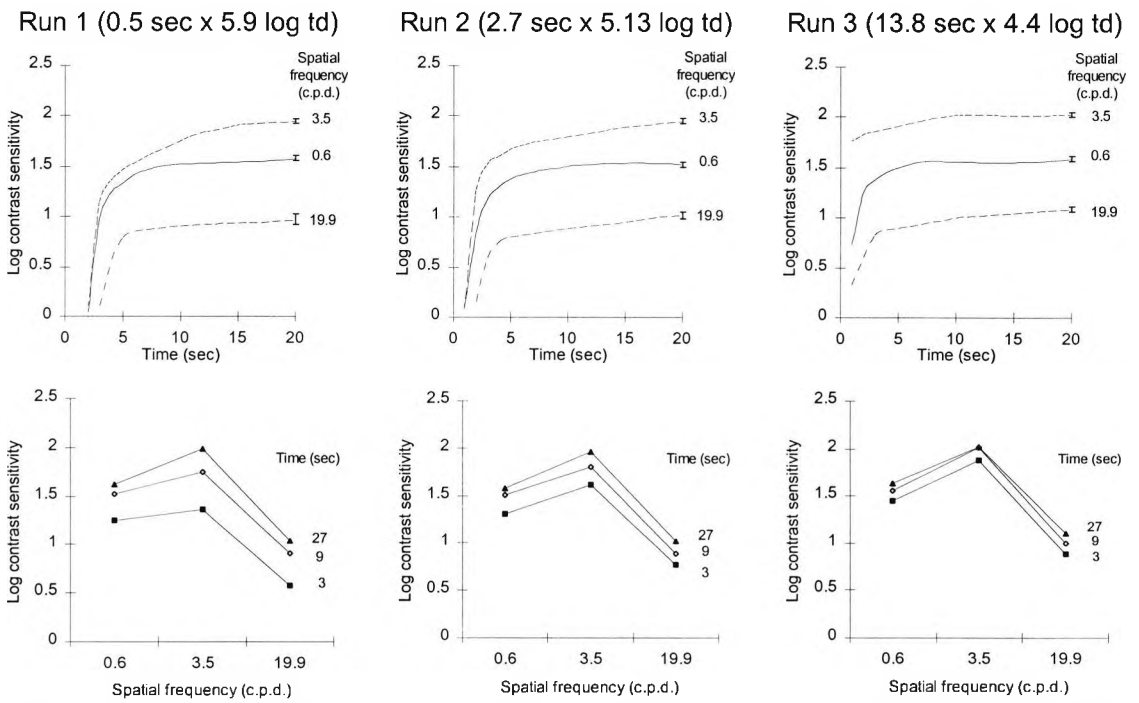

Figure 4.4 CS recovery following three equal energy bleaches that differed in intensity and duration for subject WDT. The upper row shows CS recovery functions for the three spatial frequencies examined and the lower row shows a series of contrast sensitivity functions obtained at different times following the bleach. Time of measurement is indicated to the right of each contrast sensitivity function. The error bars at the end of each curve indicate the magnitude of the mean SE.

Examination of Figures 4.3 and 4.4 shows that long and short bleaches have very different effects on CS recovery. Following the short bleach CS was markedly reduced for all spatial frequencies, so that even a high contrast grating (c=0.9) was not visible. Following exposure to the longest, least intense bleach, CS was depressed but by a relatively small amount. The effect of bleach parameters is more obvious in Figures 4.5 and 4.6 where each plot shows CS recovery for a single spatial frequency following each of the bleach conditions.

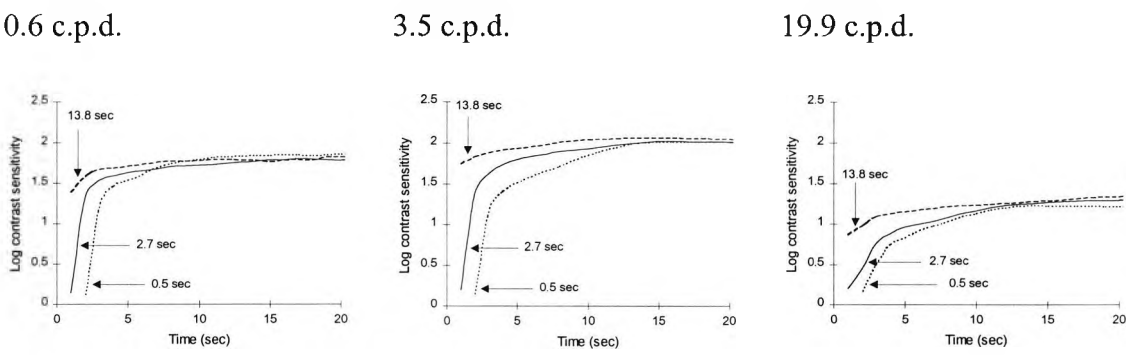

Figure 4.5 CS recovery functions for subject TM. Each plot shows recovery for a single spatial frequency for each of the 3 bleach conditions. The upper curve was obtained after a 13.8 second exposure to a 4.42 log td field, the middle curve after exposure to a 5.13 log td field for 2.7 seconds and the lower curve following a brief exposure (0.5 seconds) to a 5.9 log td field.

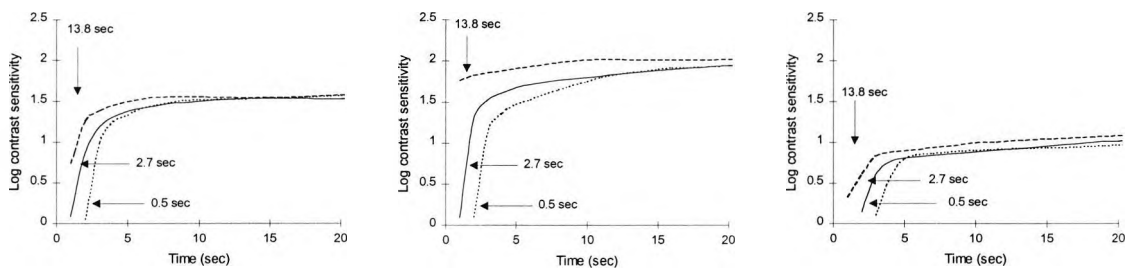

Figure 4.6 CS recovery functions for subject WDT. Each plot shows recovery for a single spatial frequency for each of the 3 bleach conditions. The upper curve was obtained after a 13.8 second exposure to a 4.42 log td field, the middle curve after exposure to a 5.13 log td field for 2.7 seconds and the lower curve following a brief exposure (0.5 seconds) to a 5.9 log td field.

Figures 4.5 and 4.6 show that the brief intense bleach reduced CS below $^{1}/_{0.9}$ for approximately 2 seconds, after which CS recovered rapidly. The longer duration (2.7 seconds) bleach only reduced CS below $^{1}/_{0.9}$ for approximately 1 second, followed by a rapid recovery and the longest bleach (13.8 seconds) only reduced subsequent CS by approximately 0.5 log units. This finding, that equal energy bleaches have a different

effect on CS recovery, does not support the hypothesis that a photoproduct is solely responsible for CS depression.

Although the results show that short and long bleaches have a very different effect on CS recovery, all spatial frequencies appear to be affected in a similar fashion. Low, intermediate and high spatial frequency gratings recover at approximately the same rate. This is most clearly shown in the series of contrast sensitivity functions in Figures 4.3 and 4.4 where each contrast sensitivity function is approximately the same shape. The only departure from this shape invariance is seen in the lower left hand panel of Figure 4.3 where the CSF is initially a low pass function.

4.6 Discussion

This set of experiments demonstrates that visual performance in photopic conditions is changed after a period of intense light adaptation. The nature of this change is critically dependant upon the intensity and duration of the adapting light. Short, intense bleaching lights dramatically reduce subsequent contrast sensitivity whereas, longer, dimmer exposures only cause a relatively small reduction in contrast sensitivity.

The finding that short and long pre-adapting exposures which bleach a similar amount of cone photopigment have a different effect on contrast sensitivity indicates that photopigment concentration is not the sole determinant of CS recovery. A long, dim exposure that bleaches 20% of cone photopigment reduces CS to a 3.5 c.p.d. grating by less than 0.3 log units but a short, intense period of light adaptation that bleaches the same amount of photopigment, reduces CS by 2 log units.

Rushton and Powell (1972) and Pugh (1975) have shown for the scotopic system that even in situations where threshold is not directly related to the fraction of unregenerated photopigment, threshold is dependant upon bleach energy. The finding that scotopic sensitivity was dependant on bleach energy (I x t) suggests that some other photoproduct must determine threshold because 'it is inconceivable that any other mechanism could integrate I x t so perfectly' (Rushton and Powell, 1972). The second experiment reported here does not support the notion that CS is determined solely by a photoproduct. However, it does not rule out the possibility that a photoproduct does

paly a role in CS depression. A photoproduct that decays rapidly, relative to the duration of the pre-adapting light, would have a higher concentration after a short exposure than a longer one.

An alternative explanation is that a "neural" mechanism is responsible for the dramatic reduction in CS following the brief bleach. Increment threshold functions obtained when a test stimulus is presented simultaneously with an adapting background rise much more steeply than a conventional increment threshold functions. The dramatic rise in threshold often referred to as "saturation" arises because adaptational mechanisms that usually protect the visual system from the unwanted effects of response compression, do not have time to operate. Hayhoe *et al.* (1987) identified several mechanisms that protect the photopic system from response compression. The brief pre-adapting exposure used here (0.5 seconds) may have had a more dramatic effect on subsequent CS than the longer exposure because a component in the visual pathway may have "saturated".

Hayhoe and Chen (1986) showed that long and short duration bleaches had a different effect on high and low flicker sensitivity. The results presented here show that although long and short duration bleaches have a different effect on CS recovery, this effect is not particularly spatial frequency dependant, i.e. the rate of CS recovery is approximately the same for all spatial frequencies. However, a subtle spatial frequency effect is evident in the lower left hand panel of Figures 4.3 and 4.4. Following the brief bleaching exposure, CS to low spatial frequencies recovers slightly more rapidly than intermediate and high spatial frequency CS. This subtle difference is explored more fully in Chapter 6 where contrast sensitivity recovery functions were obtained for 50 subjects.

5. Photostress test

5.1 Introduction

The preceding chapters have described a technique that can determine how contrast sensitivity changes following exposure to a light that bleaches a considerable fraction of photopigment. Although, this is the first time that contrast sensitivity has been measured in such circumstances, several studies have measured the time taken for acuity to return following a 'bleach'. This measurement has been found to be of clinical value and developed into a procedure known as the photostress test. The test is implemented by exposing a subject's eye to a light source, (such as a pentorch) and measuring the time taken for visual acuity to return to pre-exposure levels. Generally, a photostress recovery time (PSRT) in excess of 1 minute, or a large difference between eyes, is indicative of retinal dysfunction.

Previous chapters have shown that the recovery of contrast sensitivity following exposure to light is dependant upon 'bleach' and test parameters. Unfortunately many textbook descriptions of how the photostress test should be conducted are imprecise and it is likely that the bleaching methods proposed would produce variable results. It is perhaps for this reason that the clinical photostress test has never gained widespread acceptance. This is regrettable because under controlled conditions the test has been shown to be highly sensitive to small changes in macular function, (Collins and Brown, 1989a; Collins and Brown, 1989b). In this chapter a series of experiments are described which investigate the effects of methodology, subject age, ametropia and acuity on PSRT.

5.1.1 Normal PSRT

Chilaris (1962) provided an early description of the clinical photostress test. The technique he described involved dazzling the retina with the light from a 'slightly dimmed' ophthalmoscope for 30 seconds and measuring the time taken for acuity to return to pre-exposure levels. Recovery times less than 50 seconds were associated with

normal retinal function and times in excess of this were consistently observed in subjects with macular oedema.

Glaser *et al.* (1977) measured PSRT in 179 normal eyes as well as 63 with macular disorders and 20 with optic nerve disease. They exposed their subjects' undilated eyes to a pentorch held 3 cm from the cornea for 10 seconds and recorded the time taken to read any 3 letters on the line above pre-exposure acuity. In normal subjects mean PSRT was 27 seconds and 99% recovered within 50 seconds.

More recently Lovasik (1983) used the same pentorch technique employed by Glaser *et al.* (1977) to examine a group of 35 normal subjects. Those under 50 years of age (n=28) had a mean PSRT of 7.9 seconds (SD 2.9) and those over 50 (n=7), a mean recovery time of 15 seconds (SD 4.6).

These different estimates of normal PSRT, even when the technique is supposedly the same (Glaser et al., 1977; Lovasik, 1983), highlight the problem faced by the practitioner who wishes to differentiate between normal and abnormal recovery times. Several studies have attempted to standardise the period of light adaptation and / or measure PSRT objectively. Unfortunately many of the techniques used in such studies are beyond the resources of most clinicians.

Severin *et al.* (1967a) tried to provide a consistent level of initial light adaptation. They first dilated their subjects before fitting them with contact lenses which had a 6 mm artificial pupil. Light adaptation was achieved using a flash from a xenon arc discharge tube positioned 50 cm from the subject. The time taken for acuity (measured by Landolt-C rings in a Goldmann Weekers adaptometer) to return to normal varied from 30 to 70 seconds (mean 53 seconds).

All of the studies described so far have used the return of acuity to determine the end point of recovery but other investigations have determined recovery on the basis of the return of sensitivity to a flickering spot. Adams and Brown (1975) light-adapted their subjects (n=9) by exposing them to a 5.6×10^4 cdm^{-2} field for 10 seconds. Subjects then responded when they could see a small (5') flashing spot (4 Hz) presented on a 22 cdm^{-2} background. The test was presented at 5 discrete contrast levels. Following the period of light adaptation it took subjects approximately 40 seconds before they could see the

lowest contrast test. A similar technique was used by Collins (1989) who examined 65 normal subjects. In this study, the mean recovery time for subjects was 31 seconds (SD 24) for 16-55 year olds and 59 seconds (SD 43) for those over the age of 55.

Other investigators have measured PSRT using objective techniques. Lovasik (1983) used the pentorch technique devised by Glaser *et al.* (1977) (10 sec at 3 cm) to light adapt his subjects and PSRT was measured objectively using visual evoked responses. Bergman (1980) determined recovery times by recording the pause in optokinetic nystagmus following exposure to a photoflash. Recovery from photostress testing has also been evaluated by measuring pupil size (Zabriskie and Kardon, 1994).

5.1.2 PSRT and age

Several studies have examined the effect of age on PSRT. Most, but not all, have shown a slight increase in PSRT with advancing years. The significance of this increase is equivocal.

Severin (1967a) examined 49 subjects and compared PSRT for patients under the age of 40 to those aged 40 or over. The mean recovery time for the younger group was 51 sec (SD 9.4) and for the older group 57 sec (SD 5.9). A two sample t-test was used to show a significant difference between these two groups at the 5% level.

A smaller group of normal subjects (n=35) was examined by Lovasik (1983). He used the photostress technique described by Glaser *et al.* (1977) and fitted a non-linear regression line to the data ($PSRT = 5.403e^{0.0166.Age}$). Apparently this model is "significant at the 0.001 level" but there is no indication as to which statistic was used to substantiate this statement. Lovasik (1983) divided his subjects into 2 groups; those below 50 years of age (n=28) had PSRTs of 7.9 seconds (SD 2.7) and those over 50 (n=7) who had PSRTs of 15.2 seconds (SD 4.6).

Sloan (1968) examined 59 subjects and found no relationship between age and PSRT. Mean recovery time for right eyes was 33.8 sec (SD 10.8) and for left eyes 31.9 sec (SD 13).

The largest study of the effect of age on PSRT was conducted by Glaser *et al.* (1977). They examined 179 normal eyes using the technique described previously. The mean

PSRT for all subjects was 27 seconds (SD 11). Subjects were divided into 3 groups on the basis of age, those aged 30 or under, those aged 31 to 60 years, and those aged 61 and over. Mean PSRT for the youngest group was 26 seconds (SD 11), for the 31-60 year age group 26 seconds (SD 10) and for the oldest group 30 seconds (SD 12). The authors concluded that "increased PSRT with increased age was not striking" but they did not test for statistical differences between age groups.

5.1.3 Effect of disease and drugs on PSRT

Several retinal conditions have been shown to increase PSRT. These include cystoid macular oedema (Severin, 1980), central serous retinopathy (Natsikos and Dean Hart, 1980), age related maculopathy (Collins and Brown, 1989) macular oedema (Bailliart, 1954), macular drusen (Glaser *et al.,* 1977) and chorioretinitis (Severin, 1967b). The largest study of subjects with macular disorders was conducted by Glaser *et al.* (1977). Using the technique described earlier they showed that 83% of subjects with macular disease had PSRTs in excess of 60 seconds and the mean recovery for this group was in excess of 2.5 minutes. The same study measured PSRT in 20 eyes with optic nerve disease. This group had relatively normal PSRTs (mean 36 seconds) and 80% recovered within 50 seconds. Glaser *et al.* (1977) concluded that the photostress test was a sensitive discriminator between optic neuropathy and subtle macular disease.

Several systemic drugs have also been associated with increased PSRT including: the tranquilliser Melperon (Bergman *et al.,* 1980), Oxazepam (Bergman *et al.*, 1979), alcohol (Adams and Brown, 1975) and Chloroquine (Carr *et al.*, 1968).

5.1.4 Other factors effecting PSRT

Refractive error may also effect PSRT. It is conceivable that relatively large myopic eyes may have increased PSRTs because the retina is stretched over a greater surface area. If retinal has to move over an increased distance to recombine with opsin in the myopic eye, then PSRT may be increased.

Acuity may also effect PSRT, particularly when the Snellen chart is used. Classically the end point of the photostress test is the time taken to read the line below best acuity.

Therefore, the non-linear progression of letter sizes on the Snellen chart may effect results.

5.1.5 Clinical tests

Although a variety of techniques have been used to measure PSRT, clinicians are most likely to opt for a simple method, typically one described by a modern text book.

According to Kanski (1994), the photostress test involves measuring best acuity, exposing the patient's eye to a pentorch or an indirect ophthalmoscope held 3 cm away for 10 seconds and measuring the time taken for the patient to regain the ability to read any 3 letters of the pre-test acuity line. The result obtained is compared to that of the other eye, a slower recovery being indicative of a macular lesion (sometimes 50 seconds or more).

Alexander (1990) suggests dark adapting the subject for 1 minute then exposing the macular to the fixation target of the direct ophthalmoscope for 10 seconds. The time taken to read the line above best acuity is taken as the PSRT. Using this method the average normal recovery time is 50 seconds. There is no indication as to what constitutes an abnormal recovery time, though the authors do suggest comparing eyes and the one with the longer time may have macular oedema.

Fingeret *et al.* (1990) describe an alternative method in which the eye is exposed to a strong pentorch held 3-5 cm form the eye for 10 seconds and the time taken for the subject to read one line less than the original best acuity is measured. This is then repeated for the other eye. Normal recovery times are between 50-60 seconds and abnormal recovery times can range from 90 to 180 seconds or greater.

One of the most obvious criticisms of the clinical photostress test is lack of standardisation. Different text book descriptions of the photostress test recommend using different pieces of equipment to "photostress" the retina, e.g. pen torches, the brightness acuity tester (BAT), direct and indirect ophthalmoscopes. They also recommend different eye to source distances (3-5cm) although all agree that the eye should be exposed to the source for 10 seconds.

It is quite remarkable that these different "photostressing" methods should produce such consistent results, i.e. a normal PSRT of 50 seconds or less! Indeed this ubiquitous text book description of what constitutes a normal result is inconsistent with studies that report a range of normal PSRTs from 7 to 70 seconds, Lovasik (1983).

5.1.6 Purpose

One of the purposes of this investigation was to re-evaluate the effect of age on PSRT because previous studies provide conflicting reports. Coile and Baker (1992) have shown that both photopigment regeneration and foveal dark adaptation show a parallel slowing of recovery rate with increasing age. This finding would suggest that PSRTs for older subjects should be greater than for younger subjects. However, this tendency toward increased PSRTs with increasing age may be offset by a reduction in pupil size and in transparency of the ocular media associated with age (for a review see Weale, 1992) which would reduce retinal illuminance and thus the effectiveness of the period of light adaptation.

Another purpose was to determine what effect different, clinically applicable, bleaching strategies had on PSRT and to compare the results with a technique likely to minimise sources of error. The repeatability of each technique was determined and the effects of age, ametropia and acuity evaluated.

5.2 Materials and Methods

5.2.1 Materials

In this study 4 instruments were used to light-adapt the retina; namely, an unfocused pentorch, a focused pentorch, a Henie direct ophthalmoscope and a single channel Maxwellian view optical system.

One of the purposes of this study was to compare PSRTs obtained when using methods described in clinical textbooks with a carefully controlled test using a Maxwellian view system. Acuity was assessed using a Log MAR chart viewed from a distance of 3 m and illuminated by a tungsten halogen flood lamp[1]. In accordance with manufacturer's recommendations, the chart had a luminance of 200 cdm^{-2}. A stop clock, accurate to the nearest second, was used to measure recovery times.

5.2.2 Subjects

Subjects were members of staff and students from the Department of Optometry and Visual Science or members of the public who had attended the departmental refraction clinic.

Potential recruits to the study were examined to exclude those who had a history of retinal disease, were taking medication, had an abnormal fundal appearance, an acuity of less than 0.12 log MAR or an abnormal result with the Amsler chart. Subjects meeting these acceptance criteria were refracted to ensure they used an appropriate optical correction during the test.

In total, fifty subjects were recruited to take part in the main study, 10 subjects were in their twenties, 10 in their thirties, 10 in their forties, 10 in their fifties and 10 in their sixties.

---

[1] A Log MAR chart was chosen in preference to a Snellen chart because, unlike the Snellen chart, the progression of letter sizes increases in equal logarithmic steps. Therefore, the endpoint of recovery, one line below best acuity, was consistent irrespective of the initial acuity. The non-linear progression of letter sizes on the Snellen chart may have been a source of error in previous studies.

5.2.3 Procedures

Prior to data collection, subjects were instructed about the procedures used in the investigation. At the start of each experimental session the non-test eye was patched and log MAR acuity measured monocularly. The subjects' refractive correction (if used) was removed and one of 4 techniques (described below) was used to bleach photopigment:

Version 1 an unfocused pentorch held 3 cm from the eye for 10 seconds.

Version 2 a focused pentorch (an image of the filament was formed in the subject's pupil) held 5 cm from the eye for 10 seconds.

Version 3 the macular spot of the direct ophthalmoscope (adjusted to full intensity) was projected directly onto the macular for 30 seconds. The ophthalmoscope was held as close to the eye as possible and fixation was confirmed by the investigator.

Version 4 a 6 log td, 16°, 'white' field presented in Maxwellian view for 30 seconds.

In all cases the subject was instructed to look straight into the light. At the end of the period of light adaptation the timer was started. The subject's refractive correction (if worn) was replaced and they were encouraged to read the letter chart. The time taken for their acuity to reach 0.1 log MAR less than their best acuity (equivalent to 1 line below best acuity) was recorded as the photostress recovery time (PSRT). Subjects were not made aware of the end point. Following a recovery period of 5 minutes, the procedure was repeated for each version of the photostress test.

5.2.4 Pilot study

To highlight any problems with the methodology and to assess the repeatability of each photostress method, a pilot study was conducted on 10 subjects who attended on two separate occasions. It had been expected that version 4 of the test would be the most repeatable method and version 1 the least.

The reason for this expectation were that each method was prone to particular errors:

Version 1 of the test (holding an unfocused pen torch 3 cm from the eye for 10 seconds) had several methodological shortcomings. The retinal illuminance would depend on pupil size and errors in implementing the relatively short exposure time would have a relatively large effect on the amount of pigment bleached.

Version 2 of the test was also prone to timing errors but the retinal illuminance should have been independent of pupil size because an image of the filament of the pentorch was projected into the subject's pupil. However, in practice the experimenter found it hard to maintain the image of the filament in the subject's pupil and simultaneously observe the stop clock.

Version 3 of the test (exposing the subject to the light from a direct ophthalmoscope for 30 seconds) should have minimised possible sources of error still further. The retinal illuminance should have been independent of pupil size because ophthalmoscopes place an image of the filament in the plane of the ophthalmoscope mirror. Therefore, providing the ophthalmoscope can be held close to the pupil, the system should approximate a Maxwellian view optical system. The increased exposure time should reduce the effect of small timing errors.

Version 4 of the test involved exposing the subject for 30 seconds to a field seen in Maxwellian view. Consequently a consistent amount of pigment should have been bleached by this method.

In any comparison of clinical measurement techniques, it is of value to compare the repeatability of each method. By obtaining measurements with each method on two separate occasions for the same subjects the similarity of the repeated measurements may be determined. By plotting the measurement obtained at visit one against visit two, the degree of association between measurements may be visualised. The proximity of the points to the line of equality (visit 1 = visit 2) gives some indication of the agreement.

An alternative approach is to plot the differences between pairs of values obtained at visits one and two against the mean measurement. Such plots permit identification of any relationship between measurement error and the true value (Bland and Altman, 1986; Altman; 1991).

To determine which method is most repeatable it is necessary to calculate the standard deviation of the differences between pairs of measurements. Assuming a normal distribution of values, the coefficient of repeatability can be calculated as being twice the standard deviation of the mean differences. The test can be described as having good repeatability if differences of ±2 SD are not clinically important.

5.3 Results

5.3.1 Pilot data

The raw data from the pilot study is shown graphically in Figure 5.1. It can be seen that PSRT for versions 1 and 2 of the test were very much shorter than PSRT for versions 3 and 4. The proximity of each data set to the line of equality (visit 1 = visit 2) gives an indication of the agreement between measurements.

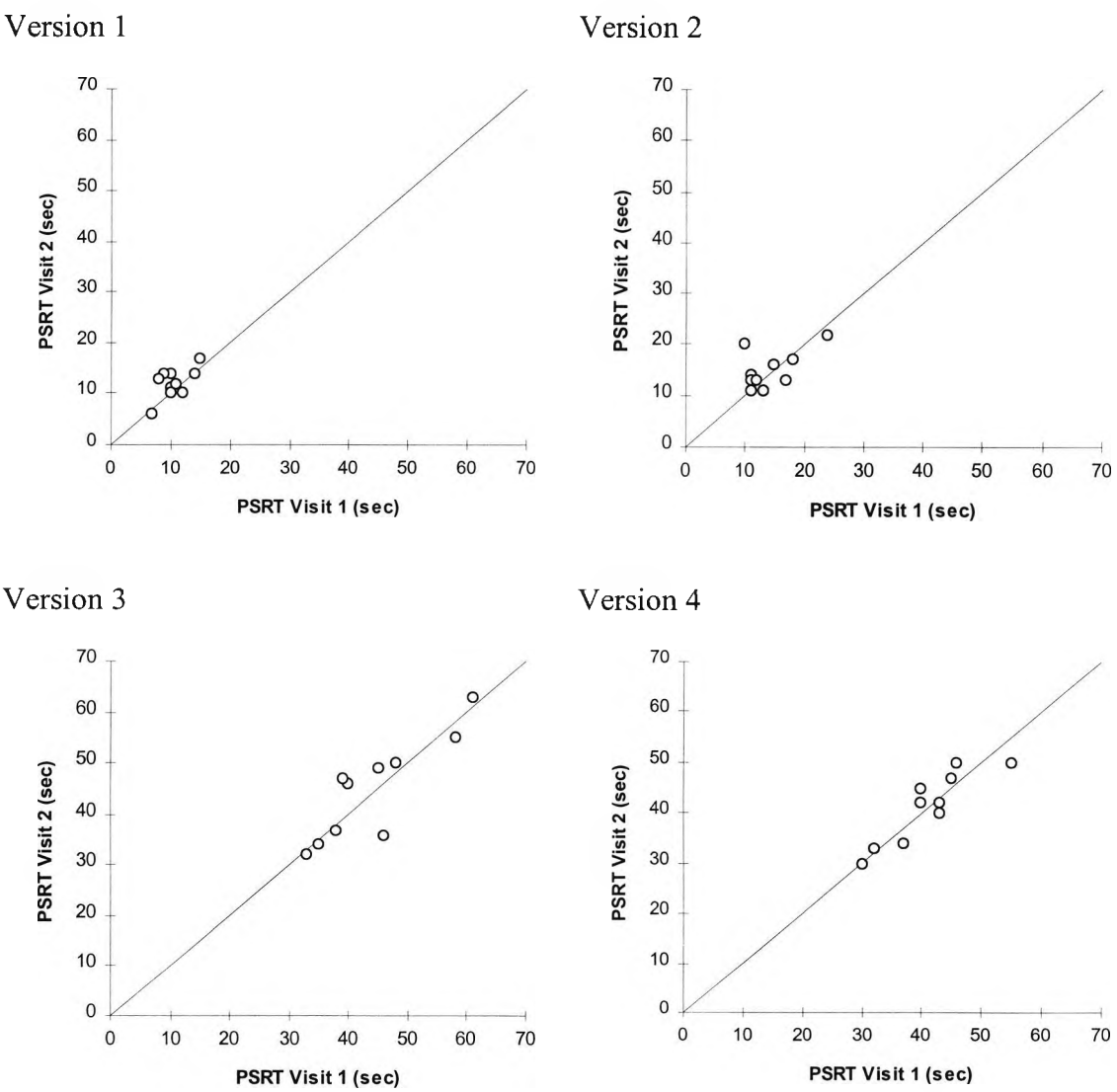

Figure 5.1 Photostress recovery time, visit 1 against visit 2. The solid line is the line of equality i.e. visit 1 = visit 2.

Figure 5.2 shows the differences between pairs of measurements plotted against the mean of the two visits (note different scales are used on the horizontal axis). The mean difference between measurements (the bias) is indicated by the solid horizontal line and the two dashed lines describe the 95% limits of agreement. These limits show how much we may expect two measurements to differ for a new subject.

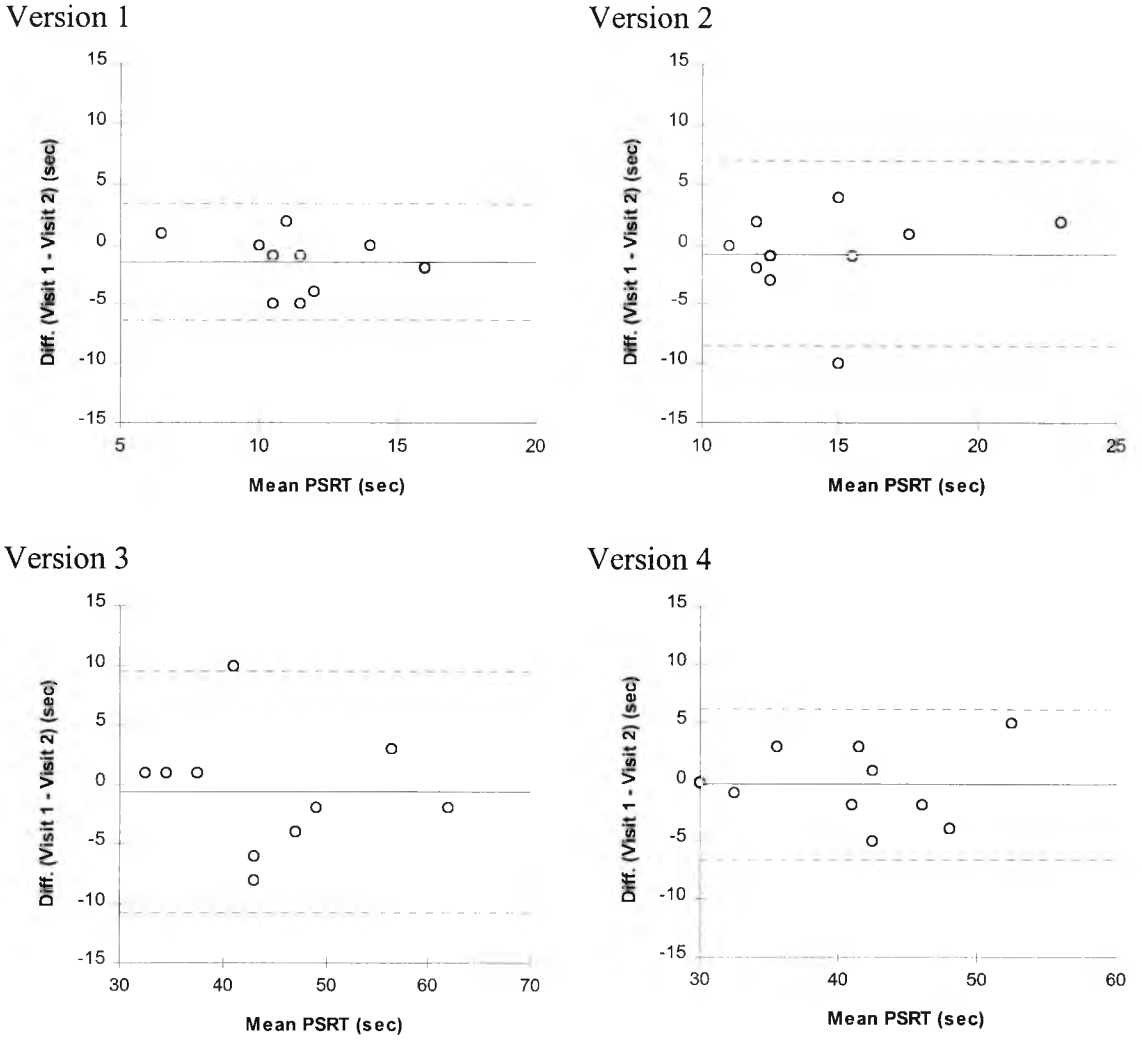

Figure 5.2 Difference in PSRT (visit 1 - visit 2) plotted as a function of mean PSRT ((visit 1 + visit 2) / 2) for each version of the photostress test studied. The solid horizontal lines shows the bias and the two dashed lines the 95% limits of agreement.

Visual examination of the plots shows that the differences in measurements are not related to the size of the measurement i.e. there is no "funnelling". However the sample size was relatively small and does not permit firm conclusions.

The repeatability results are presented in Table 5.1. The coefficient of repeatability (twice the standard deviation of the differences) is least for version 1 of the test i.e.

version 1 produced the most repeatable results. This unexpected observation highlights one disadvantage of this analysis, namely, that it does not take into account the scale of the measurement, i.e. the difference between visits for version 1 of the test is small because PSRT was relatively short.

	PSRT Visit 1 (sec)	PSRT Visit 2 (sec)	Mean Difference (sec)	Repeatability (sec)
Version 1	10.6 (SD 3)	12.1 (SD 3)	-1.5	5
Version 2	14.2 (SD 4.4)	15.0 (SD 3.7)	-0.8	7.8
Version 3	44.3 (SD 9.3)	44.9 (SD 10.0)	-0.6	10.5
Version 4	41.1 (SD 7.2)	41.3 (SD 7.1)	-0.3	6.4

Table 5.1 Repeatability data comparing visit 1 and visit 2 for each version of the photostress test. The second and third columns show the mean PSRT and SD in seconds for visits 1 and 2. The mean difference in PSRT (visit 1 - visit 2) is shown in the third column and the fourth columns specifies the coefficient of repeatability (i.e. twice the standard deviation of the of the mean difference).

Differences in measurement scale may be overcome by expressing differences in recovery time (visit 1 - visit 2) as a fraction of mean PSRT. If this is done version 4 of the test becomes the most repeatable technique as expected. The coefficient of repeatability expressed as a percentage of the mean PSRT is 44%, 52%, 22% and 14 % for versions 1 to 4 of the photostress test respectively. That is, when measuring PSRT using version 4 of the test, measurements on different occasions are likely to differ by less than 14%.

5.3.2 Effect of photostress technique on PSRT

Fifty subjects provided complete sets of data. Photostress recovery times for each of the subjects for each version of the test is presented in Appendix I.

Mean PSRT recorded with each version of the photostress test is presented graphically in Figure 5.3.

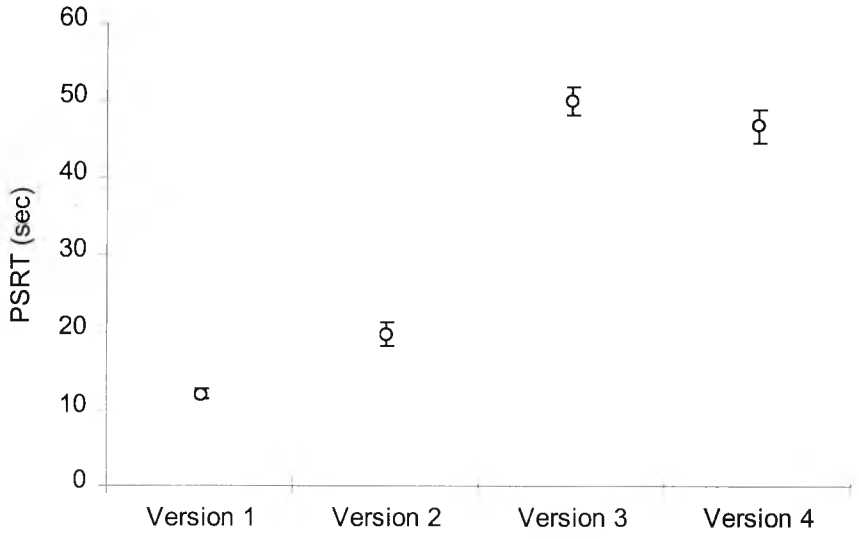

Figure 5.3 Graph showing mean PSRT obtained for each version of the photostress test for 50 normal subjects. The error bars indicate the magnitude of the standard error.

Figure 5.3 shows that PSRTs recorded using versions 1 and 2 of the photostress technique were considerably shorter than those recorded for versions 3 and 4. Using a paired t-test, this difference is highly significant for all combinations of tests except for versions 3 and 4 of the test where the difference just fails to achieves significance (two tail, df = 49, t=2.01, p = 0.052). Such large differences in PSRTs are presumably due to differences in the fraction of cone photopigment bleached by each version of the test

One purpose of this study was to compare the results obtained using the three clinically-applicable 'bleaching' methods with a Maxwellian view method ("gold standard") that might reasonably be assumed to produce the most consistent degree of initial light adaptation. This comparison is shown graphically in Figure 5.4. Each plot shows PSRT obtained with one of the versions of the test plotted against the "gold standard" PSRT. The proximity of each data set to the solid line gives an indication of the agreement between each of the techniques and the gold standard. The obvious departure from the line of equality in panels a and b of Figure 5.4 show that there is little agreement between absolute values of PSRT obtained with versions 1 and 2 of the photostress test and version 4. Version 3 of the photostress technique produces values most consistent with the "gold standard". However differences in the absolute magnitude of PSRT may be unimportant if measures of PSRT are closely associated i.e. if high values of PSRT obtained with one technique are associated with high values of another technique. The

most appropriate method of determining the association between two continuous variables is by calculating the correlation coefficient (r). The correlation coefficient was calculated for each test combination and is shown in the upper left hand corner of each plot.

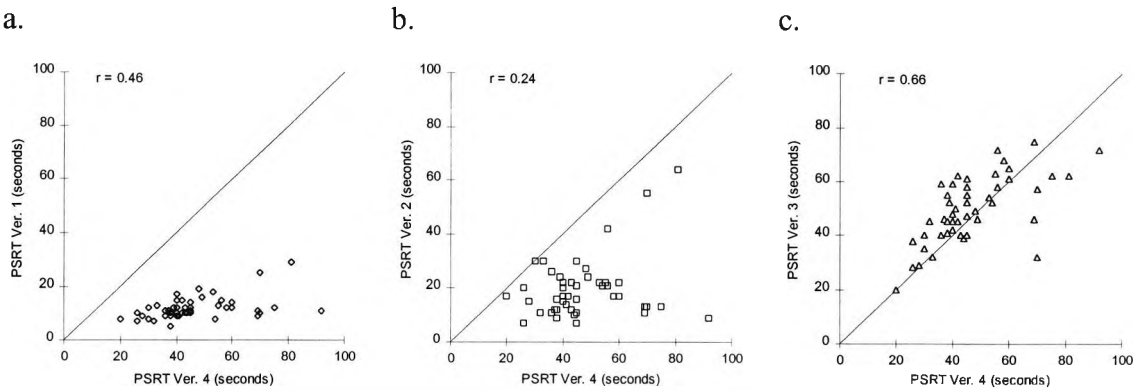

Figure 5.4 Plot of PSRT against "gold standard" PSRT (Version 4). Panel a) plots version 1 against version 4, panel b) plots version 2 against version 4 and panel c) plots version 3 against version 4. The solid line is the line of equality.

Photostress recovery time obtained with version 3 of the photostress test is most closely associated with the PSRT obtained with the "gold standard" (r = 0.66). The degree of association between version 3 of the photostress test and the gold standard suggests that version 3 of the test is likely to be the most useful in the clinic.

5.3.3 Effect of age on PSRT

When evaluating clinical measurements it is important to investigate possible relations with age. It is quite possible that the mean PSRT and the standard deviation may change with age.

The relationship between PSRT and age is best investigated by regression analysis. The equation of the least squares linear (or curvilinear) regression line may be used to describe the relationship, and the significance of this may be determined after constructing confidence intervals for the line, Altman (1991). An advantage of this technique is that the prediction interval may be used to identify the normal range of PSRTs for subjects of any age.

Best line fits were achieved using the Solver function of Excel Version 5 (working on a least squares basis) and the 95% confidence intervals were calculated in accordance with the methods described by Altman (1991).

Figure 5.5 shows four scatter diagrams plotting PSRT against age for each version of the photostress test. In the initial analysis, both linear and non-linear regression lines were fitted to the data. The non linear regression line (PSRT = $a.e^{b.Age}$) , used by Lovasik (1983) accounted for little more of the variability in the data than the linear regression function (PSRT= a + b.Age). Therefore, in the final analysis the simpler linear function was used.

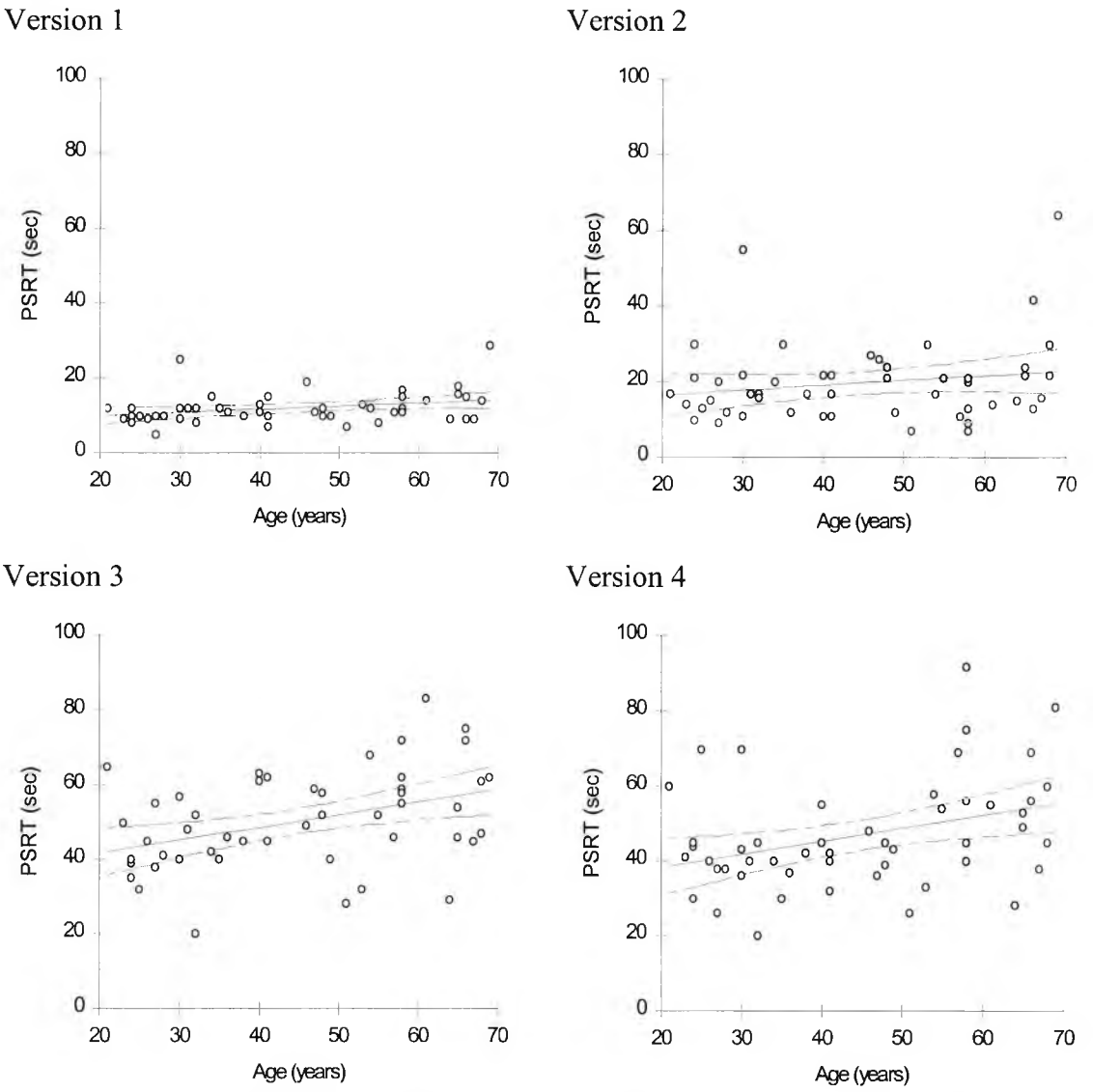

Figure 5.5 Scatter diagrams showing PSRT plotted against age for each version of the photostress test. The lines are the least squares linear regression line and 95% confidence intervals. The relationship between age and PSRT is significant (5% level) for versions 1, 3 and 4 of the test but not for version 2.

The best fit regression line for each version of the test is described below:

Version 1	PSRT = 8.13 + 0.08 x Age
Version 2	PSRT = 13.89 + 1.30 x Age
Version 3	PSRT = 34.89 + 0.34 x Age
Version 4	PSRT = 31.30 + 0.35 x Age

The regression line gives an estimate of PSRT for a given age. However the line fitted to the data is an estimate of the relationship between these variables in the population, so it is necessary to consider the uncertainty of this line. Figure 5.5 shows the regression lines together with the 95% confidence intervals for the line. This interval can be considered to contain the true relationship with 95% probability (Altman, 1991). The null hypothesis, that there is no relationship between PSRT and age, was tested by dividing the slope of the regression line, b (b in the equation PSRT= a + b.Age) by the standard error of the estimated slope and comparing this ratio with the t distribution with n-2 degrees of freedom (Altman, 1991). The t statistic for versions 1-4 of the photostress test was 2.3, 1.3, 3.0 and 2.7 respectively. The relationship between age and PSRT was significant at the 5% level for versions 1, 3 and 4 of the test but not for version 2.

It is not surprising that PSRT obtained with versions 1, 3 and 4 of the photostress test showed a significant effect with age but version 2 did not because Version 2 of the test provided the least repeatable values for PSRT.

5.3.4 Effect of ametropia and acuity on PSRT

The effect of ametropia and acuity on PSRT was investigated in a similar manner. Figure 5.6 shows a scatter diagram of PSRT obtained with version 4 of the photostress test against ametropia in dioptres. There is no significant relationship between ametropia and PSRT at the 5% level (2 tails, df = 48, t = 0.5).

A similar analysis was conducted to determine if any relationship exists between acuity and PSRT for version 4 of the photostress test. The data is presented in Figure 5.7. Again no significant relationship was seen at the 5% level (2 tails, df = 48, t = 0.6).

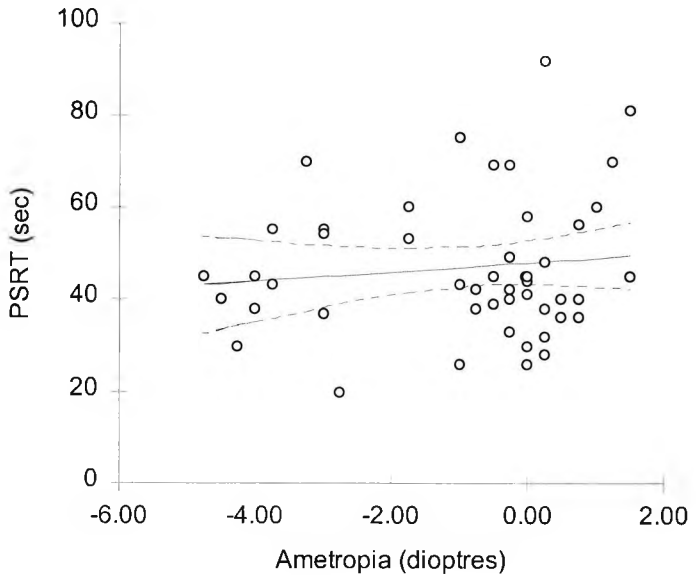

Figure 5.6 PSRT obtained for version 4 of the photostress test plotted against ametropia (D). The slope of the regression line is not significant at the 5% level.

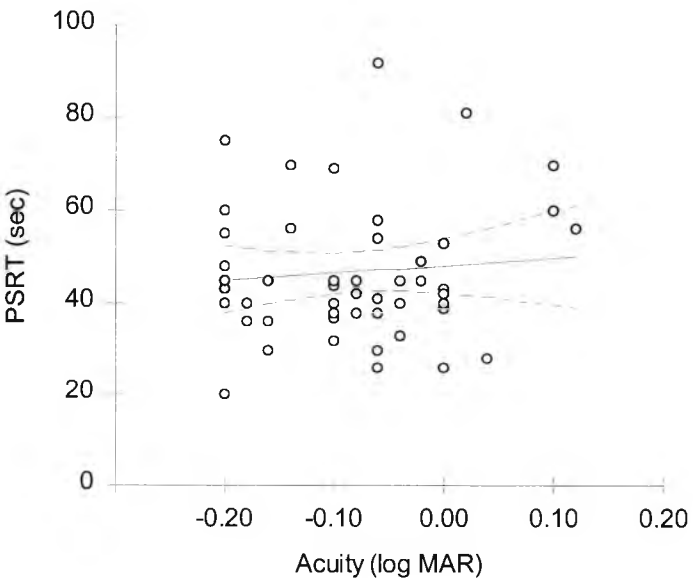

Figure 5.7 PSRT obtained for version 4 of the photostress test plotted against the log of the minimum angle of resolution. Analysis of the regression line shows no significance at the 5% level.

5.4 Discussion

For measurement of PSRT to be a useful tool in the consulting room, the clinician must know which recovery times to regard as normal. Unfortunately a variety of normal PSRTs have been reported in the literature, ranging from 7 to 70 seconds (Lovasik, 1983). This study shows that a large part of this variability may be due to differences in bleaching technique. In particular, techniques that do not bleach a substantial fraction of photopigment are likely to result in relatively short photostress recovery times. Short recovery times are difficult to measure accurately and are more variable relative to the measurement scale.

5.4.1 Comparison of photostress test methods

Each of the four methods studied, produced a different mean PSRT on the same group of subjects. Such differences are not surprising because different bleaching strategies were used and it is likely that each method bleached a different amount of photopigment. What is more surprising is that similar techniques, used in pervious studies, also produce different photostress recovery times. For example, Version 1 of the photostress test was similar to that used by Glaser *et al.* (1977) and Lovasik (1983). Here version 1 of the test produced a mean PSRT of 12 (SD 4) seconds, but Glaser *et al.* (1977) recorded a mean PSRT of 26 (SD 10) and Lovasik (1983) a mean of only 8 (SD 3) seconds. Each of these investigations used a pentorch as the adapting source held 3 cm from the cornea for 10 seconds, and the end point of recovery was noted when subjects acuity had returned to within 1 line of their previous best acuity. Such differences for supposedly identical procedures highlights the difficulty for the practitioner who wishes to identify an abnormal result on the basis of published data. The most plausible explanation for these differences is that each technique bleached a different amount of photopigment. Figure 5.8 shows the effect of bleach duration on the percentage of photopigment bleached for several different light intensities. The fraction of pigment bleached is particularly dependant upon intensity when the retinal illuminance is of an intermediate value (3.5 - 5.5 log td). For example, a retinal illuminance of 4.5 log td bleaches 50 % of cone photopigment after 120 seconds but by

increasing this level of illuminance by only half a log unit, an additional 27% of pigment is bleached.

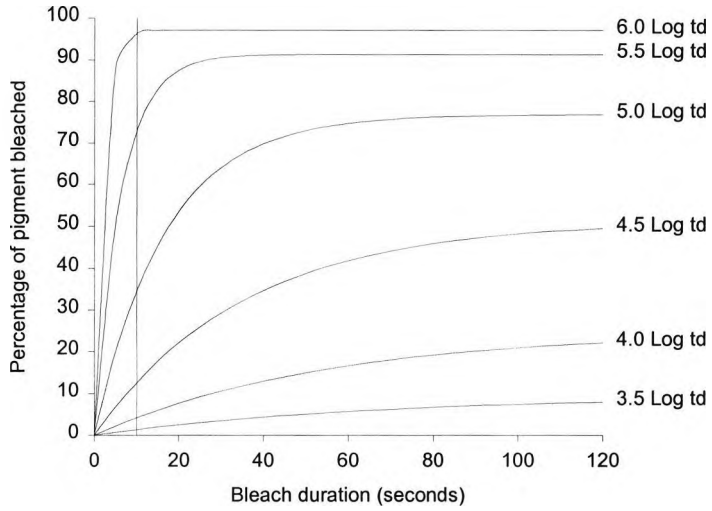

Figure 5.8 Percentage pigment bleached as a function of bleach duration for several different bleach intensities. When bleach duration is relatively short (10 seconds, vertical line) small timing errors will have a relatively large effect on the percentage of photopigment bleached especially for weak to moderate intensity bleaches up to about 5.5 log td. Calculated from the data of Hollins and Alpern (1973).

However, for more intense levels of retinal illumination, this difference is less, e.g. for the same duration exposure, raising the intensity from 5.5 to 6 log td only results in a 6% increase in the amount of photopigment bleached. Therefore, one way to minimise differences in the original bleach would be to ensure that the subject was exposed to a relatively intense light source, i.e. one that produces a retinal illuminance in excess of 5.5 log td.

To determine if the direct ophthalmoscope could provide this level of retinal illumination, five different ophthalmoscopes were taken from the departmental clinic and the retinal illuminance produced by each was determined. Assuming that each presented the adapting field in Maxwellian view (a reasonable assumption if the ophthalmoscope is held very close to the eye). The retinal illuminance produced by each instrument was 6.86, 6.81, 6.78, 6.55 and 6.18 log td. Exposing the eye to the weakest of these for 30 seconds would bleach 98% of cone photopigment and exposure to the brightest 99.6%, a relatively small difference.

The relatively longer PSRT observed for versions 3 and 4 of the test and the similarity of the two measurements is probably due to the fact that each bleached a considerable fraction of photopigment.

The amount of pigment bleached is not only dependant upon the level of retinal illumination but also the duration of the exposure. Figure 5.8 shows that when the bleach duration is relatively short (e.g. 10 seconds) small errors in exposure time, which are likely in a clinical setting, will have a relatively large effect upon the total amount of pigment bleached, particularly for intermediate levels of illumination e.g. 5.5 log td. For this level of illumination, a 2 second timing error on a 10 second bleach would make the difference between a 65% and 78% bleach. The effect of small timing errors could be minimised by increasing the exposure time, e.g. for the same example, a 2 second error on a 30 second exposure time would make the difference between a 90.2% and 90.7% bleach.

The first part of this investigation determined the repeatability of 4 photostress techniques. This is of value because a method with poor repeatability will never agree well with another method nor is it likely to be a sensitive clinical tool.

Contrary to expectations Table 5.1 shows that version 1 of the photostress test produced the most repeatable results. However the coefficient of repeatability does not take into account the fact that PSRT with version 1 of the test was the shortest (mean 11.4 sec). When the coefficient of repeatability is expressed as a percentage of mean PSRT, Version 4 of the test became the most repeatable technique and version 2 the least repeatable.

Overall, version 3 of the photostress test (holding a direct ophthalmoscope close to the eye for 30 seconds) is likely to be the most useful clinical version of the test. It provides relatively repeatable results, it produced PSRTs that agree relatively well with the "gold standard", was able to detect differences in PSRT with age and is superior to versions 1 and 2 of the test on theoretical grounds (see discussion above). However the clincial value of the technique can only be substantiated by examination of abnormal subjects.

5.4.2 Effect of age on PSRT

Many aspects of visual performance vary with age in healthy individuals and the data presented in Figure 5.5 shows that PSRT is no exception. Three of the 4 versions of the photostress test studied showed a significant increase in PSRT with age. The finding that PSRT increases with advancing years is consistent with the data obtained by Severin (1967a), Lovasik (1983) and Collins (1989). However no such increase was observed by Sloan (1968) or Glaser *et al.* (1977). This is not surprising as the increase in PSRT with age is not particularly striking and there appear to be large individual differences in PSRTs which may prevent statistical significance being achieved. Unfortunately is it not possible to evaluate Sloan's (1968) study because although he states that "there was no such correlation" between age and PSRT, he does not present any data. Glaser *et al.* (1977) failed to show a significant increase in PSRT but the mean PSRT for their oldest age group (61 years and over) was 4 seconds longer than that for both younger groups (30 and under, and 31 to 60 years).

Although the increase in mean PSRT with advancing years is small, it is important to take this into account when trying to distinguish normal from abnormal PSRTs. Data for version 3 of the photostress test is redrawn in Figure 5.9. The upper and lower limits of the shaded area describe the prediction interval i.e. 95% of new subjects tested should have a PSRT within this range. This data may be used clinically to differentiate normal from abnormal PSRTs.

5.4.3 Effect of ametropia and acuity on PSRT

At the outset it was suspected that there may have been a relationship between PSRT and refractive error, specifically, that myopes would have longer PSRTs. However, Figure 5.6 suggests that such a relationship does not exist. However, the sample did not contain a large range of refractive errors, the highest myopic prescription being -4.75D.

This study also shows that there is no relationship between acuity and PSRT. This is an important feature of a test that relies on the return of acuity as the endpoint. The equal logarithmic progression of letter sizes on the log MAR chart may have contributed to this result.

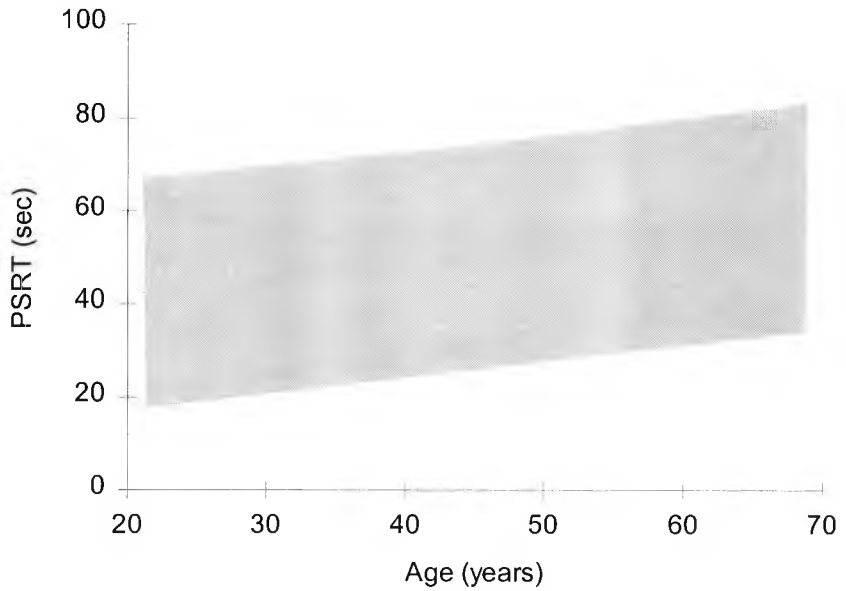

Figure 5.9 When version 3 of the photostress test is used 95% of all new subjects should have a PSRT that falls within the grey area (95% prediction interval).

In summary, the results show that PSRT is largely dependant upon the initial light-adapting technique. The results of a repeatability study and the degree of association between each of the clinical techniques and a "gold standard" suggests that the most useful clinical version of the test involves exposing the test eye to the light from a direct ophthalmoscope for 30 seconds. Regression analysis shows that PSRT increases significantly with age but that ametropia and acuity are not significant factors.

6. Analysis of CS recovery in normals

6.1 Introduction

The previous chapter describes measurements of photostress recovery time (PSRT) in 50 normal subjects using a variety of 'bleaching' techniques. Although these techniques may be of value in determining the integrity of the retina, the measurement (the time taken for acuity to return to normal) tells us little about the nature of the recovery of visual performance. To obtain a fuller understanding of how visual function changes during "photostress testing", a modified version of the contrast sensitivity recovery technique (described in Chapter 3), was used on the same 50 subjects that participated in the photostress technique investigation.

Over recent years the contrast sensitivity function (CSF) has been used widely to describe the characteristics of human spatial vision. Owsley and Sloane (1987) have shown that mid and low spatial frequency contrast sensitivity, unlike acuity, is a good predictor of visual performance to "real world" targets such as faces, road signs etc. The CSF recovery technique has a number of advantages over the conventional photostress technique. It provides information about the time taken for contrast sensitivity (CS) to return for a range of spatial frequencies, (not just a single high spatial frequency one as is the case with the photostress test). It also describes the rate at which CS returns to pre-exposure levels and, at the end of the recovery, provides the clinician with a contrast sensitivity function. It may have another advantage; PSRT has a single end point, i.e. the time taken to read a particular line of letters, therefore a single measurement of PSRT may be influenced by small short term changes in psychophysical threshold. The form of CSF recovery should be relatively independent of these fluctuations because a single contrast sensitivity recovery function contains many data points.

One purpose of this investigation was to determine if age affects CS recovery. There were several reasons for supposing that age might be a factor. Firstly, contrast sensitivity, which determines the end point of CS recovery, declines with age. Owsley *et al.* (1983) measured contrast sensitivity in 91 subjects ranging in age from 19 to 87 years. Subjects were screened to exclude ocular disease and each wore a suitable optical correction. Sensitivity to stationary gratings of low spatial frequency remained the same

throughout adulthood but sensitivity to higher spatial frequencies decreased with age. When gratings were drifted (1.1 and 4.3 deg/sec), contrast sensitivity to gratings of low spatial frequency increased particularly for young subjects. Several factors, both optical and / or neural, may account for the decline in contrast sensitivity with increasing age. Changes in the optical media associated with age result in a reduction in retinal illuminance and an increase in light scatter. Owsley *et al.* (1983) showed that reduced retinal illuminance was a significant factor in the reduction of CS with age. Another possible reason for the reduction in CS associated with age is that increased forward light scatter might directly reduce the contrast of the grating on the retina. Dressler and Rassow (1981) used a laser interference technique, to by-pass the optics of the eye, in order to determine the effect of age on the neural component of contrast sensitivity. Their data suggest there is no age-related change in "neural" contrast sensitivity.

Another reason for believing that age would have an effect on CS recovery is that there is a slowing of both foveal dark adaptation and photopigment regeneration with age, (Coile and Baker, 1992). Although, Coile and Baker (1992) claimed that a significant relationship existed between foveal dark adaptation and photopigment regeneration, their data analysis was inappropriate. They used the correlation coefficient to analyse their data despite the fact that the data was not distributed normally. Consequently the resulting correlation coefficient (r=0.75) would have been strongly influenced by just 4 pigment regeneration time constants, out of a total of 58, which were in excess of 3 minutes. Eisner (1987) also examined the effect of age on foveal dark adaptation and showed there was no slowing of the rate of foveal dark adaptation with increasing age.

6.2 Methods

In the studies described in Chapter 3 a bite bar was used to stabilise head position and cyclopentolate was instilled to paralyse accommodation. While such techniques are acceptable for laboratory studies, they would reduce the clinical acceptability of the technique. Therefore, an initial investigation was conducted in order to determine if it was possible to dispense with the bite bar and cycloplegic.

6.2.1 Development of a modified technique

Two subjects participated in this initial investigation. Contrast sensitivity recovery functions were obtained in the usual way (described in Chapter 3) and also using a modified technique. The latter used a chin rest and eye cup to maintain steady head alignment and a row of high contrast letters positioned at the centre of the CRT display to encourage stable accommodation. In all other respects the two techniques were identical. Subjects were initially light-adapted to a 5.7 log td, "white", field for 60 seconds and the retinal illuminance provided by the CRT display was set to 2.8 log td (50 cdm^{-2} through a 4 mm pupil).

The results obtained for one subject are presented in Figure 6.1. Data shown by the filled symbols were collected when the subject's head was steadied by a bite bar and accommodation was paralysed. Data shown by open symbols were collected using the modified technique.

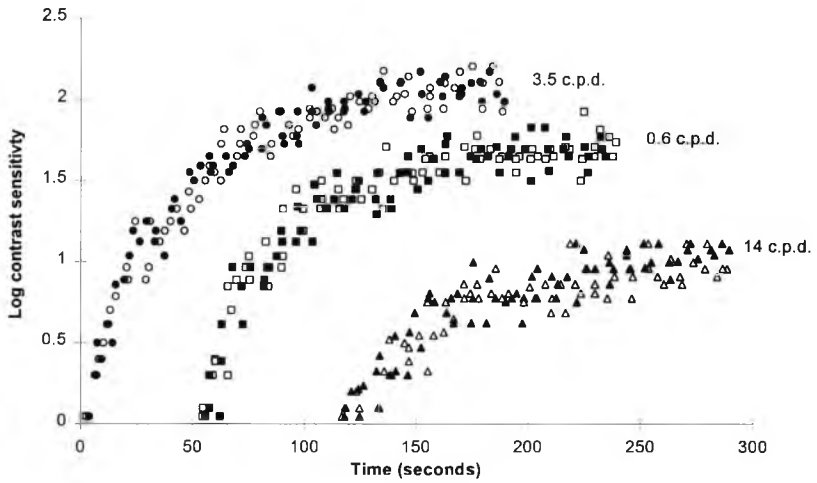

Figure 6.1. Contrast sensitivity recovery functions for 3 spatial frequencies obtained using a bite bar and cycloplegia (filled symbols) and without a bite bar or cycloplegia (open symbols). For clarity, the data for the 0.6 c.p.d. and 14 c.p.d. gratings are shifted along the horizontal axis by 50 and 100 seconds respectively.

For clarity, data for the 0.6 and 14 c.p.d. gratings have been shifted along the horizontal axis by 50 and 100 seconds respectively. Examination of Figure 6.1 shows that open and filled symbols of the same shape run together, indicating that both techniques produce similar results. The data obtained for the other subject was similar.

6.2.2 Data Analysis

It may be seen in Figure 6.1 that data were collected serially. Analysis of this type of data is problematic because individual data points are obtained at non-specific times.

Such data may be analysed in a number of ways. The most common approach is to obtain the mean value and its standard deviation at every point in time and present this graphically (see Chapter 3). The data may then be compared using a 2 sample t-test (or similar test) at each point in time to identify a significant difference. Altman (1991) criticises this approach because a) it does not take into account that consecutive data points are related, b) it cannot cope with missing values or data collected at non-specific times and c) it is difficult to interpret the importance of results that are statistically significant at a single point in time.

When evaluating serial data, a two stage method of analysis involving summary measures is more appropriate, (Altman, 1991; Matthews *et al.*, 1990). The first stage is to obtain a suitable summary of the response of an individual and the second stage is to use simple statistical techniques to analyse the summary measures as if they were raw data. This approach is statistically valid and if appropriate summary measures are used, is clinically relevant, (Matthews *et al.,* 1990). Typical summary measures might be: time to peak response, magnitude of peak response, rate of change of variable. Summary measures may also be obtained indirectly by modelling the data and extracting the values of the variables. The latter approach is adopted here.

6.2.3 Choice of model

The recovery of contrast sensitivity may be described by a number of models, each with various advantages and disadvantages. As a first step in the analysis it is necessary to identify a suitable model. To this end, 5 models were fitted to the data using the Solver function of Microsoft Excel Version 5 working on a least squares basis. The results were then evaluated against a set of criteria.

The simplest statistical model that can cope with non-linear data is the polynomial function. The particular polynomial considered here was a quadratic function:

$$CS = a + b.t + c.t^2 \qquad (1)$$

where a, b and c are variables and t = time. Together the variables may provide a description of the data but each in isolation is relatively abstract, not describing any particular feature of CS recovery.

The second model considered was a simple logarithmic function:

$$CS = a.Ln(t) + b \tag{2}$$

where a and b are variables.

The third model was a single exponential growth function.

$$CS = FS.(1 - e^{-(t-T)/To}) \tag{3}$$

where FS is the final contrast sensitivity, T is the time at which contrast sensitivity first returns and To is the time constant of recovery. Each of the variables describes a particular feature of CS recovery that may be of interest to the clinician. Although it has no direct physiological basis, single exponential models have been used extensively to describe dark adaptation data.

The fourth model was a double exponential growth function:

$$CS = FS1.(1 - e^{-(t-T1)/To1}) + FS2.(1 - e^{-(t-T2)/To2}) \tag{4}$$

where $FS1$ and $FS2$ are the contributions that the first and second exponentials make to final contrast sensitivity, (the sum of $FS1$ and $FS2$ equals the final contrast sensitivity). $T1$ and $T2$ are the times that each exponential first contributes to contrast sensitivity and $To1$ and $To2$ are the time constants for each exponential growth function. Although double exponential functions have not been fitted to dark adaptation data, the results of Baker and Donovan (1982) have shown that an additional mechanism may operate during the very early phase of dark adaptation. Here it is assumed that this additional recovery is approximately exponential on the basis of the appearance of the data presented in the inset graph in Figure 1.31.

The last model considered here is described in Appendix IV. It is based on photopigment depletion and the exponential decay of an equivalent background.

$$CS = Log\left[\frac{ML.(Io + (Po.(I + Io).e^{-t.(I+Io)/(To.Io)}/(I + Io))}{(Ct.2.10^{E.e^{-t/To1}})} + Ct\right] \tag{5}$$

where ML is twice the mean luminance of the CRT, Po is the proportion of photopigment present at the end of the bleach, I is the mean retinal illuminance of the grating, Io is the half bleach constant in td, $To2$ is the time constant of photopigment regeneration, Ct is the contrast threshold of the system (i.e. the contrast threshold after recovery), E is the intensity of the equivalent background in log units and $To1$ is the time constant of decay for the equivalent background. Although the model has some

physiological basis, the equation is complex and requires prior knowledge of the luminance of the display and the fraction of photopigment at the start of the recovery. The free parameters in the model fit were *E*, *To1*, *To2* and *Ct*. None of these variables have a direct relevance to the empirical data and their interpretation requires knowledge of the physiological processes.

When instructing the Solver function to fit Models 3, 4, and 5 to the data, a constraint on the fitting procedure was introduced. The variable *FS* in model 3, the sum of the variables *F1* and *F2* in Model 4 and the reciprocal of *Ct* in Model 5 were not allowed to exceed the highest value of log CS obtained in each data set. In this way models were forced to produce plausible estimates for final contrast sensitivity.

In this study the object of modelling was to obtain summary measures. To determine which model was most appropriate, each was evaluated against several criteria. The most appropriate model should: A) be simple, B) produce a plausible description of CS recovery, C) contain variables that describe a particular feature of the recovery, D) have only one combination of variables that produce a least squares fit and E) have a low Akacki criterion[1] value. Each of the models described above was fitted to 6 sets of raw data (each spatial frequency was represented by 2 sets of data). The raw data used in the model evaluation was chosen at random from a number of sets of data obtained from 10 subjects that participated in a repeatability study. An example of the analysis performed on data for a single subject is shown in Figure 6.2.

---

[1] The Akacki criterion is a statistic that may be used to identify an appropriate model. It determines if the inclusion of additional variables in a model is warranted on the basis of the sum of residuals squared, adjusted for measurement error. The most appropriate model has a low Akacki criterion value (AIC):

$$AIC = (n.Ln(SSr)) + (2.p)$$

where n is the number of data points, p is the number of free parameters and SSr is the residual sum of squares adjusted for the measurement error i.e.

$$SSr = \sum \frac{r^2}{vmer}$$

where r is the residual and $vmer$ is the variance of the measurement error. In this analysis the variance of the measurement error was assumed to be the variance of the data points collected over the last 10 seconds of the investigation.

Quadratic model

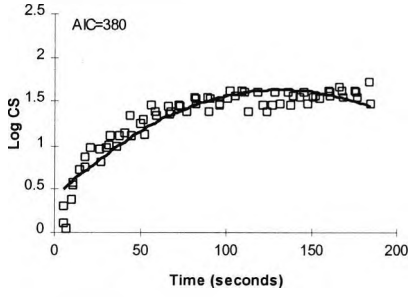

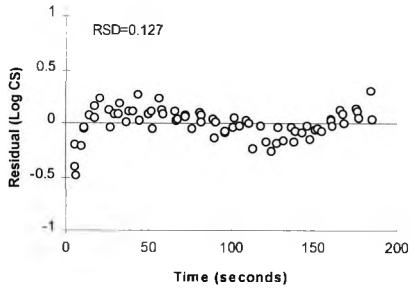

Logarithmic model

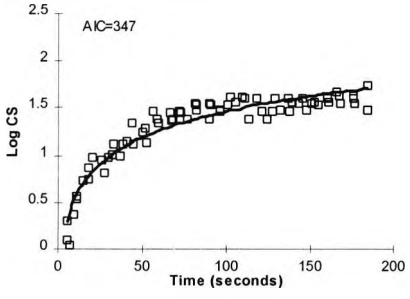

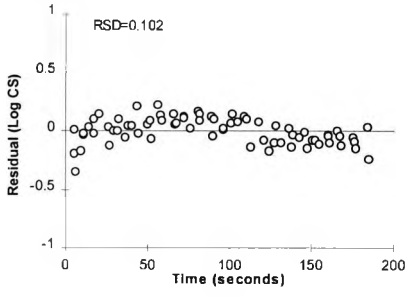

Single exponential model

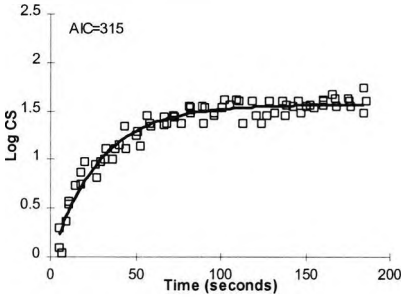

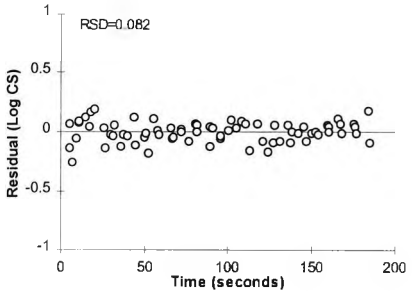

Double exponential model

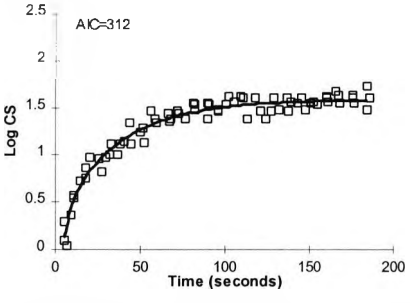

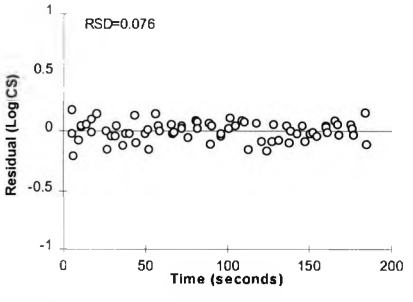

Photopigment depletion and equivalent background model

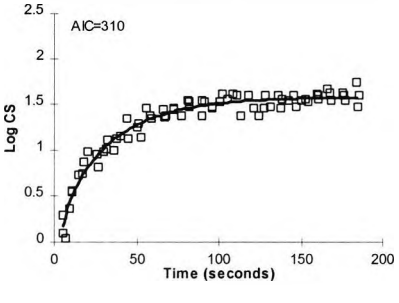

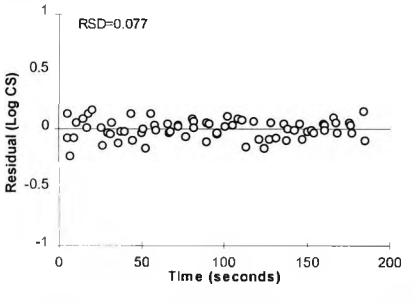

Figure 6.2. Contrast sensitivity recovery data from 1 subject fitted with 5 different models on a least squares basis. Examination of the residuals indicates how accurately each model described the data. The AIC value is the Akacki criterion value and the RSD is the standard deviation of the residuals.

6.2.3.1 Model evaluation

Table 6.1 summarises the model evaluation. In this analysis Models 1, 2, 4 and 5 were rejected in favour of Model 3, the single exponential function. The following pages elaborate on the reasons for this decision.

Model	Criteria				
	A	B	C	D	E
1	✓✓✓	✗✗✗	✗✗✗	yes	367
2	✓✓	✗	✗✗✗	yes	337
3	✓	✓✓	✓✓✓	yes	330
4	✗✗	✓✓✓	✓✓✓	no	334
5	✗✗✗	✓✓✓	✓	yes	325

Table 6.1 Summary of model evaluation. Each of the 5 models were evaluated against 5 criteria (A,B,C,D and E). The most appropriate model should: A) be simple, B) produce a plausible description of CS recovery, C) contain variables that describe a particular feature of the recovery, D) have only one combination of variables that produce a least squares fit and E) have a low Akacki criterion value. The ability of each model to fulfil criteria A, B and C was ranked subjectively from very poor ✗✗✗ to very good ✓✓✓.

Model 1 (quadratic) was rejected for several reasons: the variables a, b, and c of this quadratic function have no direct meaning individually, but must be used together to predict CS at any point in time; the least squares fit often produced a peaked function indicating misleadingly that CS declines after a period of time; the standard deviation of the residuals was relatively large and the Akacki criterion value was the largest of all the models.

Model 2 (logarithmic) provided a relatively good fit of the data and the standard deviation of the residuals was relatively small but the model was rejected because it indicates that CS continues to increase with time, e.g. after an infinite period of time, CS would be infinitely high. The plot of residuals for Model 2 in Figure 6.2 shows that this function underestimated CS half way through recovery and over estimated it toward the end of the time period.

Model 4 (double exponential) provided a very good description of the data. The plot of residuals shows an equal distribution of data points above and below zero and the mean residual standard deviation was small (0.121). However the model was rejected because the Akacki criterion value was higher than that obtained for Models 3 and 5.

Furthermore, although the double exponential function is relatively simple to understand and the parameters have real meaning i.e. *FS1* was the contribution that the first exponential made to final CS and *T1* was the time that this exponential first started to influence CS e.t.c. the least squares fitting procedure produced some unexpected values. Indeed, fitting the model to several sets of data showed that several least square fits met the Solver criteria. Figure 6.3 shows that the data for one subject is equally well fitted by the same equation when very different parameter values are used.

a.

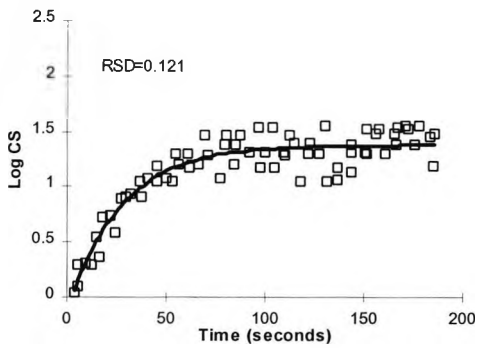

FS1 = 0.01
T1 = 68.87
To1 = 26.73
FS2 = 1.37
T2 = 0.73
To2 = 27.01

b.

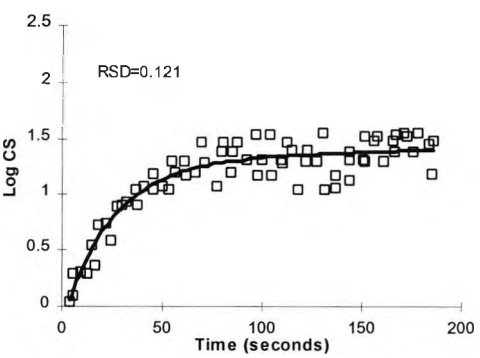

FS1 = 1.20
T1 = 4.48
To1 = 24.09
FS2 = 0.34
T2 = -79.54
To2 = 322.92

Figure 6.3 The double exponential function was fitted to the same data set on two occasions using the least squares method but different starting values. Different values were obtained for each of the variables on each occasion, indicating that there are multiple solutions to the least squares fit.

Model 5 (physiological model) provided the best description of the data. The mean residual standard deviation was only 0.115 and the Akacki criterion value was also the lowest (325) of all the models.

The values obtained for each of the parameters were in good agreement with estimates for the parameters obtained by different methods. The mean value for the time constant describing the decay of the equivalent background was 132 seconds. Which is in good agreement with that obtained by Hollins and Alpern (1973) for cone dark adaptation.

Examination of the data published by Hahn and Geisler (1995) showed that at the end of a 2 min exposure to 5.77 log td field (97% bleach), sensitivity to a 1 c.p.d. grating was equivalent to that obtained on a steady 4 log td background. Allowing for a 4 mm artificial pupil this equates to a luminance of 2.9 log cdm^{-2}, remarkably similar to the mean value of E recorded in this investigation (2.78 log cdm^{-2}).

However, the mean value for the time constant describing photopigment regeneration was 16 seconds, much less than that obtained by direct measurement, (approximately 80 seconds for subjects aged 20-30 yrs.), (Coile and Baker, 1992). This result indicates that either photopigment regenerates rapidly in the presence of a background luminance, which seems unlikely, or that the equation is an incomplete description of CS recovery.

Although Model 5 provided a good description of the data, it was rejected in the final analysis because out of the four free parameters, only parameter *Ct* (the reciprocal of final CS) has direct meaning to the clinician. The other variables describe changes in the underlying adaptational processes but are unlikely to be understood by a clinician examining the data.

Model 3 (the single exponential function) was chosen in preference to the others because of its simplicity. It contained only 3 variables, each of which described a particular feature of the data, i.e. *FS* is the final contrast sensitivity, *T* is the time taken to see a grating with a contrast of 1, and *To* is the time constant of recovery. The mean residual standard deviation was relatively low 0.122 and the Akacki criterion value was the second lowest. Its only failings were that it tended to overestimate initial CS and often produced negative values for variable *T*.

6.2.4 Subjects

The same 50 normal subjects that participated in the photostress test investigation participated in this investigation.

6.2.5 Apparatus

The apparatus was that described in Chapter 3 except that the full mouth bite bar was replaced with a chin rest and an eye cup was provided around the pinhole. The retinal illuminance of the monitor and its surround was approximately 2.8 log td and that of the

"bleaching" field 5.7 log td. Calibration was carried out periodically throughout the period of data collection in the usual way, (Westheimer, 1966).

6.2.6 Procedure

Prior to each experimental session, the subjects' optical correction (adjusted for the eye to monitor distance) was placed immediately behind the pinhole. After clear instructions subjects signalled their readiness to begin each experiment by pressing a button which caused the "bleaching field" to be exposed to the test eye for 60 seconds. Following this period of light-adaptation, the subject responded when the grating became just visible throughout the duration of the experiment (180 seconds). Three sets of measurements were taken for each spatial frequency (0.6, 3.5 and 14 c.p.d.). The order of grating presentation was randomised to balance order effects. Each experiment took approximately 45 minutes to complete and subjects were encouraged to take a break if they felt tired.

6.2.7 Pilot study

To highlight any problems with the methodology and to assess the repeatability of the technique, a pilot study was conducted on 10 subjects. Data was collected from each subject on two separate occasions.

6.3 Results

The raw data for each subject and the best fitting single exponential functions are shown in Appendix III.

6.3.1 Pilot study

The data were fitted with the single exponential model described earlier. Values for the variables; final contrast sensitivity (*FS*), the time that contrast sensitivity first returned i.e. when c=1 (*T*) and the time constant of recovery (*To*) provided a summary of each CS recovery function and were treated as raw data.

The data obtained from the pilot study for variable *FS* (the final contrast sensitivity) is presented in Figure 6.4. The proximity of each data set to the line of equality (visit 1 = visit 2) gives an indication of the agreement between measurements. The coefficients of repeatability (twice the standard deviation of the differences) for the 0.6, 3.5 and 14 c.p.d. gratings were 0.15, 0.11 and 0.24 log CS respectively. Subjects found it difficult to establish a reliable criteria for detection of the 14 c.p.d. grating and this is reflected by a relatively large coefficient of repeatability.

The repeatability data for variable *T* (the time at which the grating was first seen) is shown in Figure 6.5. The data for the 0.6 and 3.5 c.p.d. gratings appear to be clustered around a particular value. The mean value of *T*, for the 0.6 c.p.d. grating was -3.1 seconds (SD 4.4) and -1.2 seconds (SD 1.5) for the 3.5 c.p.d. grating. The coefficient of repeatability for the 0.6, 3.5 and 14 c.p.d. gratings were 6.9, 3.9 and 8.8 seconds respectively.

Figure 6.6 shows the repeatability data for variable *To* (time constant of recovery). The coefficient of repeatability for the 0.6, 3.5 and 14 c.p.d. gratings were 10.3, 12.4 and 13.4 seconds respectively. The importance of this level of variability in terms of the clinical value of the test can only be determined when the effects of disease on these parameters is known.

In all cases the agreement between repeated measurements is most readily assessed by examination of the difference plots. In such plots, individual data points should be evenly distributed above and below the mean and there should be no "funnelling". In all cases the data appear to be spread about the mean value and there is no obvious "funnelling".

0.6 c.p.d.

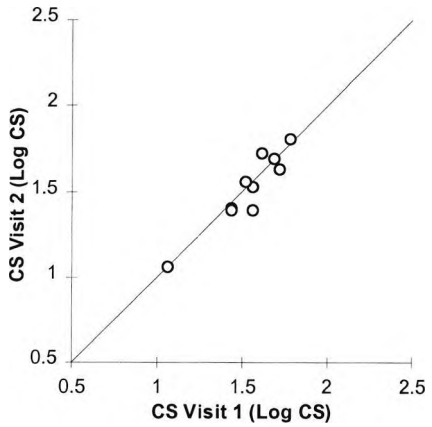

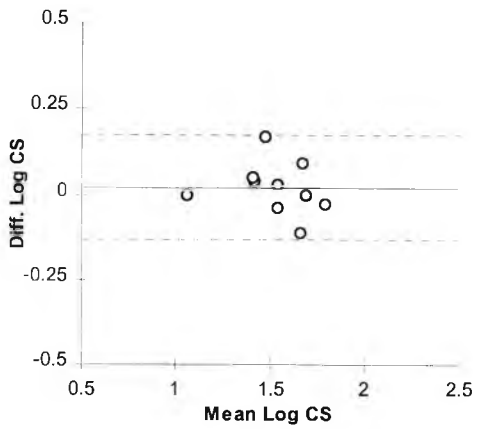

3.5 c.p.d.

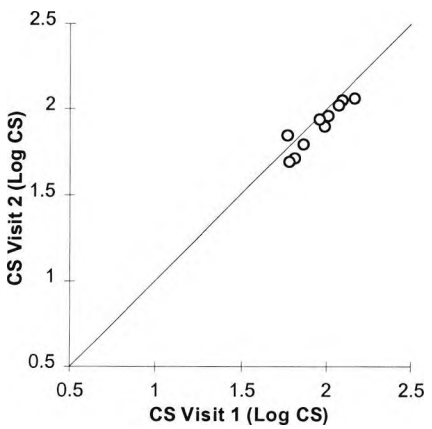

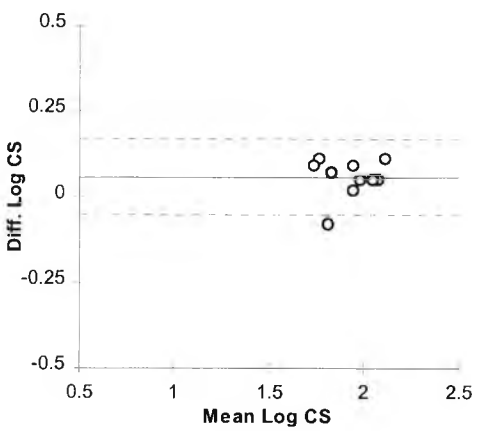

14 c.p.d.

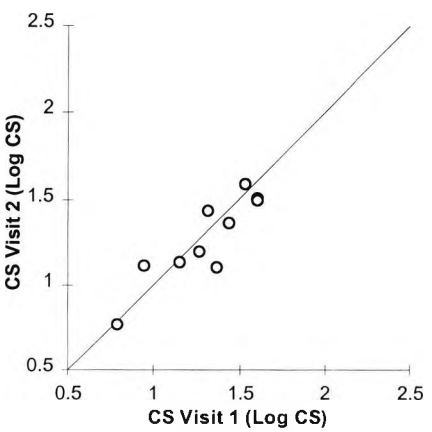

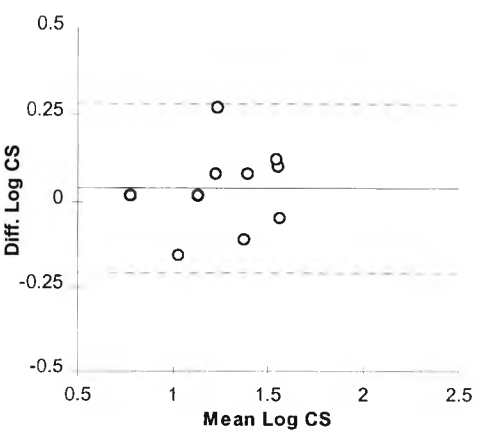

Figure 6.4 Repeatability data obtained for variable *FS* (final contrast sensitivity). Proximity of the data to the line of equality in the scatter plots gives an impression of the repeatability of the data. The mean bias between visits 1 and 2 is shown by the solid line in the residuals plot and the two dashed lines show the 95 % limits of agreement.

0.6 c.p.d.

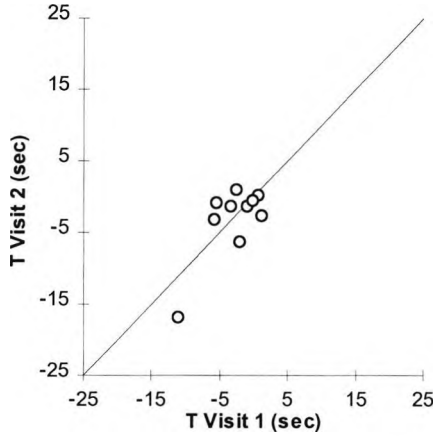

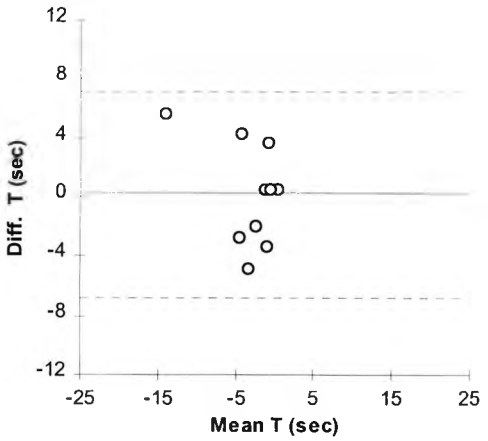

3.5 c.p.d.

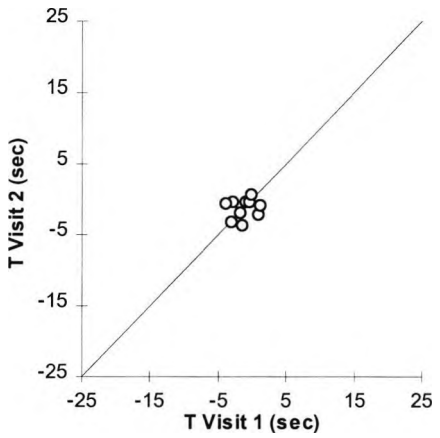

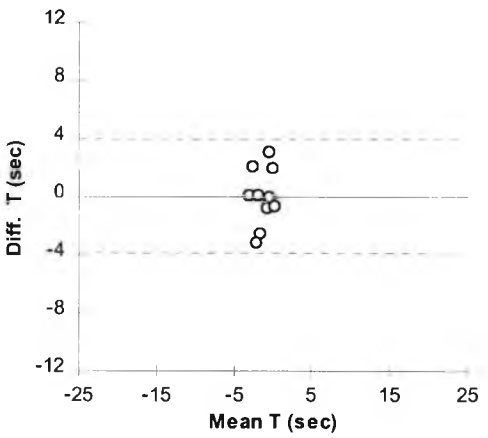

14 c.p.d.

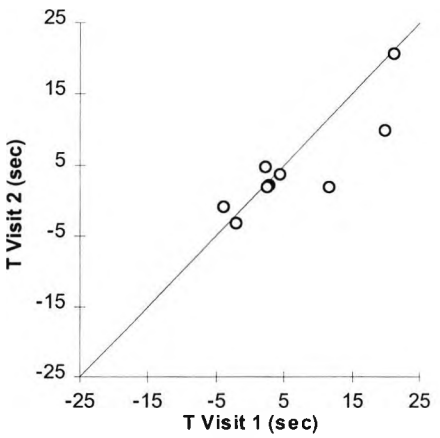

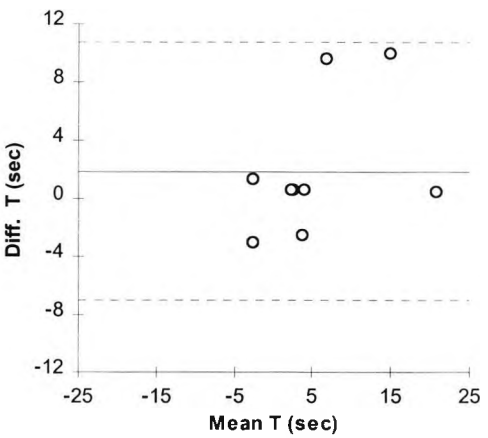

Figure 6.5 Repeatability data for the variable *T* (time that contrast sensitivity first returned). The cluster of points in a and b indicates that the CS returned for all subjects at approximately the same time.

0.6 c.p.d.

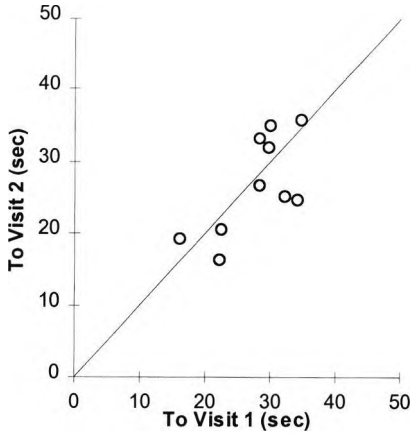

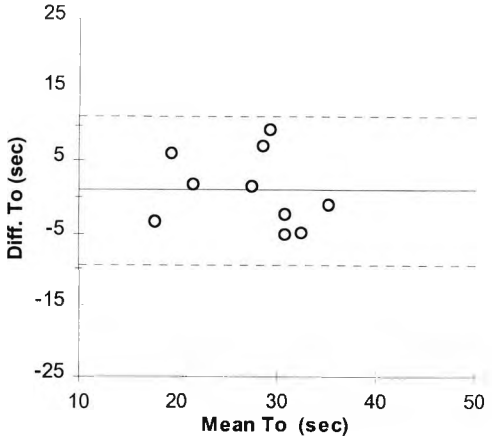

3.5 c.p.d.

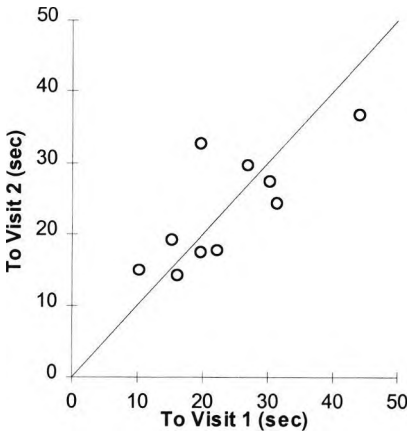

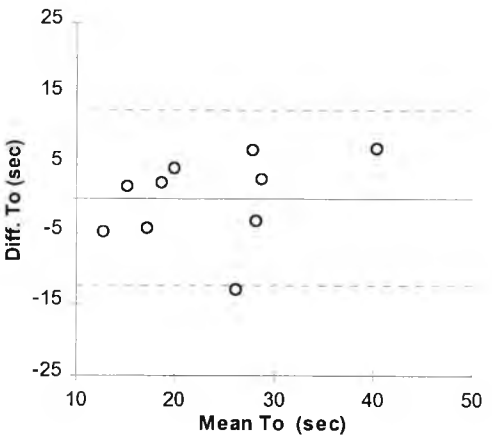

14 c.p.d.

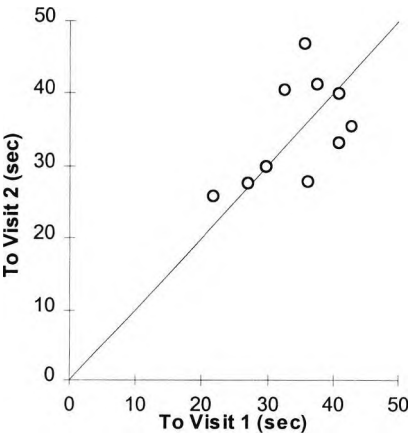

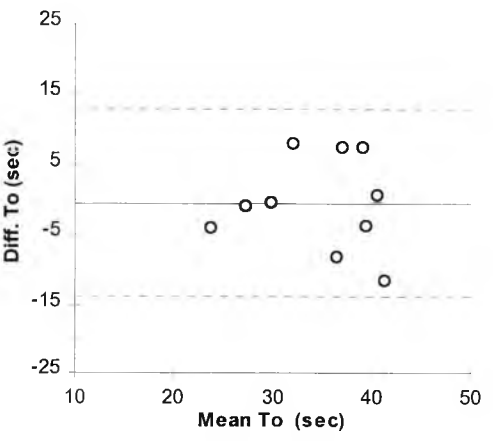

Figure 6.6 Repeatability data for variable *To* (the time constant of recovery). Although the data is relatively scattered it does follow the line of equality. The coefficient of repeatability for the 0.6, 3.5 and 14 c.p.d. gratings were 10.3, 12.4 and 13.4 seconds respectively.

6.3.2 CS recovery

Typically, following a period of intense light adaptation subjects were "blinded" by a dense afterimage that obscured even a high contrast grating (c = 0.9). After a few seconds CS started to return but the nature of CS recovery was subtly different for each spatial frequency. Initial recovery of CS to the 0.6 and 3.5 c.p.d. gratings began several seconds before that of the 14 c.p.d. grating. Once seen at their highest contrast, the rate at which CS subsequently improved was also spatial frequency dependant. Recovery of contrast sensitivity was particularly rapid for the intermediate spatial frequency and particularly slow for the highest spatial frequency.

Each CS recovery curve is described by just three variables FS, T and To, the values for each of these variables, is shown (for each subject) in Appendix III and summarised in Figure 6.7.

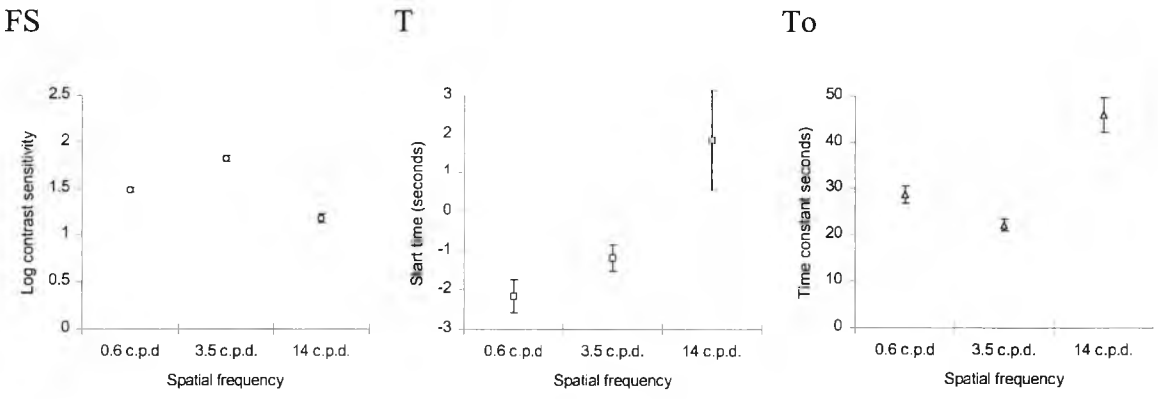

Figure 6.7. Three graphs showing the mean values obtained for the variables FS, T and To which summarise CS recovery for 50 normal subjects. The error bars indicate the magnitude of the standard error.

Final contrast sensitivity (FS) was greatest for the intermediate spatial frequency and least for the highest spatial frequency. This finding is unremarkable because the contrast sensitivity function is a band pass function in photopic conditions when a fixed grating area is used.

Variable T (start time) describes the time when contrast sensitivity first returned, c = 1.0 (i.e. where the CS recovery curve cuts the x (time) axis. The negative values obtained for this variable highlight the fact that it provides a theoretical description of when CS first returned rather than an actual estimate of the return of CS. Values for T suggest that that CS returns first to the lowest spatial frequency and last for the highest spatial

frequency. This difference is statistically significant, (one way analysis of variance, df=2, p=0.0017).

The time constant of recovery (To) was greatest for the highest spatial frequency and least for the intermediate spatial frequency, i.e. contrast sensitivity recovery was slowest for the 14 c.p.d. grating and fastest for the 3.5 c.p.d. grating. The difference in recovery rates between spatial frequencies was significant, (one way analysis of variance, df=2, p<0.0001).

6.3.3 Effect of age on CS recovery

Several statistical methods may be used to determine the effect of age on the recovery of CS. One of the most popular is the correlation coefficient (r), which describes the degree of association between two continuous variables. However the use of this statistic is not appropriate because subjects were not chosen at random from the population (10 subjects were recruited from each decade of life). A more appropriate analysis is to conduct a one way analysis of variance to determine if there is a significant difference in the means of each age group. The mean values obtained for each of the parameters (FS, T and To) and their standard deviations are presented in tabular form below, together with the results of the analysis.

Age group	Final contrast sensitivity, *FS* (log CS)		
	0.6 c.p.d.	3.5 c.p.d.	14 c.p.d.
20s	1.49 (0.23)	1.92 (0.15)	1.37 (0.20)
30s	1.55 (0.12)	1.86 (0.34)	1.25 (0.44)
40s	1.53 (0.10)	1.72 (0.24)	1.01 (0.28)
50s	1.52 (0.18)	1.84 (0.18)	1.22 (0.23)
60s	1.34 (0.17)	1.78 (0.12)	1.04 (0.33)

Table 6.2 Mean log final contrast sensitivity by age group. Values in brackets are standard deviations.

Age group	Start time, *T* (seconds)		
	0.6 c.p.d.	3.5 c.p.d.	14 c.p.d.
20s	-2.33 (3.39)	-1.16 (2.18)	1.96 (12.69)
30s	-1.38 (2.76)	-0.33 (2.00)	1.47 (12.69)
40s	-0.91 (2.39)	-0.11 (2.00)	3.06 (9.69)
50s	-2.70 (2.32)	-1.92 (1.95)	0.30 (5.33)
60s	-3.49 (3.85)	-2.43 (3.18)	2.49 (10.00)

Table 6.3 Mean start time (*T*) by age group. Values in brackets are standard deviations.

Age group	Time constant, *To* (seconds)		
	0.6 c.p.d.	3.5 c.p.d.	14 c.p.d.
20s	25.80 (9.14)	24.58 (12.64)	47.02 (25.46)
30s	24.46 (9.54)	19.90 (11.12)	42.78 (40.04)
40s	24.69 (3.44)	17.39 (7.23)	44.31 (28.82)
50s	30.90 (15.56)	21.73 (5.78)	53.58 (19.55)
60s	37.03 (19.76)	27.17 (7.52)	42.60 (14.66)

Table 6.4 Mean time constant of recovery by age group. Values in brackets are standard deviations.

To assess the effect of age on log contrast sensitivity (*FS*) for each spatial frequency a one way analysis of variance was carried out. According to this analysis age does not have a significant effect on contrast sensitivity: for 0.6 c.p.d, $F=2.39$, $p = 0.07$; for 3.5 c.p.d. $F=1.17$, $p = 0.33$, and for 14 c.p.d. $F=2.38$, $p = 0.07$.

Analysis of the data showed that age did not have a significant effect on the value of *T*: for 0.6 c.p.d, $F=1.19$, $p = 0.33$; for 3.5 c.p.d. $F=1.86$, $p = 0.13$, and for 14 c.p.d. $F=0.12$, $p = 0.97$.

Again, this analysis showed that age did not have a significant effect on the rate at which CS returned: for 0.6 c.p.d, $F=1.87$, $p = 0.13$; for 3.5 c.p.d. $F=1.72$, $p = 0.16$, and for 14 c.p.d. $F=0.29$, $p = 0.88$.

The analysis of variance is an appropriate statistic but it does not make best use of the data, in particular, it does not take into account the fact that the groups are related by a continuous variable, age. Consequently one important feature of the data is overlooked.

A more appropriate analysis uses the technique of regression. Regression analysis mathematically describes the relationship between two continuous variables. Unlike the correlation coefficient, the sample does not need to be random and the predictor variable (x) does not need to be distributed normally. However, three assumptions underlie this method of analysis: the values of the outcome variable (y) should have a normal distribution for each value of x, the variability of y should be the same for all values of x, and in the case of linear regression, the relationship should be linear, Altman (1991).

Figures 6.8, 6.9 and 6.10 plot the values obtained for *FS*, *T* and *To* respectively for all subjects.

Examination of the individual plots in Figures 6.8, 6.9 and 6.10 show that the assumptions necessary for regression analysis are broadly met. There do not appear to be any systematic differences in the variability of each variable with increasing age and there does not appear to be any justification for assuming anything other than a linear relationship.

Each set of data was fitted with a least squares regression line (solid line) (described by the equation in the top left hand corner of each plot). The two dotted lines show the 95% confidence intervals for the regression line, i.e. there is a 95% chance that the true relationship falls within these lines. To determine if the relationship between age and each variable was significant, the hypothesis that the slope of the regression line equalled zero, i.e. that b=0 was tested. This analysis produced a value (shown in the upper right hand corner of each plot) that may be compared with the t distribution with 48 (n-2) degrees of freedom.

Figure 6.8 shows that contrast sensitivity (*FS*) tends to decline with increasing age. This trend is significant at the 5% level for the 0.6 c.p.d and 14 c.p.d. gratings but not for the 3.5 c.p.d. grating.

Figure 6.9 shows that the time at which recovery first begins (*T*) is independent of age for all spatial frequencies. The mean value for the "start time" (*T*) was -2.16 (SD 3.02), -1.19 (SD 2.39) and 1.85 (SD 9.17) seconds for the 0.6, 3.5 and 14 c.p.d. gratings respectively. Values of T were particularly variable for the 14 c.p.d. grating.

Figure 6.10 shows a small increase in the variable To with increasing age. This increase is only significant for the 0.6 c.p.d. grating. For all subjects the mean time constant of recovery for the 0.6, 3.5 and 14 c.p.d. gratings were 28.58 (SD 12.93), 22.16 (SD 9.52) and 46.06 (26.32) seconds respectively.

0.6 c.p.d.

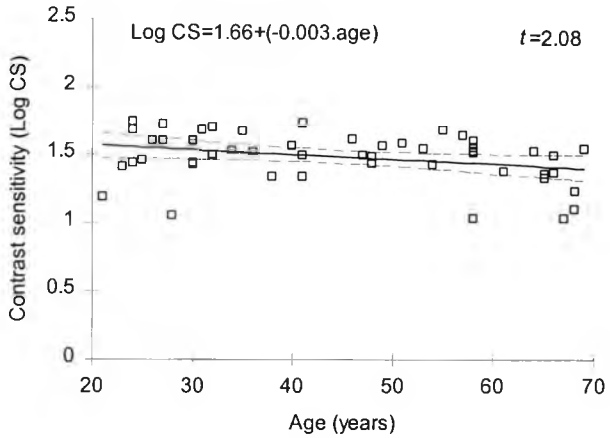

3.5 c.p.d.

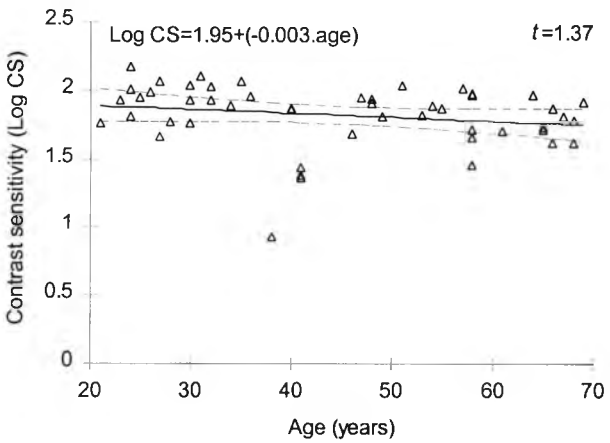

14 c.p.d.

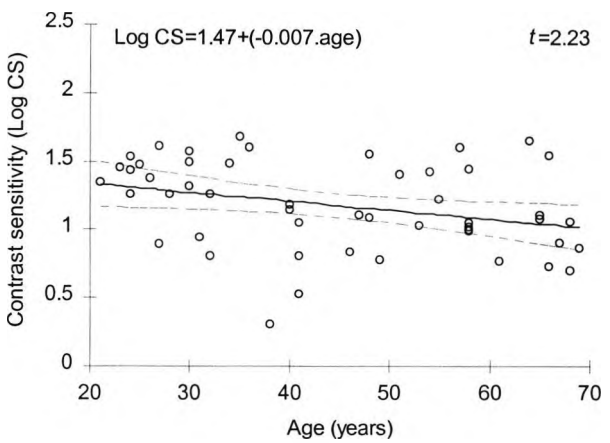

Figure 6.8 Variable *FS* (final contrast sensitivity) as a function of age, for 3 spatial frequencies. The regression line (solid line) is described by the equation at the top left of each plot and the t statistic indicates the significance of the slope. Values for *t* in excess of 2.011 and 2.407 indicate significance at the 5% and 1% levels respectively with 48 degrees of freedom.

0.6 c.p.d.

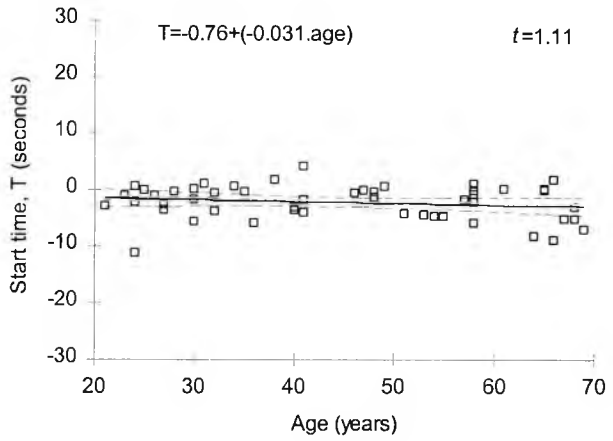

3.6 c.p.d.

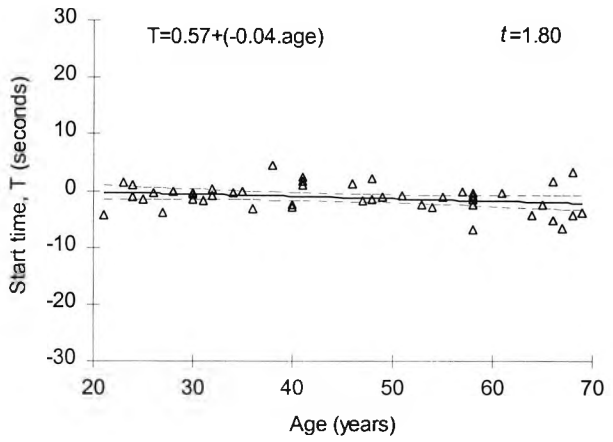

14 c.p.d.

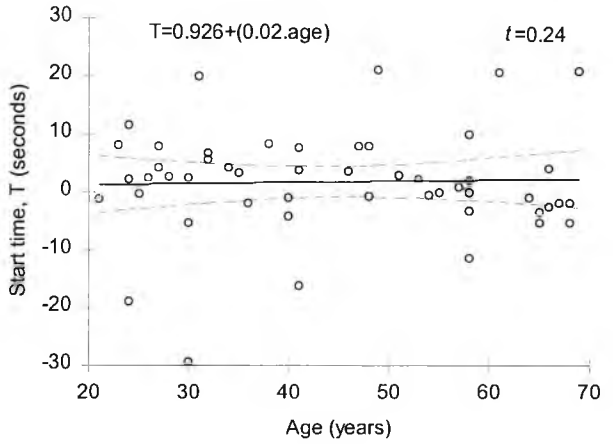

Figure 6.9 Variable *T* (time that CS first returns) as a function of age, for 3 spatial frequencies. The regression line (solid line) is described by the equation at the top left of each plot and the t statistic indicates the significance of the slope. Values for *t* in excess of 2.011 and 2.407 indicate significance at the 5% and 1% levels respectively with 48 degrees of freedom.

0.6 c.p.d.

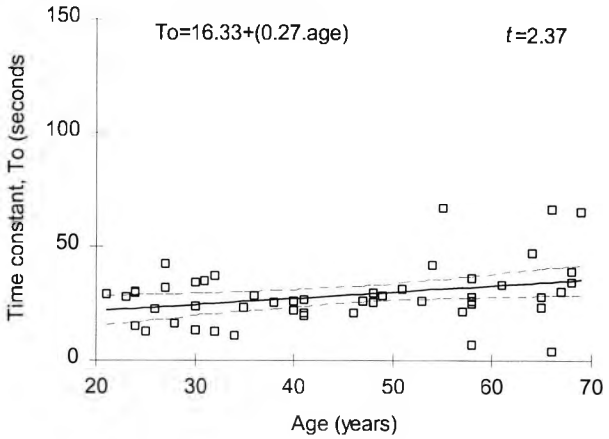

3.5 c.p.d.

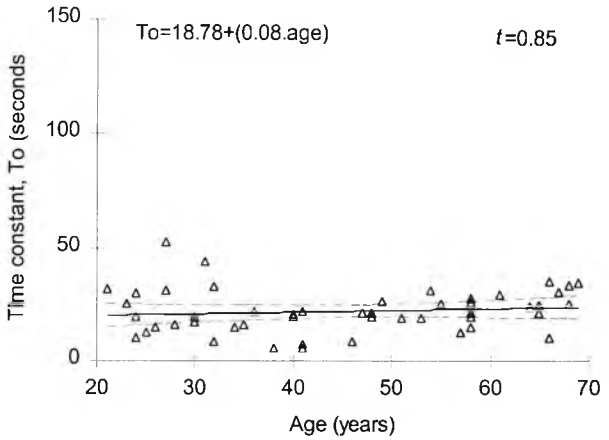

14 c.p.d.

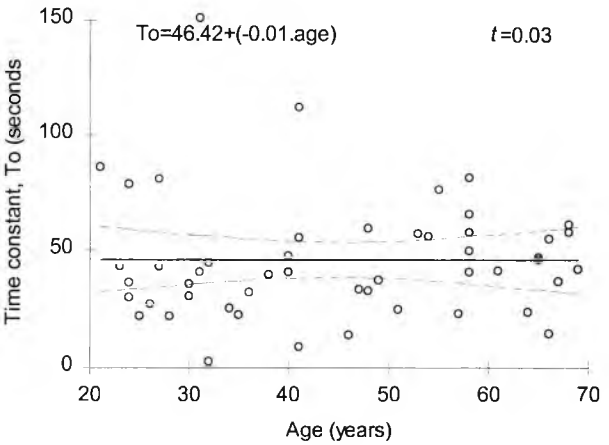

Figure 6.10 Variable *To* (time constant of recovery) as a function of age, for 3 spatial frequencies. The regression line (solid line) is described by the equation at the top left of each plot and the t statistic indicates the significance of the slope. Values for *t* in excess of 2.011 and 2.407 indicate significance at the 5% and 1% levels respectively with 48 degrees of freedom. Note the outlying value of 151 seconds for a 30 year old subject in (c.), if this outlying value is removed the regression is described by *To*=31.96+(0.25.age) and the associated *t* statistic becomes *t*=1.30.

6.4 Discussion

A technique for measuring the recovery of the CSF following intense light adaptation has been described. The information provides a good description of a subject's "real world" visual performance following exposure to bright light which may be of some clinical value.

The main object of this study was to determine if age has an effect on the recovery of contrast sensitivity. The effects of age are discussed below.

The variable *FS* provides an estimate of steady-state contrast sensitivity. Analysis of this variable indicates a small decline in contrast sensitivity with advancing years. The decline is greatest for the highest spatial frequency (14 c.p.d.), (see lower panel in Figure 6.8). This finding is in good agreement with previous studies of the effect of age on steady-state contrast sensitivity, (Owsley *et al.,* 1983; Derefeld *et al.,* 1979). Indeed, values for the parameter *FS* were similar to measurements of contrast sensitivity obtained by Owsley *et al.* (1983) despite methodological differences. Owsley *et al.* (1983) showed that CS to a 16 c.p.d. grating was 1.47 (SD 0.23) log CS for subjects in their twenties and 1.05 (SD 0.4) for subjects in their sixties. In this study, variable *FS* for a 14 c.p.d grating had a value of 1.37 (SD 0.2) log for subjects in their twenties and 1.04 (SD 0.33) for those in their sixties.

The loss of CS associated with increasing age was most evident for the highest spatial frequency grating (14 c.p.d.). Although, high spatial frequency CS is particularly susceptible to optical blur it is unlikely that this factor is responsible because all subjects wore their best optical correction. Owsley *et al.* (1983) suggest that loss of high spatial frequency CS is due to a reduction in retinal illuminance and increase in light scatter associated with age.

The least squares fitting procedure often produced negative values for variable *T* (the time at which CS first returned). It therefore provides a theoretical, rather than a practical, description of the time that CS first returned. Analysis of variable *T* indicates that it is independent of age for all spatial frequencies. Contrast sensitivity returned fastest for the low spatial frequency grating and slowest for the high spatial frequency grating. This finding is not surprising because variable *T* is analogous to the

measurement of conventional PSRT. During a conventional photostress test subjects are first able to see the large letters, which are high contrast stimuli containing relatively low spatial frequencies. Some time elapses before subjects are able to see small letters, which are also high contrast stimuli but ones composed of relatively high spatial frequencies. If a much higher spatial frequency grating (specifically one approaching the limits of resolution) had been used as a test stimuli then presumably the value for variable *T* would be similar to PSRT.

Values for variable *To*, the time constant of CS recovery, generally increased with age. However, the increase was small and only significant for the 0.6 c.p.d. grating (at the 5 % level). An increase in the value of *To* is not apparent from the regression line in the lower panel of Figure 6.10, because of an outlying value obtained for subject No. 3 (*To*=151). If this value is removed, the equation for the regression line becomes *To*=31.96+(0.25.age). The shortest time constants of recovery were generally observed for the 3.5 c.p.d. grating and the longest for the 14 c.p.d. grating. Although there have been no previous investigations of the recovery of the CSF following exposure to light, the slight slowing of the recovery may be related to a slowing of foveal dark adaptation with age, (Coile and Baker, 1992).

Although this study has demonstrated that the CSF recovery technique could be used clinically to describe an individual's recovery of visual performance, its diagnostic value may only be determined by examining abnormal subjects. An abnormal result would be indicated if data from an individual fell outside the 95% prediction intervals. Figure 6.11. describes the range of normal values, the 95% prediction intervals (shaded in grey), for each variable. This data may be used in a subsequent investigation to identify an abnormal result.

In summary, The effects of age on the recovery of the CSF are small, final contrast sensitivity declines with age, the time constant of recovery slightly increases with age but the start of the recovery is independent of age. Statistical significance (at the 5% level) was only observed for the decline in FS with age for the 0.6 and 14 c.p.d. gratings, and for the increase in To for the 0.6 c.p.d. grating.

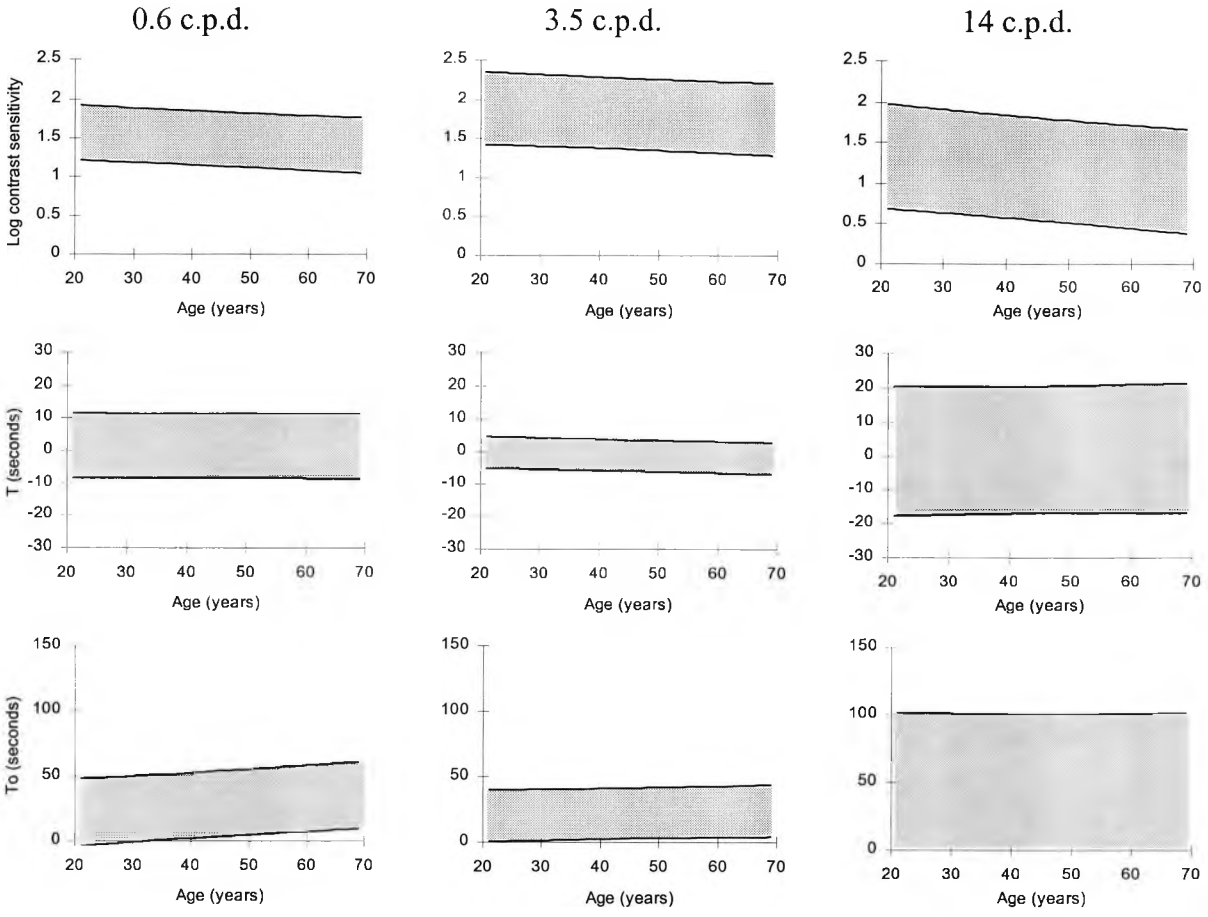

Figure 6.12 The 95 % prediction intervals for each of the variables. 95% of all new subjects data should fall within these zones. Each column shows the prediction intervals for each spatial frequencies, 0.6 c.p.d. (first column), 3.5 c.p.d. (second column), 14 c.p.d. (third column). Each row shows the prediction intervals for a particular variable, FS (top), T (middle), To (bottom).

7. Summary and conclusions

When we move from bright daylight to the relative gloom of a building interior it often takes several seconds or even minutes for vision to adjust. Although this is a familiar and invariably inconvenient aspect of visual function, relatively little is known about the recovery of spatial vision in such circumstances. For example, there have been no previous investigations of how sensitivity to sinusoidal gratings varies throughout the full course of dark adaptation. Four studies have measured threshold to square wave gratings but the results of these are rather contradictory. Coletta *et al*, (1986) and Naarendorp *et al*, (1988) showed that threshold to high spatial frequency gratings increased during the 'rod' phase of dark adaptation (a phenomenon attributed to suppressive rod-cone interaction) but, studies by Brown *et al*, (1953) and Brown *et al*, (1969) showed no such effect. Further information about the recovery of spatial vision following a period of intense light adaptation has been provided by several 'photostress' studies. Typically these investigations measure the time taken for acuity to return following a period of light adaptation. Although these results are of interest clinically (long PSRTs are associated with retinal dysfunction) they provide only limited information about the recovery of spatial vision under "everyday" conditions.

This thesis examines various aspects of the recovery of spatial vision after a period of intense light adaptation.

In chapter 1 the anatomy and electrophysiology of the visual system is reviewed with particular emphasis on the retina - the principal site for adaptation. The possible roles of the six main types of retinal neurones in the adaptation process are described and the contribution of rod-cone interactions is discussed. The two hypotheses (the photochemical and equivalent background hypotheses) that have dominated much of the experimental work on dark adaptation are also described. In classical dark adaptation experiments, the luminance threshold for the detection of a test target is measured as a function of time. Such studies typically yield a biphasic recovery curve where an initial rapid increase in sensitivity (attributed to cones) is followed by a slower recovery phase (attributable to rods). Other studies have measured changes in sensitivity to temporally and spatially periodic stimuli. Dark adaptation functions obtained using high frequency

flicker or high spatial frequency gratings (stimuli only detected by cones) do not show the typical two stage recovery. Instead, following an initial increase in sensitivity, sensitivity decreases again as the rods recover and start exercising a suppressive influence on the cones. This phenomenon of suppressive rod-cone interaction (SRCI) is reviewed.

A series of experiments to investigate the recovery of spatial vision during dark adaptation are described in chapter 2. There were several reason for conducting this study. Firstly, all previous studies of dark adaptation have used square wave gratings and the harmonics contained in such stimuli may have influenced the results. Secondly, evidence for the existence of grating SRCI is equivocal. Coletta *et al.* (1986) and Naarendorp *et al.* (1988) showed that sensitivity to high spatial frequency gratings declines during the rod phase of dark adaptation but studies by Brown *et al.* (1953) and Brown *et al.* (1969) showed no such effect. A third reason for conducting the study was to determine if the recovery of spatial vision was similar in colour normal and dichromatic subjects.

Seven subjects (4 colour normals, 2 protanopes and a deuteranope) were exposed to a 16°, 6 log td, 'white', field for 10 sec which bleached about 96% of cone photopigment. Luminance thresholds for sinusiodal gratings of various spatial frequencies were then measured as a function of time as the eye dark adapted.

Data obtained for low spatial frequency gratings were qualitatively similar to conventional dark adaptation functions showing distinct cone and rod limbs. For colour normal and deuteranopic subjects, threshold for the highest spatial frequency grating declined for the first 5 minutes of dark adaptation and then rose by up to 1 log unit, confirming the existence of grating SRCI. However, this increase in threshold was not observed in the two protanopes studied. The absence of grating SRCI in protanopes suggests a distil site for this interaction involving LWS cones. This finding is at odds with a report which indicates that grating SRCI is a post-retinal phenomenon (light adaptation of the non test eye abolishes grating SRCI but has no effect on flicker SRCI), (Frumkes *et al.*, 1995). However, it is argued that the reduction in grating SCRI observed when the non-test eye is light-adapted, may be attributable to an improvement in sensitivity of the test eye (due to a reduction in central noise) which masks SRCI.

This hypothesis may be tested by obtaining dark adaptation functions while the non-test eye is partially light adapted. If partial light adaptation of the non-test eye improves sensitivity to high spatial frequency gratings then a protanope should show a drop in threshold (for a 14 c.p.d. grating) during the rod phase of dark adaptation approximately equivalent to the apparent reduction of grating SRCI in colour normal subjects.

While dark adaptation investigations are of theoretical interest, they tell us little about 'every day' visual performance. Rarely are we required to 'see' in absolute darkness and the important quantity for the visual system to extract form the environment is not threshold luminance but contrast. Chapter 3 describes a technique that may be used to measure changes in the contrast sensitivity function (CSF) following intense light adaptation.

Two subjects participated in the experiment. Accommodation was paralysed using 0.5% cyclopentolate and the test eye was aligned at a Maxwellian view optical system and exposed to a 5.7 log td uniform white field subtending 16° for a period of 2 minutes. Initially, a high contrast sinusoidal grating (c=0.9) of a predetermined spatial frequency was displayed on a CRT display and subjects were required to respond when it was first seen 'through' the after image. Thereafter, the contrast of the grating was continuously ramped up from sub-threshold levels under computer control until the subject responded that it was just visible (ascending method of limits). In this way contrast sensitivity could be monitored until recovery was complete. This procedure was repeated three times and mean contrast sensitivity (CS) was calculated as a function of time using a linear interpolation method. This entire procedure was repeated for five spatial frequencies (0.6, 1.4, 3.5, 8.3 and 19.9 c.p.d.) at five mean luminance levels (50, 5, 0.5, 0.05 and 0.005 cdm^{-2}).

When the mean luminance of the grating was relatively high (50 and 5 cdm^{-2}), CS returned relatively rapidly (being complete after about 2-3 minutes) and the rate of CS recovery was similar for all spatial frequencies suggesting that the recovery of CS for all spatial frequencies was determined by the same mechanism. Such results could be accounted for by receptoral adaptation. When the mean luminance of the grating was reduced to 0.5 cdm^{-2}, CS recovery was slower, the peak CS shifted from 3.5 to 1.5 c.p.d. and there was some evidence that recovery for low spatial frequencies continued

tocincrease after high frequency CS had plateaued. This difference in recovery rate may be accounted for if low spatial frequency pathways continued to operate in accordance with Weber's law whilst higher spatial frequency pathways operated in accordance with square root law. At lower luminances (0.05 and 0.005 cdm^{-2}) low spatial frequency CS recovered in two phases - an initial phase that lasted about 10-15 min followed by a further increase in CS presumably attributable to rod activity.

Experiments to investigate the effect of varying 'bleach' intensity and duration on CS recovery are described in chapter 4. The principal reason for investigating the effects of bleach intensity and duration was to determine if the concentration of a photoproduct might determine CS recovery. Two experiments were conducted using the same equipment and procedures used in the preceding chapter.

In the first investigation the intensity (I) and duration (t) of the bleach were varied in such a way that different I.t combinations bleached the same fraction of photopigment (20, 50, 86 and 95%). If CS recovery was related to the concentration of photopigment alone, brief intense bleaches should have had the same effect on subsequent CS recovery as long, dim ones providing the fraction of pigment bleached in each case was the same. Results from 2 subjects plotted as log CS as a function of time, show that brief, intense bleaches depress CS to a greater extent and for longer than long, dim ones.

In the second investigation the more general photochemical hypothesis was investigated. The intensity and duration of the bleach was varied to produce equal energy bleaches (i.e. I.t=k, the Bunsen-Roscoe law). Again short, intense bleaches were found to reduce CS by a greater amount and produce longer recovery times than equal energy long, dim ones, indicating failure of the more general photochemical hypothesis. These results suggest that CS recovery in photopic conditions is not simply determined by the concentration of a photoproduct.

It has been suggested that the rate of recovery of spatial vision following intense light adaptation is of clinical value. A procedure for implementing such measurements is described in the literature and has been termed the photostress test. This test, which involves exposing the eye to an intense light and then measuring the time taken for acuity to recover, is capable of differentiating retinal from post-retinal causes of visual loss. A wide range of normal photostress recovery times (PSRT) have been reported in

the literature (7-70 seconds) and it is perhaps for this reason that the test has never gained widespread acceptance with clinicians. A study to compare 3 clinically applicable versions of the photostress test with a method likely to minimise sources of error is described in chapter 5. The purpose of this comparison was to identify the most suitable clinical technique and to determine the effect of age, ametropia and acuity on PSRT.

Fifty normal subjects aged (21-76 years) participated in the study. Subjects were light adapted using: a) a pentorch held 3 cm from the eye for 10 seconds; b) a focused pentorch for 10 seconds; c) a direct ophthalmoscope for 30 seconds and d) a Maxwellian view optical system (the 'gold standard'). The repeatability of each technique was evaluated in a pilot study (n = 10). The third bleaching strategy (directing a subject to fixate the light from a direct ophthalmoscope for 30 seconds) produced PSRTs most closely associated with the 'gold standard' technique. Linear regression analysis showed that PSRT increased significantly with age but that PSRT was independent of ametropia and acuity.

Although the photostress test has been shown to be of value clinically, the recovery of visual acuity provides us with limited information about the more general properties of spatial vision during this process. Chapter 6 describes the development of a modified versions of the CS recovery technique and shows how the CSF recovers in conditions analogous to those employed in the photostress test. The primary objective was to determine the effect of age on the recovery of CSF.

The same subjects (n = 50) that participated in the photostress study took part in this investigation. Following exposure to a 5.7 log td field for 60 seconds, the recovery of CS to a variety of gratings (0.6, 3.5 and 14 c.p.d.) was monitored for 3 minutes. Raw CS recovery data was modelled with a single exponential growth function in the form $CS = FS.(1 - e^{-(t-T)/To})$ where FS was the final recovered CS, T was the time that elapsed before the high contrast grating was seen and To was the time constant of recovery. Analysis of these variables showed that final recovered CS (FS) declined with age and that the time constant of recovery (To) increased with age but that the time taken for the grating to first be seen (T) was independent of age. The technique provides a fuller description of the recovery of visual performance than the conventional

photostress test. Further studies involving patients with various forms of retinopathy are required in order to establish the clinical value of this test.

In summary, this thesis presents a series of experiments designed to further our understanding of the recovery of spatial vision following a period of intense light adaptation. The results show, for the first time, how threshold to sinusiodally modulated gratings varies during the course of dark adaptation. The existence of a phenomenon known as grating suppressive rod-cone interaction is confirmed and results from dichromatic subjects indicates that this interaction takes place at a distal retinal site. The recovery of contrast sensitivity following a period of intense light adaptation was also investigated. The recovery of contrast sensitivity is dependant on several factors; the spatial frequency and mean luminance of the grating, the intensity and duration of the adapting field and the age of the subject. The data presented in this thesis makes a further contribution to our understanding of how visual performance changes when 'the lights go out'.

Appendix I

Subject	*Age*	*BVS*	*MAR*	*Pupil*	*Ver. 1*	*Ver. 2*	*Ver. 3*	*Ver. 4*
1	31	-0.25	0.00	4	12	17	48	40
2	26	0.75	-0.20	4	9	15	45	40
3	30	0.75	-0.06	4	9	11	40	36
4	58	0.75	-0.20	3	17	20	59	40
5	49	-3.75	-0.10	4	10	12	40	43
6	41	0.25	-0.20	4	7	11	45	32
7	27	-4.00	-0.14	3	5	9	55	38
8	51	0.00	-0.10	3	7	7	28	26
9	58	-4.75	-0.06	3	12	7	55	45
10	54	0.00	-0.06	3	12	17	68	58
11	41	-4.50	0.00	3	10	22	45	40
12	27	-1.00	-0.10	4	10	20	38	26
13	28	-0.75	-0.20	4	10	12	41	38
14	38	-0.25	-0.20	4	10	17	45	42
15	53	-0.25	-0.06	4	13	30	32	33
16	32	-2.75	0.00	4	8	17	20	20
17	41	-0.75	-0.04	4	15	17	62	42
18	35	0.00	-0.10	3	12	30	40	30
19	55	-3.00	-0.06	3	8	21	52	54
21	58	-1.00	0.04	4	12	13	62	75
22	32	-0.50	0.00	4	12	16	52	45
23	24	0.00	-0.18	4	10	10	39	44
24	34	0.50	-0.20	4	15	20	42	40
25	30	-1.00	-0.20	4	12	22	40	43
26	24	0.00	-0.16	4	12	21	40	45
28	25	-3.25	-0.20	4	10	13	32	70
29	21	-1.75	-0.08	4	12	17	65	60
30	66	0.75	-0.14	3	15	42	72	56
31	30	1.25	-0.20	4	25	55	57	70
32	24	-4.25	-0.08	4	8	30	35	30
36	57	-0.25	-0.10	3	11	11	46	69
37	58	0.25	-0.06	4	11	9	72	92
38	46	0.25	-0.10	4	19	27	49	48
39	36	-3.00	-0.08	4	11	12	46	37
40	40	-4.00	0.00	3	11	11	61	45
41	47	0.50	-0.02	3	11	26	59	36
42	48	-0.50	-0.02	3	10	21	58	45
43	61	-3.75	-0.18	3	14	14	83	55
44	65	-0.25	-0.16	3	16	24	46	49
45	48	-0.50	-0.06	4	12	24	52	39
46	23	0.00	-0.16	4	9	14	50	41
47	58	0.75	-0.04	4	15	21	58	56
48	40	-3.00	-0.10	4	13	22	63	55
49	68	1.50	0.10	4	14	30	47	45
50	64	0.25	0.00	5	9	15	29	28
51	69	1.50	0.02	4	29	64	62	81
52	67	0.25	0.10	4	9	16	45	38
53	66	-0.50	0.12	4	9	13	75	69
54	65	-1.75	-0.10	4	18	22	54	53
55	68	1.00	-0.04	4	14	22	61	60
Mean	44.7	-0.88	-0.08	3.7	12.0	19.9	49.5	46.7
SD	15.3	1.75	0.09	0.50	4.3	10.9	12.2	15.0

Table showing age, best vision sphere (BVS), Log of the minimal angle of resolution (MAR) and pupil size to nearest mm in 50 normal patients. The last 4 columns show photostress recovery times for 4 versions of the photostress test.

Appendix II

Subject	Age	BVS	0.6 c.p.d.			3.5 c.p.d.			14 c.p.d.		
			FS	T	To	FS	T	To	FS	T	To
1	31	-0.25	1.69	1.09	34.69	2.10	-1.71	44.06	0.95	19.99	40.92
2	26	0.75	1.61	-0.90	22.50	1.99	-0.38	15.14	1.38	2.58	27.00
3	30	0.75	1.61	-1.70	24.1	2.04	-0.24	17.25	1.50	-29.23	151.52
4	58	0.75	1.56	-5.73	36.08	1.98	-6.75	27.80	1.02	9.91	41.01
5	49	-3.75	1.57	0.79	28.30	1.81	-1.06	26.81	0.78	21.16	37.61
6	41	0.25	1.50	-4.02	26.74	1.38	1.69	7.30	0.81	-16.12	112.39
7	27	-4.00	1.61	-3.52	42.43	1.67	-3.84	52.59	0.90	7.88	81.46
8	51	0.00	1.59	-4.13	31.23	2.04	-0.84	18.86	1.41	2.95	25.09
9	58	-4.75	1.04	1.15	6.85	1.46	-1.55	14.98	1.00	-11.36	66.01
10	54	0.00	1.43	-4.75	41.70	1.89	-2.99	31.01	1.43	-0.43	56.47
11	41	-4.50	1.73	-1.70	21.02	1.36	2.33	5.84	0.53	3.92	8.98
12	27	-1.00	1.72	-2.49	32.18	2.07	-3.77	31.41	1.61	4.28	42.94
13	28	-0.75	1.06	-0.14	16.15	1.78	-0.09	16.05	1.26	2.78	21.89
14	38	-0.25	1.35	1.82	25.59	0.93	4.61	5.82	0.31	8.42	39.84
15	53	-0.25	1.55	-4.40	26.09	1.82	-2.42	19.20	1.03	2.25	57.39
16	32	-2.75	1.50	-0.43	12.76	1.93	0.33	8.62	0.81	5.62	2.67
17	41	-0.75	1.35	4.19	19.82	1.44	1.10	22.02	1.05	7.78	55.77
18	35	0.00	1.68	-0.29	23.12	2.07	-0.07	16.34	1.68	3.49	23.01
19	55	-3.00	1.69	-4.56	66.63	1.87	-1.09	25.39	1.23	-0.02	76.57
21	58	-1.00	1.52	-2.16	27.64	1.66	-0.78	19.80	0.99	-3.17	57.80
22	32	-0.50	1.71	-3.74	37.32	2.03	-0.82	32.85	1.26	6.77	45.14
23	24	0.00	1.44	-2.03	29.79	2.01	1.10	30.16	1.54	11.66	36.15
24	34	0.50	1.53	0.67	10.96	1.89	-0.32	15.25	1.49	4.22	25.81
25	30	-1.00	1.44	-5.59	34.16	1.77	-1.48	19.65	1.32	2.58	35.54
26	24	0.00	1.69	0.74	15.33	1.82	-1.09	19.97	1.26	-18.93	78.83
28	25	-3.25	1.46	-0.05	12.67	1.95	-1.61	12.96	1.48	-0.22	22.31
29	21	-1.75	1.19	-2.77	29.04	1.77	-4.38	31.97	1.35	-1.23	86.40
30	66	0.75	1.50	-8.79	66.24	1.87	-5.27	35.47	1.54	-2.61	54.93
31	30	1.25	1.43	0.21	13.60	1.93	-0.56	17.09	1.57	-5.30	30.82
32	24	-4.25	1.74	-11.17	30.01	2.17	1.04	10.34	1.44	2.38	29.88
36	57	-0.25	1.65	-1.57	21.32	2.02	-0.05	12.75	1.60	0.94	23.18
37	58	0.25	1.61	-0.09	25.19	1.97	-0.37	21.29	1.45	-0.10	82.08
38	46	0.25	1.62	-0.35	20.73	1.69	1.27	8.90	0.84	3.65	14.10
39	36	-3.00	1.52	-5.87	28.33	1.96	-3.05	22.11	1.60	-1.90	32.47
40	40	-4.00	1.62	-8.34	33.18	1.87	-2.79	19.84	1.42	-14.33	94.69
41	47	0.50	1.50	-0.08	26.09	1.95	-1.67	21.35	1.11	7.86	33.24
42	48	-0.50	1.44	-1.26	29.70	1.91	2.09	19.91	1.55	-0.71	59.46
43	61	-3.75	1.39	0.24	33.33	1.71	-0.35	29.80	0.77	20.65	41.38
44	65	-0.25	1.34	0.16	23.40	1.74	-2.47	21.68	1.11	-5.16	47.31
45	48	-0.50	1.49	-0.22	25.78	1.94	-1.55	21.24	1.09	7.96	32.94
46	23	0.00	1.41	-0.97	27.88	1.93	1.42	25.21	1.46	8.09	43.34
47	58	0.75	1.53	-0.79	26.31	1.72	-2.34	26.21	1.05	2.07	50.17
48	40	-3.00	1.57	-3.06	26.40	1.86	-2.54	20.71	1.19	-0.92	47.65
49	68	1.50	1.24	-3.10	34.05	1.62	3.46	33.79	0.70	-1.71	57.92
50	64	0.25	1.53	-8.12	47.35	1.97	-4.36	24.23	1.65	-0.96	24.01
51	69	1.50	1.55	-6.93	64.87	1.92	-3.86	34.56	0.87	20.97	42.04
52	67	0.25	1.04	-5.06	29.97	1.81	-6.61	30.81	0.91	-1.72	36.78
53	66	-0.50	1.38	1.78	4.00	1.62	1.76	10.53	0.73	4.08	14.51
54	65	-1.75	1.37	-0.05	28.12	1.72	-2.35	25.14	1.08	-3.39	45.95
55	68	1.00	1.10	-5.07	38.97	1.79	-4.22	25.70	1.06	-5.26	61.20
MEAN	44.7	-0.88	1.49	-2.16	28.58	1.82	-1.19	22.16	1.18	1.85	46.06
SD	15.3	1.75	0.18	3.02	12.93	0.22	2.39	9.52	0.32	9.17	26.32

Table showing data obtained from 50 subjects after fitting each contrast sensitivity recovery curve with a single exponential growth function. *FS* is the final contrast sensitivity (Log CS), *T* is the time that contrast sensitivity first returned and *To* is the time constant of recovery, both are in seconds.

Appendix III

Raw contrast sensitivity recovery data (open symbols) and single exponential model (closed symbols), for 50 normal subjects, plotted as log contrast sensitivity as a function of time. Each row shows data obtained from a single subject and each column contains data for a single spatial frequency (see Chapter 6).

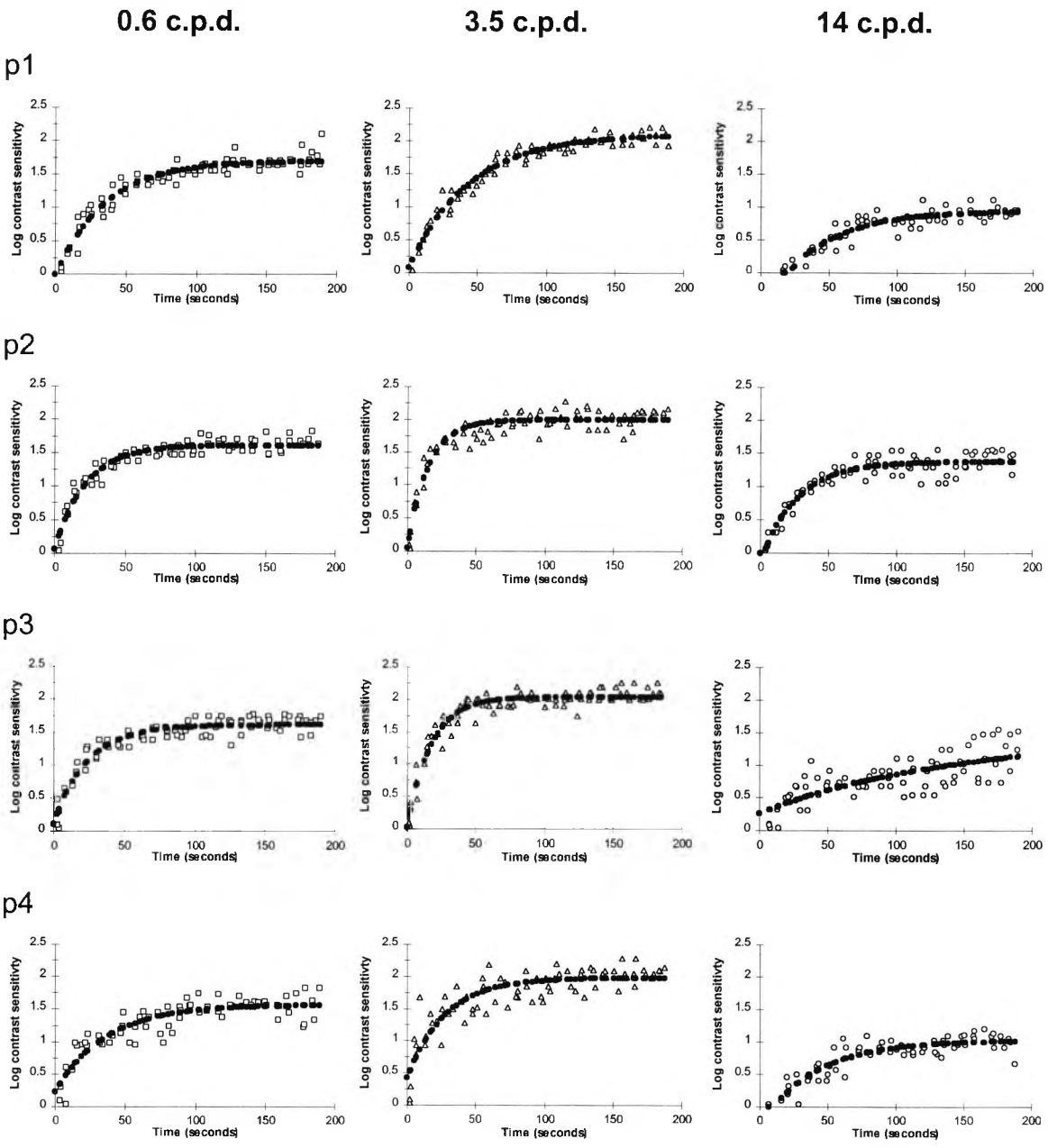

p5

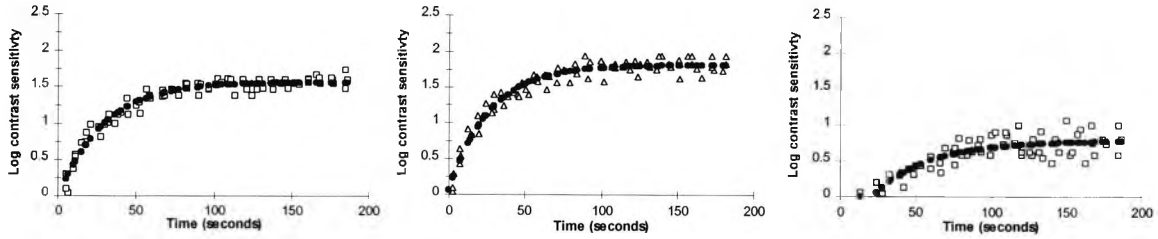

p6

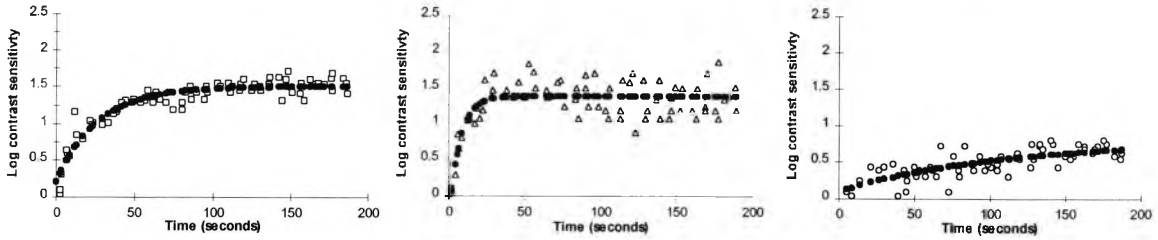

p7

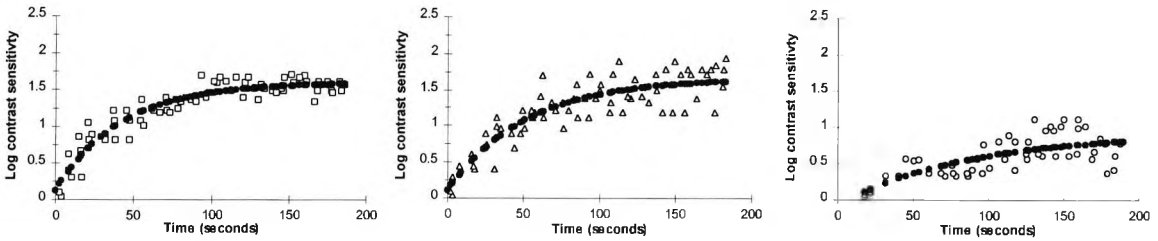

p8

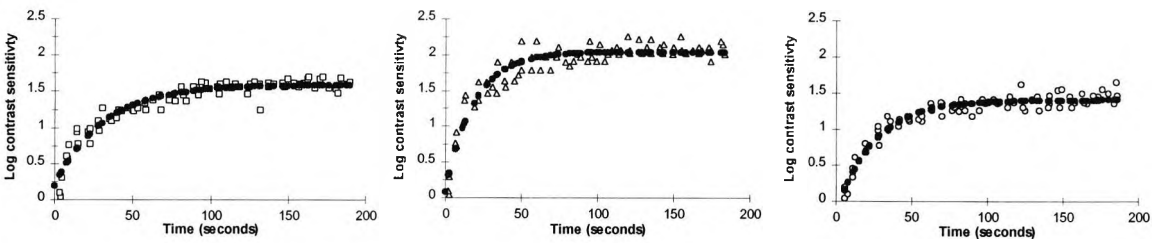

p9

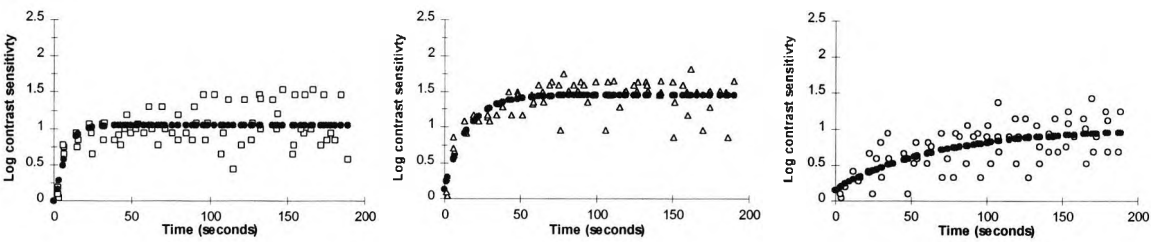

p10

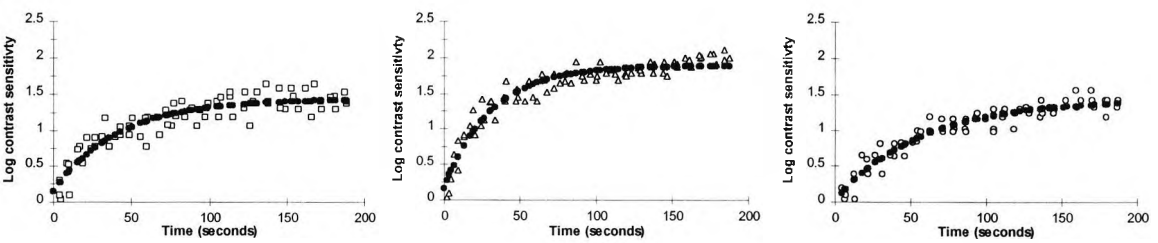

p11

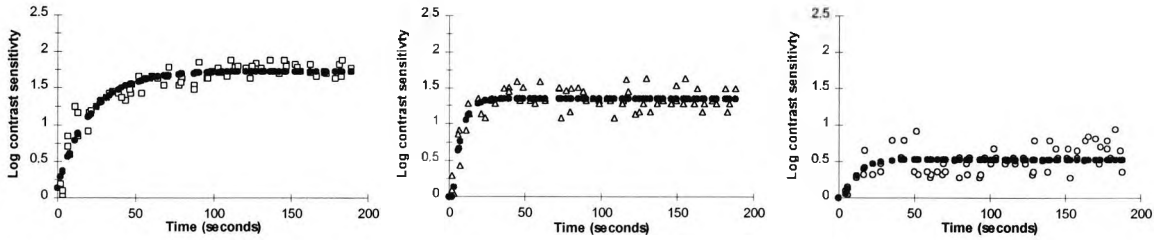

p12

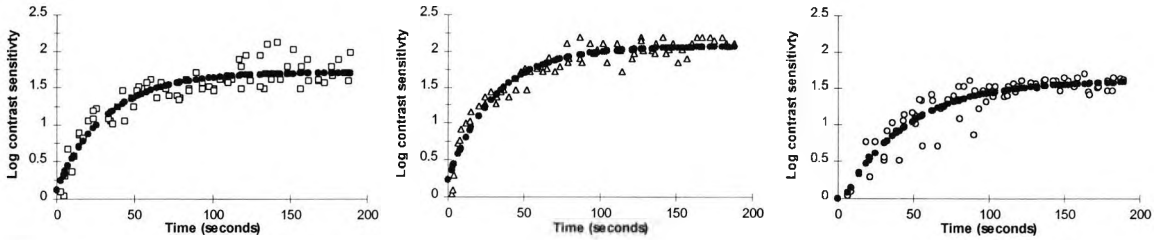

p13

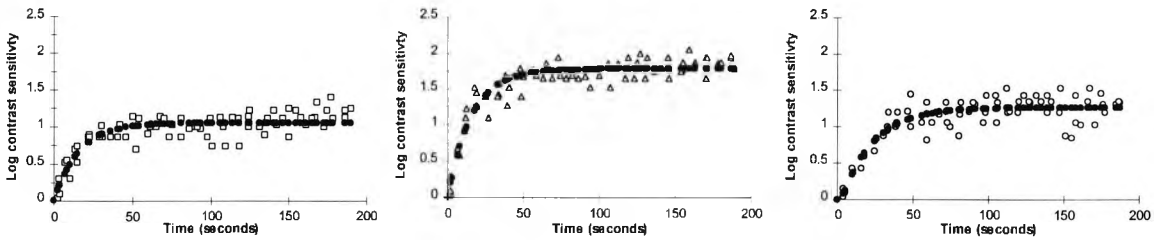

p14

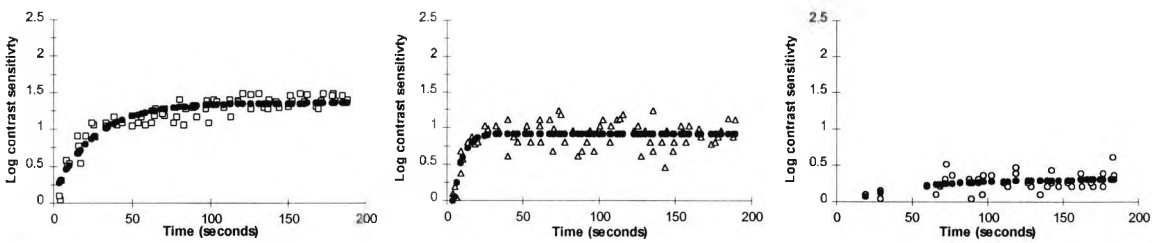

p15

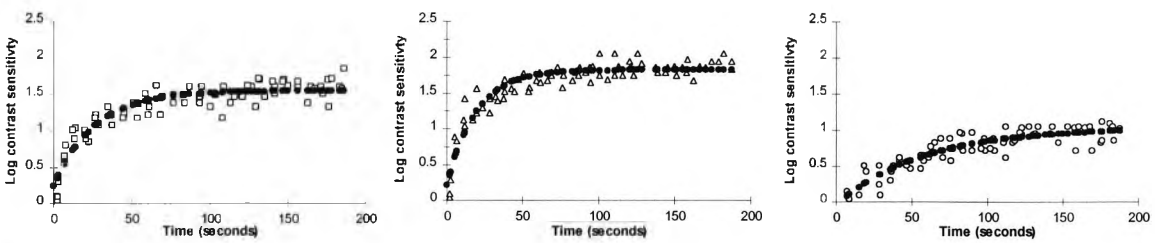

p16

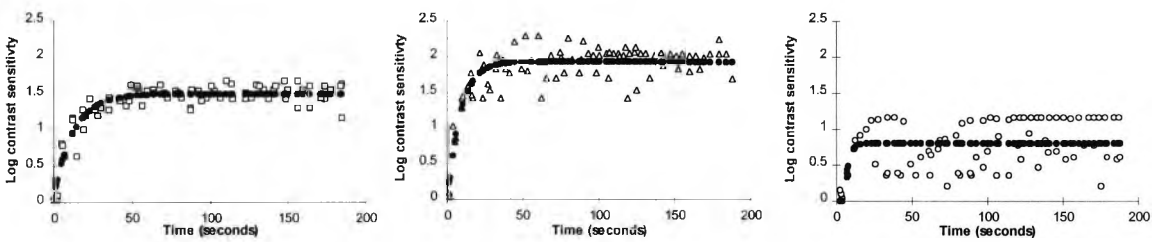

p17

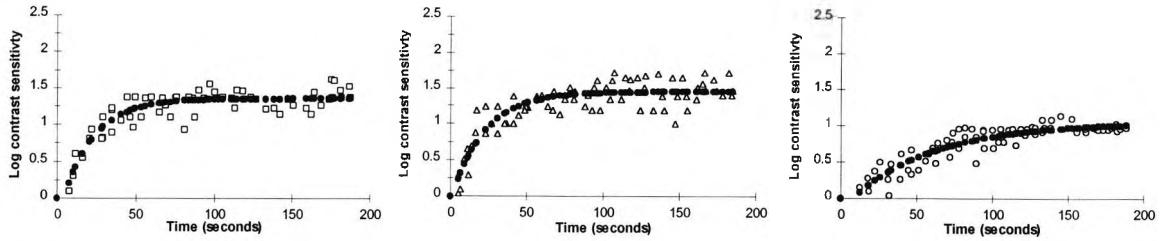

p18

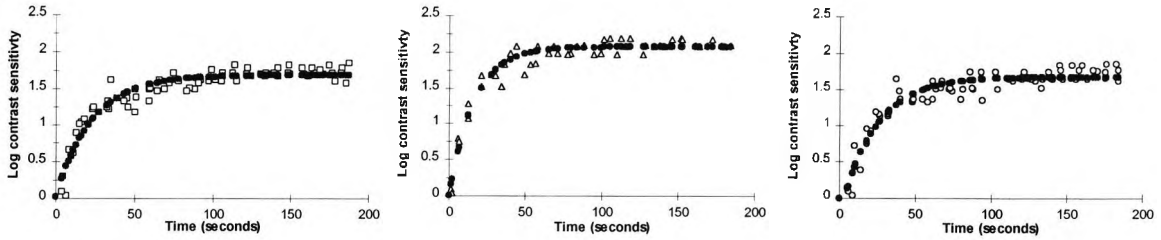

p19

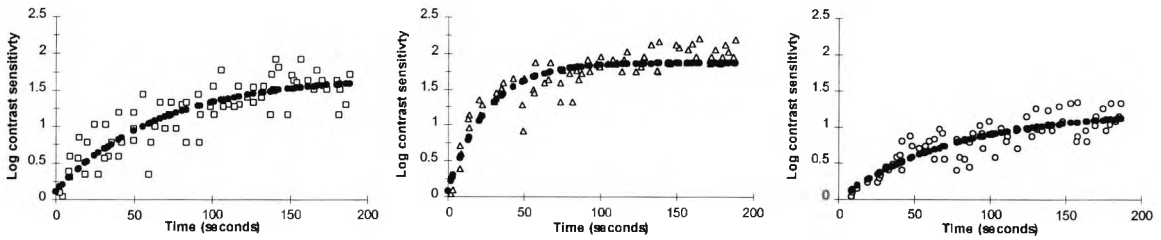

p21

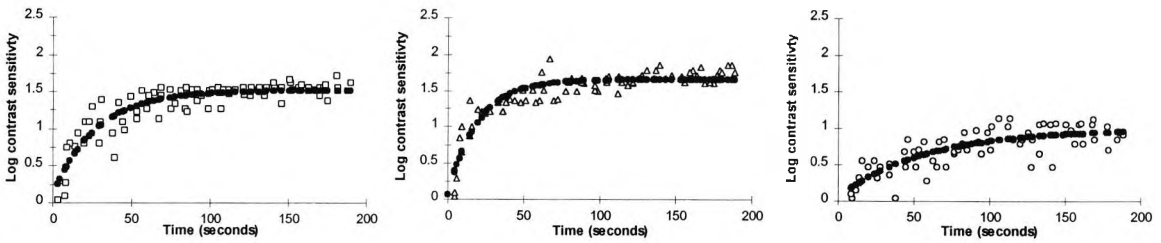

p22

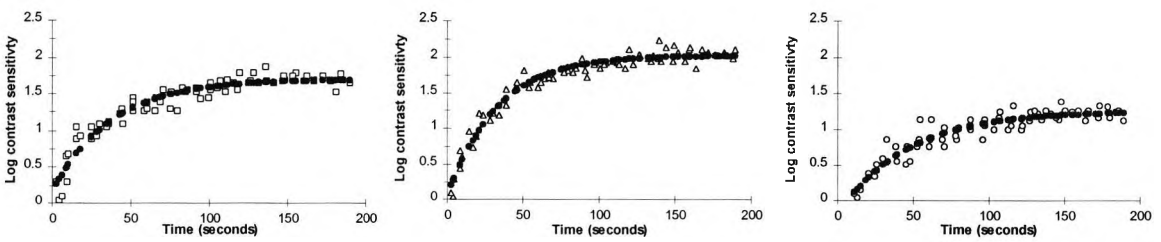

p23

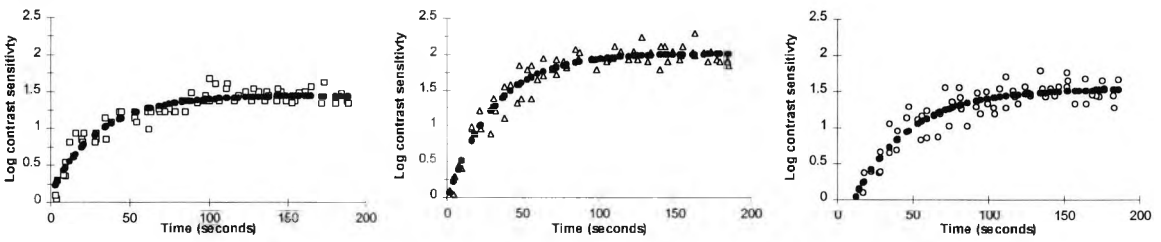

p24

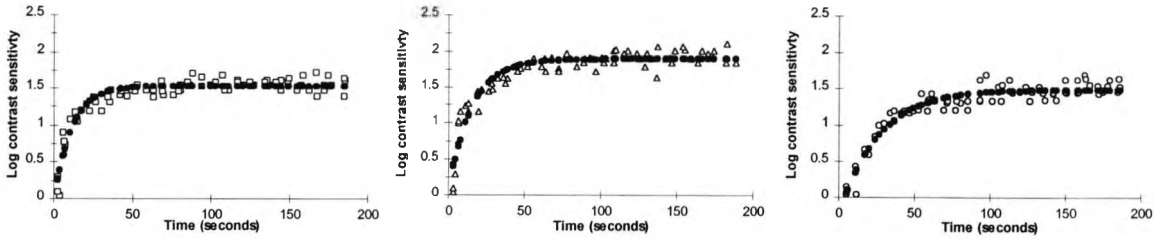

p25

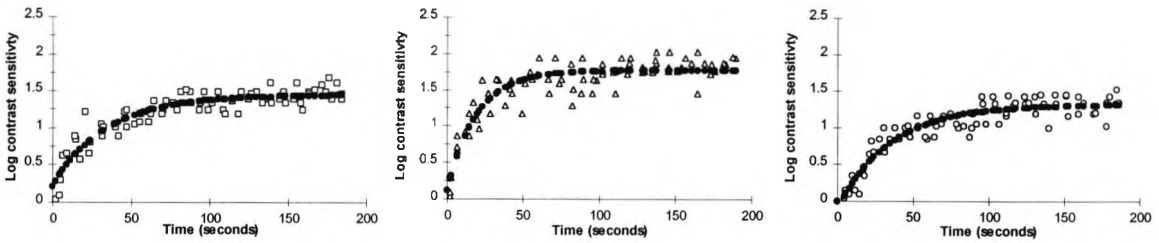

p26

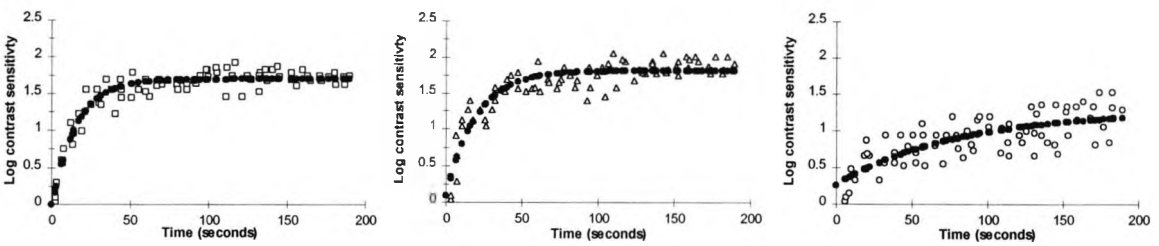

p28

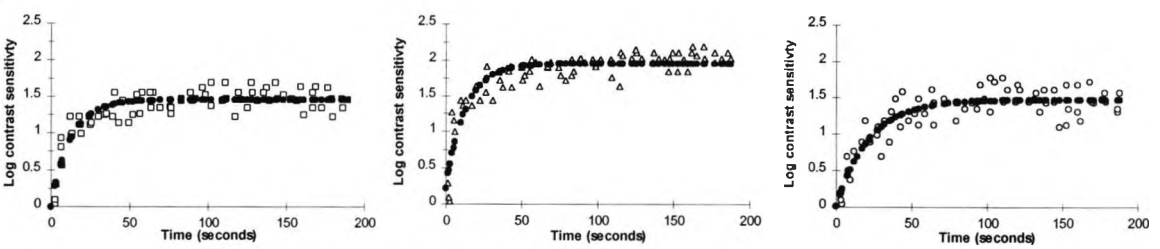

p29

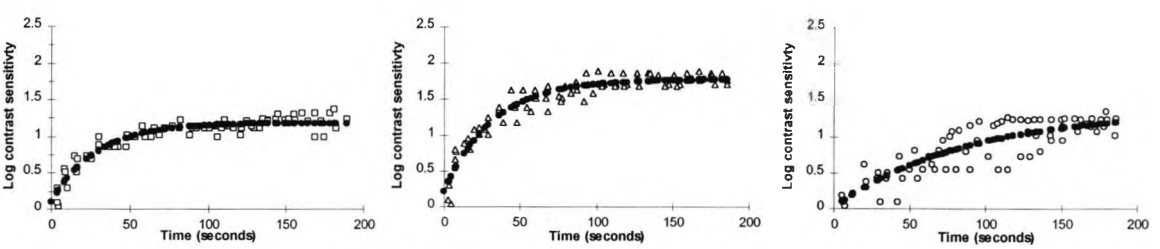

p30

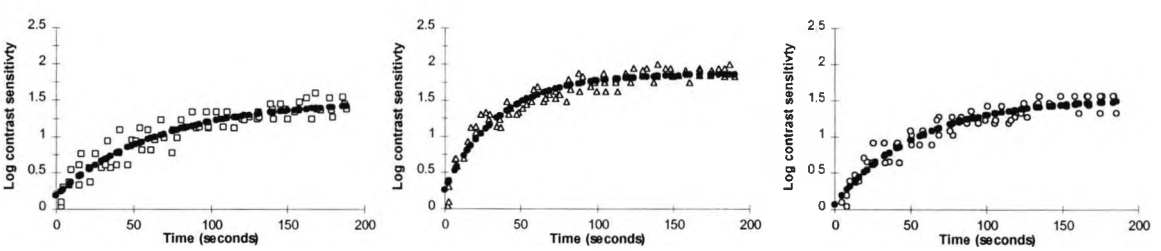

p31

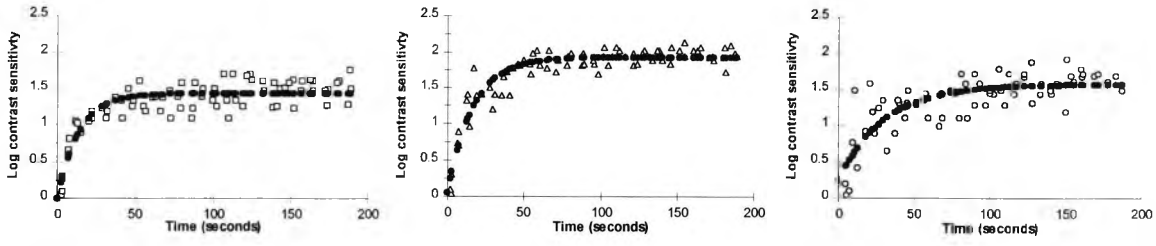

p32

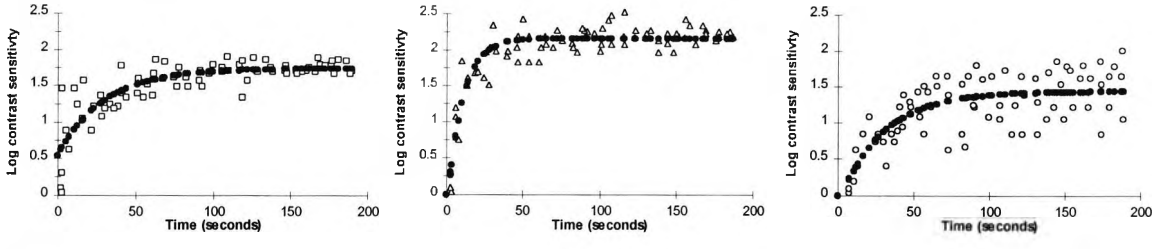

p33

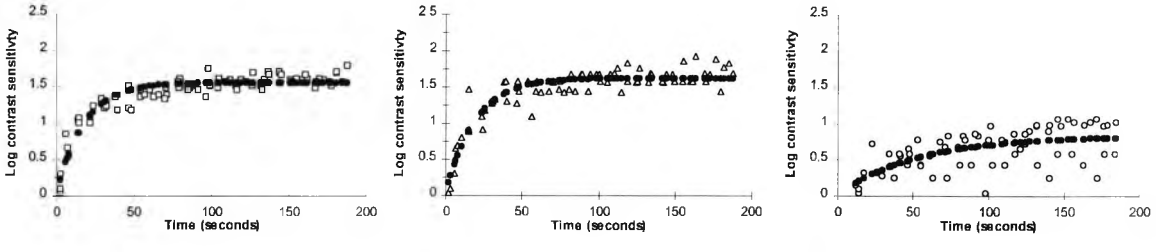

p36

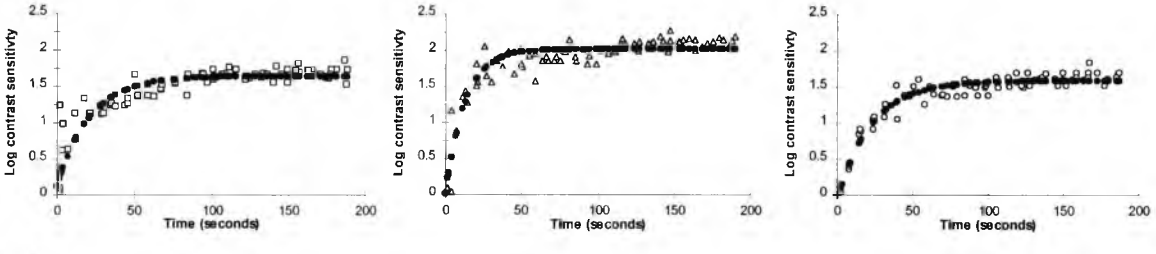

p37

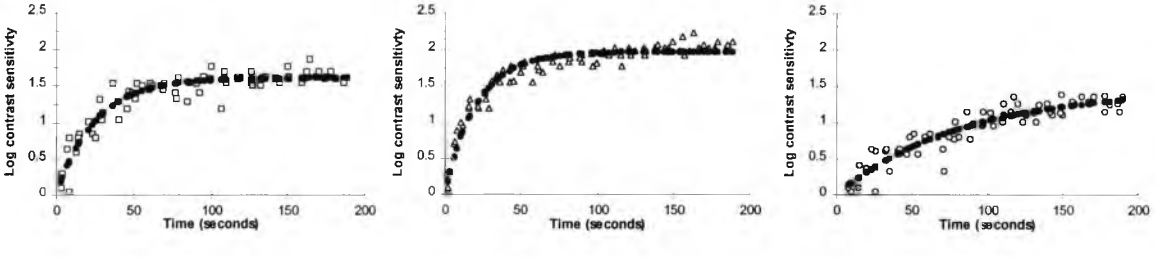

p38

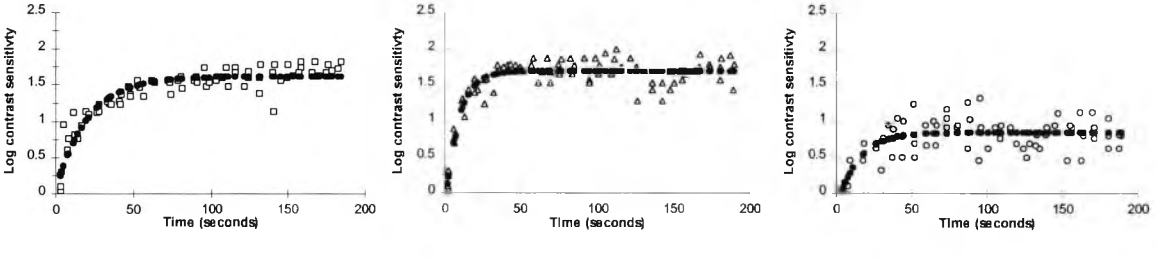

p39

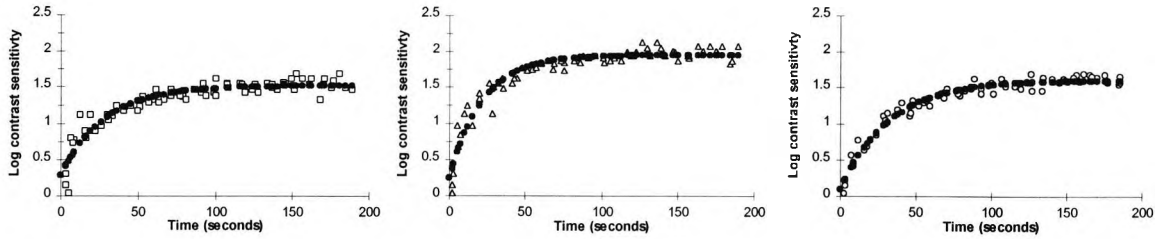

p40

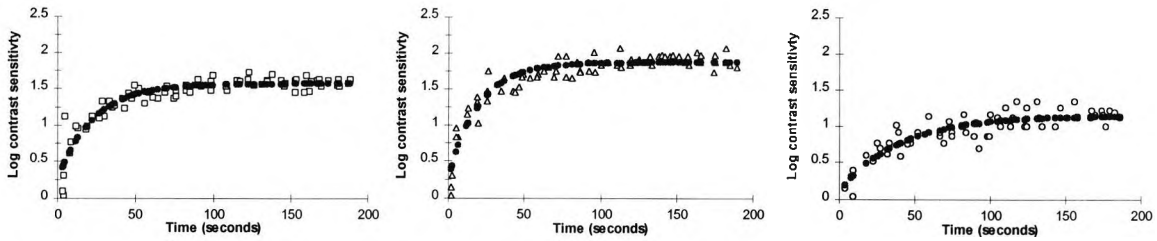

p41

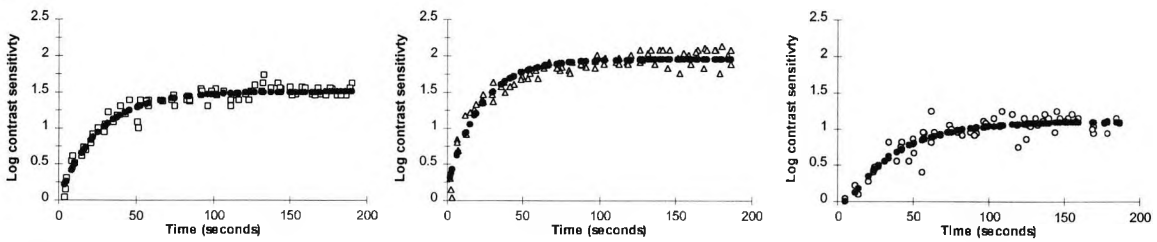

p42

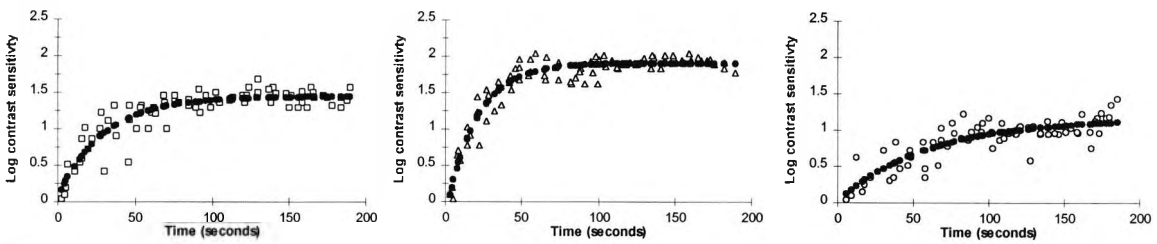

p43

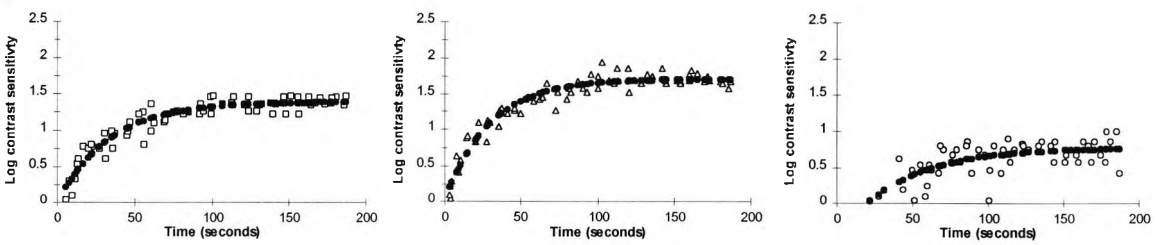

p44

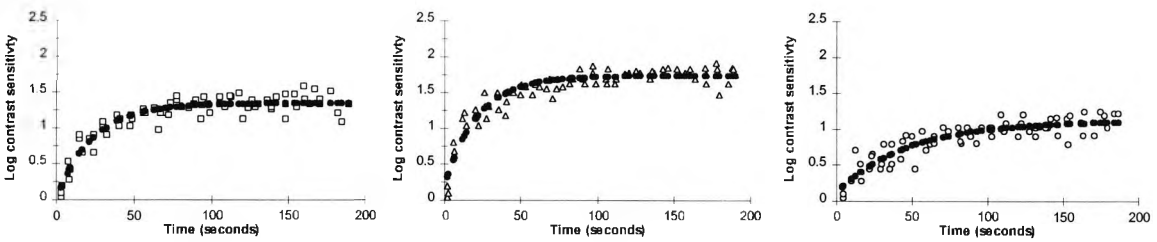

p45

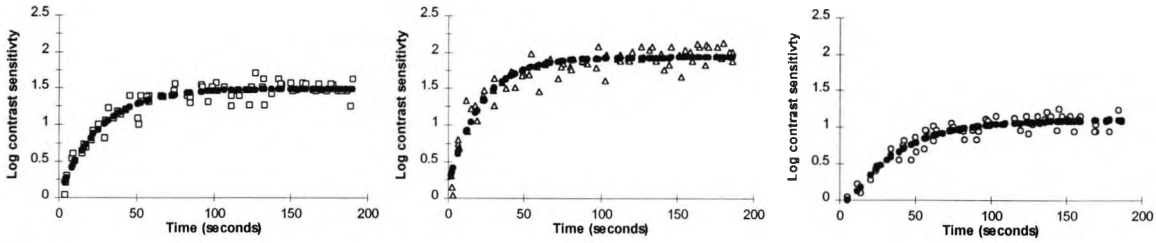

p46

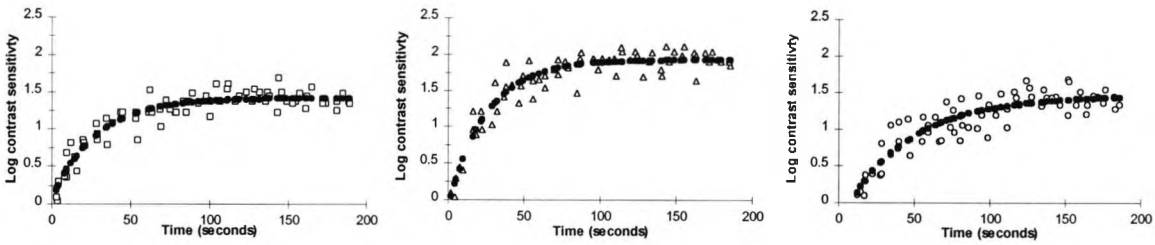

p47

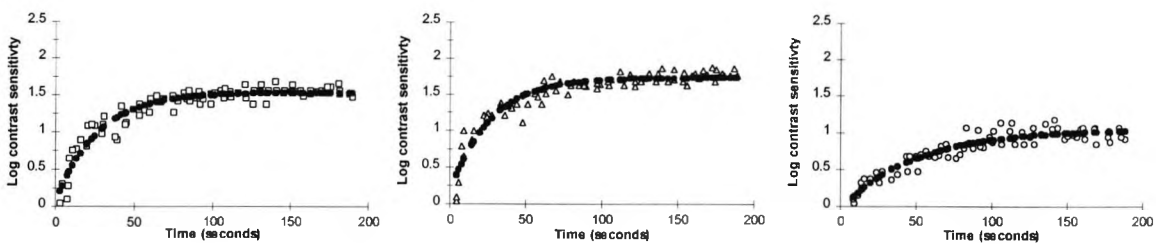

p48

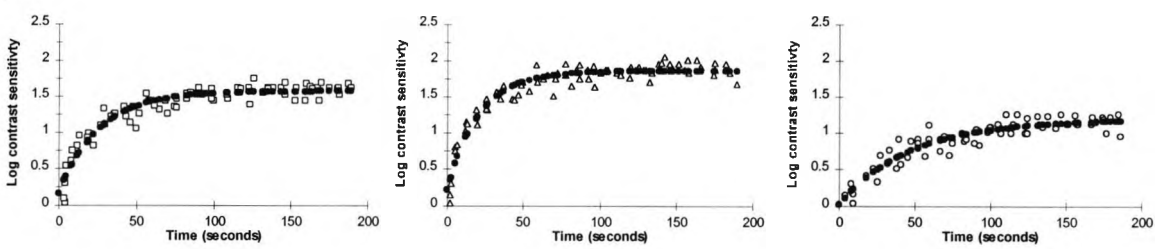

p49

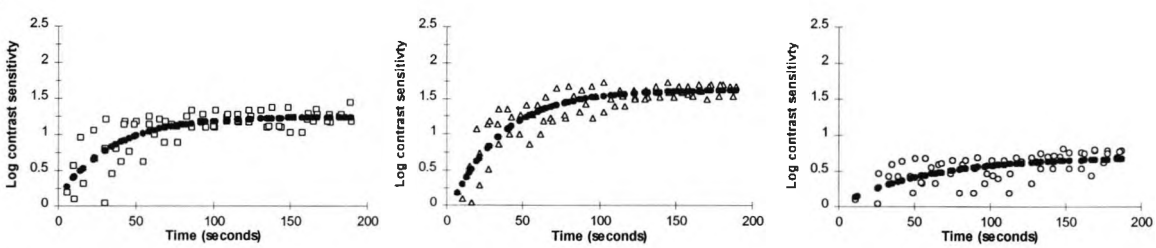

p50

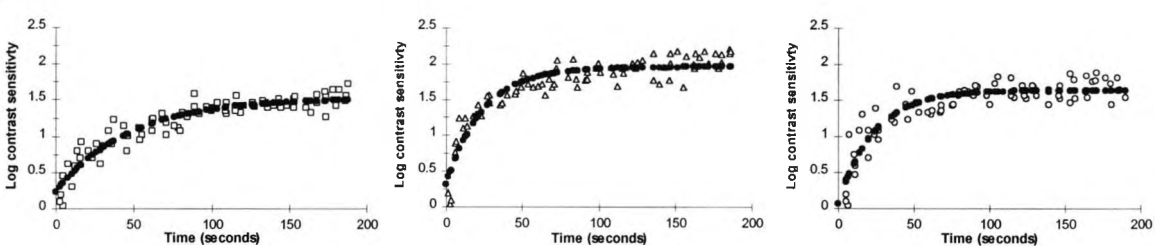

p51

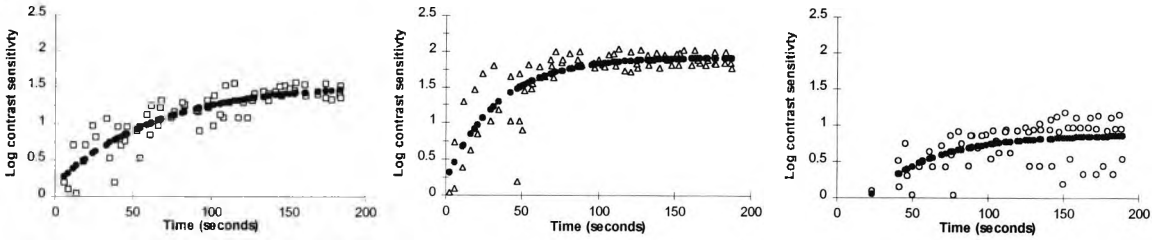

p52

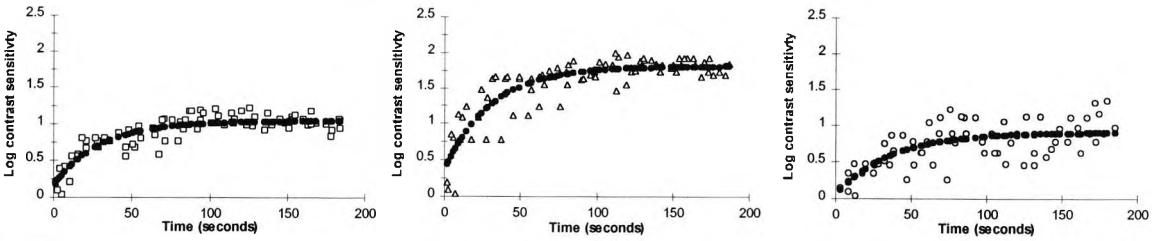

p53

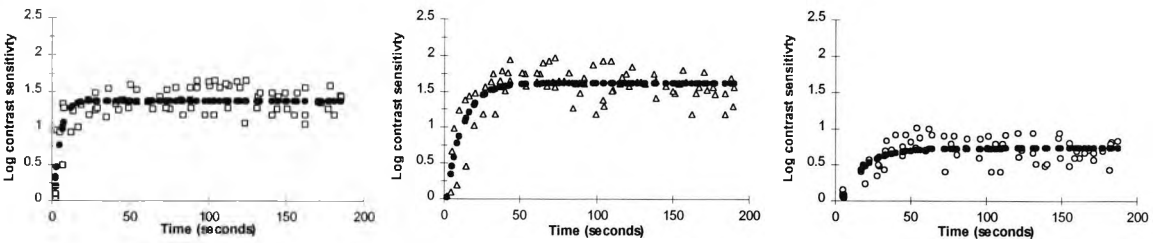

p54

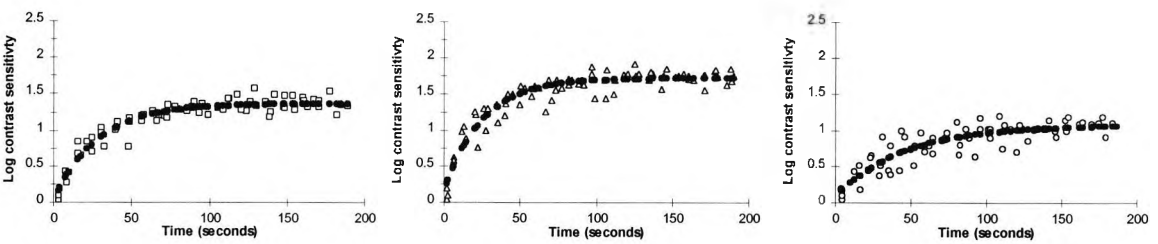

p55

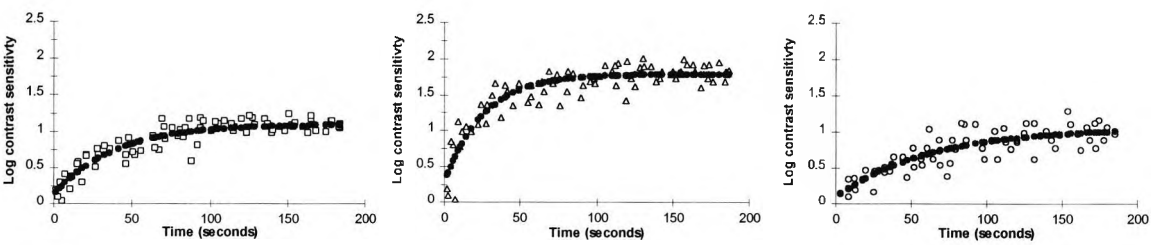

p58

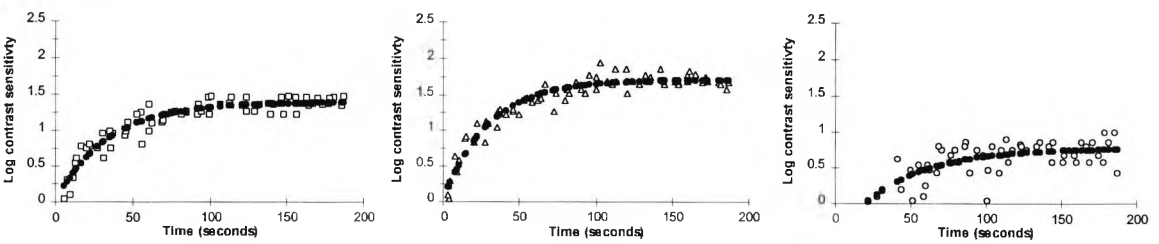

p60

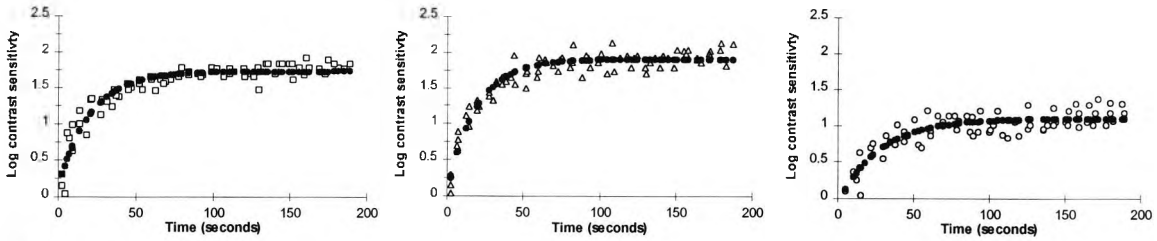

p61

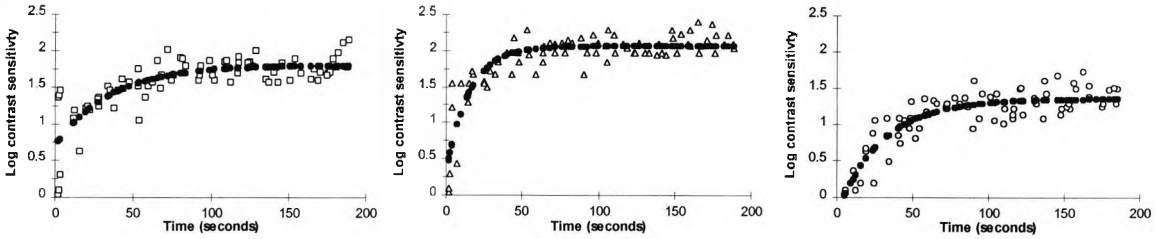

p62

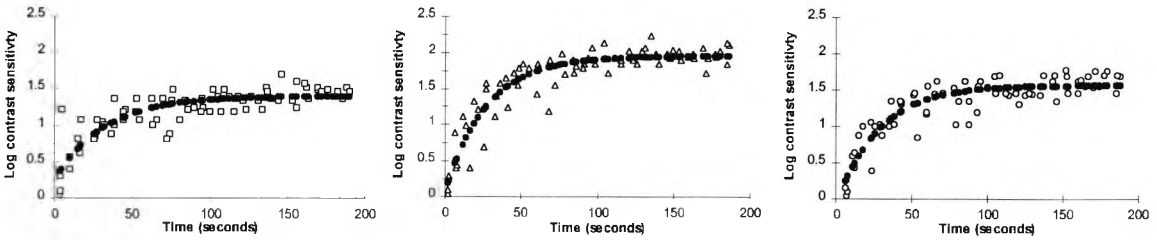

p63

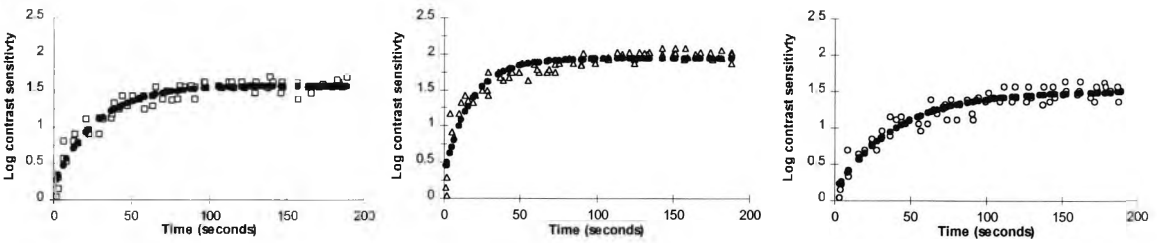

p64

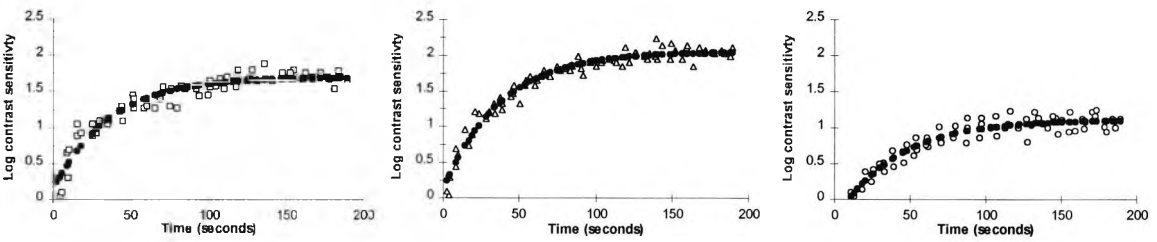

p65

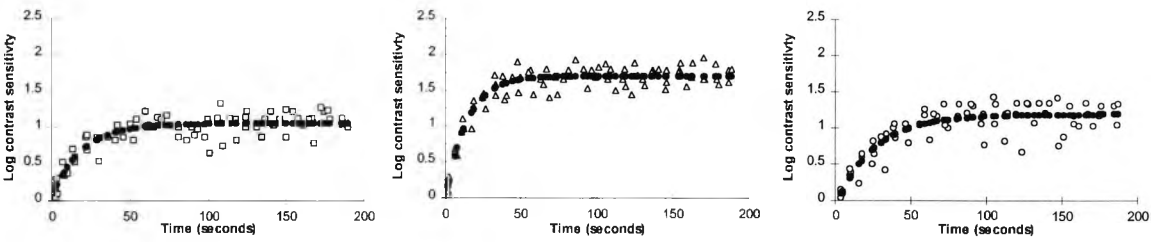

p66

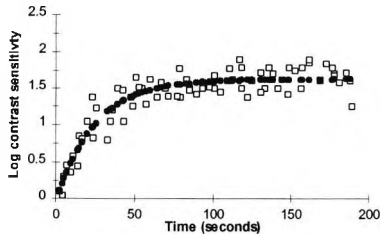
Log contrast sensitivty
Time (seconds)

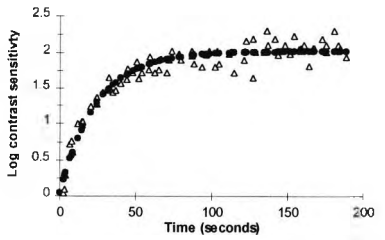
Log contrast sensitivty
Time (seconds)

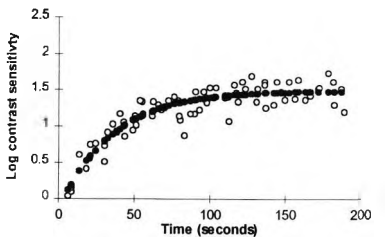
Log contrast sensitivty
Time (seconds)

p67

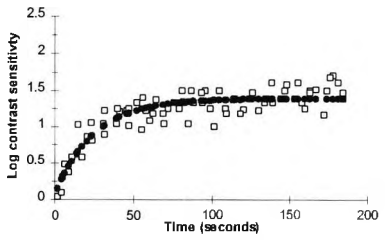
Log contrast sensitivty
Time (seconds)

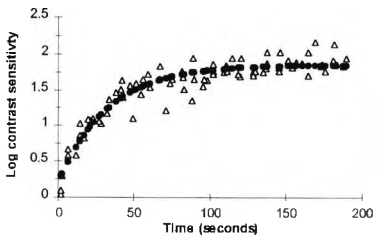
Log contrast sensitivty
Time (seconds)

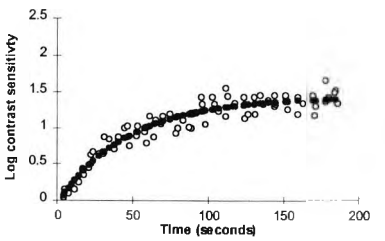
Log contrast sensitivty
Time (seconds)

Appendix IV

A model of CS recovery

Although dark adaptation and CS recovery experiments are not the same, the same adaptational mechanisms operate during both types of experiment. The following paragraphs describe a model of contrast sensitivity recovery for the photopic system based upon two factors that will affect how the receptors respond to the bars of a grating; namely photopigment bleaching and the equivalent background of excitation. This model is evaluated against empirical data in chapter 6.

Unlike the rod system, photopigment depletion in cones accounts for a substantial component of dark adaptation, (Geisler, 1980). The reduction in photopigment concentration reduces the retina's quantum catching power and so the chance of light initiating the transduction cascade is reduced. A correction for pigment depletion is given by:

$$Ir = I \,.\, p \qquad (1)$$

where Ir is the effective intensity of the light after correction for photopigment depletion, I is the uncorrected intensity and p is the proportion of unbleached pigment, (Geisler, 1980).

The luminance profile of a square wave grating presented on a CRT is shown in the left hand panel of Figure 1. Photopigment depletion reduces the quantum catching power of the receptors and so the effective luminance of the grating is scaled by the factor p. The right hand panel of Figure 1 shows the effective luminance of the grating when only 10% of the receptoral photopigment is available.

Photopigment depletion acts in a multiplicative way, i.e. it simply scales the effective luminance of the grating, but has no effect on the contrast of the grating.

A.

$$c = \frac{Imax - Imin}{Imax + Imin}$$

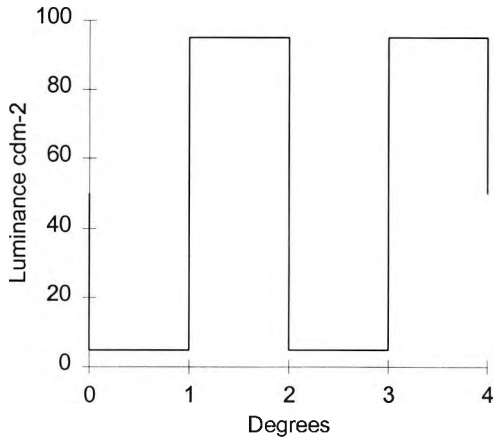

B.

$$c = \frac{(p.Imax) - (p.Imin)}{(p.Imax) + (p.Imin)}$$

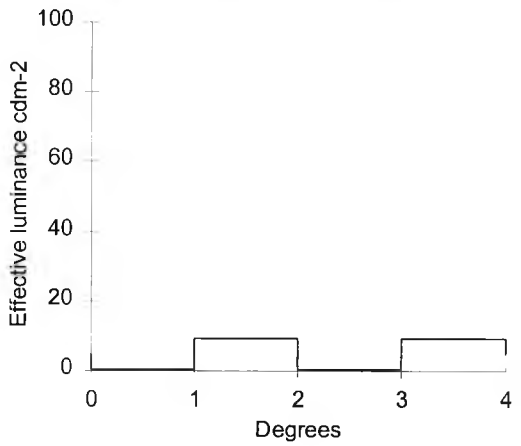

Figure 1 shows how the effective luminance of the bars of a grating on a CRT display (A.) are transformed by a 90% reduction in photopigment concentration (B.). It may be seen from the equations above each plot that contrast is unaffected by photopigment depletion (at this stage).

The technique of retinal densitometry has been used to investigate photopigment regeneration in the intact human retina, (Hollins and Alpern, 1973; Rushton and Henry, 1968; Smith *et al*, 1983). When photopigment regeneration takes place in the dark, the fraction of photopigment present may be described by:

$$(1 - p) = (1 - Po).e^{-t/To} \qquad (2)$$

where p is the fraction of pigment present at time t, Po is the fraction present when t=0 and To is the time constant of recovery. However, in an investigation of contrast sensitivity, regeneration does not take place in the dark but in the presence of a background (the mean luminance of the grating), therefore equation 2 becomes a little more complex:

$$p = \frac{Io + \left(Po.(I + Io) - Io\right)e^{-t.(I+Io)/To.Io}}{(I + Io)} \qquad (3)$$

where Io is the retinal illuminance that bleaches half the pigment at equilibrium (3×10^4 td) and I is the intensity of the background field in trolands. Figure 2 shows how the fraction of cone photopigment changes in the presence of a 628 td (i.e. 50 cdm^{-2} viewed through a 4 mm pupil) background field, following exposure to 6 log td for 10 seconds.

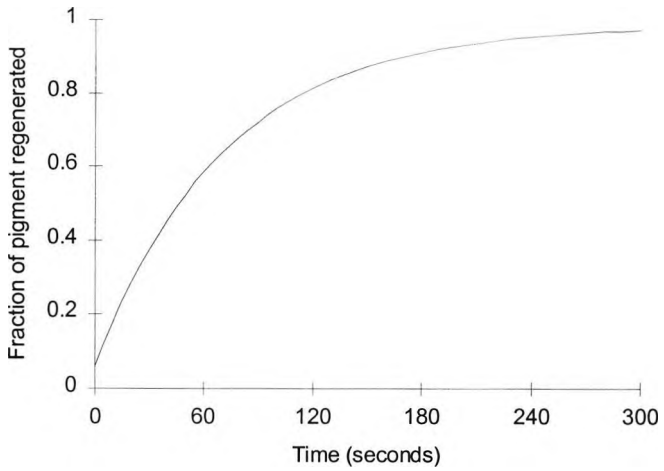

Figure 2. Graph showing the regeneration of cone photopigment in accordance with equation (2) assuming a time constant of recovery (To) of 74 seconds, and a half bleach constant of (3 x 10^4 td).

During dark adaptation and CS recovery, the transduction cascade is activated both by absorbed quanta and putatively by opsin which creates an equivalent background of excitation. Therefore the receptors "see" the test stimulus superimposed on an equivalent background. Figure 3 shows how the scaled response to the bars of a high contrast grating, brought about by photopigment depletion, is further transformed by the presence of an equivalent background (E).

A.

$$c = \frac{(p.Imax) - (p.Imin)}{(p.Imax) + (p.Imin)}$$

B.

$$c = \frac{(E + (p.Imax)) - (E + (p.Imin))}{(E + (p.Imax)) + (E + (p.Imin))}$$

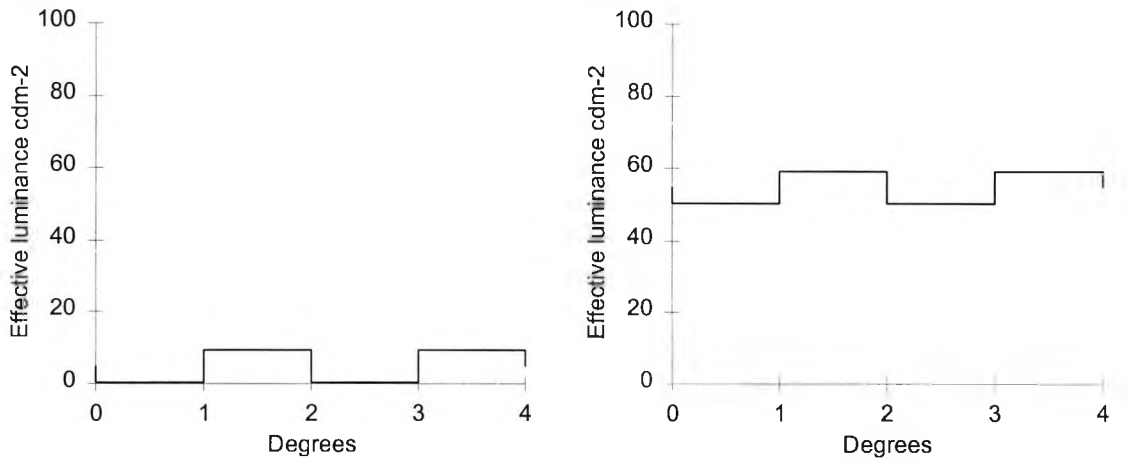

Figure 3 Graph showing how the luminance profile of the grating shown in Figure 1 (B.) is further transformed by the addition of an equivalent background (E).

The addition of an equivalent background has several effects: it acts like a d.c. offset device increasing the effective mean luminance of the grating and consequently reducing its contrast. Furthermore, this d.c. input makes the system sensitive to changes in pigment density, i.e. changes in p will now alter contrast.

In rod dark adaptation, where the effects of photopigment depletion are small, dark adaptation functions (log threshold vs. time) may be described by an exponential function. Likewise cone dark adaptation functions may also be described by an exponential function after the effects of photopigment depletion have been corrected for. On the assumption that the equivalent background hypothesis is a reasonable working hypothesis and assuming that any increment threshold function is a straight line[1] (log threshold vs. log background) then log equivalent background should also decay in an exponential fashion. Figure 4 describes the decay of an equivalent background that alters exponentially according to:

$$E = 10^{(Ei.e^{(-t/To)}} \qquad (4)$$

where E is the illuminance of the equivalent background, Ei is the initial intensity of the background in log units at t=o and To is the time constant of recovery.

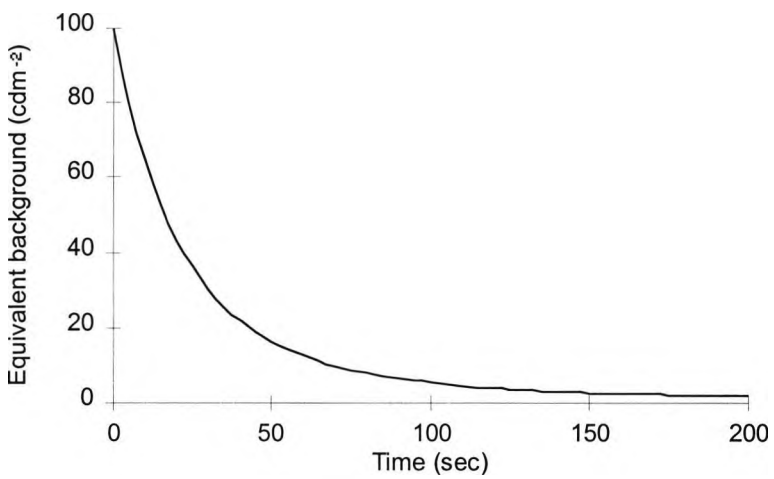

Figure 4 Decay of equivalent background during dark adaptation based on equation (4) assuming that the initial background is equivalent to 2 log cdm^{-2} and To is 100 seconds.

[1] Although departures form a straight line are common, for example when going from square root to Weber like behaviour or when encountering "saturation" in the scotopic system, such departures are unlikely when retinal illuminance is at or above 2.8 log td because most spatial frequencies display Weber behaviour above this level (this does not apply to relatively high spatial frequencies) and saturation does not occur in the cone system.

To determine how contrast sensitivity changes following exposure to light it is necessary to assume that the visual system's threshold to "effective" contrast remains constant. This is a reasonable assumption in photopic conditions because contrast threshold is largely determined by contrast gain which is relatively stable above a certain level of illumination. Suppose that the visual system's steady-state contrast sensitivity to a grating is 2 log CS i.e. its contrast threshold is 0.01, then following the period of light adaptation the grating will be at threshold when its adjusted contrast reaches 0.01. Specifically the grating will be at threshold when:

$$\frac{(E+(p.Imax))-(E+(p.Imin))}{(E+(p.Imax))+(E+(p.Imin))}=0.01 \qquad (5)$$

By extracting values for the 2 unknown quantities *Imin* and *Imax* it is possible to predict how CS would change after a bleach. Values for *Imax* and *Imin* may be obtained after solving the simultaneous equations (5) and (6).

$$Ml = Imax + Imin \qquad (6)$$

where *Ml* is twice the mean luminance of the CRT display. For clarity the simultaneous equations are solved below:

$$Ct=\frac{E+(Imax.p)-(E+(Ml-Imax).p)}{E+(Imax.p)+E+((Ml-Imax).p)} \qquad (7)$$

$$Ct=\frac{Imax.p-Ml.p+Imax.p}{2E+Ml.p} \qquad (8)$$

$$1=\frac{2.Imax.p-Ml.p}{Ct.2.E+Ct.Ml.p} \qquad (9)$$

$$Imax.2.p=Ct.2.E+Ct.Ml.P+Ml.p \qquad (10)$$

$$Imax=\frac{Ct.2.E+Ct.Ml.p+Ml.p}{2.p} \qquad (11)$$

$$Imin = Ml - Imax \qquad (12)$$

where *Ct* is the contrast threshold of the system, *Ml* is twice the mean luminance of the monitor, *E* is the luminance of the equivalent background and *p* is the fraction of cone

photopigment. By substituting equations (11) and (12) in the equation for Raleigh contrast, contrast sensitivity following light adaptation may be described by:

$$CS = \frac{Ct.2.E}{p.Ml} + Ct \qquad (13)$$

By substituting equations (3) and (4) for E and p in equation (13) contrast sensitivity may be predicted at any time:

$$CS = Log\left[\frac{ML.(Io + (Po.(I + Io).e^{-t.(I+Io)/(To.Io)}/(I + Io))}{(Ct.2.10^{E.e^{-t/Tol}})} + Ct\right] \qquad (14)$$

Figure 5 shows the models prediction for the recovery of contrast sensitivity if the contrast threshold for the system is 0.01, and the initial light adaptation period bleached 96.3% of cone photopigment (6 log td, for 10 seconds). The time constant of recovery for pigment regeneration was taken as 73 seconds, on the basis of densitometric data obtained by Hollins and Alpern (1973) for a 10 second bleach. The equivalent background after the bleach was assumed to be equivalent to 1000 cdm^{-2} (based on results of Hahn and Geisler (1995) for a 1 c.p.d. grating) and its time constant was 100 seconds.

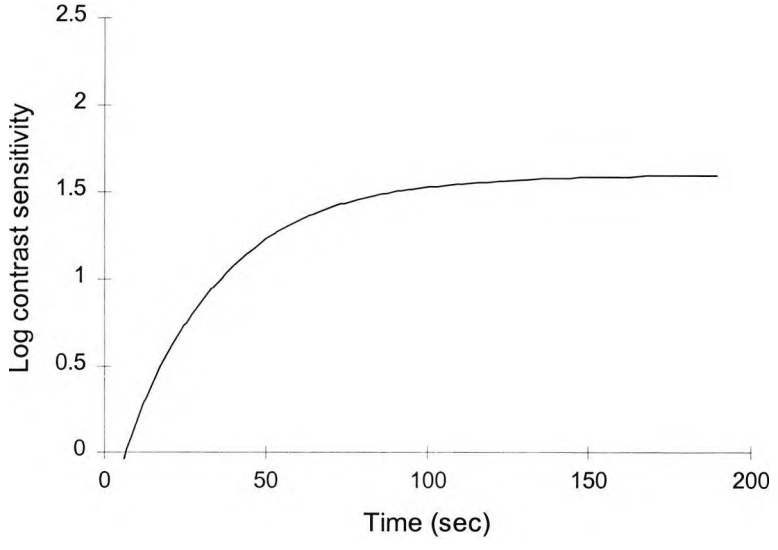

Figure 5 Plot showing how contrast sensitivity would recover following a 96.3% bleach, if the equivalent background produced by the period of light adaptation had an equivalent luminance of 1000 cdm^{-2}.

References

Adams, A.J. and Brown, B. (1975). Alcohol prolongs time course of glare recovery. *Nature*. **257**, 481-483.

Adelson, E.H. (1982). Saturation and adaptation in the rod system. *Vision Res*. **22**, 1299-1312.

Aguilar, M. and Stiles, W.S. (1954). Saturation of the rod mechanism of the retina at high levels of stimulation. *Optica Acta*. **1**, 59-65.

Alexander, K.R. and Fishman, G.A. (1983). Rod-cone flicker interaction: Evidence for a distal retinal locus. *J. opt. Soc. Am*. **68,** 1915.

Alexander, K.R. and Fishman, G.A. (1984). Rod-cone interaction in flicker perimetry. *Br J Ophthal*. **68**, 303-309.

Alexander, K.R. and Fishman, G.A. (1985). Rod-cone interaction in flicker perimetry: evidence for a distil retinal locus. *Doc. Ophthalmol*. **60**, 3-36

Alexander, L.J. (1990). Macular photostress recovery test. In *Primary care of the posterior segment*. (ed. L. J. Alexander), Appelton and Lange, Norwalk, Connecticut, pp.17-18.

Alpern, M., Rushton, W.H.A. and Torii, S. (1970). The attenuation of rod signals by bleachings. *J. Physiol*. **207**, 449-461.

Altman, D.G. (1991). *Practical statistics for medical research*. Chapman and Hall, London.

Arden, G.B. and Hogg, C.R. (1985). Rod-cone interactions and analysis of retinal disease. *Br. J. Ophthalmol*. **69,** 404-415.

Arden, G.B. and Weale, R.A. (1954). Nervous mechanisms and dark adaptation. *J. Physiol*. **125,** 417-426.

Baker, H.D. and Donovan, W.J. (1982). Early dark adaptation, the receptor potential and lateral effects on the retina. *Vision Res*. **22,** 645-651.

Baker, H.D. and Rushton, W.A.H. (1965). The red-sensitivie pigment in normal cones. *J. Physiol. Lond*. **176**, 56-72.

Barbur, J.L. (1995). Personal communication.

Barlow, H.B. (1958b). Intrinsic noise of cones. In *Visual Problems of Colour Vol II*. H. M. Stationary Office, London. pp. 617-630.

Barlow, H.B. (1965). Optic nerve impulses and Weber's law. *Cold Spring Harb. Symp. quant. Biol*. **30,** 539-546.

Barlow, H.B. (1972). Dark and light adaptation: Psychophysics. In *Handbook of sensory physiology Vol VII/4.* (ed. D. Jameson. and L.M. Hurvich). Springer-Verlag, Berlin, pp. 1-28.

Barlow, H.B. and Andrews, D.S. (1967). Sensitivity of receptors and receptor "pools". *J. opt. Soc. Am.* **57,** 837-838.

Barlow, H.B. and Levick, W.R. (1969). Three factors limiting the reliable detection of light by retinal ganglion cells of the cat. *J. Physiol.* **200,** 1-24.

Battersby, W. and Wagman, I. (1962). Neural limits of visual excitability. IV. Spatial determinants of retrochiasmal interaction. *Am. J. Physiol.* **203,** 359-365.

Baylor, D.A. and Hodgkin, A.L. (1974). Changes in time scale and sensitivity in turtle photoreceptors. *J. Physiol.* **242,** 729-758.

Baylor, D.A., Matthews, G. and Yau, K.W. (1980). Two components of electrical dark noise in toad retinal rod outer segments. *J Physiol.* **309,** 561-591.

Baylor, D.A., Nunn, B.J. and Schnapf, J.L. (1984). The photocurrent, noise and spectral sensitivity of rods of the monkey Macaca Fascicularis. *J. Physiol.* **357,** 575-607.

Bergman, H., Borg, S., Hogman, B., Larsson, H. and Tengroth, B. (1979). The effects of oxazepam on ocular readaptation time. *Acta. Ophthal.* **57**, 145-150.

Bergman, H., Borg, S., Hogman, B., Larsson, H. and Tengroth, B. (1980). The effects of melperon on ocular readaptation time assessed by a new recording technique. *Acta. Ophthal.* **57**, 145-150.

Blackwell, H.R. (1946). Contrast thresholds of the human eye. *J. Opt. Soc. Am.* **55,** 624-643.

Blakemore, C.B. and Rushton, W.A.H. (1965a). Dark adaptation and increment threshold in a rod monochromat. *J. Physiol.* **181,** 612-628.

Blakemore, C.B. and Rushton, W.A.H. (1965b). The rod increment threshold during dark adaptation in normal and rod monochromat. *J. Physiol.* **181,** 629-640.

Bland, J.M. and Altman, D.G. (1986). Statistical methods for assessing agreement between two methods of clinical measurement. *Lancet*, **i**, 307-310.

Blanks, J.C. (1989). Morphology of the retina. In *Retina. volume 1 - Basic science and inherited retinal disease.* (ed. S.J.Ryan, T.E. Ogden and A.P. Schachat), The C.V. Mosby Company, St Louis, Baltimore, pp. 37-52.

Boycott, B.B. and Wassle, H. (1974). The morphological types of ganglion cells of the domestic cat's retina. *J. Physiol.* **240,** 397-419.

Boynton, R.M. and Whitten, D.N. (1970). Visual adaptation in monkey cones: recordings of late receptor potentials. *Science,* **170**, 1423-1426.

Brown, A.M. (1983). Dark adaptation of the long-wavelength sensitive cones. *Vision Res.* **23**, 837-843.

Brown, J.L., Graham, C.H., Leibowitz, H. and Ranken, H.B. (1953). Luminance thresholds for the resolution of visual detail during dark adaptation. *J. Opt. Soc. Am.* **43**, 197-202.

Brown, J.L., Metz, J.W. and Yohman, J.R. (1969). Test of scotopic suppression of the photopic process. *J. opt. Soc. Am.* **59,** 1677-1678.

Burkhardt, D.T. (1995). The influence of center-surround antogonism on light adaptation in cones in the retina of the turtle. *Visual Neuroscience*, **12**, 877-885.

Campbell, F.W. and Gurbisch, R.W. (1966). Optical quality of the human eye. *Journal of Physiology*. **187,** 437-445.

Campbell, F.W. and Robson, J.G. (1968). Application of Fourier analysis to the visability of gratings. *J. Physiol.* **197**, 551-566.

Campbell, F.W. and Rushton, W.A.H. (1955). Measurement of scotopic pigments in the living human eye. *J. Physiol.* **130,** 131-147.

Carr, R.E., Henkind, P., Rothfield, N. and Siegel, I. M. (1968). Ocular toxicity of antimalerial drugs. *Am. J. Ophthalmol.* **66**, 738-744.

Chilaris, G.A. (1962). Recovery time after macular illumination. *Am. J. Ophthalmol.* **53**, 311-314.

Cicerone, C.M. and Hayhoe, M.M. (1990). The size of the pool for bleaching adaptation in human rod vision. *Vision Res.* **30**, 693-697.

Cicerone, C.M., Hayhoe, M.M .and MacLeod, D.I.A. (1990). The spread of adaptation in human foveal and parafoveal cone vision. *Vision Res.* **30**, 1603-1615.

Coile, D.C. and Baker, H.D. (1992). Foveal dark adaptation, photopigment regeneration, and aging. *Visual Neuroscience,* **8**, 27-39.

Coletta, N.J. and Adams, A.J. (1984). Rod-cone interactions in flicker detection. *Vision Res.* **24**, 1333-1340.

Coletta, N.J. and Adams, A.J. (1985). Loss of flicker sensitivity on dim backgrounds in normal and dichromatic observers. *Invest. Ophthal. Visual Sci. Suppl.* **26**, 187.

Coletta, N.J., Schefrin, B.E. and Adams, A.J. (1986). Rod adaptation influences cone spatial resolution. *Invest. Ophthal. Visual Sci. Suppl.* **27**, 71.

Collins, M. (1989). The onset of prolonged glare recovery with age. *Ophthal. Physiol. Opt.* **9**, 368-371.

Collins, M. and Brown, B. (1989a). Glare recovery and age related maculopathy. *Clin. Vision Sci.* **4**, 145-153.

Collins, M. and Brown, B. (1989b). Glare recovery and its relation to other clinical findings in age related maculopathy. *Clin. Vision. Sci.* **4**, 155-163.

Coolen, C.C. and van Norren, D. (1988). Kinetics of human cone photopigments explained with a Rushton-Henry model. *Biol. Cybern.* **58**, 123-128.

Cornwall, M.C. and Fain, G.L. (1994). Bleached pigment activates transduction in isolated rods of the salamander retina. *J. Physiol.* **480**, 261-279.

Corson, D.W., Cornwall, M.C., MacNichol, E.F., Jin, J..Johnson, R., Derguini, F., Crouch, R.K., and Nakanishi, K. (1990). Sensitization of bleached rod photoreceptors by 11-cis-locked analogues of retinal. *Proc. Natl. Acad. Sci.* USA. **87**, 6823-6827.

Craik, K.J.W. and Vernon, M.D. (1941). The nature of dark adaptation. *Brit. J. Psychol.* **32**, 62-81.

Crawford, B.H. (1937). The change of visual sensitivity with time. *Proc. R. Soc. Lond.* B. **123**, 69-89.

Crawford. B.H. (1947). Visual adaptation in relation to brief conditioning stimuli. *Proc. R. Soc. Lond. B.* **134**, 283-302.

Croner, L.J. and Kaplan, E. (1995). Receptive fields of P and M Ganglion cells across the primate retina. *Vision Res.* **35,** 7-24.

Curcio, C.A. and Sloan, K.R. (1992). Packing geometry of human cone photoreceptors: Variation with eccentricity and evidence of local anisotropy. *Visual Neuroscience.* **9**, 169-180.

Curico, C.A., Sloan, K.R., Packer, O., Hendrickson, A.E. and Kalina, R.E. (1987). Distribution of cones in human and monkey retina: individual variability and radial asymetry. *Science.* **23**, 579-582.

Daitch, J.M. and Green, D.G. (1969). Contrast sensitivity of the human peripheral retina. *Vision Res.* **9**, 947-952.

Das, S.R., Bhardwaj, N., Kjeldby, H. and Gouras, P. (1992). Muller cells of chicken retina synthesize 11-cis retinol. *Biochemical Journal.* **285,** 907-913.

Dawis, S.M. and Purple, R. (1982). Adaptation in cones: a general model. *Biophys J.* **39,** 151-155.

Derefeld, F.D., Lennerstrand, G. and Lundh, B. (1979). Age variations in normal human contrast sensitivity. *Acta. Ophthal.* **57,** 679-690.

Derrington, A.M. and Lennie, P. (1984). Spatial and temporal contrast sensitivities of neurones in lateral geniculate nucleus of macaque. *J. Physiol.* **357,** 219-240.

Dowling, J.E. (1960). Chemistry of visual adaptation in the rat. *Nature (Lond.)* **188**, 114-118.

Dowling, J.E. (1987). *The retina an approachable part of the brain*. The Belknap Press of Harvard University Press, Massachusetts.

Dressler, M. and Rassow, B. (1981). Neural contrast sensitivity measurements with a laser interference system for clinical screening application. *Invest. Ophthalmol. visual Sci.* **21**, 737-744.

Eisner, A. (1987). Comparisons across age of selected visual functions. *Documenta Ophthalmologica Proceedings Series*. **46**, 99-109.

Enroth-Cugell, C. and Lennie, P. (1975). The control of retinal ganglion cell discharge by receptive field surrounds. *J. Physiol.* **247**, 551-578.

Enroth-Cugell, C. and Robson, J.G. (1966). The contrast sensitivity of retinal ganglion cells of the cat. *J. Physiol.* **233,** 271-309.

Enroth-Cugell, C., Hertz, B.G. and Lennie, P. (1977b). Convergence of rod and cone signals in the cat's retina. *J. Physiol.* **269**, 297-318.

Eysteinsson, T. and Frumkes, T.E. (1989). Physiological and Pharmologic Analysis of Suppressive Rod-Cone in Necturus Retina. *J. Neurophysiology*. **61**, 866-877.

Fain, G.L. (1976). Sensitivity of toad rods: dependance on wavelength and background illumination. *J. Physiol.* **261,** 71-101.

Fain, G.L. and Cornwall, M.C. (1993). Light and dark adaptation in vertebrate photoreceptors. In *Contrast sensitivity: from receptors to clinic*, (ed. R. Shapley and D.K. Lam), MIT Press, Boston, MA, USA, pp 3-32.

Fingeret, M., Casser, L. and Woodcome, H.T. (1990). Photostress recovery test. In *Atlas of primary eyecare procedures* (ed. M. Fingeret, L. Casser and H.T. Woodcome), Appelton and Lange, Norwalk, Connecticut, pp. 222-223.

Frishman, L.J. and Sieving, P.A. (1995). Evidence for 2 sites of adaptation affecting the dark-adapted ERG of cats and primates. *Vision Research*. **35**, 435-442.

Frishman, L.J., Reddy, M.G. and Robson, J.G. (1996). Effects of background light on the human dark-adapted electroretinogram and psychophysical threshold. *Journal of the Optical Society of America A-Optics Inage Science and Vision*, **13**, 601-612.

Frumkes, T.E. (1989). Suppressive rod-cone interaction. In *Principals and practice of clinical electrophysiology of vision*. (ed. G.B. Arden and J.R. Heckenlively), Mosby, St. Louis, pp. 469-474.

Frumkes, T.E. (1990). Classical and modern psychophysical studies of dark and light adaptation and their relationship to underlying retinal function. In *The Science of Vision*. (ed. K.N. Leibovic), Springer Verlag, New York, pp. 172-210.

Frumkes, T.E. and Eysteinsson, T. (1988). The cellular basis for suppressive rod-cone interaction. *Visual Neuroscience*. **1**, 263-273.

Frumkes, T.E. Naarendorp, F. Goldberg, S.H. (1988). Abnormalities in retinal neurocircuitary in protanopes: evidence provided by psychophysical investigation of temporal-spatial interactions. *Invest. Ophthal. Visual Sci. Suppl.* **29**, 163.

Frumkes, T.E., Lange, G., Naarendorp, F and Eysteinsson, T. (1995). Suppressive rod-cone interactions: underlying mechanisms and practical application. In *Colour Vision Deficiencies XII* (ed. B. Drum), Kluwer Academic Publishers, Dordrecht, pp. 329-334.

Geisler, W.S. (1979). Evidence for the equivalent background hypothesis in cones. *Vision Res.* **19**, 799-805.

Geisler, W.S. (1980). Comments on the testing of two prominent dark-adaptation hypotheses. *Vision Res.* **20**, 807-811.

Geisler, W.S. (1981). Effects of bleaching and backgrounds on the flash response of the cone system. *J. Physiol.* **312**, 413-434.

Geisler, W.S. (1983). Mechanisms of visual sensitivity: backgrounds and early dark adaptation. *Vision Res.* **23**, 1423-1432.

Ginsburg, A.P. and Cannon, M.W. (1983). Comparison of three methods for rapid determination of threshold contrast sensitivity. *Invest. Ophthalmol. and Visual Sci.* **24**, 798-800.

Glaser, J.S., Savino, P.J., Sumers, K.D., McDonald, S.A. and Knighton, R.W. (1977). The photostress recovery test in the clinical assessment of visual function. *Am. J. Ophthalmol.* **83**, 255-260.

Goldberg, S.H. and Frumkes, T.E. (1983). A distal retinal locus for rod-cone interaction? *Invest. Ophthal. visual Sci. Suppl.* **24,** 187.

Goldberg, S.H., Frumkes, T.E. and Naygaard, R.W. (1983). Inhibitory influence of unstimulated rods in the human retina: evidence provided by examining cone flicker. *Science*, N.Y. **221**, 180-182.

Granit, R. (1947). *Sensory mechanisms of the retina*. Oxford University Press, London.

Green, D. (1986). The search for the site of visual adaptation. *Vision Res.* **26,** 1417-1429.

Green, D.G., Dowling, J.E., Siegel, I.M. and Ripps, H. (1975). Retinal mechanisms of visual adaptaiton in the skate. *The J. Gen. Physiol.* **65**, 483-502.

Guyer, D.R., Schachat, A.P. and Green, W.R. (1989). The choroid: structural considerations. In *Retina. volume 1 - Basic science and inherited retinal disease*, (ed. S.J. Ryan, T.E. Ogden and A.P. Schachat), The C.V. Mosby Company, St Louis, Baltimore, pp. 17-31.

Hahn, L.W. and Geisler, W.S. (1991). Contrast sensitivity functions measured during dark adaptation and on steady backgrounds. *Optical Soc. Am. Annual Meeting Technical Digest*, **17,** 164.

Hahn, L.W. and Geisler, W.S. (1995). Adaptation mechanisms in spatial vision I: bleaches and backgrounds. *Vision Res.* **35**, 1585-1594.

Hartline, H.K. (1938). The response of single optic nerve fibres of the vertebrate eye to illumination of the retina. *Am. J. Physiol.* **121**, 400-415.

Hayhoe, M.M, Benimoff, N.J. and Hood, D.C. (1987). The time-course of multiplicative and subtractive adaptation process. *Vision Res.* **27**, 1981-1996.

Hayhoe, M.M, Levin, M.E. and Koshel, R.J. (1992). Subtractive processes in light adaptation. *Vision Res.* **32**, 323-333.

Hayhoe, M.M. (1979). Lateral interactions in human cone adaptation. *J. Physiology.* **296**, 125-140.

Hayhoe, M.M. and Chen, B. (1986). Temporal modulation sensitivity in cone dark-adaptation. *Vision Res.* **26**, 1715-1725.

Hayhoe, M.M. and Smith, M.V. (1989). The role of spatial filtering in sensitivity regulation. *Vision Res.* **29**, 457-469.

Hecht, S. (1924). The visual discrimination of intensity and the Weber-Fechner Law. *J. gen. Physiol.* **7,** 235-267.

Hecht, S. (1937). Rods, cones, and the chemical basis of vision. *Physiol. Rev.* **17**, 239-290.

Hecht, S., Haig, C., and Chase, A. (1937). The influence of light adaptation on subsequent dark adaptation of the eye. *J. Gen. Physiol.* **20**, 831-850

Hess, R.F. (1990). Rod-mediated vision: role of post receptoral filters. In *Night Vision*, (ed. R.F. Hess, L.T. Sharpe. and K. Nordby), Cambridge University Press, Cambridge, pp. 3-48.

Hess, R.F. and Nordby, K. (1986). Spatial and temporal limits of vision in the achromat. *J. Physiol.* **371**, 365-385.

Hollins, M. and Alpern, M. (1973). Dark adaptation and visual pigment regeneration in human cones. *J. Gen. Physiol.* **62**, 430-447.

Hubel, D.H. (1988). *Eye, brain, and vision*. Scientific American Library, New York.

Jin, J., Jones, G.J. and Cornwall, M.C. (1994). Movement of retinal along cone and rod photoreceptors. *Visual Neuroscience.* **11**, 389-399.

Kanski, J.J.(1994) *Clinical ophthalmology a systematic approach, third edition*, Butterworth-Heinemann Ltd, London.

Kaplan E. and Shapley R.M. (1986). The primate retina contains two types of ganglion cells, with high and low contrast sensitivity. *Proc. Natl. Acad. Sci.* **83,** 2755-2757.

Kelly, D.H. (1972). Adaptation effects on spatio-temporal sine-wave thresholds. *Vision Res.* Vol. **12,** 89-101.

Kitterle, F.L. and Leguire, L.E. (1975). The effects of borders and contours on threshold during early dark adaptation. *Vision Res.* **15**, 1217-1224.

Kolb, H. (1994). The architecture of functional neural circuits in the vertebrate retina. *Invest. Ophthalmol. Visual Sci.* **35**, 2385-2404.

Kolb, H. and Famiglietti, Jr. E.V. (1976). Rod and cone pathways in the retina of the cat. *Investigative Ophthalmology* **15**, 935-946.

Kolb, H., Linberg, K.A. and Fisher, S.K. (1992). Neurones of the human retina: a golgi study. *The Journal of Comparitive Neurology*. **318**, 147-187.

Kuffler S. W. (1953). Discharge patterns and functional organization of mamalian retina. *J. Neurophysiol.* **16,** 37-68.

Lamb, T.D. (1980). Spontaneous quantal events induced in toad rods by pigment bleaching. *Nature* **287**, 349-351.

Lamb, T.D. (1981). The involvement of rod photoreceptors in dark adaptation. *Vision Res.* **21**, 1773-1782.

Lamb, T.D. (1990). Dark adaptation: a re-examination. In *Night Vision* (ed. R.F. Hess, L.T. Sharpe. and K. Nordby), Cambridge University Press, Cambridge, pp.177-222.

Lange, G. and Frumkes, T.E. (1992). Influence of rod-light adaptation upon the visibility of displays modulated concurrently in the temporal and spatial domains. *Invest. Ophthal. Visual Sci. Suppl.* **35**, 1261.

Lange, G. and Frumkes, T.E. (1993). Separate spatial and temporal forms of suppressive rod-cone interaction (SRCI). *Invest. Ophthalmol. Vis. Sci. Suppl.* **34**, 818.

Lansford, T.G. and Baker, H.D. (1969). Dark adaptation: An interocular light adaptation effect. *Science*. **164**, 1307-1309.

Linberg, K.A. and Fisher, S.K. (1986). An ultrastructural study of interplexiform cell synapses in the human retina. *The Journal of Comparative Neurology*, **243**, 561-576.

Lovasik, J.V. (1983). An electrophysiological investigation of the macular photostress test. *Invest. Ophthalmol. Visual Sci.* **24**, 437-441.

Makous, W. (1990). Absolute sensitivity. In *Night Vision* (ed. R.F. Hess, L.T. Sharpe. and K. Nordby), Cambridge University Press, Cambridge, pp.146-176.

Margrain, T.H. and Thomson, W.D. (1994). Recovery of CSF following exposure to bright lights. *Invest. Ophthalmol. Visual Sci. Suppl.* **35**, 1371.

Margrain, T.H. and Thomson, W.D. (1997). Recovery of spatial vision during dark adaptation in normal subjects. *Ophthal. Physiol. Opt.* **17**, 509-515.

Matthews, J.N.S., Altman, D.G., Campbell, M.J. and Royston, J.P. (1990). Analysis of serial measurements in medical research. *Br. Med. J.* **300,** 230-235.

McDonnell, J.M. (1989). Ocular embryology and anatomy. In *Retina. volume 1 - Basic science and inherited retinal disease* (ed. S.J.Ryan, T.E. Ogden. and A.P. Schachat), The C.V. Mosby Company, St Louis, Baltimore.

Merigan, W.H. and Maunsell, J.H.R. (1990). Macaque vision after magnocellular lateral geniculate lesions. *Visual Neuroscience.* **5**, 347-352.

Miller, R.F. (1989). The physiology and morphology of the vertebrate retina. In *Retina. volume 1 - Basic science and inherited retinal disease* (ed. S.J.Ryan, T.E. Ogden. and A.P. Schachat), The C.V. Mosby Company, St Louis, Baltimore, pp. 83-108.

Naarendorp, F. (1987). The effects of long term and short term adaptation on cone-mediated spatial vision. PhD thesis: The City University of New York, Graduate Faculty in Psychology.

Naarendorp, F., Denny, N. and Frumkes, T.E. (1988). Rod light and dark adaptation influence cone-mediated spatial acuity. *Vision Res.* **28**, 67-74.

Natsikos, J.V. and Dean Hart, J.C. (1980). Photostress recovery times in cases of serous retinopathy. *J. R. Soc. Med.* **73**, 793-797.

Nelson, R. (1977). Cat cones have rod input: a comparison of the response properties of cones and horozontal cell bodies in th eretina of the cat. *J. Comp. Neurol.* **172**, 109-136.

Norman, R.A. and Werblin, F.S. (1974). Control of retinal sensitivity. *The J Gen. Physiol.* **63**, 37-61.

Normann, R.A. and Perlman, I. (1990). Background and bleaching adaptation in luminosity type horozontal cells in the isolated turtle retina. *Journal of Physiology.* **421**, 321-341.

Ogden, T.E. (1989). Topography of the retina. In *Retina. volume 1 - Basic science and inherited retinal disease* (ed. S.J.Ryan, T.E. Ogden. and A.P. Schachat), The C.V. Mosby Company, St Louis, Baltimore, pp. 31-36.

Owsley, C. and Sloane, M.E. (1987). Contrast sensitivity, acuity, and the perception of real-world targets. *Br. J. Ophthalmol.* **71.** 791-796.

Owsley, C., Sekuler, R. and Siemsen, D. (1983). Contrast sensitivity throughout adulthood. *Vision Res.* **23,** 689-699.

Palczewski, K. (1994). Is vertebrate phototransduction solved? new insights into the molecular mechanism of phototransduction. *Invest. Ophthalmol. Visual Sci.* **35**, 3577-3581.

Pugh, E.N. (1975). Rushtons paradox: rod dark adaptation after flash photolysis. *J. Physiol* **248**, 413-431.

Pugh, E.N.Jr. and Lamb, T.D. (1990). Cyclic GMP and Calcium: the internal messengers of excitation and adaptation in vertebrate photoreceptors. *Vision Res.* **30**, 1923-1948.

Purpura, K., Kaplan, E. and Shapley, R.M. (1988). Background light and the contrast gain of primate P and M retinal ganglion cells. *Proc. Natl. Acad. Sci.* **85,** 4534-4537.

Purpura, K., Tranchina, D., Kaplan, E. and Shapley, R.M. (1990). Light adaptation in the primate retina: analysis of changes in gain and dynamics of monkey retinal ganglion cells. *Vis. Neurisci.* **4**, 75-93.

Rodieck R. (1965). Quantitative analysis of cat retinal ganglion cell response to visual stimuli. *Vision Res.* **5,** 583-601.

Rose, A. (1948). The sensitivity performance of the human eye on an absolute scale. *J. opt Soc. Am.* **38**, 196-208.

Rovamo J., Virsu, V. and Nasanen R. (1978). Cortical magnification factor predicts the photopic contrast sensitivity of peripheral vision. *Nature (London)* **27,** 54-56.

Rovamo, J and Virsu, V (1979). An estimation and application of the human cortical magnification factor. *Experimental Brain Res.* **37**, 495-510.

Rushton, W.A.H. (1957). Physical measurement of cone pigments in the living human eye. *Nature (Lond.)* **179**, 571-573.

Rushton, W.A.H. (1961b). Rhodopsin meaasurement and dark adaptation in a subject deficient in cone vision. *J. Physiol.* **156**, 193-205.

Rushton, W.A.H. (1965). The Ferrier Lecture, 1962. Visual Adaptation. Proc. *R. Soc. Lond.* B **162,** 20-46.

Rushton, W.A.H. (1972). Light and dark adaptation. *Invest. Ophthalmol.* **11**, 503-517.

Rushton, W.A.H. and Henry, G.H. (1968). Bleaching and regeneration of cone photopigments in man. *Vision Research.* **8**, 617-631.

Rushton, W.A.H. and Powell, D.S. (1972). The early phase of dark adaptation. *Vision Res.* **12**, 1083-1093.

Ruskell, G. (1988). Neurology of visual perception. In *Optometry* (ed. K. Edwards and R. Llewellyn), Butterworths, London, pp 3-24.

Ryan, M.K. and Hendrickson, A.E. (1987). Interplexiform cells in macaque monkey retina. *Exp. Eye Res.* **45**, 57-66.

Saari, J.C. (1990). Enzymes and proteins of the mammalian visual cycle. In *Progress in Retinal Research* (ed. N. Osborne and J. Chandler), Permagon Press, Oxford, pp. 363-381.

Schiller, P.H., Logothetis, N.K., and Charles, E.R. (1990). Functions of the colour-opponent and broad-band channels of the visual system. *Nature* **343,** 68-70.

Schnapf, J.L. and Baylor, D.A. (1987). How photoreceptor cells respond to light. *Scientific American*. **256**, 40-47.

Schneeweis, D.M. and Schnapf, J.L. (1995). Photovoltage of rods and cones in the macaque retina. *Science*. **268**, 1053-1056.

Severin, S.L. (1980). Qualitative photostress testing for the diagnosis of cystoid macular oedema. *Am. Intra-Ocular Implant Soc.* J. **6**, 25-27.

Severin, S.L., Tour, R.L. and Kershaw, R.H. (1967a). Macular function and the photostress test 1. *Arch Ophthalmol*. **77**, 2-7.

Severin, S.L., Tour, R.L. and Kershaw, R.H. (1967b). Macular function and the photostress test 2. *Arch Ophthalmol*. **77**, 163-167.

Shapley, R. (1991). Neural mechanisms of contrast sensitivity. In *Spatial vision* (ed. D.M. Regan), MacMillan, London, pp. 290-305.

Shapley, R. and Enroth-Cugell, C. (1984). Visual adaptation and retinal gain controls. In *Progress in Retinal Research Vol 3* (ed. N. Osborne and G. Chandler), Permagon, Oxford, pp. 263-346.

Shapley, R., Kaplan, E. and Purpura, K. (1993). Contrast sensitivity and light adaptation in photoreceptors or in the retinal network. In *Contrast sensitivity: from receptors to clinic*. (ed. R. Shapley and D.K. Lam), MIT Press, Boston, MA, pp. 103-3116.

Sharpe, L.T. (1990). The light-adaptation of the human rod visual system. In *Night vision basic, clinical and applied aspects*. (ed. R.F. Hess, L.T. Sharpe and K. Nordby), Cambridge University Press, Cambridge, pp. 49-124.

Sharpe, L.T. and Nordby, K. (1990). The photoreceptors in the achromat. In *Night vision basic, clinical and applied aspects*. (ed. R.F. Hess, L.T. Sharpe and K. Nordby), Cambridge University Press, Cambridge, pp 335-389.

Sharpe, L.T., Stockman, A., Fach, C.C. and Marksthler, U. (1993). Temporal and spatial summation in the human rod visual-system. *J. Physiol*. **463**, 325-348.

Sloan, P.G. (1968). Clinical application of the photostress test. *Am. J. Optometry and Arch. Am. Academy of Optometry*. 617-623.

Smith, V.C., Pokorny, J. and van Norren, D. (1983). Densitometric measurement of human cone photopigment kinetics. *Vision Res*. **23**, 517-524.

Smith, V.C., Porknoy, J. and van Norren, D.K. (1983). Densitometric measurement of human cone photopigment kinetics. *Vision Res.* **23**, 517-534.

Sneyd, J. and Tranchnia, D. (1989). Phototransduction in cones: and inverse problem in enzyme kinetics. *Bull. Math. Biol.* **51**, 749-784.

Stabell, B. and Stabell, U. (1993). Rod-cone interaction in form detection. *Vision Res.* **33**, 195-201.

Stiles, W.S. and Crawford, B.H. (1932). Equivalent adaptation levels in localized retinal areas. In *Report of a joint discussion on vision,* Physical Society of London, Cambridge University Press, Cambridge, pp. 194-211.

Stockman, A., Sharpe, T.L., Ruther, K. and Nordby, K. (1995). 2 signals in the human rod visual-system - A model-based on electrophysiological data. *Visual Neuroscience.* **12**, 951-970.

Stone, J. and Hoffman, K.P. (1972). Very slow-conducting ganglion cells in the cat's retina: a major, new functional type? *Brain Res.* **43**, 610-616.

Tamura, T., Nakatani, K. and Yau, K.W. (1989). Light adaptation in cat retinal rods. *Science.* **245,** 755-758.

Valeton, M.J. and van Norren, D. (1983). Light adaptation of primate cones: an analysis based on extra cellular data. *Vision Res.* **23,** 1539-1547.

van Nes, F.L. and Bouman, M.A. (1967). Spatial modulation transfer in the human eye *J. opt. Soc. Am.* **57**, 401-406.

Verweij, J. (1996). *Synaptic interactions in the outer retina of goldfish.* PhD thesis: University of Amsterdam, Laboratory of Medical Physics.

Virsu, V. (1974). Dark adaptation shifts apparent spatial frequency. *Vision Res.* **14**, 433-435.

Walraven, J., Enroth-Cugell, C., Hood, D.C., MacLeod, D.I.A. and Schnapf, J.L. (1990). The control of visual sensitivity receptoral and post receptoral processes. In *Visual perception the neurophysiological foundations*, (ed. L. Spillmann. and J.S. Werner), Academic Press Inc, San Diego, California, pp. 53-102.

Weale, R.A. (1992). *The senescence of human vision*, Oxford University Press, Oxford.

Werblin, S.F. (1974). The control of sensitivity in the retina. Sci. Amer. **228**, 70-79.

Westheimer, G. (1966). The maxwellian view. *Vision Res.* **6**, 669-682.

Whittle, P. and Challands, P.D.C. (1969). The effect of background luminance on the brightness of flashes. *Vision Res.* **9**, 1095-1110.

Wilson, H.R., Levi, D., Lamberto, M., Rovamo, J. and DeValois, R. (1990). The perception of form: Retina to striate cortex. In *Visual perception the neurophysiological*

foundations, (ed. L. Spillmann. and J.S. Werner), Academic Press Inc., San Diego, California, pp. 231-272.

Witovsky, P. and Dearry, A. (1992). Functional roles of dopamine in the vertebrate retina. In *Progress in Retinal Research Vol 11*, Permagon Press, Oxford, pp 247-292.

Woods, R.L. and Thomson, W.D. (1993). A comparison of psychometric methods for measuring the contrast sensitivity of experienced observers. *Clinical Vision Sciences*. **8**, 401-415.

Wyszecki, G. and Stiles, W.S. (1982). *Colour Science: Concepts and Methods, Quantitative data and formulas, second edition,* Wiley, New York.

Yau, K.W. (1994). Phototransduction mechanism in retinal rods and cones. *Invest. Ophthalmol. Visual Sci*. **35**, 9-32.

Zabriskie, N.A. and Kardon, R.H. (1994). The pupil photostress test. *Ophthalmology,* **101**, 1122-1130.

Zeki, S. (1993). *A vision of the brain*. Blackwell Scientific Publications, Oxford.

Bibliography

Alexander, K. R. and Kelly, S.A. (1984) The influence of cones on rod saturation with flashed backgrounds. Vision Res. 24, 507-511.

Arden, G.B. and Hogg, C.R. (1985). A new cause for difficulty in seeing at night. *Documenta Ophthalmologica*. **60**, 121-125.

Arnold, K. and Anstis, S. (1993). Properties of the visual channels that underlie adaptation to gradual change of luminance. *Vision Res*. **33**, 47-54.

Bauer, G.M., Frumkes, T.E. and Holstein, G.R. (1983). The influence of rod light and dark adaptation upon rod-cone interaction. *J. Physiol*. **337**, 121-135.

Brown, B. and Kitchin, J.L. (1983). Dark adaptation and the acuity/luminance response in senile macular degeneration (SMD). A*m. J. Optom. and Physiol. Optics*. **60**, 645-650.

Buck, S.L. (1985). Cone-rod interaction over time and space. *Vision Res*. **25**, 907-916.

Burns, S.A., Elsner, A.E., Lobes,L.A. and Doft, B. H. (1987). A psychophysical technique for measuring cone photopigment bleaching. *Invest. Ophthalmol. Vis. Sci*. **28**, 711-717.

Coile, D.C. (1989). Foveal dark adaptation, photopigment regeneration, and aging. PhD thesis, The Florida State University.

Djamgoz, M.B.A. and Wagner, H.J. (1992). Localization and function of dopamine in the adult vertebrate retina. *Neurochem Int*. **20**, 139-191.

Drum, B. (1982). Summation of rod and cone responses at absolute threshold. *Vision. Res*. **22**, 823-826.

Eisner, A. (1989). Losses of foveal flicker sensitivity during dark adaptation following extended bleaches. *Vision Res*. **29**, 1401-1423.

Eisner, A. (1992). Losses of flicker sensitivity during dark adaptation: effects of test size and wavelength. *Vision Res*. **32**, 1975-1986.

Elliot, D. B. and Bullimore, M.A. (1993). Assessing the reliability, discriminative ability, and validity of disability glare tests. *Invest. Ophthalmol. and Visual Sci*. **34**, 108-119.

Fitzke, F.W., Holden, A.L. and Sheen, F.H. (1985). A maxwellian-view optometer suitable for electrophysiological and psychophysical research. *Vision Res*. **25**, 871-874.

Frumkes, T.E. and Wu, S.M. (1990). Independant influences of rod adaptation on cone-mediated responses to light onset and offset in distil retinal neurones. *J. Neurophysiology*. **64**, 1043-1054.

Frumkes, T.E., Lange, G., Denny, N. and Beczkowska, I. (1992). Influence of rod adaptation upon cone responses to light offset in humans:I. Results in normal observers. *Visual Neuroscience*. **8**, 83-89.

Frumkes, T.E., Lembessis, E.,Vollaro, J., Moshe, D. and Eysteinsson, T. (1995). Influence of rod-adaptation upon chromatic and achromatic cone-vision. Unpublished manuscript.

Gardner, M.J. and Altman, D.G. (1986). Confidence intervals rather than P values: estimation rather than hypothesis testing. *British Medical Journal*. **292**, 746-750.

Gilchrist, J. (1988). The psychology of vision. In *Optometry*, (ed. K. Edwards and R. Llewellyn), Butterworths, London, pp. 25-43.

Graham, N. and Hood, D.C. (1992). Modeling the dynamics of light adaptation: the merging of two traditions. *Vision Res*. **32**, 1373-1393.

Graham, N. (1972). Spatial frequency channels in the human visual system:effects of luminance and pattern drift rate. *Vision Res*. **12,** 53-68.

Hahn, L.W. and Geisler, W.S. (1995). Local light-adaptation mechanisms in grating detection. Unpublished manuscript.

Hayhoe, M.M, Benimoff, N.J. and Hood, D.C. (1987). The time-course of multiplicative and subtractive adaptation process. *Vision Res*. **27**, 1981-1996.

Hayhoe, M.M. (1990). Spatial interactions and models of adaptation. *Vision Res*. **20**, 957-965.

Hess, R.F. and Howell, E.R. (1988). Detection of low spatial frequencies: a single filter of multiple filters. *Ophthal. Physiol. Opt*. **8**, 378-385.

Hess, R.F., Mullen, K.T. and Nordby, K. (1992). Mutual rod-cone suppression within the central visual field. *Ophthal. Physiol. Opt.* **12**,183-188.

Hinrichs, C.S., Newsome, D.A. and Blacharski, P.A. (1992). New macular photostress device indicates recovery time differences with and without macular edema and between drusen and macular degeneration. *Invest. Ophthalmol. Visual Sci. Suppl*. **35**, 724.

Jenness, J.W. (1992). Blough's effect measured in humans: a rise in the cone-mediated detection threshold during dark adaptation. PhD thesis, The University of Michigan.

Kaufman, D.A. (1991). The luminance dependance of spatiotemporal response of cat area 17 and area 18 units. PhD thesis. University of Pensylvania.

Lange, G. and Frumkes, T.E. (1992). Influence of rod adaptation upon cone responses to light offset in humans: II. results in an observer with exaggerated suppressive rod-cone interaction. *Visual Neuroscience*. **8**, 91-95.

Le Grand, Y. (1957). Retinal illumination. In *Light, colour and vision*. Chapman and Hall, London.

Lie, I. (1969). Dark adaptation and the photochromatic interval. *Doc. Ophthalmol.* **17**, 411-510.

Logothesis, N.K., Schiller, P.H., Charles, E.R. and Hurlbert, A.C. (1990). Perceptual deficits and the activity of the colour-opponent and broad band pathways at isoluminance. *Science*. **247**, 214-217.

Lorenceau, J. (1987). Recovery from contrast adaptation: effects of spatial and temporal frequency. *Vision Res*. **27**, 2185-2191.

MacLeod, D.I.A. (1978). Visual sensitivity. *Ann. Rev. Psychol.* **29**, 613-645.

Miller, W.H. (1990). Dark mimic. *Invest. Ophthalmol. Visual Sci.* **31**, 1664-1673.

Mollon, J.D. and Bowmaker, J.K. (1992). The spatial arrangement of cones in the primate fovea. *Nature*. **360**, 677-679.

Mustonen, J., Rovamo, J. and Näsänen, R. (1993). The effects of grating area and spatial frequency on contrast sensitivity as a function of light level. *Vision Res*. **33**, 2065-2072.

Naarendorp, F. and Frumkes, T.E. (1991). The influence of short-term adaptation of human rods and cones on cone-mediated grating visibility. *Journal of Physiology*. **432**, 521-541.

Oehler, R. and Sharpe, L.T. (1989). Dark adaptation and increment threshold in rhesus monkey and man. *Experimental Brain Res*. **75**, 664-668.

Prestude, A.M., Watkins, L. and Watkins, J. (1978). Interocular light adaptation effect on the lie "specific threshold". *Vision Res* **18**, 855-857.

Rudnicka, A. R.. Steele, C.F., Crabb, D.P. and Edgar, D.E. (1992). Repeatability, reproducibility and intersession variability of the Allergan Humphrey ultrasonic biometer. *Acta Ophthalmologica*. **70**, 327-334.

Rushton, W.A.H. and MacLeod, D.I. (1986). The equivalent background of bleaching. *Perception*. **15**, 689-703.

Rushton, W.H.A. (1965). The sensitivity of rods under illumination. *J. Physiol.* **178**, 141-160.

Sandberg, M.A., Berson, E. L. and Effron, M.H. (1981). Rod-cone interaction in the distil human retina. *Science*. **212**, 829-831.

Schiller, P.H. and Logothetis, N.K. (1990). The colour-opponent and broad-band channels of the primate visual system. *Trends in Neurosciences*. **13,** 392-398.

Schneck, M.E., Adams, A.J., Volbrecht, V.J. and Haegerstrom-Portnoy, G. (1990). LWS cone effects on rod threshold and saturation in achromats with residual cone function. *Vision Res*. **30**, 973-983.

Sivak, M.m Olson, P.L. and Zeltner, K. A. (1989). Effect of prior headlight experience on ratings of discomfort glare. *Human Factors*. **31**, 391-395.

Smith, R.G., Freed, M.A. and Sterling, P. (1986). Microcircuitry of the dark-adapted cat retina: functional architecture of the rod-cone network. *The Journal of Neuroscience*. **6**, 3505-3517.

Sterling, P., Freed, M.A. and Smith, R.G. (1988). Architecture of rod and cone circuits to the on-beta ganglion cell. *The Journal of Neuroscience*. **8**, 523-642.

Sturgis, S.P. and Osgood, D.J. (1982). Effects of glare and background luminance on visual acuity and contrast sensitivity: implications for dirver night vison testing. *Human Factors*. **24**, 347-360.

Thompson, H.S. (1987). The Pupil. In *Adler's Physiology of the eye, 8th Ed.* (ed. R.A. Moses, W.M. Hart, Jr.), Mosby, St Louis, pp. 311-338.

Valeton, J.M. (1983). Photoreceptor light adaptation models: an evaluation. *Vision Res.* **23**, 1549-1554.

Virsu, V. (1978). Retinal mechanisms of visual adaptation and afterimages. *Medical Biology*. **56**, 84-96.

Yeh, T., Lee, B.B. and Kremers, J. (1996). The time course of adaptation in macaque retinal ganglion cells. *Vision Res*. **36**, 913-931.